UNIVERSITEIT VAN PRETORIA
UNIVERSITY OF PRETORIA
YUNIBESITHI YA PRETORIA

Physico-chemical modification of kafirin microstructures for application as biomaterials

By

Joseph Ochieng' Anyango

Submitted in the partial fulfilment of the requirements for the

Degree

PhD Food Science

in the

Department of Food Science

Faculty of Natural and Agricultural Sciences

University of Pretoria

South Africa

August 2012

UNIVERSITEIT VAN PRETORIA
UNIVERSITY OF PRETORIA
YUNIBESITHI YA PRETORIA

DECLARATION

I hereby declare that this thesis submitted at the University of Pretoria for the award of PhD degree is my work and has not been submitted by me for a degree at any other University or Institution of Higher Education.

Joseph Ochieng' Anyango
August 2012

ABSTRACT

Physico-chemical modification of kafirin microstructures for application as biomaterials

Joseph Ochieng' Anyango

Supervisor: Prof John RN Taylor

Co-supervisor: Dr Janet Taylor

Co-supervisor: Prof Vinny Naidoo

Microparticles produced from kafirin, the sorghum grain prolamin protein, by molecular self-assembly using coacervation with acetic acid solvent are vacuolated. They have shown considerable potential for encapsulation of antioxidants and for preparation of high quality free-standing bioplastic films. However, the functional quality of these kafirin microstructures needs to be improved to exploit their potential application, particularly as biomaterials.

Wet heat, transglutaminase and glutaraldehyde treatments were used to modify the physical structure and chemical properties of the kafirin microstructures. Heat treatment (50–96°C) increased microparticle average size by up to four-fold to ≈20 μm, probably due to disulphide cross-linking of kafirin proteins. The vacuoles within these microparticles enlarged up to >10-fold, probably due to greater expansion of air within the microparticles with higher temperature, as the vacuoles are probably footprints of air bubbles. As with heat treatment, glutaraldehyde (10–30%) treatment resulted in oval microparticles, up to about four-fold larger than the control, probably due to covalent glutaraldehyde-polypeptide linkage. Transglutaminase (0.1–0.6%) treatment had only slight effect on the size and shape of microparticles, probably because kafirin has very low lysine content, inhibiting transglutaminase-catalysed cross-linking through ε-(-glutamyl)-lysine bonding. Surface morphology using atomic force microscopy indicated that the microparticles apparently comprised coalesced nanostructures. With heat and transglutaminase treatments, the microparticles seemed to be composed of round nanostructures that coalesced into random irregular shapes, indicative of non-linear protein aggregation. In contrast, with glutaraldehyde treatment, the nanostructures were spindle-shaped and had a unidirectional orientation,

probably due to linear alignment of the nanostructures controlled by glutaraldehyde-polypeptide linkage.

Thin (<50 µm) films prepared from kafirin microparticles and conventional cast kafirin films were compared in terms of their water stability and other related properties. Films cast from microparticles were more water-stable compared to conventional kafirin films, probably because the large vacuoles within the kafirin microparticles may have enhanced protein solubility in the casting solution, thereby improving the film matrix cohesion. The films prepared from microparticles treated with glutaraldehyde were more water-stable compared to the control, despite the loss of plasticizer, probably due to formation of the covalent glutaraldehyde-polypeptide linkages.

The potential of modified kafirin microparticles to bind bone morphogenetic protein-2 (BMP-2) was investigated. Compared to a collagen standard, the BMP-2 binding capacity of control, heat-treated, transglutaminase-treated and glutaraldehyde-treated kafirin microparticles were 7%, 18%, 34% and 22% higher, respectively, probably mainly due to the vacuoles within the microparticles creating greater binding surface area. The safety, biodegradability and effectiveness of kafirin microparticle film and kafirin microparticle film-BMP-2 system in inducing bone growth were determined by a subcutaneous bioassay using a rat model. Kafirin microparticle film and kafirin microparticle film-BMP-2 system was non-irritant to the animals, probably because kafirin is non-allergenic. The kafirin microparticle film implants showed signs of some degradation but a large proportion of these implants was still intact by Day 28 post implantation, probably because of the low susceptibility of kafirin to mammalian proteolytic enzymes. Kafirin microparticle film-BMP-2 system did not induce bone growth, probably mainly due to low BMP-2 dosage and short study duration.

Modification of kafirin microparticles by wet heat or glutaraldehyde treatment both result in increased size of the microparticles with similar gross structure. However, it is apparent that with both treatments the proteins within the pre-formed kafirin microparticles undergo some form of further assisted-assembly through different mechanisms. It seems that heat-induced disulphide cross-linking reinforces a layer around the nanostructures, probably rich in γ-kafirin polypeptides, that stabilizes the structure of the nanostructures. In contrast, glutaraldehyde-treatment appears to destabilize this structure-stabilizing layer through formation of γ-kafirin polypeptide-glutaraldehyde covalent bonding. This probably offsets the balance of attractive and repulsive forces between the different kafirin subclasses within the

nanostructures, thereby resulting in collapsed nanostructures and linear realignment. A deeper understanding of the mechanism of kafirin self-assembly will be important for further development of kafirin microstructures for different applications.

DEDICATION

This thesis is dedicated to:

My lovely wife Carol,

Daughters Natalie and Hope,

And son Brad

For their love, patience and unwavering support

ACKNOWLEDGEMENTS

I would like to express my gratitude to my supervisor, Prof John Taylor, first for the opportunity to work with him during my masters and doctoral studies, spanning about five years. Secondly, his constructive guidance and timely comments were most valuable throughout this work.

I am also grateful to my co-supervisor, Dr Janet Taylor. Apart from her supervisory role, she introduced me to the practical preparation of kafirin microstructures. Her innate ability to listen and offer carefully planned guidance is much appreciated.

I thank my co-supervisor, Prof Vinny Naidoo who was valuable especially in the animal study.

I wish to thank Dr Nicolaas Duneas of Altis Biologics, who introduced me to the work on bone morphogenetic proteins (BMPs).

I wish to thank Mr Alan Hall, Mr Chris van der Merwe and Mrs Antoinette Buys for their help with microscopy.

I want to thank Mrs Ilse Janse van Rensburg of University of Pretoria Biomedical Research Centre who helped with the preparation of the research animals for surgical procedures.

I am grateful to Prof Resia Pretorius of the Department of Physiology, University of Pretoria for her comments on histology data.

I thank Dr W.S. Botha of Idexx Laboratories who kindly discussed with me the findings of the independent post-mortem histopathological evaluation of the study animals.

I am grateful for University of Pretoria Postgraduate Research Support Bursary and Ralph Waniska Sorghum and Millet Bursary.

I am grateful to the rest of academic staff, support staff and fellow postgraduate students at the Department of Food Science, University of Pretoria, for the time I spent with them during my study. Their company was a source of encouragement.

Above all, I am greatly indebted to my family, for their love and understanding.

TABLE OF CONTENTS

LIST OF TABLES

LIST OF FIGURES

1 INTRODUCTION

'Microparticles' is a collective name for microcapsules and microspheres, which are colloidal microstructures with size 1–250 µm (reviewed by Allemann, Leroux and Gurny, 1998; Reis, Neufeld, Ribeiro and Veiga, 2006). These microstructures can be made from synthetic polymers, natural biodegradable polymers, or a combination (reviewed by Sinha and Trehan, 2003). The common synthetic polymers used for preparing microparticles are polyesters such as poly(lactic acid) (PLA) or poly-lactic-*co*-glycolic acid (PLGA) (Freitas, Merkle and Gander, 2005), while examples of the natural polymers are proteins such as zein (Wang and Padua, 2010), kafirin (Taylor, Taylor, Belton and Minnaar, 2009a), albumin (Coombes, Breeze, Lin, Gray, Parker and Parker, 2001; MacAdam, Shaft, James, Marriott and Martin, 1997), gelatin (Mohanty and Bohidar, 2005) and polysaccharides such as chitosan (Guerrero, Teijón, Muñiz, Teijón and Dolores Blanco, 2010), alginate (X. Wang, Wenk, Hu, Castro, Meinel, Wang, Li, Merkle and Kaplan, 2007), starch (Heritage, Loomes, Jianxiong, Brook, Underdown and McDermott, 1996), cellulose (Kumar, Kang and Hohl, 2001) and dextran (Franssen and Hennink, 1998).

Most applications of microparticles are in the pharmaceutical industry, especially as carriers for drug delivery (reviewed by Tan, Choong and Dass, 2010). Microparticles can also be used in tissue engineering as scaffolds for cell transplantation to facilitate tissue regeneration for bone repair and for soft tissues regeneration in wound healing (Babensee, Anderson, McIntire and Mikos, 1998; Quirk, France, Shakesheff and Howdle, 2004). In the food sector, protein microparticles are used for improving flavour, aroma, stability, appearance, nutritional value and texture of food products (Stark and Gross, 1991). Microencapsulation has been used to incorporate health-promoting ingredients such as vitamins, antioxidants and essential minerals as well as fatty acids, into food (Schrooyen, Van der Meer and De Kruif, 2001). Protein microparticles have also been used to increase the survival of probiotic bacteria during their transit through the gastro intestinal (GI) tract by protecting bacteria in both the carrier food and in the human stomach (Marteau, Minekus, Havenaar and Huis In't Veld, 1997; Picot and Lacroix, 2004). It is projected that microparticles might be applied to improve absorption and bioavailability of nutrients and as nano-sensors for traceability and monitoring the condition of food during transport and storage (reviewed by Chaudhry, Scotter, Blackburn, Ross, Boxall, Castle, Aitken and Watkins, 2008).

Protein microparticles are natural products, which are biocompatible and normally have generally recognized as safe (GRAS) status (reviewed by Sinha and Tehran, 2003). Plant proteins in particular are widely available as by-products of food processing, such as the distillers dried grains with solubles (DDGS) which is the main co-product from grain-based ethanol production (reviewed by Wang, Tilley, Bean, Sun and Wang, 2009), brewers spent grains (Mussatto, Dragone and Roberto, 2006), brewing and milling (Lawton, 2002). Using proteins to make microparticles is technically advantageous as proteins are amenable to various chemical modifications that enhance microparticle surface hydrophilicity or hydrophobicity (reviewed by Chen, Remondetto and Subirade, 2006; MacAdam et al., 1997). For example, MacAdam et al. (1997) modified albumin microspheres to prepare hydrophobic and hydrophilic albumin microspheres with chemically reactive groups (carboxylic acid and amino residues) on the surface to which ligands could be attached and hence improve their drug delivery efficiency. In addition, proteins have natural capacity to bind potentially useful bioactive molecules (Wang, Yin and Padua, 2008). Such modifications may be necessary to improve the end-use functionality of protein microparticles. Microparticles produced from kafirin, the storage prolamin protein of sorghum, using simple coacervation with acetic acid as the solvent are vacuolated (Taylor et al., 2009a). This gives them a very large internal surface area, hence the ability to bind bioactive compounds as demonstrated with phytochemicals (Taylor et al., 2009b). These kafirin microparticles can also be used to prepare high quality free-standing bioplastic films (Taylor et al., 2009c). However, the quality of kafirin microparticles needs to be enhanced to broaden their potential applications and possibly to open up market opportunities for them.

2 LITERATURE REVIEW

In this review the term microparticles is defined in detail, and the principle behind the formation of protein microparticles is explained. Technologies for the preparation of protein microparticles are discussed. Properties of protein microparticles that are vital for their potential applications as well as the suitability of proteins to use for preparation of microparticles are discussed. A comparison between the functional quality of protein microparticles and other biodegradable microparticles is provided. Since kafirin will be the basic material in this research, a brief review of characteristics of kafirin proteins is given. Research into various methods used to improve the functionality of protein microparticles is reviewed. The principle behind the formation of protein microparticle films, techniques for their preparation and their quality compared to conventional protein films are described. A review is given of current and potential applications of protein microparticles and potential bioactives that can be bound or encapsulated by protein microparticles. Lastly, some of the techniques for studying the structures of protein microparticles are briefly discussed.

2.1 PROTEIN MICROPARTICLES

2.1.1 Definitions

Microparticles that have a shell and an inner core, in which active substances dissolve, although adsorption of these substances may also occur at their surfaces, are called microcapsules (Figure 2.1a). In contrast, microspheres have a matrix-type structure where active compounds can be adsorbed at their surface, entrapped or dissolved in the matrix (Figure 2.1b). Similar to microparticles, nanoparticles refer to nanocapsules and nanospheres with similar differences for capsules and spheres in the nanometre range. In this review, the term microparticles will be used for both unless specified otherwise. Microencapsulation refers to the process of enveloping a substance within another in a microscale (Schrooyen et al., 2001). In this thesis the term ‘microstructures’ will be used as a general term for protein structures including microparticles and films.

2.1.2 Formation of protein microparticles

There are two main ways to form protein microparticles. One approach involves reducing coarse protein powders to fine powders with microscale particle size through milling process

using ball mills, colloid mills, hammer mills and jet or fluid-energy mills (reviewed by Johnson, 1997).

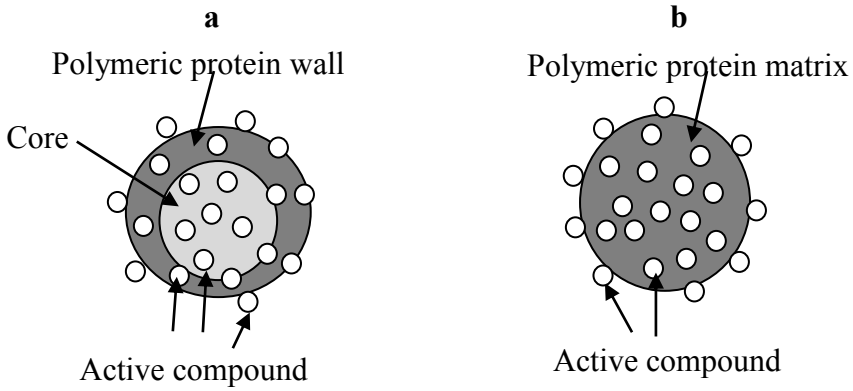

Figure 2.1 Schematic representation of protein microparticles. **a**. Microcapsules. **b**. Microspheres. Adapted from Reis et al. (2006).

Among these milling techniques, the jet mill is the most commonly used to prepare protein microparticles (reviewed by Shoyele and Cawthorne, 2006). Jet milling process involves micronization by interparticle collision and attrition, which typically produces particles size 1–20 µm (reviewed by Johnson, 1997). Alternatively, protein microparticles can be formed by molecular self-assembly (reviewed by Zhang, 2002; Lowik and van Hest, 2004; Wang and Padua 2010, 2012). Molecular self-assembly is the spontaneous organization of molecules under thermodynamic equilibrium conditions into structurally well-defined and rather stable arrangements (protein aggregates) (Whitesides, Mathias and Seto, 1991). As explained by Lowik and van Hest (2004), amphiphilicity is one of the main driving forces for self-assembly. Molecules containing both polar and apolar elements tend to minimize unfavourable interactions with the aqueous environment through a protein aggregation process, in which the hydrophilic domains become exposed and the hydrophobic moieties remain shielded. Self-assembly relies on weak non-covalent interactions, which typically include hydrogen bonds, ionic bonds and van der Waals' bonds. Protein aggregation usually irreversibly leads to the formation of amorphous, flocculent aggregates often heterogeneous in structure (Kentsis and Borden, 2004). As explained by Van der Linden and Venema (2007), the macroscopic and microscopic properties of materials that contain protein assemblies (aggregates) depend on the assembly structure, size, and interactions of the assemblies with the material matrix. Therefore, understanding the aggregation process of proteins may be useful in fabrication of protein microparticles for various applications. For

example, Wang and Padua (2010) working on zein used evaporation induced self-assembly (EISA) to form microspheres, packed spheres and films depending on zein concentration in aqueous ethanol solution. Wang, Crofts and Padua (2003) reported the formation of zein nanoscale tubes (cylinders) by self-assembly.

Protein aggregation is associated mostly with the presence of β-sheet conformation, as was found with zein aggregates (Mizutani, Matsumura, Imamura, Nakanishi and Mori, 2003). Militello, Vetri and Leone (2003) working on bovine serum albumin observed an increase in β-sheet structure at the expense of α-helical conformation after thermal aggregation of the protein. Yeo, Lee, Lee and Kim (2003) using silk protein, fibroin, compared the structures of pure amorphous fibroin and fibroin microparticles by studying their Fourier transform-infrared (FTIR) spectra. The amorphous fibroin sample had typical amide I and amide II bands at 1653 and 1531 cm^{-1}, respectively, which correspond to a random coil conformation. On the other hand, in fibroin microparticles, these peaks were shifted to lower frequencies, 1621 cm^{-1} and 1526 cm^{-1}, respectively, representing β-sheet conformation. The significance of β-sheet structure in the formation of protein microparticles has also been shown in kafirin microparticles (Taylor et al., 2009a). Despite the importance of the β-sheet conformation in aggregation, some proteins seem to deviate from this property as they maintain their native structure in their aggregated form. For example, human lithostathine has been shown to retain its native structure, during fibril formation through domain swapping (Laurine, Gregoire, Fandrich, Engemann, Marchal, Thion, Mohr, Monsarrat, Michel, Dobson, Wanker, Erard and Verdier, 2003).

Protein aggregation can be linear (also referred to as fibrillar) and non-linear (also known as particulate or aggregate) (reviewed by Van der Linden and Venema, 2007). The type of protein aggregation depends primarily on the general state of the protein when aggregation occurs (i.e. the concentration, temperature, pH, salt concentration, salt type and solvent added), rather than the specific amino acid sequence of the protein (Krebs, Devlin and Donald, 2007). These authors demonstrated this aspect when they worked with proteins that differ substantially from each other, but are all known to exhibit linear aggregation. They noted that after incubation at a pH near each protein's isoelectric point (pI), at an elevated temperature, all the proteins exhibited non-linear aggregation. Protein aggregations in foods are normally induced by heating and/or acidification. These treatments often induce unfolding of the proteins, thereby exposing certain sites, which are normally hidden within

the protein, and together with other properties triggers assembly (reviewed by Van der Linden and Venema, 2007).

Linear aggregation, also referred to as 'amyloid-like assembly', is created by linear association of protein molecules maintained by hydrophobic interactions (reviewed by Chen et al., 2006). It can occur through end-to-end aggregation of protein molecules (reviewed by Yeates and Padilla, 2002). Linear assemblies are formed when proteins are heated at pH values far from their pIs and at low ionic strength, when they are highly charged (Bolder, Hendrickx, Sagis and Van der Linden, 2006). The strong electrostatic repulsion that occurs under these conditions and the cross-β sheet structure imposes essentially a one-dimensional aggregation (Krebs et al., 2007).

Non-linear aggregation, also known as particulate or aggregate form is produced by random aggregation of structural units essentially controlled by van der Waals' forces (reviewed by Chen et al., 2006). The structural units are composed of large and almost spherical aggregates characterised by less elastic behaviour and lower rupture resistance. Particulate form occurs within pH range close to the proteins isoelectric point where net charge on the molecules is minimal (Krebs et al., 2007). This low charge, which offers minimal barrier to aggregation, together with partial unfolding of proteins at elevated temperature, results in fast and non-specific aggregation. Because the aggregation is non-specific, there is no directionality to the aggregates, resulting in the formation of three-dimensional spherical particles.

2.1.3 The technology for preparation of protein microparticles

The most common techniques for preparation of protein microparticles are spray-drying, solvent extraction/evaporation and phase separation/coacervation (reviewed Sinha and Trehan, 2003; Chen and Subirade, 2007). Other techniques are modifications of these three methods (reviewed by Freitas et al., 2005). The choice of the method depends on the properties of the protein and the purpose for which the microparticle is intended. Preparation method may be challenging when sensitive ingredients are to be encapsulated due to the possible damaging effect of formulation and process parameters, such as type of organic solvent, shear forces and temperature. Sinha and Trehan (2003) provided some factors to consider when selecting a method for encapsulation of active ingredients for controlled delivery. These include: optimum ingredient loading, high yield of microspheres, stability of the encapsulated material, batch uniformity and inter-batch reproducibility, adjustable release

profiles, low burst effect and free-flow properties of microspheres especially if they are intended for syringeable drugs. The most popular methods for the preparation of microparticles from hydrophobic polymers are organic phase separation and solvent removal techniques (reviewed by Herrmann and Bodmeier, 1998). A brief review of a few common techniques is dealt with next.

2.1.3.1 *Spray-drying*

In this process a feed protein solution is atomized into droplets that dry rapidly due to their high surface area and intimate contact with the drying gas (generally compressed air) (reviewed by Shoyele and Cawthorne, 2006). The solidified particles pass into a second chamber and are trapped in a collection flask. The advantages of this method include control of drug release properties of the resultant microspheres as well as the process being tolerant to small changes of polymer specifications (reviewed by Sinha and Trehan, 2003). Spray-drying is typically a process for preparing 1–10 µm size microspheres (reviewed by Sinha and Trehan, 2003) although slightly larger microparticles may be formed (Young, Sarda and Rosenberg, 1993). Young et al. (1993) used this technique to microencapsulate anhydrous milk fat using whey proteins. They observed that the whey protein capsules were spherical with smooth, wrinkle-free surfaces. Particle size ranged from 1–25 µm. However, this process requires high capital investment and has low recovery as it can result in huge losses through the exhaust vent (reviewed by Sinha and Trehan, 2003), which was noted using laboratory scale spray dryer (Yu, Rogers, Hu, Johnston and Williams III, 2002). Moreover, there is a risk of protein denaturation by physical stresses particularly high shear rates during atomization (reviewed by Johnson, 1997). Spray-drying technique is mostly applied in pharmaceutical industry for production of inhalant or aerosol drugs because it produces microparticles with suitable aerodynamic properties (Chan, Clark, Gonda, Mumenthaler and Hsu, 1997; Maa, Nguyen, Sweeney, Shire and Hsu, 1999).

2.1.3.2 *Solvent evaporation/removal*

In a typical solvent evaporation technique, the protein is dissolved in an aqueous organic solvent (Freitas et al., 2005; Tice and Gilley, 1985). An emulsion is formed by adding this suspension or solution to a vigorously stirring water (often containing a surface-active agent to stabilize the emulsion). The organic solvent is evaporated while continuing to stir. Evaporation results in precipitation of the protein, forming solid microcapsules containing

core material. When solvent removal method is used, the protein is typically dissolved in an oil miscible organic solvent (reviewed by Sinha and Trehan, 2003). The difference in this case is that the organic solvent is removed by diffusion into the oil phase while continuing to stir. No elevated temperatures or phase separating chemicals are required (reviewed by Sinha and Trehan, 2003; Freitas et al., 2005). Controlled particle sizes in the nano- to micro- metre range can be achieved. Cook and Shulman (1998) used this technique for preparation of zein microparticles.

2.1.3.3 *Phase separation/coacervation*

In this technique a protein solution is prepared and, while continuing to stir the solution, an *antisolvent* (a solvent in which the protein is insoluble) is slowly added to the solution (reviewed by Sinha and Trehan, 2003). Depending on the solubility of the protein in the solvent and antisolvent, either the protein precipitates or phase separates into a protein-rich and a protein-poor phase. Under suitable conditions, the protein in the protein-rich phase (coacervate) will migrate to the interface with the continuous phase. The proposed principle behind this technique is that when a protein solution is dispersed in an antisolvent, the binary mixture becomes a marginal solvent for the protein molecules, which precipitate (Mohanty and Bohidar, 2005; Taylor, 2008; Wang and Padua, 2010). Additionally, the poor solvation environment compels the protein molecules to reduce their spatial expansion thereby bringing charged protein functional groups ($-NH_3^+$ and $-COO^-$) to each other's vicinity through electrostatic interactions. This results in collapse of some single protein molecules through intramolecular interactions (self-charge neutralization), yielding the proteins microparticles with smaller radii. On the other hand, most other protein molecules associate (aggregate) to form large protein aggregates of larger radii through intermolecular electrostatic interactions. The morphology of the protein microparticles is attributed to the acquisition of a spherical shape needed for minimising the surface free energy through smallest surface area for a given volume if there is no contribution of other factors (Taylor, 2008).

Mathiowitz, Chickering III, Jong and Jacob (2000) working with zein developed an improvement of this technique in which the microparticle size was determined by non-stress parameters such as protein concentration, viscosity, solvent/antisolvent miscibility and solvent:antisolvent volumetric ratios. These workers claim that their modification is advantageous as it produces microparticles with minimal losses of the material to be encapsulated. This procedure produces microparticles of typical size 10 nm to 10 µm. The

microparticles produced by this technique are characterised by a homogenous size distribution and are thus expected to have well-defined, predictable properties. The phase separation technique has been used for preparation of zein microparticles for encapsulation of essential oils such as oregano, cassia and red thyme (Parris, Cooke and Hicks, 2005), for preparation of zein microspheres to deliver ivermectin (parasiticide) (Liu, Sun, Wang, Zhang and Wang, 2005), for preparation of ovalbumin-loaded zein microspheres (Hurtado-López and Murdan, 2005) and for preparation kafirin microparticles (Taylor et al., 2009a). The kafirin microparticles prepared by simple coacervation in which microparticles were expelled from a solution of kafirin in glacial acetic acid using distilled water were vacuolated (Taylor et al., 2009a). The existence of vacuoles greatly increases the surface area of materials, which may provide a matrix for the growth of cells (reviewed by Gong, Wang, Sun, Xue and Wang, 2006; H.-J. Wang, Gong, Lin, Fu, Xue, Huang and Wang, 2007) and binding with bioactive compounds such as polyphenols (Taylor et al., 2009b) and horseradish peroxidase (X. Wang et al., 2007). A disadvantage of coacervation is frequent impairment by residual solvents and coacervating agents found in the microspheres (reviewed by Freitas et al., 2005).

2.1.4 Properties of protein microparticles important for their application

To function appropriately, protein microparticles need to possess particular characteristics relevant to their intended use. A predominant use for microparticles is in encapsulation, which involves the envelopment of minute solid particles, liquid droplets or gases in a coating (Schrooyen et al., 2001; Reis et al., 2006). Encapsulation is aimed at providing delivery systems for various functional agents such as vitamins, minerals, antioxidants, polyunsaturated fatty acids and drugs. Weiss, Takhistov and McClements (2006) identified four functions that an effective delivery system must possess. First, it should carry the functional ingredient to the desired site of action. Second, in order to maintain the functional ingredient in its active state, it must protect the functional ingredient from physical, chemical or biological degradation during processing, storage, and utilization. Third, it should regulate the release of the functional ingredient, such as the release rate or the specific environmental conditions that trigger release (for example, pH, ionic strength, or temperature). Fourth, the delivery system has to be compatible with the other components in the system, as well as being compatible with the physicochemical and qualitative attributes (that is, appearance, texture, taste, and shelf life) of the final product. Protein microparticles intended for the food industry must be safe, non-toxic, edible and biodegradable. For biomedical applications, the

microparticles need to be biocompatible, resistant to possible attack by immune system *in vivo*, biodegradable and/or reabsorbable in the body once its function is accomplished and small enough for easy introduction into the body (Coombes, Lin, O'Hagen and Davis, 2003).

The size of protein microparticles appears to be a major factor that affects their applications. For example, when Liu et al. (2005) tested the suitability of zein microspheres for delivery of ivermectin, they found that ivermectin-loaded zein microspheres were suitable for use in drug targeting system because the diameter of the microspheres (0.3–1.2 μm) is appropriate for phagocytosis by macrophages. These workers stated, however, that microspheres with an average diameter of 1 μm were so small which may lead to a fast release because of the increased ratio of surface area to volume as the microspheres decrease in size. Chen and Subirade (2007) working on nutrient release properties of alginate–whey protein microspheres suggested that sustained release of encapsulated materials by larger particles is probably due to their smaller surface area/volume ratios and longer diffusion path lengths. On the other hand, syringeable drug-loaded microparticles are better if they are of smaller sizes.

The surface morphology of protein microparticles also affects their applications. Porosity of microparticles may be necessary for tissue engineering as it helps in tissue regeneration (reviewed by Karageorgiou and Kaplan, 2005; Gong et al., 2006). In addition, the presence of vacuoles (pores) within microparticles creates a large internal surface area for binding of bioactive compounds. For example, as discussed Taylor et al. (2009b) showed that vacuolated kafirin microparticles have the ability to bind antioxidants. The protein characteristics also influence the functionality of microparticles prepared from them. For example, studies using zein microparticles have shown that the zero-order release of ivermectin in the presence of pepsin (Liu et al., 2005) or sustained release of encapsulated lysozyme in an aqueous environment (Zhong, Jin, Davidson and Zivanovic, 2009), probably as a result of the the relatively high hydrophobicity of zein protein.

2.1.5 Quality of protein microparticles compared with other biodegradable microparticles

Synthetic biodegradable polymer microparticles are made from polyesters, polyanhydrides, polyorthoesters, polyphosphazenes, and pseudopolyamino acids of which polyesters have found most widespread application (reviewed by Sinha and Trehan, 2003). Synthetic microparticles have advantages over protein microparticles as they can be reproducibly

synthesized, easily purified and are well characterised (Hurtado-López and Murdan, 2005). However, the low toxicity, biodegradability and GRAS status of protein microparticles are their major advantage. In terms of performance, generally, synthetic polymer microparticles have higher active ingredients loading efficiency than microparticles prepared using natural polymers, probably enhanced by the longer period of their use and research. For example, Liggins, Toleikis and Guan (2008) produced polyethylene glycol (PEG) microparticles that could be loaded with a drug at a concentration of greater than 50% (weight drug/weight microparticle). High loading capacity may facilitate less frequent dosing and may increase efficacy. However, the use of synthetic polymers in the preparation of microparticles has some drawbacks. The instability of agent to be delivered (e.g. sensitive protein drugs) is one of the concerns (reviewed by X. Wang et al., 2007). Reviewing formulation aspects of polymeric biodegradable microspheres for antigen delivery, Tamber, Johansen, Merkle and Gander (2005) noted that the organic solvents used during microencapsulation and the acidic microenvironment generated during PLGA degradation can negatively affect the activity of many encapsulated proteins as well as labile molecules. In addition, there are some indications that the breakdown of PLGA and similar polymers to acids such as lactic and glycolic acids can lead to inflammatory reactions in some circumstances when used as scaffold materials (reviewed by Babensee et al., 1998; Quirk et al., 2004).

Concerning the use of natural non-protein polymers to prepare microparticles, some potential technical limitations may be encountered. For example, alginates, which are seaweed derived gel-forming polysaccharides comprising chains of alternating α-L-guluronic acid and β-D-mannuronic acid residues, can be used to prepare biocompatible drug carriers. This can be done through controlled gelation by chelation between the carboxyl groups of its α-L-guluronic acid residues with either Ca^{2+}, Ba^{2+} or poly(L-lysine) (Draget, Skjåk-Bræk and Smidsrød, 1997; Smidsrød and Skjåk-Bræk, 1990). However, X. Wang et al. (2007) reviewing characteristics of alginate microspheres explained that alginate microparticles may be unstable in physiological environments as phosphate and citrate ions can extract Ca^{2+} from the alginate and liquefy the system. In addition, these authors raised concerns regarding the low mechanical strength of alginate drug delivery carriers. Similarly, starch microparticles have a disadvantage, as starch is susceptible to degradation in the gut (Heritage et al., 1996). Hence, these natural non-protein microparticles have to be stabilized often with synthetic polymers to be useful. For example, Heritage et al. (1996) grafted starch microparticles with a hydrophobic silicone polymer coating, 3-(triethoxysilyl)-propyl-terminated

polydimethylsiloxane (TS-PDMS) to effectively deliver orally human serum albumin (HSA). Therefore there is need to prepare microparticles from natural polymers which are stable in aqueous environment but still degradable. Microparticles made from kafirin may be suitable.

2.2 KAFIRIN

Kafirins are the aqueous alcohol soluble storage proteins (prolamins) of sorghum (Paulis and Wall, 1979) and located in protein bodies in the grain starchy endosperm (Taylor, Novellie and Liebenberg, 1985). Kafirins are very similar to zeins, the prolamin storage proteins of maize (DeRose, Ma, Kwon, Hasnain, Klassy and Hall, 1989) but are more hydrophobic (more strictly speaking, less hydrophilic) (reviewed by Duodu, Taylor, Belton and Hamaker, 2003; Belton, Delgadillo, Halford and Shewry, 2006). Four kafirin sub-classes have been identified as α-, β-, γ- and δ-kafirins (Shull, Watterson and Kirleis, 1991; Belton et al., 2006). Kafirins can be classified based on their differences in molecular weight, structure (Shull et al., 1991), cross-linking behaviour (El Nour, Peruffo and Curioni, 1998), amino acid composition and sequence (Belton et al., 2006; Mokrane, Lagrain, Gebruers, Courtin, Brijs, Proost and Delcour, 2009) (Table 2.1). From the hydration energy values, δ-kafirin is the most hydrophobic of the kafirin sub-classes. It is interesting to note from the hydration energies that γ-kafirin is more hydrophobic than α- and β-kafirins despite γ-kafirin being the only kafirin that is water soluble (Duodu et al., 2003). This may appear counterintuitive but Belton et al. (2006) explained that this is probably due to the high level of histidine in γ-kafirin (9 mols %) (De Freitas, Yunes, Da Silva, Arruda and Leite, 1994). As the pKa of histidine is about six (Edgcomb and Murphy, 2002), there may be a high degree of ionisation which leads to electrostatic repulsion and hence water solubility. The relative proportions of the different kafirin subclasses in total kafirin, which has been used by all workers on kafirin films and microparticles, are given in Table 2.1.

Hydrophobicity of a protein is important in regulating the release profile of encapsulated materials in the protein microspheres. For example, using soya protein isolate (SPI)/zein blend microspheres Chen and Subirade (2009) found that the encapsulated riboflavin release rate decreased progressively with increasing zein content. This was probably attributed to the resulting increased hydrophobicity due to zein proteins and hence decreased rate of hydration of the microspheres.

Table 2.1 Relative proportions of the different kafirin sub-classes in total kafirin

Kafirin	Molecular weight[a,b,c]	Proportion (%) of total kafirin[c,e]	Amino acid composition and sequence[a,b]	Hydration energy (kcal/ mol of 100 residues)[a]	Cross-linking behaviour[a, d]
α_1-	25–27k	66–84	Rich in non-polar amino acids, no Lys, one Trp, 10 blocks of repeated amino acids VIIPQXSLAPXAXXS	-144	Monomers oligomers and polymers
α_2-	22–24k			-133	
β-	16–20k	7–13	Rich in Met and Cys, two Trp LQMPGMGLQDLYGAGALMTM (M)GA (Q)X	-123	Monomers and polymers
γ-	28–31k	9–16	Rich in Pro, Cys, His. No Lys, Asn, Asp, Trp. Four repeats TLTTGGXGXQ	-100	Oligomers and polymers
	49k[*†]		Unknown		
δ-	13–15k		Rich in Met, no Lys, 1 Trp THIPGHLPLVM	-99	Unknown

[a]Belton et al. (2006); [b]Mokrane et al. (2009); [c]Shull et al. (1991); [d]El Nour et al. (1998); [e]Hamaker, Mohamed, Habben, Huang and Larkins (1995); [*]Evans, Schüssler and Taylor (1987); [†]Da Silva, Taylor and Taylor (2011)
X – Unidentified amino acid

2.2.1 Kafirin structure: physical and chemical properties

A study by Gao, Taylor, Wellner, Byaruhanga, Parker, Mills and Belton (2005) on native sorghum kafirins, using FTIR spectroscopy, showed a 58% α-helical conformation content. Similarly, working with both normal and mutant sorghums, Duodu, Tang, Wellner, Belton and Taylor (2001) found a 54–58% α-helical conformation content for uncooked sorghum kafirin. In addition, Wang et al. (2009) characterised the composition as well as chemical and physical properties of kafirin proteins in the distillers dried grains with solubles (DDGS), which is the main co-product from grain-based ethanol production. They extracted kafirin using three different methods: Acetic acid method (Taylor, Taylor, Dutton and De Kock, 2005a), HCl-ethanol method (Xu, Reddy and Yang, 2007) and NaOH-ethanol method (Emmambux and Taylor, 2003). The secondary structure of kafirin extracts from the three methods showed α-helical conformation dominance in all the three types of extracts with smaller proportions of β-sheet conformation. Therefore, it may be concluded that the native secondary structure of kafirin is rich in α-helical conformation.

However, when subjected to physical stress such as heat, the kafirin secondary structures generally become richer in β-sheet conformation as a result of unfolding (Duodu et al., 2001; Byaruhanga, Emmambux, Belton, Wellner, Ng and Taylor, 2006; Emmambux and Taylor, 2009). The pI of kafirin is 6 (Csonka, Murphy and Jones, 1926). This may be a useful parameter in manipulating the type of kafirin aggregation formed. This is because by adjusting the pH from above to below their isoelectric point the charge on proteins can be changed from negative to positive thereby resulting into different protein structures (reviewed by Van der Linden and Venema, 2007).

2.2.2 Kafirin digestibility

Kafirin has somewhat poor digestibility relative to other cereal prolamins, which worsens on wet cooking (reviewed by Duodu et al., 2003; Hamaker, Kirleis, Butler, Axtell and Mertz, 1987). The poor digestibility of wet-cooked kafirin is probably mainly due to disulphide cross-linking between the γ- and β- kafirin species, which inhibit the digestion of the major kafirin protein component, α-kafirin (Da Silva et al., 2011). As with microparticles prepared with poorly digestible zein (Parris et al., 2005; Hurtado-López and Murdan, 2006), the poor digestibility of kafirin may make kafirin microparticles more resistant to enzymatic degradation, enabling delivery of the encapsulated material to the desired site. A positive correlation has been shown between protein digestibility (under simulated gastric conditions) and the rate of release of antioxidant activity of catechin and condensed tannins encapsulated with kafirin microparticles (Taylor et al., 2009b).

2.2.3 Kafirin microparticles

As stated, kafirin microparticles, size 1–10 μm, as prepared by (Taylor et al., 2009a) using simple coacervation with acetic acid solvent are vacuolated. These kafirin microparticles produced high quality free-standing bioplastic films when about 11 times acetic acid as a proportion to kafirin content was used (Taylor et al., 2009c). In addition, these microparticles had the capacity to encapsulate bioactive compounds such as antioxidants (Taylor et al., 2009b), probably because their vacuolated structure provided larger binding surface area. However, as indicated the functionality of kafirin microparticles needs to be enhanced to broaden their potential applications.

2.3 MODIFICATION OF THE FUNCTIONAL QUALITY OF PROTEIN MICROPARTICLES

To prevent problems such as the fragility of protein microparticles and because of the short *in vivo* half-lives of bioactive compounds (time it takes for the bioactives to lose half their activity in a physiological environment), there is need to develop microparticles with improved functional quality such as physical strength and stability in aqueous environment (reviewed by Stark and Gross, 1994; Balmayor, Feichtinger, Azevedo, Van Griensven and Reis, 2009). Modification of proteins to enhance the functional properties of protein microparticles can be achieved by physical treatment (Patil, 2003; Vandelli, Romagnoli, Monti, Gozzi, Guerra, Rivasi and Forni, 2004), chemical cross-linking (Vandelli, Rivasi, Guerra, Forni and Arletti, 2001; Lee and Rosenberg, 1999), treatment with food components such as polyphenols (Xing, Cheng, Yang and Ma, 2004) and lipids (Önal and Landon, 2005), and enzymatic treatment (Dong, Xia, Hua, Hayat, Zhang and Xu, 2008). Such modifications can produce proteins with altered thermal stability, surface reactivity, lipophilicity, molecular weight, charge, shear stability and resistance to proteases (reviewed by Stark and Gross, 1994).

2.3.1 Physical treatment of protein microparticles

2.3.1.1 *Heat*

Heat has been applied to improve the functionality of protein microparticles. For example, Zhang and Zhong (2010) used thermal pre-treatment to enhance the heat stability of whey protein nanoparticles. This was aimed at averting the formation of aggregates or gels (at high protein concentrations e.g. >5%) when whey is heated above 60^{o}C. As deduced from this study heat treatment generally increased microparticles size through protein cross-linking, which results in protein polymerization. With certain protein microparticle preparation techniques, especially that involve particle micronization, an increase in temperature during microparticle preparation may result in a decrease in the size of protein microparticles. This was found by Bustami, Chan, Dehghani and Foster (2000) who used an Aerosol Solvent Extraction System (ASES) to generate microparticles from different types of proteins for aerosol delivery from aqueous-based solution. Their operating temperature was in the range 20–45°C. These authors found that at higher temperatures, the diameters of the microparticles were generally smaller compared to sizes obtained at relatively lower operating temperatures.

According to these authors, it seems that higher temperature during spray drying enhances mass transfer, and lowers density, both of which may induce a higher degree of super-saturation resulting in higher nucleation rate with correspondingly less particle agglomeration. Patil (2003) working with albumin microspheres explained that thermal stabilization occurs through direct reaction between functional groups on the albumin polypeptide side chains forming by inter-chain amide links (self-cross-linking), which renders the albumin insoluble. Thermal stabilization of albumin occurs at temperatures above 50^{o}C, although temperatures between 90–180^{o}C are commonly applied (Dubey, Parikh and Parikh, 2003). When Dubey et al. (2003) heat-stabilized albumin, there was a reduction in both particle size of the albumin microspheres and their drug entrapment efficiency for 5-fluorouracil (5-FU), an anticancer drug, with increasing temperature and time. This finding indicated that modification of protein microparticles by conventional heat treatment might not be an ideal method for heat sensitive encapsulated active ingredients. Microwave cross-linking has also been explored as a means of improving the loading and the drug release properties of gelatin microspheres loaded with diclofenac, a non-steroidal anti-inflammatory agent (Vandelli et al., 2004). This heat treatment enhanced the loading capacity and protection of the drug from degradation.

2.3.1.2 *Application of mechanical stress*

During the preparation of protein microparticles stress may be introduced through, for example, mechanical shearing and/or agitation or through exposure to ultrasound (reviewed by Bilati, Allemann and Doelker, 2005). Generally, smaller protein microparticles are formed by increased speed and longer mixing times due to the formation of smaller emulsion droplets (Patil, 2003; Whittlesey and Shea, 2004; Freitas et al., 2005), which result from stronger shear forces and increased turbulence. A study of kafirin microparticles prepared using aqueous ethanol as the solvent showed an increase the size of holes (vacuoles) in the microparticles when higher shear was applied during mixing (Taylor et al., 2009a). As explained by these authors, it seems that the increased turbulence with high shear would incorporate more air into the liquid phase, thereby creating bubbles. Then small bubbles would possibly coalesce to form larger bubbles before being entrapped within the microparticles as the protein precipitates. However, in the same study, it was observed that kafirin microparticles prepared using a different solvent (glacial acetic acid), lost their spherical structure instead forming a continuous matrix apparently being broken into

fragments, which aggregated together. This study highlighted the necessity of choosing an appropriate solvent for preparation of microparticles for particular applications. It also underscored the need to explore possibilities of including additives such as porogens in certain solvent systems if needed to improve the porosity of protein microparticles. A porogen is a soluble additive included during microparticle preparation, which after microparticle formation is leached out, generating a highly porous matrix (Lee, Soles, Vogt, Liu, Wu, Lin, Kim, Lee, Volksen and Miller, 2008). Nonetheless, agitation can be used to manipulate vacuole sizes of protein microparticles thereby increasing their encapsulation capacities (Taylor et al., 2009a). As discussed, stirring to create a flow instead of turbulence can be used to enhance formation of fibrils (Bolder, Sagis, Venema and Van der Linden, 2007). This shows that regulation of the amount of stress in the system can be used to manipulate the structure of the protein microparticles to suit specific applications.

2.3.1.3 *Manipulation of acid concentration*

Increasing the concentration of an acid used in the preparation of protein microparticles has been shown to result in larger kafirin microparticles with a less continuous structure (Taylor et al., 2009a), possibly due to aggregation of protein molecules through denaturation. As a possible cause of protein aggregation, these authors suggested that higher acid concentration may unfold the kafirin secondary structure from a predominately α-helical structure to β-sheet conformation. As the β-sheet conformation is more mobile from a molecular perspective, this would expose previously hidden hydrophobic amino acids allowing hydrophobic interactions between polypeptide chains. The increase in molecular mobility due to the β-sheet conformation would also expose other ionic and neutral amino acids which would then be available to form inter- and intra- molecular hydrogen bonds. The combination of hydrogen bonding and hydrophobic interaction between polypeptide chains would then result in protein aggregation. Similarly, working with SPI-zein composite, Chen and Subirade (2009) noted that swelling of microspheres was minimal near the isoelectric point (pI) and greater at lower pH (pH 1.2) or higher pH (pH 7.4), which probably indicated that swelling behaviour is governed mainly by the net charge of the protein molecules. As discussed, near the pI the numbers of charged groups on the polypeptide chains ($-NH_3^+$ and $-COO^-$) are presumed to be nearly equal, and few ionized groups are free to repel each other (Krebs et al., 2007). At lower pH, the chains bear a strong positive net charge due to $-NH_3^+$ groups, whereas at higher pH, they bear a strong negative net charge because of $-COO^-$ groups. The

resulting electrostatic repulsion allows the solvent medium to diffuse into the protein network causing more swelling and larger microspheres. Therefore, during preparation, the pH of the system can be manipulated to form microparticles with the required size and structure for particular applications.

2.3.2 Cross-linking proteins with enzymes

The stability of a protein can be improved by cross-linking the protein prior to preparation of microparticles by phase separation process by addition of an enzyme, which catalyses intra- and/or inter-molecular cross-linking of the protein, such as transglutaminase, or protein disulphide isomerase (Mathiowitz, Bernstein, Morrel and Schwaller, 1993). Transglutaminase (protein-glutamine:amine γ-glutamyl transferase) catalyses an acyl transfer reaction in which carboxyamide groups of peptide-bound glutamine residues are the acyl donors and a variety of primary amines are the acyl acceptors (Figure 2.2a) (Ohtsuka, Sawa, Kawabata, Nio and Motoki, 2000).

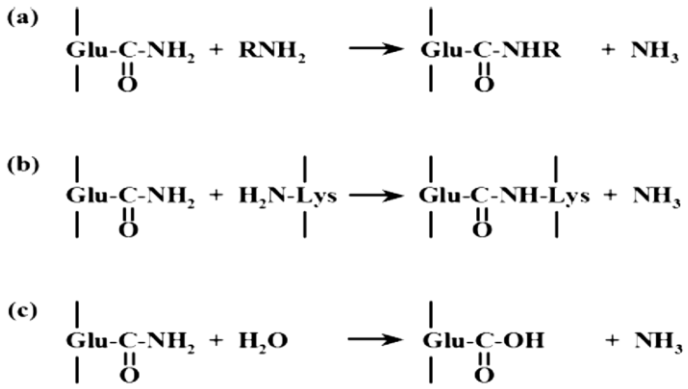

Figure 2.2 Reactions catalysed by transglutaminase. (**a**) Acyl-transfer reaction; (**b**) Cross-linking reaction between glutamine and lysine residues of proteins or peptides. The resultant bridge is called ε-(γ-glutamyl)-lysine bond; (**c**) Deamidation (Yokoyama et al., 2004).

When ε-amino groups of peptide-bound lysine residues are the acceptors, protein cross-linking occurs through ε-(γ-glutamyl)-lysine bridges (Figure 2.2b). In the absence of available amines, the enzyme may also catalyse the hydrolysis of glutamine residues to glutamate residues during which water molecules are used as acyl acceptors (Figure 2.2c) (Yokoyama, Nio and Kikuchi, 2004; Motoki and Seguro, 1998). The action of this enzyme leads to the post-translational modification of proteins through either the formation of intra- and intermolecular isopeptide bonds or the covalent attachment of amines such as polyamine

and putrescine (Ikura, Goto, Yoshikawa, Sasaki and Chiba, 1984). The large polymers so formed may be chemically and enzymatically resistant and mechanically strong. Transglutaminase has been widely applied commercially in the food industry in protein cross-linking reactions (reviewed by Lantto, 2007). Enzyme concentration may be an important parameter especially when enzymatic modification is used to enhance the functionality of protein microparticles. An example is demonstrated in the work of Dong et al. (2008) on transglutaminase-hardened gelatin-gum arabic spherical multinuclear microcapsules (SMMs) prepared by complex coacervation. These authors found that lower concentrations of transglutaminase led to lower structural stability in the resulting SMMs. This was probably because decreasing the transglutaminase concentration results in lower enzymatic activity per volume and thus possibly lower microcapsule cross-linking density. Therefore, the microcapsule hardening ability becomes poor, and the resulting structure disintegrates easily.

Sometimes protein microparticles are preferred with lower molar mass. For example, peptides of gluten of molar mass <10 kDa, preferably 3–5 kDa may be required due to their water-retaining capacity and their conditioning effect (reviewed by Auriol, Paul and Monsan, 1996). As stated by these authors, these low molecular weight peptides can be obtained through enzymatic hydrolysis with proteases such as Alcalase (Novozymes), pepsin or acid protease from *Aspergillus niger*. The peptides so derived have marked hydrophobic characteristics. The functionality, surface properties and molecular weight distribution of the protein can also be modified by hydrolysis with other proteases, such as papain or chymotrypsin, to yield peptides having similar solubility characteristics as the untreated protein (Haralampu, Sands and Gross, 1993).

2.3.3 Cross-linking protein microparticles with chemicals

Chemical cross-linking procedures have been applied to overcome the problem of rapid solubilisation of protein microparticles in aqueous environments, which results in fast drug release profiles (Digenis, Gold and Shah, 1994). Furthermore, as hydrophilic polymeric system, protein microparticles have difficulties achieving sustained drug release as when the system absorbs water and swells, drugs will rapidly diffuse out (reviewed by Latha, Rathinam, Mohanan and Jayakrishnan, 1995). The chemicals commonly used to cross-link protein microparticles for microparticle stability in aqueous environment include aldehydes such as glutaraldehyde (Lee and Rosenberg, 1999, 2000), formaldehyde and glyceraldehyde (Vandelli et al., 2001). Cross-linking of protein with an aldehyde involves the reaction of free

amino groups of peptide chains with the aldehyde (carbonyl) groups (Bigi, Cojazzi, Panzavolta, Roveri and Rubini, 2002) (Figure 2.3). The carbonyl groups of the aldehydes can react with any nitrogen in a protein (Kiernan, 2000). Intra- and intermolecular links are formed that could connect atoms of neighbouring but not interacting molecules, yielding artificial protein oligomers that lack biological significance (reviewed by Fadouloglou, Kokkinidis and Glykos, 2008).

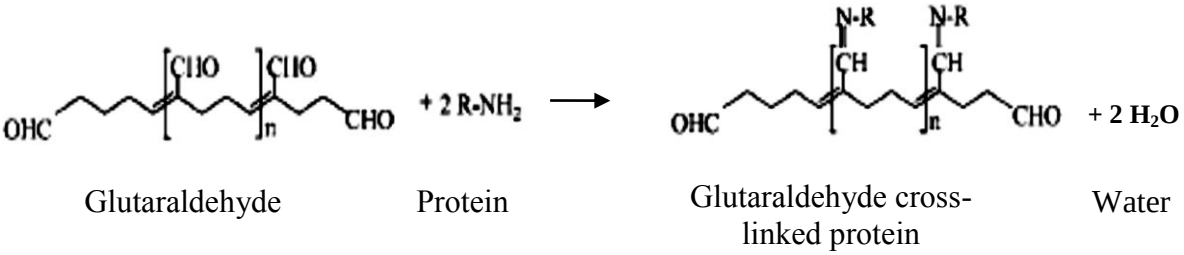

Figure 2.3 Cross-linking reaction between glutaraldehyde and protein (adapted from Migneault, Dartiguenave, Bertrand and Waldron, 2004; Kiernan, 2000).

Glutaraldehyde is the most efficient among these three aldehydes in cross-linking of food proteins (reviewed by Gerrard and Brown, 2002). This is probably due to the presence of dicarbonyl groups in a glutaraldehyde molecule, which provide two reactive moieties (Gerrard and Brown, 2002) and the fact that it has five-carbon species considered optimal for protein cross-linking reactions (reviewed by Meade, Miller and Gerrard, 2003). According to Migneault et al. (2004), it is the polymeric forms of glutaraldehyde that are involved in the cross-linking reaction. The core release properties of a protein microparticle can substantially be improved by cross-linking protein with glutaraldehyde. For example, to improve the efficiency of encapsulation of theophylline (a water-soluble drug used in therapy for respiratory diseases such as asthma) with whey microparticles, Lee and Rosenberg (1999) cross-linked the whey protein with glutaraldehyde-saturated toluene. This great improvement in the encapsulation efficiency through cross-linking was probably due to creation of a dense microparticle wall matrix occasioned by the formation of whey protein-glutaraldehyde-saturated toluene meshwork, which impeded diffusion of the microencapsulated theophylline molecules. In addition, Vandelli et al. (2001) working with gelatin microspheres loaded with clonidine hydrochloride (an antihypertension drug), found that cross-linking with D,L-glyceraldehyde resulted in a more gradual and sustained systolic blood pressure (SBP) reduction and the antihypertensive effect than uncross-linked microspheres. A main disadvantage of using chemical cross-linking as opposed to heat or transglutaminase cross-

linking is the toxicity of the residuals of chemical cross-linking agents and the *in vivo* biodegradation products of the chemical cross-linked macromolecule (reviewed by Vandelli et al., 2004).

2.3.4 Cross-linking with polymeric food components

Tannins are plant polyphenols with an exceptional ability to precipitate protein (Emmambux and Taylor, 2003; Charlton, Baxter, Khan, Moir, Haslam, Davies and Williamson, 2002). Xing et al. (2004) studied the influence of the tannins on the morphology and structures of the gelatin-acacia complex microcapsules used to microencapsulate capsaicin (the main pungent ingredient in hot peppers). These authors found that when compared to the use of glutaraldehyde, tannin cross-linked microcapsules had relatively high encapsulation efficiency and relatively high drug content with a good dispersion and an even distribution and shape. Similarly, the ability of polyphenols to inhibit degradation of protein microparticles was reported by Taylor et al. (2009b) who found little degradation of the kafirin microparticles encapsulating sorghum condensed tannin and catechin while still releasing reasonably good antioxidant activity. This was probably a result of synergistic actions of hydrogen bonding and hydrophobic effects when tannins interact with proteins (Kawamoto, Mizutani and Nakatsubo, 1997). Studies have shown an intrinsic complexity of the molecular recognition processes that occur between tannins and proteins such as gelatin (Madhan, Muralidharan and Jayakumar, 2002).

The performance of protein microparticles for delivery of bioactives can also be improved by using food compounds. For example, by adding different types of lipids, Önal and Landon (2005) found a substantial improvement in quality of zein microparticles, measured by encapsulation, delivery and retention efficiencies of riboflavin in early fish larvae. These workers did not provide a clear explanation why this was so. However, the introduction of lipid in to the system may have induced protein-lipid interaction.

2.4 PROTEIN MICROPARTICLE FILMS

These are bioplastic films prepared from protein microparticles. There are two process pathways used for producing bioplastic protein films, the dry (melt process) and the wet process (reviewed by Cuq, Gontard and Guilbert, 1998; Zhang and Mittal, 2010). The dry process uses a thermal or thermo-mechanical process based on thermoplastic properties of

biopolymers when plasticized and heated above their glass transition temperatures under low water content. For example, Lai, Padua and Wei (1997) used the dry process to prepare 0.5 mm thick zein films (sheets) plasticized with palmitic and stearic acids. In the wet process (solvent process) or also known as casting, the protein microparticles are typically dissolved or dispersed in suitable solvents with plasticizers. The resulting solutions or dispersions form free-standing films or coatings on a plate by casting the mixture and subsequent drying. This procedure is generally used for pre-formed films and coatings (reviewed by Cuq et al., 1998). Casting is the most often used protein film-forming method (reviewed by Zhang and Mittal, 2010). These protein films in general are water sensitive and lack mechanical strength but are good oxygen barriers (reviewed by Cuq et al., 1998; Zhang and Mittal, 2010).

Studies have shown that films produced from protein microparticles have superior functional quality than conventional protein films. For example, Taylor et al. (2009c) found that kafirin microparticle films had smoother film surface and lower water vapour permeability than the conventional cast films from kafirin. Likewise, Cook and Shulman (1998) working with zein found that zein microparticle films had no voids or porosity in contrast to conventional zein films, which had large void spaces as assessed by scanning electron microscopy (SEM). Researchers have shown that protein microparticle films have potential for useful novel applications. For example, Dong, Sun and Wang (2004) prepared zein microparticle films onto which human liver cells and mice fibroblast cells could attach and proliferate. Similarly, in a study by Wang, Lin, Liu, Sheng and Wang (2005), they reported a heparin-loaded zein microsphere films with potential for application as drug-eluting coating films used for cardiovascular devices such as stents.

2.5 APPLICATION OF PROTEIN MICROPARTICLES

The majority of applications of protein microparticles is in the medical field, especially as carriers for drug delivery (reviewed by Haidar, Hamdy and Tabrizian, 2009; Tan et al., 2010). However, the boundaries between food, medicine and cosmetics are already obscure and the advent of nanoparticles that can interact with biological entities at a near-molecular level is likely to blur further these boundaries (reviewed by Chaudhry et al., 2008). Some food and cosmetic companies are collaborating to develop cosmetic nutritional supplements. For example, in 2002, L'Oréal and Nestlé formed a joint venture, Laboratoires Innéov (Charles, 2002). Innéov's first product, called "Innéov Firmness," contains lycopene (Marketing Week, 2003). Applications of protein microparticles in the food industry include delivery of

bioactive compounds or agents for development of improved flavour, colour, texture and consistency of foodstuffs, increased absorption and bioavailability of nutrients and health supplements (reviewed by Jones and McClements, 2010; Livney, 2010; Schrooyen et al., 2001). Table 2.2 highlights representative bioactive agents delivered by protein microparticles/nanoparticles. Protein microparticles can also be used as new food packaging materials with improved mechanical, barrier and antimicrobial properties, and nano-sensors for traceability and monitoring the condition of food during transport and storage (reviewed by Chaudhry et al., 2008).

In the patent of Stark and Gross (1991), they claim that their microparticles, with size 0.1–4.0 µm, can be used as a fat substitute in food. Protein microparticles could increase the survival of healthy probiotic bacteria during their transit through the gastrointestinal tract by protecting bacteria in both the carrier food and in the human stomach (Marteau et al., 1997; Picot and Lacroix, 2004) with potential health benefits. Protein microparticles have potential for application in the biomedical sector in tissue engineering (Gong et al., 2006) as scaffolds or sutures, carrier for bioactive compounds such as bone morphogenetic proteins (Haidar et al., 2009). Biomaterials applied as carriers for controlled delivery of bioactives offer many advantages over the inorganic systems such as fullerene, gold, silver and silica. Some of the advantages of biomaterials include the increase of treatment effectiveness and significant reduction of toxicity, due to their biodegradability property (reviewed by Xu et al., 2011).

Table 2.2 Examples of bioactive compounds or agents delivered by protein microparticles

Bioactive category	Bioactive agent	Protein
Nutraceuticals	*Vitamins:*	
	D (Semo, Kesselman, Danino and Livney, 2007)	Casein
	B1 (Benichou, Aserin and Garti, 2007)	Whey protein isolate
	riboflavin (Chen and Subirade, 2009)	Soy-Zein blend
	Minerals:	
	Fe^{2+} (Sugiarto, Ye and Singh, 2009)	Casein/ Whey protein isolate
	Mg^{2+} (Bonnet, Cansell, Berkaoui, Ropers, Anton, and Leal-Calderon, 2009)	Casein
	Omega 3 oils and other health promoting fatty acids:	
	fish oil (Patten, Augustin, Sanguansri, Head and Abeywardena, 2009)	Casein
	flax oil (Quispe-Condori, Saldaña and Temelli, 2011)	Zein
	docosahexaenoic acid (DHA) (Zimet and Livney, 2009)	β-lactoglobulin
	Essential oils:	
	oregano, cassia and red thyme (Parris et al., 2005)	Zein
	Carotenoids:	
	β-carotene (López-Rubio and Lagaron, 2012)	Whey protein concentrate
	lycopene (Gouranton, El Yazidi, Cardinault, Amiot, Borel and Landrier, 2008)	Bovine serum albumin
	Polyphenols:	
	resveratrol (Bharali, Siddiqui, Adhami, Chamcheu, Aldahmash, Mukhtar and Mousa, 2011)	Bovine serum albumin
	condensed tannins and catechin (Taylor et al., 2009b)	Kafirin
	epigallocatechin gallate (EGCG) (Shutava, Balkundi and Lvov, 2009)	Gelatin
Probiotics and other microorganisms	Bifidobacteria (Picot and Lacroix, 2004)	Whey protein
	recombinant yeasts (Hebrard, Blanquet, Beyssac, Remondetto, Subirade and Alric, 2006)	Whey protein

Bioactive category	Bioactive agent	Protein
Therapeutics	*Anti-microbial:*	
	nisin and thymol (Xiao, Davidson and Zhong, 2011)	Zein
	Parasiticide (endectocide):	
	ivermectin (Gong, Sun, Sun, Wang, Liu and Liu, 2011; Liu et al., 2005)	Zein
	Cancer therapy:	
	paclitaxel (Gong, Huo, Zhou, Zhang, Peng, Yu, Zhang and Li, 2009)	Bovine serum albumin
	5-fluorouracil (Maghsoudi, Shojaosadati and Farahani, 2008)	Bovine serum albumin
	Anti-diabetic drug:	
	metformin (Xu, Jiang, Reddy and Yang, 2011)	Zein
	Peptidic-drugs:	
	bone morphogenetic protein-2 (Bessa, Balmayor, Hartinger, Zanoni, Dopler, Meinl, Banerjee, Casal, Redl, Reis and Van Griensven, 2010)	Silk fibroin
	Other drugs:	
	theophylline (asthma drug) (Latha et al., 1995)	Casein
Enzymes	bile salt-hydrolase (Lambert, Weinbreck and Kleerebezem, 2008)	Whey protein
Flavours/aromas/fragrances	ethyl hexanoate (Giroux and Britten, 2011)	Whey protein

2.6 TECHNIQUES FOR STUDYING THE STRUCTURE OF PROTEIN MICROPARTICLES

The techniques used to study the structure of protein microparticles depend on the information required. Some of the common techniques are microscopy, spectroscopy, electrophoresis, and differential scanning calorimetry (DSC). Often these techniques are used in combination for verification. The more important methods will be discussed briefly.

2.6.1 Microscopy

Microscopy is an important technique for visualization in the study of protein and protein products structure. Yang, Wang, Lai, An, Li and Chen (2007) provides a summary of some of the common microscopy techniques that are used in studying the structure of protein microparticles. The use of a number of different imaging techniques is recommended in order to compare and confirm results. The main features of some the microscopy techniques and protein microparticle type applications are shown in Table 2.3.

2.6.2 Fourier transform infrared (FTIR) spectroscopy

FTIR spectroscopy provides information about the secondary structure composition of proteins. Each protein has a characteristic set of absorption bands in its infrared spectrum. Typical bands found in the infrared spectra of proteins and polypeptides include the Amide I and Amide II, which arise from the amide bonds that link the amino acids (reviewed by Pelton and McLean, 2000; Surewicz, Mantsch, and Chapman, 1993). The Amide I band is due mainly to C═O stretch (80%) and weak N–H bend, and the stretching of the C−N bond, while Amide II band is due to N–H bend (60%) and C–N stretch (40%). Conformational sensitivity of amide bands are mainly influenced by H-bonding and the coupling between transition dipoles (reviewed by Pelton and McLean, 2000). In kafirin, the Amide I band occurs at wave number ≈1650–1620 cm^{-1} while Amide II band occurs in the ≈1550–1500 cm^{-1} region (Duodu et al., 2001). FTIR has been used by many workers to determine the secondary structure of protein microparticles and in turn relate the findings to the functionality of the protein microparticles.

Table 2.3 Characteristics of different microscopy techniques and their application in protein microparticle type research (adapted from Yang et al., 2007)

Microscopy	Advantages	Disadvantages	Examples of application
Light microscopy	Large scan area; Fast scan speed; Cheap	Only 2D; Need pre-treatment; Low resolution and magnification	Kafirin microparticle films (Taylor et al., 2009c); Microwave-treated gelatin microspheres (Vandelli et al., 2004)
Scanning electron microscopy (SEM)	High resolution; Fast scan speed	Only 2D; Need pre-treatment; Not native status	Zein films (Lai and Padua, 1997), zein scaffolds (Gong et al., 2006), zein microspheres (Suzuki, Sato, Matsuda, Tada, Unno and Kato, 1989; Parris et al., 2005); whey protein based microcapsules (Lee and Rosenberg, 1999)
Transmission electron microscopy (TEM)	Nanoscale; High resolution; Fast scan speed	Only 2D; Need pre-treatment; Not native status	Ovalbumin nanospheres (Coombes et al., 2001); Whey protein beads (Beaulieu, Savoie, Paquin and Subirade, 2002); Kafirin microparticles (Taylor et al., 2009a)
Confocal laser scanning microscopy (CLSM)	Study dynamic process; Fast scan speed; 2D and 3D; In situ	Limited excitation wavelengths available with common lasers, occurring over narrow bands and are expensive to produce in the ultraviolet region; Need pre-treatment	Silk fibroin microspheres (X. Wang, Wenk, Matsumoto, Meinel, Li and Kaplan, 2007)
Atomic force microscopy (AFM)	High resolution (nanoscale); Minimal sample preparation; 2D and 3D; In air or liquid, in situ, continuous process; Can be manipulated	Small scan size; Slower scan speed; Difficult for soft material	Zein films (Guo, Liu, An, Li and Hu, 2005), Zein globules (Gao, Ding, Zhang, Shi, Yuan, Wei and Chen, 2007), Zein microparticles (Wang et al., 2008), Gliadins (McMaster, Miles, Kasarda, Shewry and Tatham, 2000).

For example, Taylor et al. (2009a) working on kafirin microparticles used FTIR with which they found that formation of kafirin microparticles was associated with β-sheet conformation at the expense of α-helical conformation. Similarly, Chen and Subirade (2009) working with riboflavin as the model drug used FTIR to characterise SPI, zein, and SPI/zein blends as potential delivery systems for nutraceutical products. Other workers who have used FTIR to study protein microparticles include López-Rubio and Lagaron (2012) working on whey protein capsules obtained through electrospraying for the encapsulation of β-carotene. Most studies on protein microparticles with FTIR use the Amide I band determination of protein secondary structure rather than the amide II band. This is probably because Amide I band mainly arises from only one of the amide functional groups, in contrast to the Amide II mode (Jackson and Mantsch, 1995).

2.6.3 Electrophoresis

This is a technique that separates proteins under the influence of an electric field, through a sieving medium, usually a polyacrylamide gel (reviewed by Yada, Jackman, Smith and Marangoni, 1996). The proteins are separated based on their differences in molecular size and/or charge. A common method, Sodium Dodecyl Sulphate-Polyacrylamide Gel Electrophoresis (SDS-PAGE) separates protein molecules based on their sizes. SDS-PAGE has been used often in determination of molecular weight distribution in many studies of protein microparticles. For example, Parris et al. (2005) used SDS-PAGE to measure the rate of zein nanosphere digestion thereby determining the rate of release of essential oils encapsulated by zein nanospheres. Taylor et al. (2009a) working on kafirin microparticles used SDS-PAGE to show that despite evidence of aggregation of the kafirin proteins during microparticle formation, there was no significant polymerisation, in contrast to what happens when kafirin is heated under moist conditions. In a related study, these workers used SDS-PAGE to show little enzymatic degradation of the kafirin microparticles encapsulating sorghum condensed tannin, which contrasted the almost complete degradation of kafirin microparticles not encapsulating the tannins (Taylor et al., 2009c). Zhang, Luo and Wang (2011) used SDS-PAGE to determine the stability of zein microparticles in mild acidity (pH 6.5) where they found that zein retained its primary structure upon the mild pH treatment.

2.7 CONCLUSIONS

Protein microparticles have potential for use in preparation of useful biomaterials. However compared to similar products prepared using synthetic materials, protein biomaterials have shortcomings such as poor mechanical properties, poor water stability and relatively lower binding capacity for bioactive compounds. These limitations must be addressed to realize the full potential of protein microparticles. This could be achieved by modifying the properties of the protein microparticles, and hence improving their functional properties, which will in turn increase their end use application. Modification of the protein microparticles can be achieved by physical, chemical and enzymatic cross-linking or a combination of these treatments. These treatments are usually performed on the proteins prior to or during preparation of the microparticles. An alternative approach that is not often applied is treatment of the protein microparticles after their preparation. The relatively high hydrophobicity and slow enzymatic hydrolysis of sorghum kafirin and the fact kafirin can be used to produce vacuolated microparticles, provides an opportunity to produce high quality microparticles that have potentially many applications in the food and pharmaceutical industry as well as the biomedical field. However, to make them more useful as biomaterials it is important to increase the size of the kafirin microparticles to suit applications where large structures with a high degree of interconnected porosity are required. In addition, it is also necessary to improve both the tensile properties and water resistance of the bioplastic films prepared from the kafirin microparticles in order to make them applicable in aqueous conditions.

3 HYPOTHESES AND OBJECTIVES

3.1 HYPOTHESES

a. Treating kafirin microparticles with heat, transglutaminase and glutaraldehyde will change the morphology of the microparticles. These microparticles will be larger and more inert as a result of kafirin protein polymerization. Heat treatment has been shown to result in kafirin polymerization as a result of disulphide cross-linking of kafirin proteins (Emmambux and Taylor, 2009; Duodu et al., 2003). Despite the fact that kafirin has very low lysine content (Belton et al., 2006), in the absence of lysine, transglutaminase catalysed reactions should proceed through deamidation, which is a secondary reaction pathway, where kafirin glutamine in converted to glutamic acid (Yokoyama et al., 2004). Glutaraldehyde cross-linking occurs through the formation of non-disulphide bonding between the carbonyl groups (C═O) of the aldehyde and free amino groups ($-NH_2$) of the protein amino acid (Farris, Song and Huang, 2010).

b. Modification of kafirin microparticles by heat, transglutaminase and glutaraldehyde will result in an improvement in the quality of products prepared from kafirin microparticles such as bioplastic films and delivery devices for bioactive compounds. This is because of kafirin protein polymerization. It has been shown that protein polymerization by heat, transglutaminase or glutaraldehyde slows down the rate of release of bioactive compounds bound by protein microparticles (Prata, Zanin, Ré and Grosso, 2008) and improves protein film water stability and related properties (Byaruhanga, Erasmus and Taylor, 2005; Chambi and Grosso, 2006; Sessa, Mohamed, Byars, Hamaker and Selling, 2007), probably as result of increase in the protein hydrophobicity (Reddy, Tan, Li and Yang, 2008). By slowing down rate of release of bound bioactive compounds as result of increased kafirin hydrophobicity, the kafirin microparticle-bioactive system will be more efficacious. The efficacy of a bioactive compound is achieved by maintaining its concentration at the target site for a sufficient period of time (Bessa, Casal and Reis, 2008).

c. The kafirin microparticle-bioactive compound complex will be a safe biomaterial system as kafirin is non-allergenic (Ciacci, Maiuri, Caporaso, Bucci, Del Giudice, Massardo, Pontieri, Di Fonzo, Bean, Ioerger and Londei, 2007) due to the fact that it does not contain any of the protein amino acid sequences known to be toxic to coeliacs (reviewed

by Wieser and Koehler, 2008). As explained by these authors, protein toxicity is associated with repeating amino acid sequences such as QPQPFPPQQPYP and (Q) QPQQPFP, which are absent in kafirin proteins.

3.2 OBJECTIVES

The overall objective of this study is to improve the quality of kafirin microparticles in order to expand their potential application.

Specific objectives:

1. To determine the effects of modification with heat, transglutaminase and glutaraldehyde on the functionality of kafirin microparticles with respect to their size, structure and chemical properties.
2. To determine the effects of modification of kafirin microparticles on the quality of products prepared from them such as bioplastic films and binding devices for bioactive molecules such as bone morphogenetic proteins (BMPs).

To establish the safety, biodegradability and efficacy of kafirin microparticle-bioactive system.

4 RESEARCH

CHAPTER 1

4.1 PHYSICO-CHEMICAL MODIFICATION OF KAFIRIN MICROPARTICLES FOR APPLICATION AS A BIOMATERIAL

4.1.1 Abstract

Vacuolated spherical kafirin microparticles, mean diameter 5 µm, can be formed by self-assembly from an acidic solution with water addition. Three-dimensional scaffolds for hard tissue repair require large microstructures (e.g. particle size 80–200 µm for injectable dental implants) with a high degree of interconnected porosity. Heat, transglutaminase and glutaraldehyde cross-linking treatments were investigated to modify the properties of kafirin microparticles to enhance their potential application. The microparticles treated with heat or glutaraldehyde during their formation were only slightly larger than the control, with the glutaraldehyde-formed microparticles being fairly uniform in size, whereas-the heat formed microparticles were less homogeneous. In terms of appearance, the heat- and glutaraldehyde-formed microparticles differed from the untreated control in that they had smooth surfaces and fewer internal vacuoles. Cross-linking the formed kafirin microparticles using wet heat or glutaraldehyde treatment resulted in larger microparticles (approx. 20 µm), which whilst similar in size and external morphology, were apparently formed by further assisted-assembly by two substantially different mechanisms. In addition, heat treatment increased vacuole size. In contrast, transglutaminase treatment had little effect on the size of individual microparticles but resulted in agglomeration of kafirin microparticles into large lumps. Heat treatment involved kafirin polymerization by disulphide bonding with the microparticles being formed from round, coalesced nanostructures, as shown by AFM. Kafirin polymerization of glutaraldehyde-treated microparticles was not by disulphide bonding and the nanostructures, as revealed by AFM, were spindle-shaped. Thus, kafirin microparticles, particularly modified with heat or glutaraldehyde, have potential as natural, non-animal protein scaffolds.

4.1.2 Introduction

Cereal prolamin proteins such as zein and kafirin can be self-assembled into nano- and micro-particles (Muthuselvi and Dhathathreyan, 2006; Taylor et al., 2009a). These particles have potential applications as delivery systems for drugs (Muthuselvi and Dhathathreyan, 2006), nutraceuticals (Patel, Hu, Tiwari and Velikov, 2010; Taylor et al., 2009b), antimicrobials (Xiao et al., 2011), essential oils (Parris et al., 2005), as biomaterials in tissue engineering as scaffolds (Gong et al., 2006), and as biomedical coatings for arterial/vascular prostheses (Wang et al., 2005). Zein and kafirin are natural, plant-based, non-allergenic, and slowly biodegradable therefore have some advantages over animal-based biomaterials such as silk and collagen, especially for biomedical applications. Collagen and silk have poor wet strength and bovine collagen has potential immunogenicity and has been reported to transmit diseases such as bovine spongiform encephalopathy (reviewed by Reddy and Yang, 2011).

Wang and Padua (2012) recently described a possible nanoscale mechanism for the self-assembly of zein into various mesostructures. This self-assembly appears to be driven by the amphiphilic nature of the zein protein and occurred when changes were made to the polarity of an aqueous ethanol solution of zein by evaporation. An earlier paper by the same workers indicated that, at larger scale, the zein self-assembly is by layering onto a central core (Wang and Padua, 2010). They suggested radial growth occurred by hydrophobic interactions as the solvent became more hydrophilic due to the evaporation of the ethanol.

Kafirin is very similar to zein in amino acid composition but is more hydrophobic, or more strictly speaking less hydrophilic (Belton et al., 2006) and so can be considered amphiphilic in nature. Kafirin microparticles can be made by a process that is almost opposite to that used by Wang and Padua et al. (2010, 2012). Instead of dissolving the protein in aqueous ethanol and increasing the polarity of the solution by evaporation of the ethanol, the kafirin is dissolved in a primary solvent, glacial acetic acid, water is then added resulting in the self-assembly of kafirin microparticles (Taylor et al., 2009a). In both cases, there is a change in solvent polarity, causing protein self-assembly as described by Wang and Padua (2010, 2012) for zein.

Comparison of the structure of zein and kafirin microparticles show that the kafirin microparticles are generally larger (1–10 µm, mean diameter of 5 µm) (Taylor et al., 2009a) than zein microparticles (ranges from 0.3–1.7 µm (Muthuselvi and Dhathathreyan, 2006)

when made by similar processes. Kafirin microparticles have a rough surface and internal vacuoles resulting in a large surface area, whereas, zein microparticles are generally smooth and solid (Parris et al., 2005). The vacuoles in the kafirin microparticles are thought to be the footprint of air bubbles incorporated in the very viscous protein solution, which become entrapped within the microparticles as they self-assemble (Taylor et al., 2009a).

Although there is considerable interest in nano-sized particles, some potential biomaterial applications, particularly for three dimensional scaffold type structures for hard tissue repair, require large particles with a high degree of interconnected porosity (Hou, De Bank and Shakesheff, 2004). For example, an injectable dental implant, requires a particle size 80–200 µm (Weiss, Layrolle, Clergeau, Enckel, Pilet, Amouriq, Daculsi and Giumelli, 2007). Cross-linking by physical (Zhang and Zhong, 2009), chemical (Kim, Kang, Krueger, Sen, Holcomb, Chen, Wenke and Yang, 2012) and enzymic (Zhang and Zhong, 2009) methods have been applied to water-soluble protein nano- and micro-particles, such as whey protein (Zhang and Zhong, 2009) and gelatin (Kim et al., 2012), to increase water resistance and reduce swelling. However, there has been little research on cross-linking of prolamin protein microparticles, probably because the proteins are relatively hydrophobic (Belton et al., 2006).

The main objectives of this research were to determine whether cross-linking could increase the size of kafirin microparticles to improve their potential utility as biomaterial scaffolds and to attempt to understand the underlying mechanism involved.

4.1.3 Materials and methods

4.1.3.1 *Materials*

A mixture of two similar white, tan-plant non-tannin sorghum cultivars PANNAR PEX 202 and 606, was used. Whole grain sorghum was milled using a laboratory hammer mill (Falling Number 3100, Huddinge, Sweden) fitted with a 500 µm opening screen. An analytical grade 25% glutaraldehyde solution (Saarchem, Krugersdorp, South Africa) was used. Microbial transglutaminase (Activa® WM), activity 100 U/g was kindly donated by Ajinamoto Co., Paris, France.

4.1.3.2 *Extraction of kafirin*

Kafirin was extracted from whole sorghum flour according to method of Emmambux and Taylor (2003). Briefly, milled sorghum was mixed with 70% (w/w) aqueous ethanol containing 5% sodium hydroxide (w/w) and 3.5% sodium metabisulphite (w/w) at 70^{o}C for 1 h with vigorous stirring. The clear supernatant was recovered by centrifugation and the ethanol evaporated. Kafirin was precipitated by adjusting the pH of the protein suspension to 5. The precipitated kafirin was recovered by filtration under vacuum, freeze-dried, defatted with hexane at ambient temperature and air-dried. The protein contents of defatted air-dried kafirin extracts was 84% (N × 6.25, dry matter basis) determined by Dumas nitrogen combustion method (AACC International, 2000) Method 46-30.

4.1.3.3 *Preparation of kafirin microparticles*

These were prepared essentially according to Taylor et al. (2009a), which is a simple coacervation in which microparticles are expelled from a solution of kafirin in glacial acetic acid. Some modification was made. After dissolution of the kafirin in glacial acetic acid and equilibration of the kafirin solution, distilled water was added at rate of 1.4 mL/min using a Watson-Marlow Bredel peristaltic pump (Falmouth, England) while mixing using a magnetic stirrer at 600 rpm to form kafirin microparticle suspension. The kafirin microparticle suspension contained 2% kafirin protein and 5.4% acetic acid and pH 2.0. For microparticles intended for analysis in dry form, the acetic acid was removed by washing three times with distilled water by centrifugation at 3150 *g*, then the pellets freeze-dried before storage at 10^{o}C.

4.1.3.4 *Treating kafirin microparticles*

Heat or glutaraldehyde treatment during microparticle formation

Hot distilled water (96^{o}C) or a solution of 6.85% (w/w) glutaraldehyde was added to the solution of kafirin in glacial acetic acid (24% w/w) using a peristaltic pump at the rate of 1.4 mL/h, while stirring, to give a final kafirin concentration of 2% (w/w) in 0.9 M acetic acid. The final temperature of the heat treatment was approximately 75^{o}C and the final glutaraldehyde concentration was 75% (w/w) (protein basis). Lower glutaraldehyde concentrations did not increase kafirin microparticle size (data not shown).

Wet heat treatment of kafirin microparticles

A kafirin microparticle suspension was prepared and washed free of acetic acid, as described above. The resultant pellet was re-suspended in 91% (w/w) water. Wet heat treatment was carried out by heating the kafirin microparticle suspensions at 50°C, 75°C and 96°C for 1 h. A control sample was maintained at 22°C.

Glutaraldehyde treatment of kafirin microparticles

Kafirin microparticle suspensions were prepared as described above. Glutaraldehyde was added to 4.0 g kafirin microparticle suspensions containing 2% protein (w/w) in 0.9 M acetic acid (pH 2.0), resulting in final glutaraldehyde concentrations of 0%, 10%, 20%, and 30% (w/w) on protein basis. Samples were then vortex-mixed and held at 22°C for 12 h.

Transglutaminase treatment of kafirin microparticles

Kafirin microparticle suspensions (4.0 g) were weighed in plastic centrifuge tubes. The acetic acid was washed off with distilled water as described. The supernatant was discarded while the wet kafirin microparticle pellet was retained. A working transglutaminase enzyme solution was prepared by mixing 25% Activa® WM, enzyme activity 100 U/g, in a 0.02 M Tris-HCl buffer (pH 7.0), preheated to 50°C. Transglutaminase enzyme (0.1%, 0.3% and 0.6% w/w on protein basis), was added to the wet kafirin microparticle pellets and the total mass made up to the original 4.0 g using the preheated 0.02 M Tris-HCl buffer. Pure maltodextrin (1%) solution in the buffer was used as a control. The target transglutaminase/protein (kafirin) ratio (mg/g) was 0 (control), 1, 3, and 6, which was based on work by Bruno, Giancone, Torrieri, Masi and Moresi (2008). Transglutaminase reaction was carried out at 30°C for 12 h after which the supernatants were removed and pellets washed with distilled water as described.

4.1.3.5 *SDS-PAGE*

Kafirin microparticles were characterised by SDS-PAGE under reducing and non-reducing conditions. An XCell SureLock™ Mini-Cell electrophoresis unit (Invitrogen Life Technologies, Carlsbad, CA) was used with 15-well 1 mm thick pre-prepared Invitrogen NuPAGE® 4-12% Bis-Tris gradient gels. The protein loading was ≈10 µg. Invitrogen

Mark12™ Unstained Standard was used. Proteins were stained with Coomassie® Brilliant Blue R250 overnight and then destained.

4.1.3.6 *Microscopy*

Light microscopy

Kafirin microparticle suspensions were viewed and photographed using a Nikon Optiphot light microscope (Kanagawa, Japan).

Electron microscopy

Suspensions of kafirin microparticles were prepared for SEM and TEM according Taylor et al. (2009a). Briefly, the liquid fraction of the microparticle suspension was removed and the microparticles fixed with glutaraldehyde before staining with osmium tetraoxide. Then the samples were dehydrated sequentially in different concentrations of acetone. SEM preparations were mounted on an aluminium stub using a double-sided carbon tape, sputter-coated with gold and viewed using a Jeol JSM-840 Scanning Electron Microscope (Tokyo, Japan). TEM preparations were infiltrated with Quetol resin and polymerized at 60^{o}C. Sections were cut using a microtome, stained in ural acetate and lead citrate and viewed with a Jeol JEM-2100F Field Emission Electron Microscope (Tokyo, Japan).

AFM

Freeze-dried kafirin microparticles were embedded on the surface of aluminium stubs. Then the microparticles were viewed with a Veeco Icon Dimension Atomic Force Microscope (Bruker, Cambridge, U.K.) using tapping-in-air mode. A silicon tip on nitride lever cantilever, tip size 8 nm was used. To determine the mechanical properties of the kafirin microparticles, the kafirin microparticles were embedded on a glass slide using custom-made glue. Then the mechanical properties of the microparticles were determined using Quantitative NanoMechanics (QNM) mode with the following parameter settings: Scan size 1 µm, Scan rate 0.500 Hz, Deflection sensitivity 80.2 nm/V, Deformation sensitivity 507 nm/V, and 256 scans per line. A silicon tip on nitride lever cantilever, tip size 9 nm with a spring constant 4.461 N/m was used. Force-deformation curves were generated and slopes calculated from the linear portions of these curves.

4.1.3.7 *Determination of size of the kafirin microparticles*

Microparticle size was determined by comparing their images with that of a scale bar of the same magnification. For each treatment, duplicate measurements were made each with at least 100 microparticles.

4.1.3.8 *In vitro protein digestibility (IVPD)*

An IVPD assay was performed on freeze-dried kafirin microparticles using a micro-scale pepsin digestion protocol described by Taylor and Taylor (2002), which is a modified procedure of Hamaker, Kirleis, Mertz and Axtell (1986). Accurately weighed samples (10 mg) were digested with a P7000-100G pepsin (Sigma, Johannesburg, South Africa), activity 863 units/mg protein for 2 h at 37^{o}C and the products of the digestion were pippeted off. The residue was washed with distilled water and dried at 100^{o}C overnight. The residual protein was determined by Dumas nitrogen combustion method (AACC International, 2000) method 46-30. IVPD was calculated by the difference between the total protein and the residual protein after pepsin digestion divided by the total protein and expressed as a percentage.

4.1.3.9 *FTIR spectroscopy*

FTIR spectroscopy was done as described by Taylor et al. (2009a). Freeze-dried microparticles were scanned using a Vertex 70v FT-IR spectrometer (Bruker Optik, Ettlingen, Germany), using 64 scans, 8 cm^{-1} band and an interval of 1 cm^{-1} in the Attenuated Total Reflectance (ATR) mode at wavenumber 600–4000 cm^{-1}. At least four replicates were performed for each treatment. The FTIR spectra were Fourier-deconvoluted with a resolution enhancement factor of 2 and 12 cm^{-1} bandwidth. The proportions of the α-helical conformations (≈1650 cm^{-1}) and the β-sheet structures (≈1620 cm^{-1}) were calculated by measuring the heights of the peaks assigned to these secondary structures on the FTIR spectra. The relative proportion of α-helical conformations was calculated thus:

$$\%\ \text{of α-helical conformation} = \frac{\text{Abs α-helix peak}}{\text{Abs α-helix peak} + \text{Abs β-sheet peak}} \times 100$$

Where:

Abs α-helix peak = Absorbance at ≈1650 cm^{-1} after baseline correction
Abs β-sheet peak = Absorbance at ≈1620 cm^{-1} after baseline correction

4.1.3.10 *Statistical analyses*

The IVPD and FTIR data as well as the data on mechanical properties of the kafirin microparticles were analysed by one-way analysis of variance (ANOVA). These measured parameters were the dependent variables while and heat, transglutaminase and glutaraldehyde treatments were the independent variables. All the experiments were repeated at least once. The mean differences assessed by Fischer's Least Significant Difference (LSD) test. The calculations were performed using Statistica software version 10 (StatSoft, Tulsa, OK).

4.1.4 Results and discussion

4.1.4.1 *Morphology and size distribution of treated kafirin microparticles*

Heat and glutaraldehyde treatments during microparticle preparation

Kafirin microparticles prepared at ambient temperature (22°C) were spherical, between 1 and 10 µm in diameter, with pores (vacuoles) between 0.5 and 2 µm (Figure 4.1), as reported previously (Taylor et al. 2009a). The majority of the microparticles were between 1 and 5 µm (Figure 4.2). The microparticles treated with heat or glutaraldehyde during their formation were only slightly larger than the control, with the glutaraldehyde-formed microparticles being fairly uniform in size, whereas the heat formed microparticles were less homogeneous. In terms of appearance, the heat- and glutaraldehyde-formed microparticles differed from the untreated control in that they had smooth surfaces and fewer internal vacuoles. Since the aim of the study was to substantially increase the size of the microparticles, the approach of cross-linking after the self-assembly process was investigated.

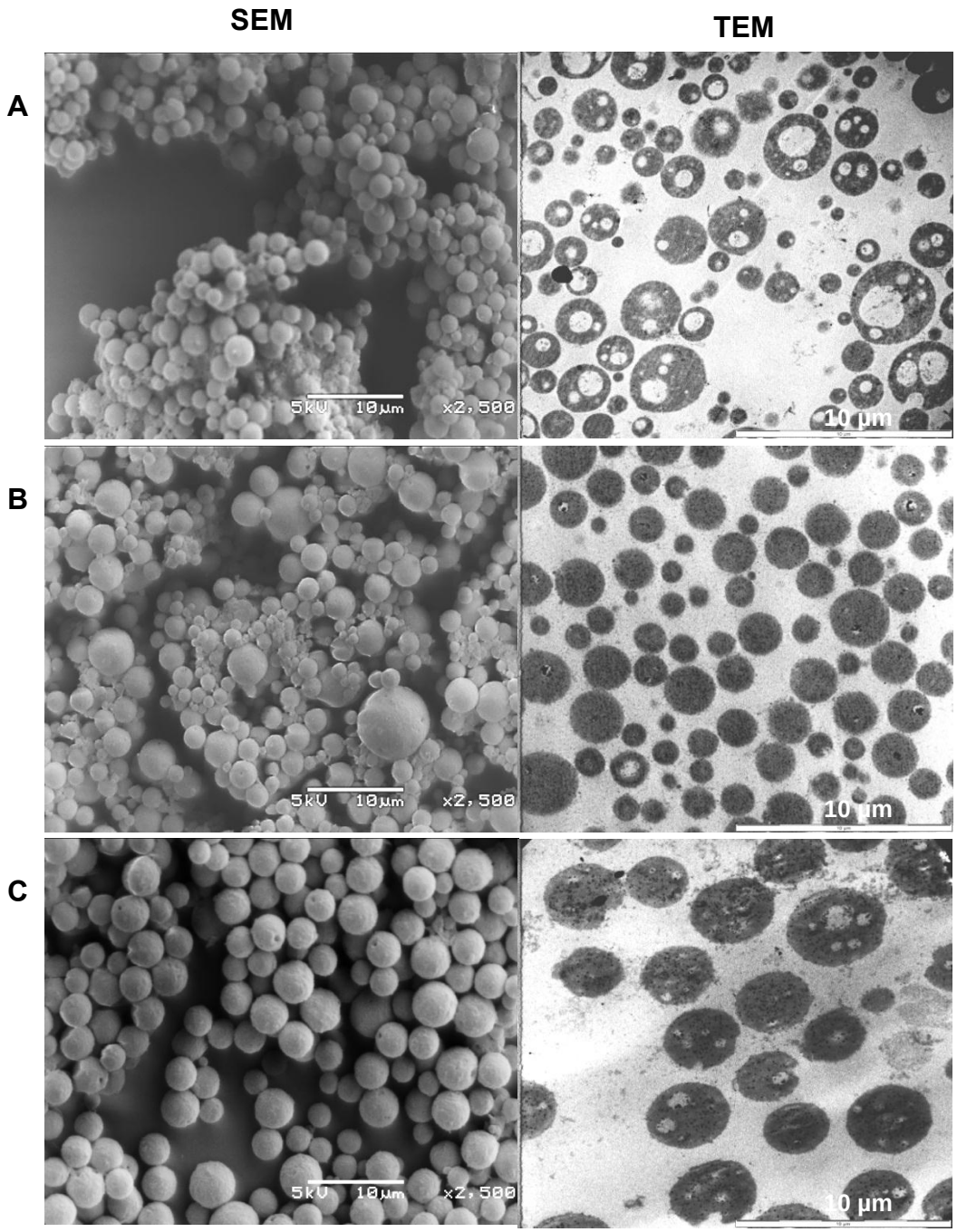

Figure 4.1 Electron microscopy of kafirin microparticles treated during preparation (formation). **A.** Control. **B.** Heat treatment. **C.** Glutaraldehyde treatment.

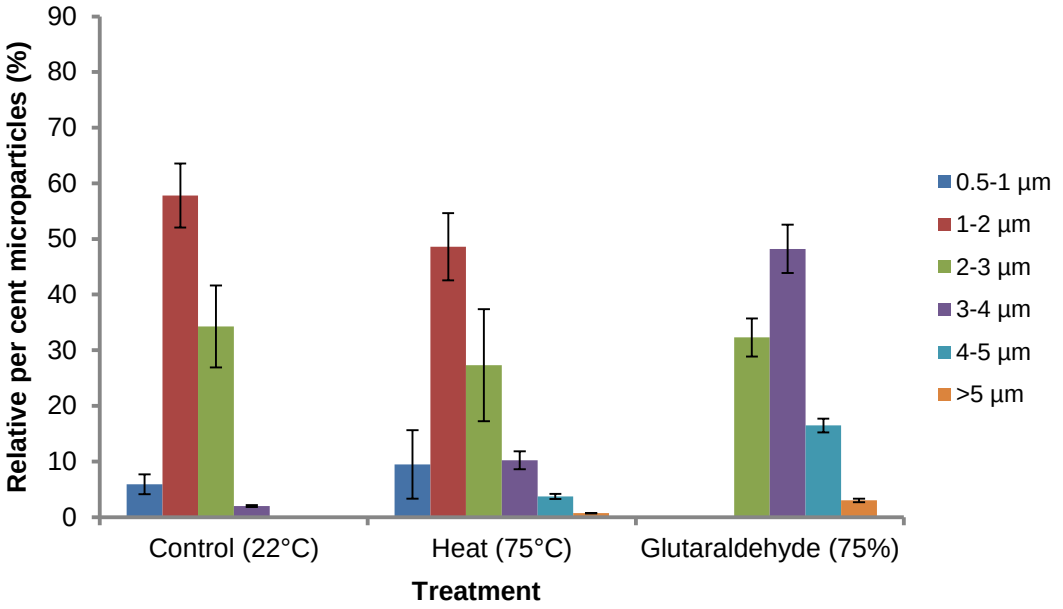

Figure 4.2 Particle size distribution of kafirin microparticles treated with heat and glutaraldehyde during microparticle formation. Error bars are standard deviations for two replicate measurements each of at least 100 particles.

Treatment following microparticle preparation

Wet heat treatment following the microparticle self-assembly changed the shape of the larger kafirin microparticles to oval and increased their average size to ≈20 µm thereby skewing the microparticle size distribution (Figure 4.3). Particle size increased with increasing severity of the heat treatment up to 75°C, after which there was no further increase in microparticle size with increased temperature. Vacuoles within the heat-treated kafirin microparticles showed a >10-fold increase in size compared to the control to a maximum of about 17 µm. The increase in vacuole size with heat treatment was probably due to greater expansion of air with higher temperature within the microparticles, since the vacuoles are probably footprints of air bubbles (Taylor et al., 2009a). The relative proportion of microparticles of size >20 µm increased by up to about 40% with increase in temperature up to 75^{o}C (Figure 4.4). Increasing the temperature to 96^{o}C did not increase further the microparticle size. The oval shape of the larger heat-treated microparticles was probably due to the rate of particle coalescence being inversely proportional to particle size, as proposed by Lehtinen and Zachariah (2001), who studied the effect of coalescence energy release on the temporal shape evolution of nanoparticles.

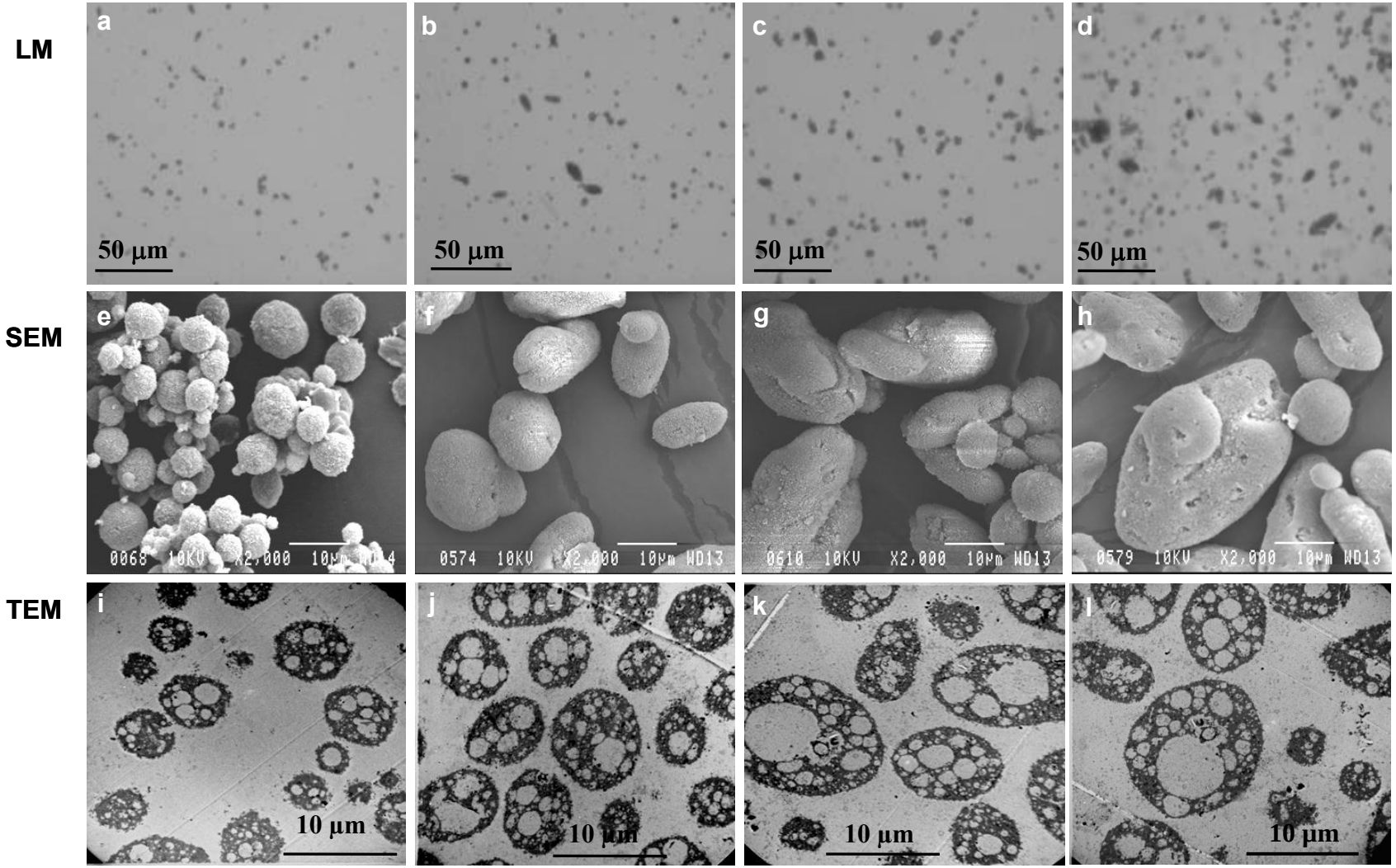

Figure 4.3 Microscopy of heat-treated kafirin microparticles. **a, e, i**- Control (22°C); **b, f, j** - 50°C; **c, g, k** - 75°C; **d, h, i**- 96°C. LM – Light microscopy; SEM – Scanning electron microscopy; TEM – Transmission electron microscopy.

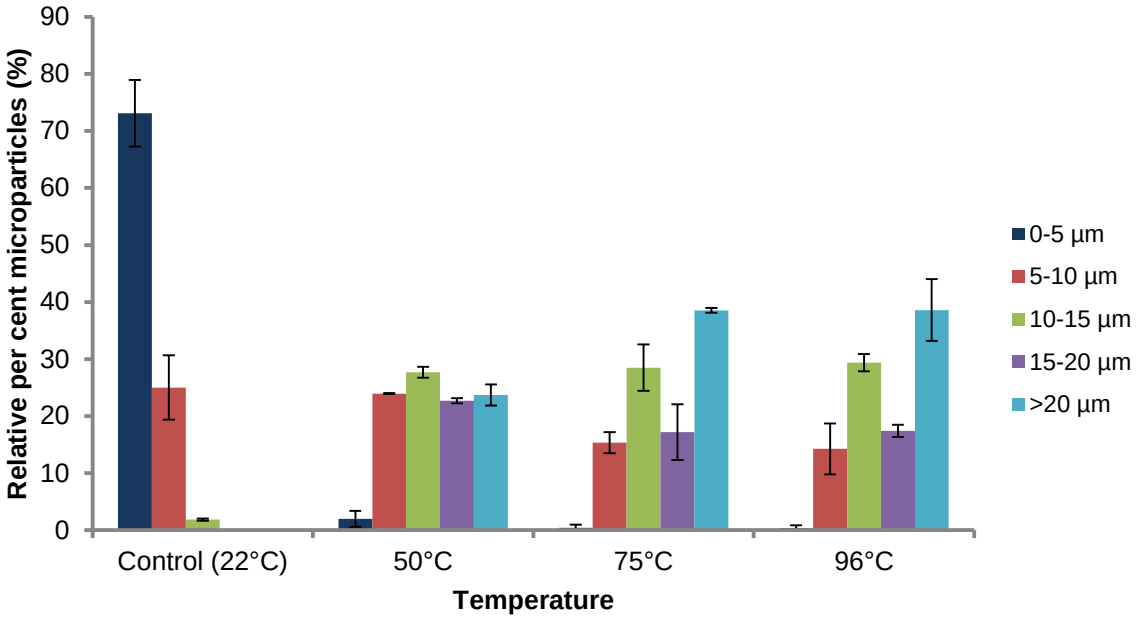

Figure 4.4 Particle size distribution of heat-treated kafirin microparticles. Error bars are standard deviations for two replicate measurements each of at least 150 particles.

Transglutaminase treatment resulted in formation of large masses (>200 µm across) of agglomerated kafirin microparticles (Figure 4.5). Evidence of kafirin microparticle agglomeration was also shown by increase in volume of kafirin microparticle sediments with transglutaminase treatment (Figure 4.6). Agglomerated particles would probably exhibit a loose packing characteristic as more interstitial spaces would not be filled, thereby resulting into particles occupying a large volume. However, individual transglutaminase-treated kafirin microparticles were round-shaped; most of them were of size 5–10 µm (Figure 4.7). Even with the higher level of transglutaminase treatment (0.6% transglutaminase), only a small proportion of microparticles (about 4%) was >20 µm in size. The fact that kafirin essentially contains no lysine (Belton et al., 2006) may have inhibited transglutaminase catalysed cross-linking through the ε-(-glutamyl)-lysine bonding mechanism (Motoki and Seguro, 1998), thereby causing the small increase in particle size. Unlike with heat treatment, the vacuole size did not change with transglutaminase treatment, probably because the reaction temperature was low (30°C), hence no air expansion. Much larger particle sizes have been reported with other proteins. For example Gan, Cheng and Easa (2008) working with SPI treated with transglutaminase at 1.0 U/g protein reported up to 280 µm microcapsule size, probably because SPI is rich in lysine.

Glutaraldehyde treatment following the self-assembly increased the microparticle size (Figure 4.8).

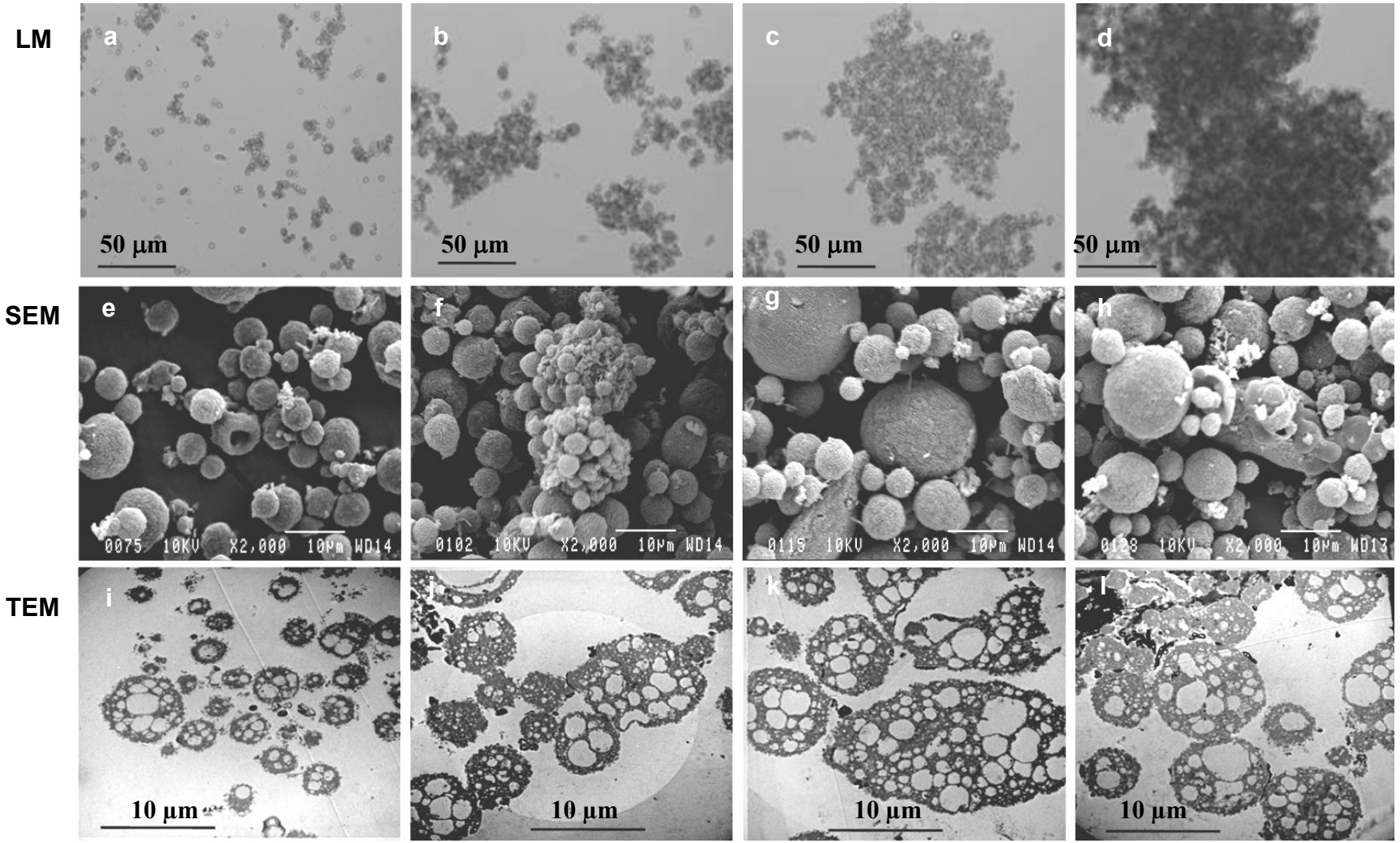

Figure 4.5 Microscopy of transglutaminase (TG)-treated kafirin microparticles. **a, e, i** - Maltodextrin (control); **b, f, j** - 0.1% TG + Maltodextrin; **c, g, k** - 0.3% TG + Maltodextrin; **d, h, i**- 0.6% TG + Maltodextrin. LM – Light microscopy; SEM – Scanning electron microscopy; TEM – Transmission electron microscopy.

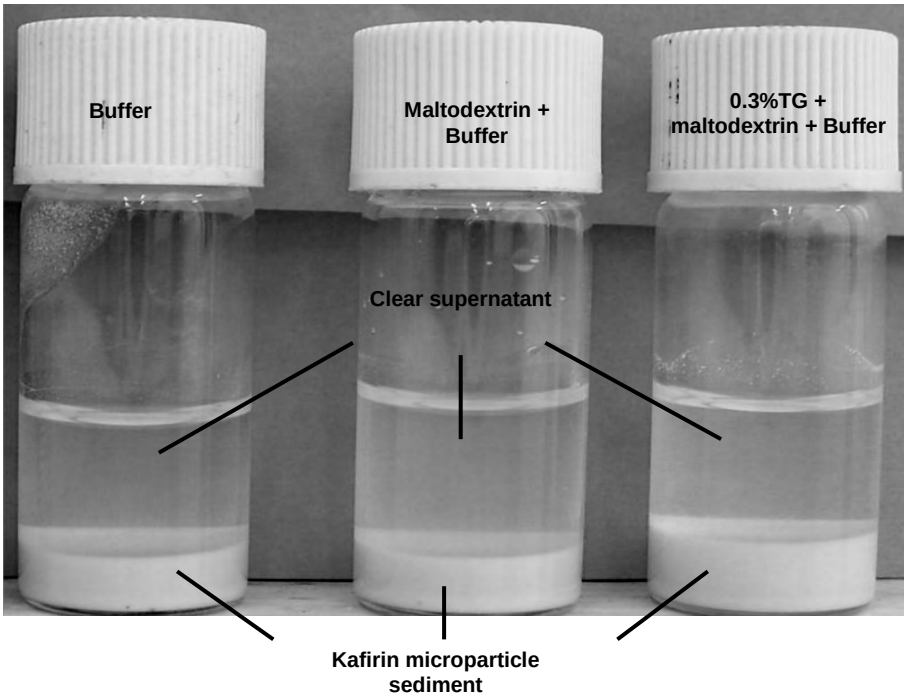

Figure 4.6 Photograph showing the volume of kafirin microparticle sediment after incubation in buffer, maltodextrin and transglutaminase (TG) for 12 h at 30°C. The same amount of microparticles was used in each treatment.

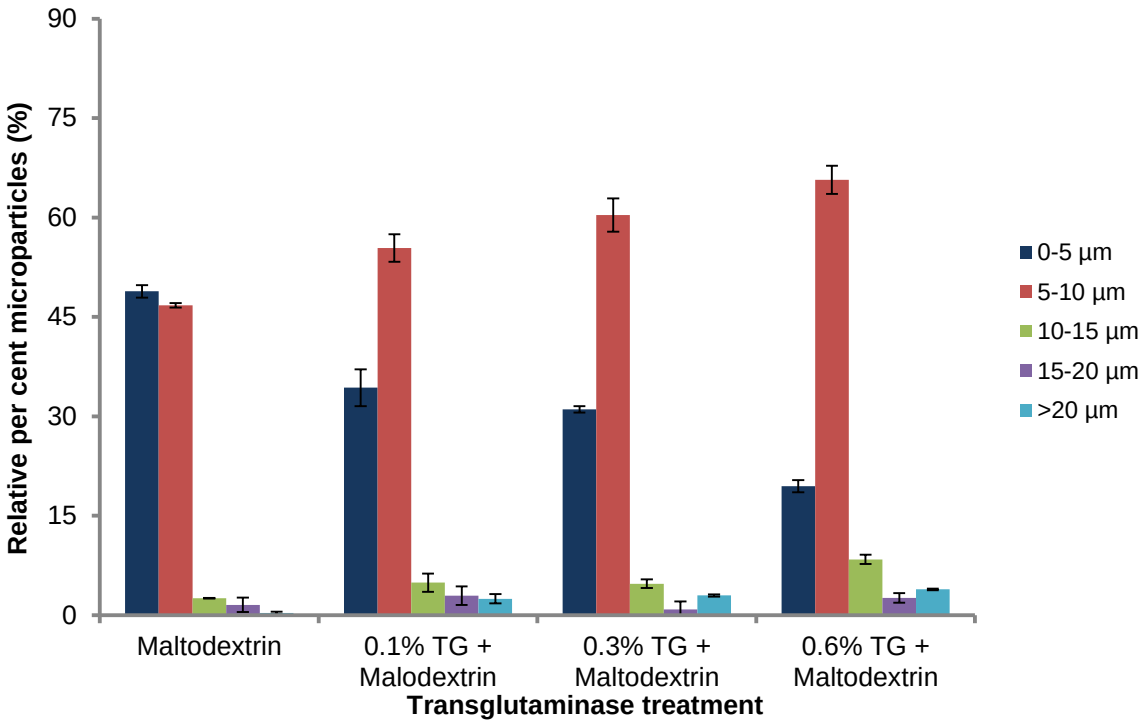

Figure 4.7 Particle size distribution of transglutaminase-treated kafirin microparticles. Error bars are standard deviations for two replicate measurements each of at least 100 particles.

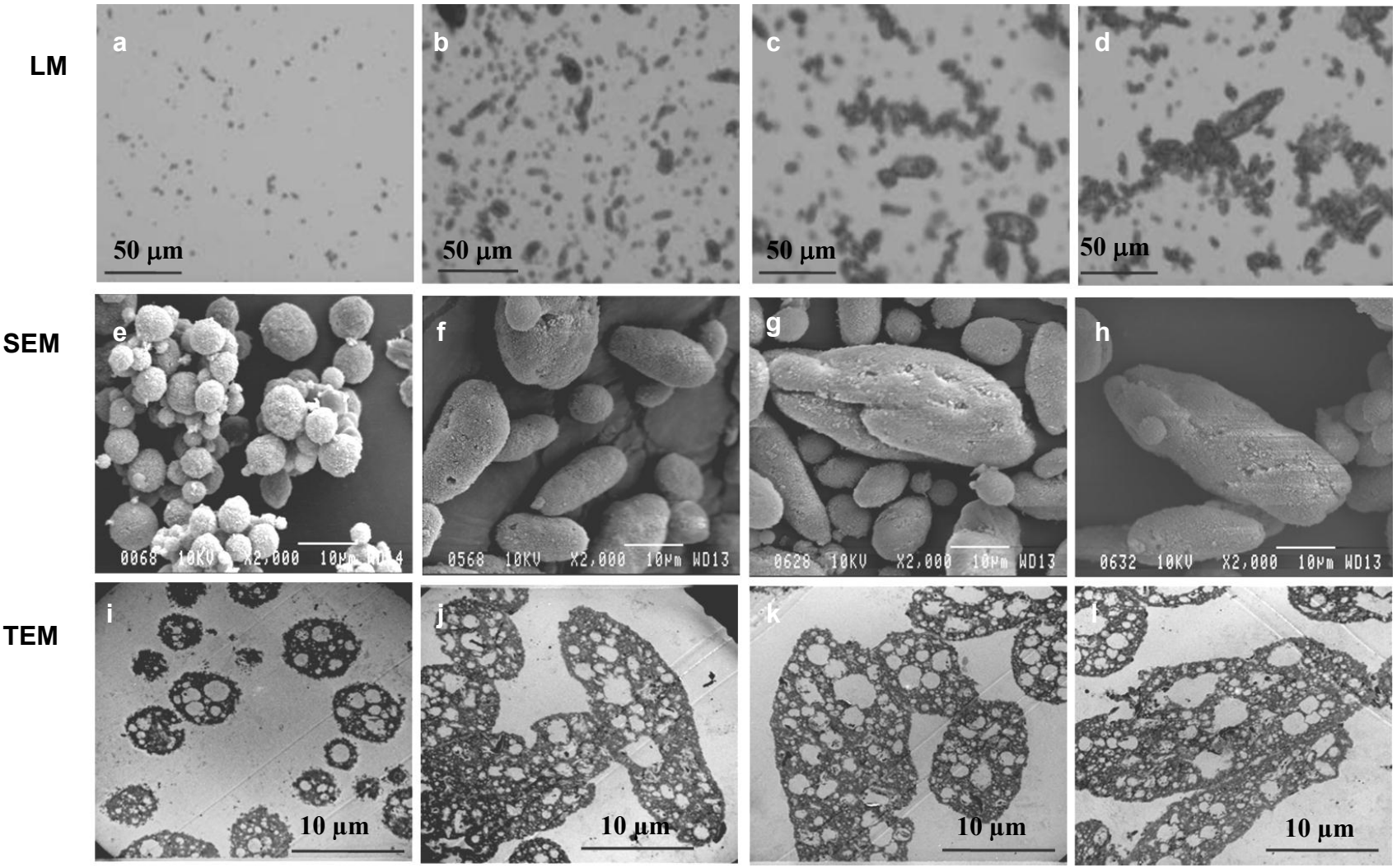

Figure 4.8 Microscopy of glutaraldehyde (GTA)-treated kafirin microparticles. . **a, e, i** - Control; **b, f, j** - 10% GTA; **c, g, k** - 20% GTA; **d, h, i** -30% GTA. LM – Light microscopy; SEM – Scanning electron microscopy; TEM – Transmission electron microscopy.

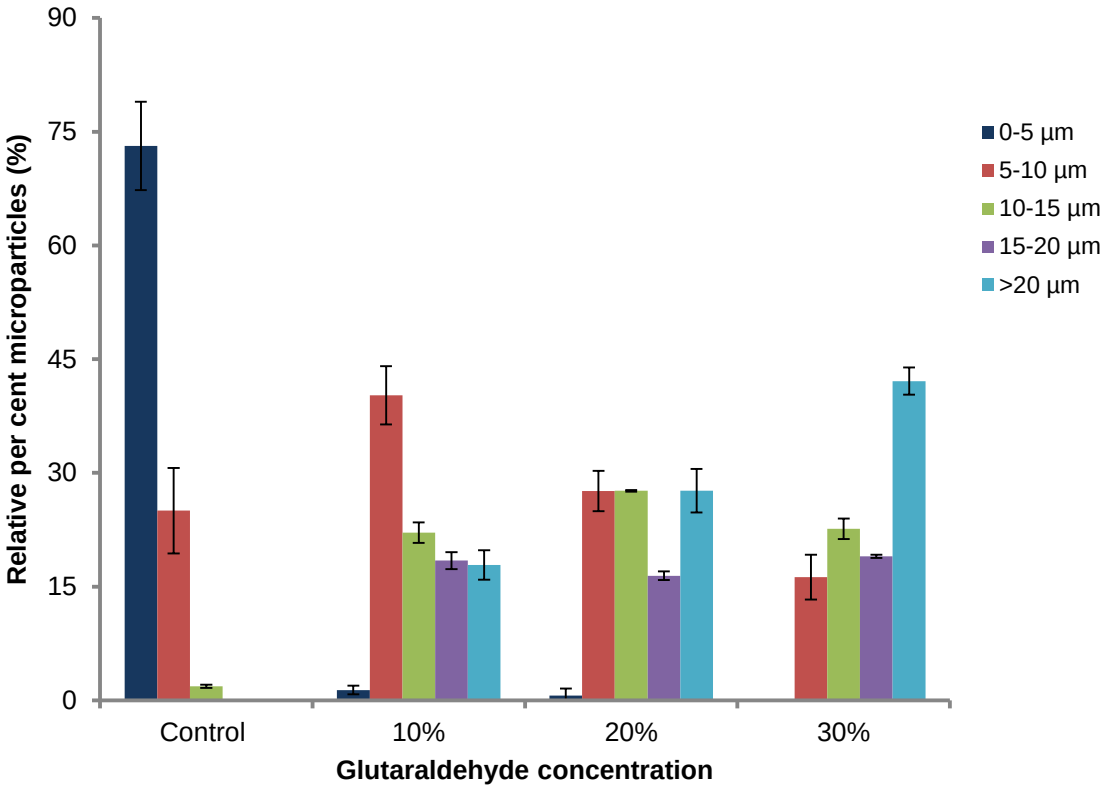

Figure 4.9 Particle size distribution of glutaraldehyde-treated kafirin microparticles. Error bars are standard deviations for two replicate measurements each of at least 100 particles.

As with increasing severity of wet heat treatment, the average microparticle size increased with severity of the glutaraldehyde treatment, from 1-5 µm of the control to >20 µm with 30% glutaraldehyde. Ezpeleta, Rache, Gueguen and Orecchioni (1997) reported a similar increase in particle size of vicilin microparticles with glutaraldehyde treatment. The relative proportion of microparticles of size >20 µm was also increased, up to about 45% with 30% glutaraldehyde (Figure 4.9). Glutaraldehyde treatment also resulted in particles that were of more elongated oval shape than heat-treated microparticles. Unlike heat treatment, the size of the vacuoles in the microparticles did not change with glutaraldehyde treatment. This is presumably, because there was no heating involved with the glutaraldehyde treatments therefore the expansion of entrapped air was not possible.

AFM indicated that the kafirin microparticles had a surface characterized by a rough morphology (marked X) (Figure 4.10A-E). Figure 4.10A illustrates the surface of a single control microparticle. More detailed study showed that the microparticle surface was composed of nanosized protuberances. Figure 4.10B shows the surface of a single heat-treated microparticle. In this case, more detailed study showed that nano-sized protuberances

of irregular shape and size (≈50–300 nm) were responsible for the final surface topography. As viewed by SEM (Figures 4.3, 4.5 and 4.8) the morphology is most likely due to non-linear (random) aggregation of the structural units (polypeptides). Similar nanostructure images have been reported with zein nanoparticles precipitated from aqueous ethanol (Xu et al., 2011) and with zein film droplets deposited onto silica (Panchapakesan, Sozer, Dogan, Huang and Kokini, 2012). Non-linear protein aggregation with heat treatment is a generic property of polypeptides (Krebs et al., 2007). As explained by these authors, non-linear protein aggregation is fast and non-specific, which decreases the likelihood of substantial structural rearrangements during the aggregation process. Furthermore, as the non-linear protein aggregation is not specific, there is no directionality to the aggregates, probably resulting in the round shapes. AFM of transglutaminase treated microparticles showed similar morphology as with heat treatment **(**Figure 4.10D).

On the contrary, with glutaraldehyde treatment, the presumed kafirin nanostructures were spindle-shaped with a unidirectional orientation, probably due to linear glutaraldehyde-protein linkage, as discussed (Figure 4.10E**)**. These nanostructures were ≈100–350 nm long and ≈20–100 nm wide (Figure 4.10Ei). The image in Figure 4.10Eii is probably a cross-sectional view of the spindles (represented by circular shapes). No reference to similar shaped protein particle structures visualized by AFM could be found in the literature. The spindle-shape formed with glutaraldehyde treatment suggests a linear polymerization of the kafirin polypeptides during their reaction with glutaraldehyde. This is in agreement with Migneault et al. (2004) who suggested that glutaraldehyde-protein reaction results in a cross-linked structure consisting of a linear aldol-condensed oligomer of glutaraldehyde linked to Schiff base (imine) from the protein. The variation in size of nanostructures viewed by AFM is probably dependent on how homogenous the nanoparticles were in the sites viewed. The nanostructures viewed from rough areas (R, Figure 4.10A-E) had larger diameter compared to those from flat areas (F, Figure 4.10A-E). This was probably because of the broadening phenomenon, where the side of the AFM probe is involved in imaging (reviewed by Shakesheff, Davies, Jackson, Roberts, Tendler, Brown, Watson, Barrett, and Shaw, 1994). The broadening effect is due to tip-sample convolution, which results when the radius of curvature of the tip is similar to, or greater than, the size of the feature that is imaged (reviewed by Shakesheff et al., 1994).

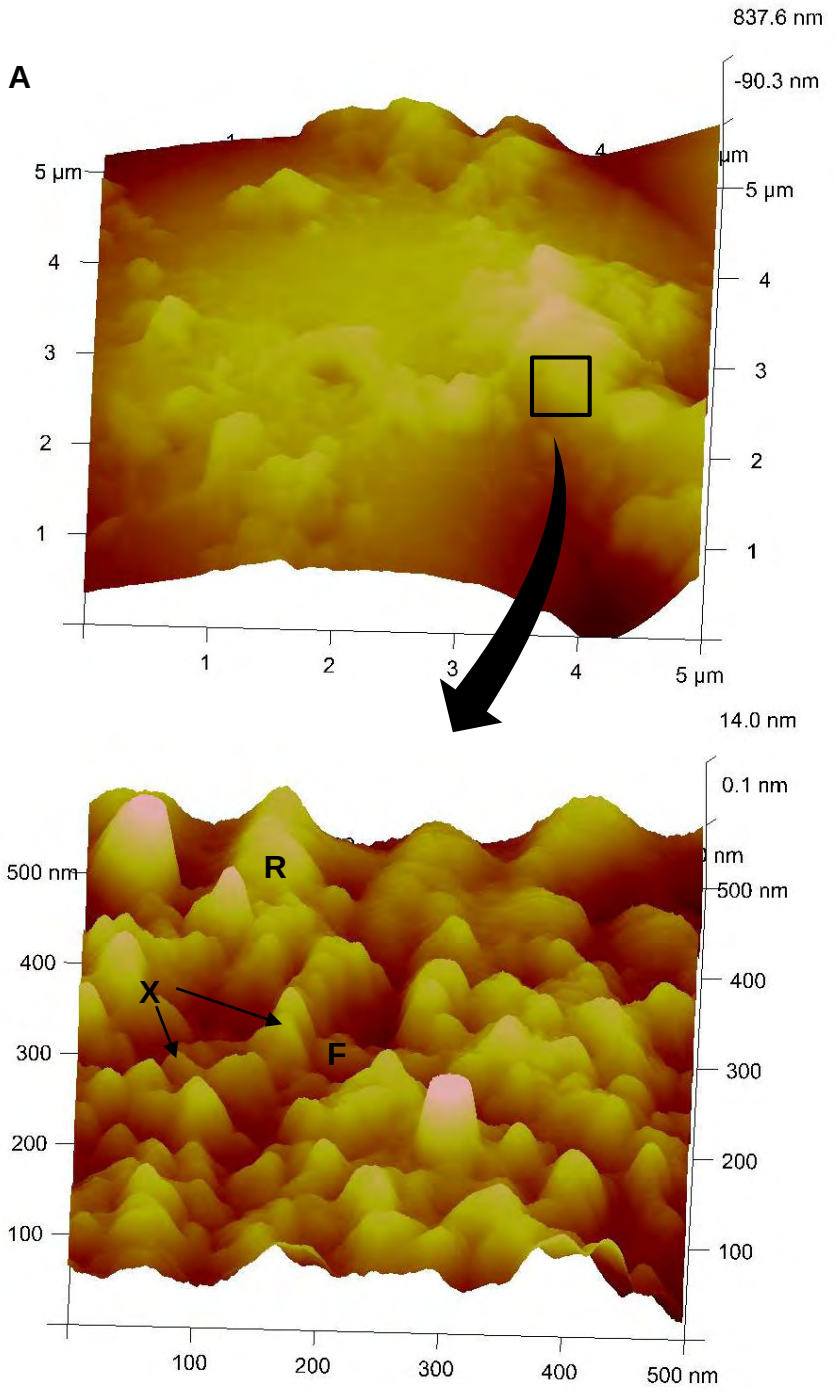

Figure 4.10 AFM topographs of treated kafirin microparticles at two different levels of magnification.

A. Control (22ºC). **B**. Heat treatment (96ºC).

C. Maltodextrin.

D. Transglutaminase treatment (0.6% transglutaminase + maltodextrin).

E. Glutaraldehdye treatment (30%). (**i**) Side view. (**ii**) View from end of nanostructures.

F-flat area, R- rough area. X –nanostructures (nanosized protuberances).

B

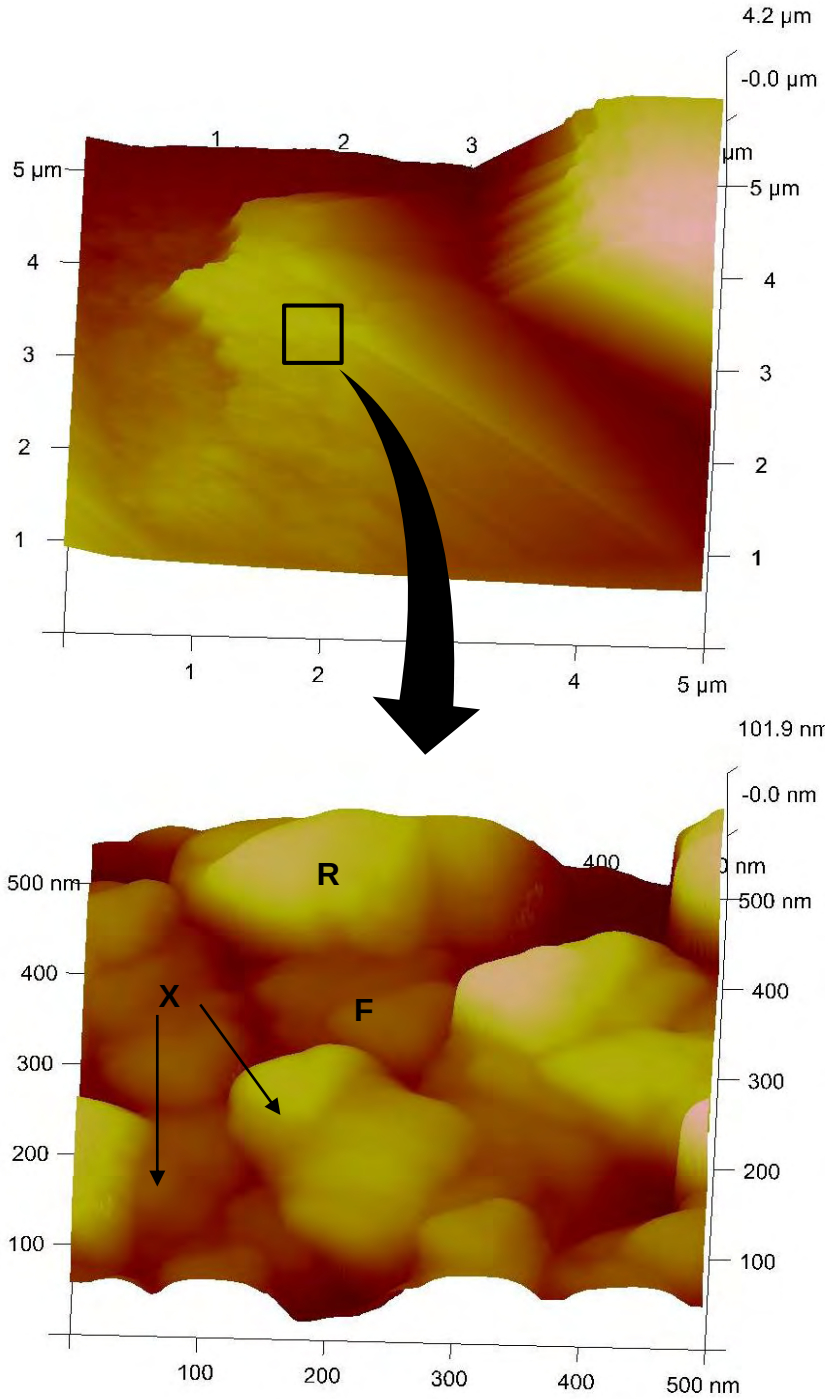
4.2 µm
-0.0 µm
µm
5 µm
4
3
2
1
1
2
3
5 µm
4
3
2
1
1
2
4
5 µm
101.9 nm
-0.0 nm
nm
500 nm
400
300
200
100
R
F
X
400
500 nm
400
300
200
100
100
200
300
400
500 nm

C

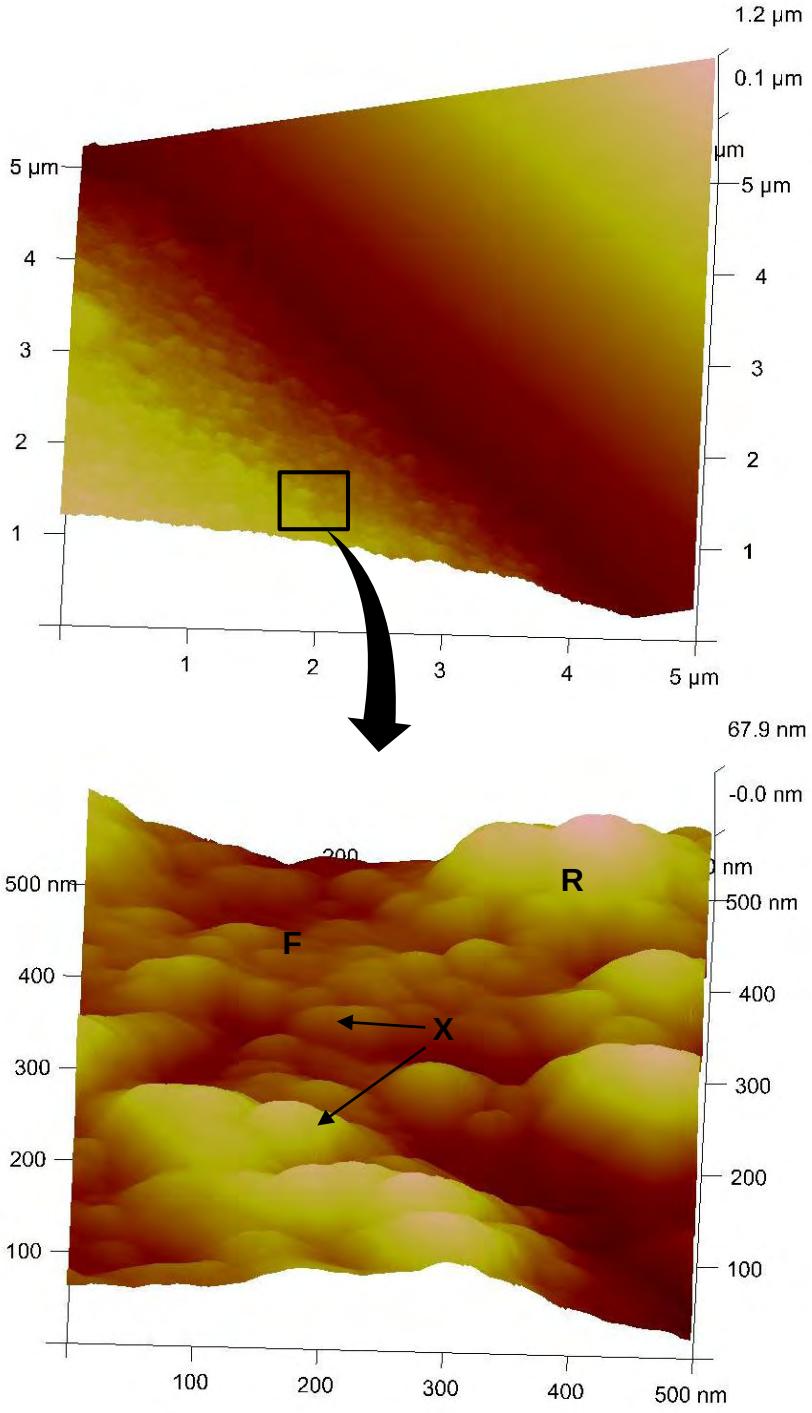
1.2 µm
0.1 µm
µm
5 µm
4
3
2
1
5 µm
4
3
2
1
67.9 nm
-0.0 nm
500 nm
400
300
200
100
R
F
X
500 nm
400
300
200
100

D

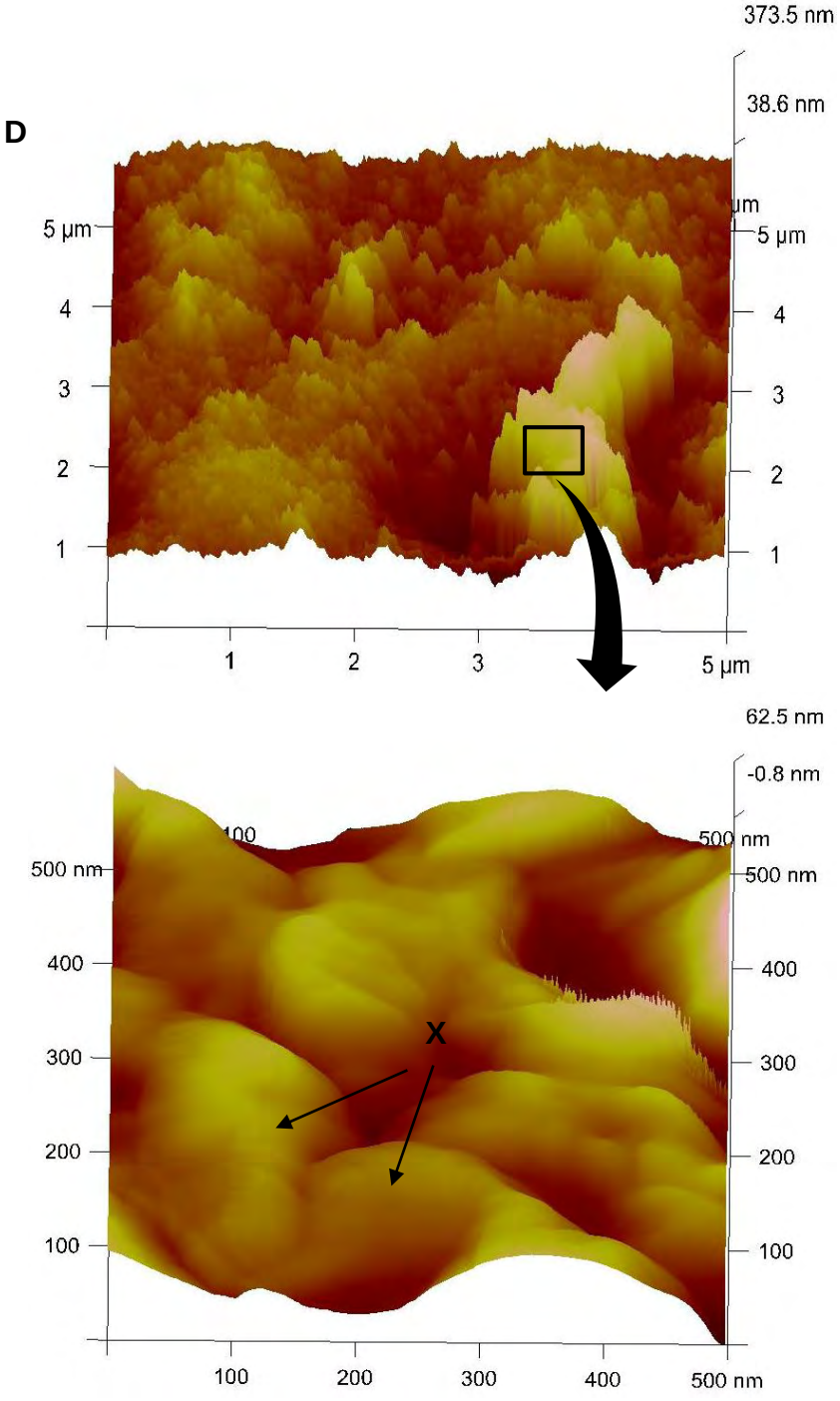
373.5 nm
38.6 nm
5 µm
4
3
2
1
1
2
3
5 µm
62.5 nm
-0.8 nm
500 nm
400
300
200
100
X
100
200
300
400
500 nm

E (i)

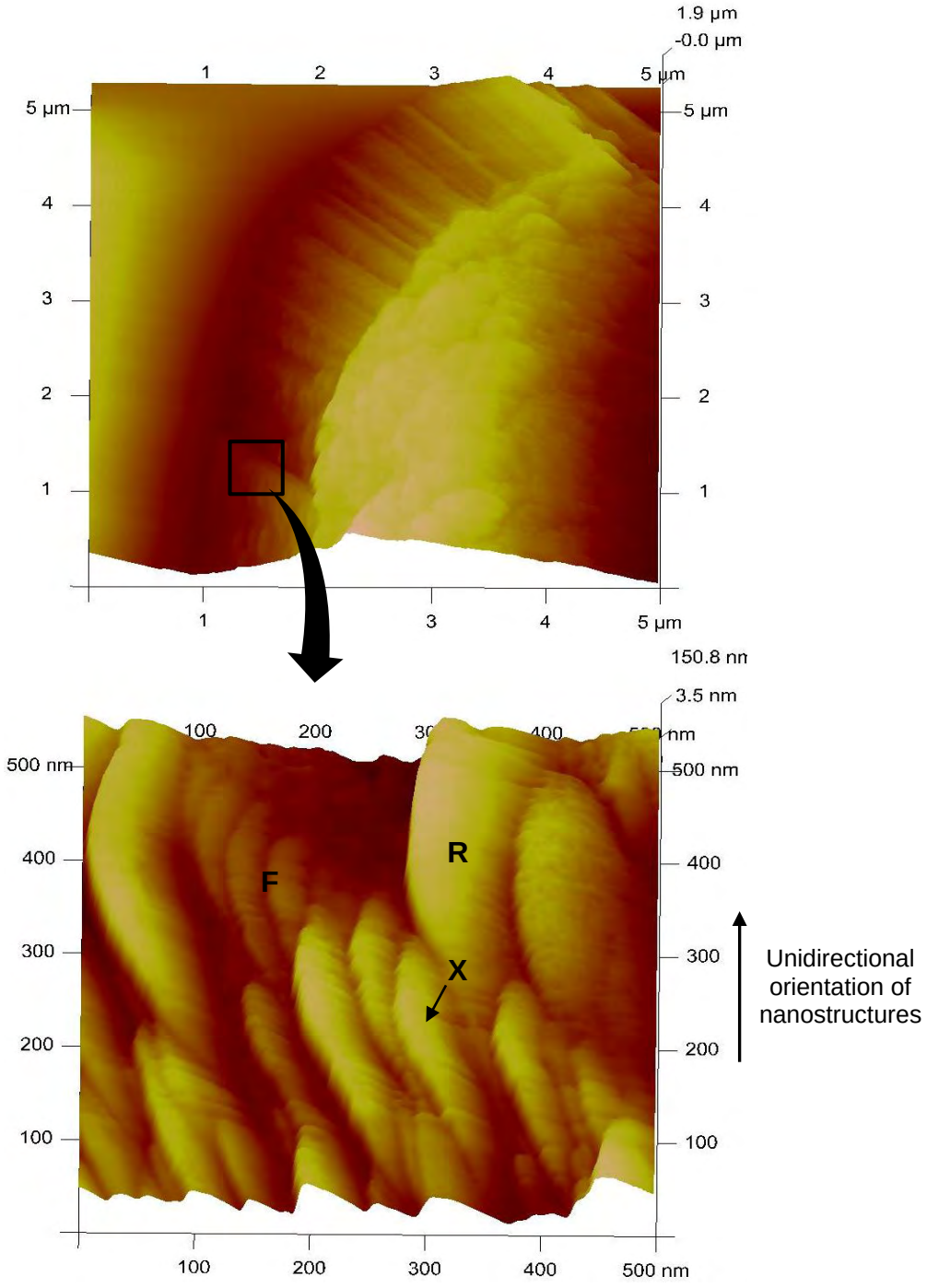
1.9 µm
-0.0 µm
5 µm
150.8 nm
3.5 nm
500 nm
R
F
X
Unidirectional orientation of nanostructures

E (ii)

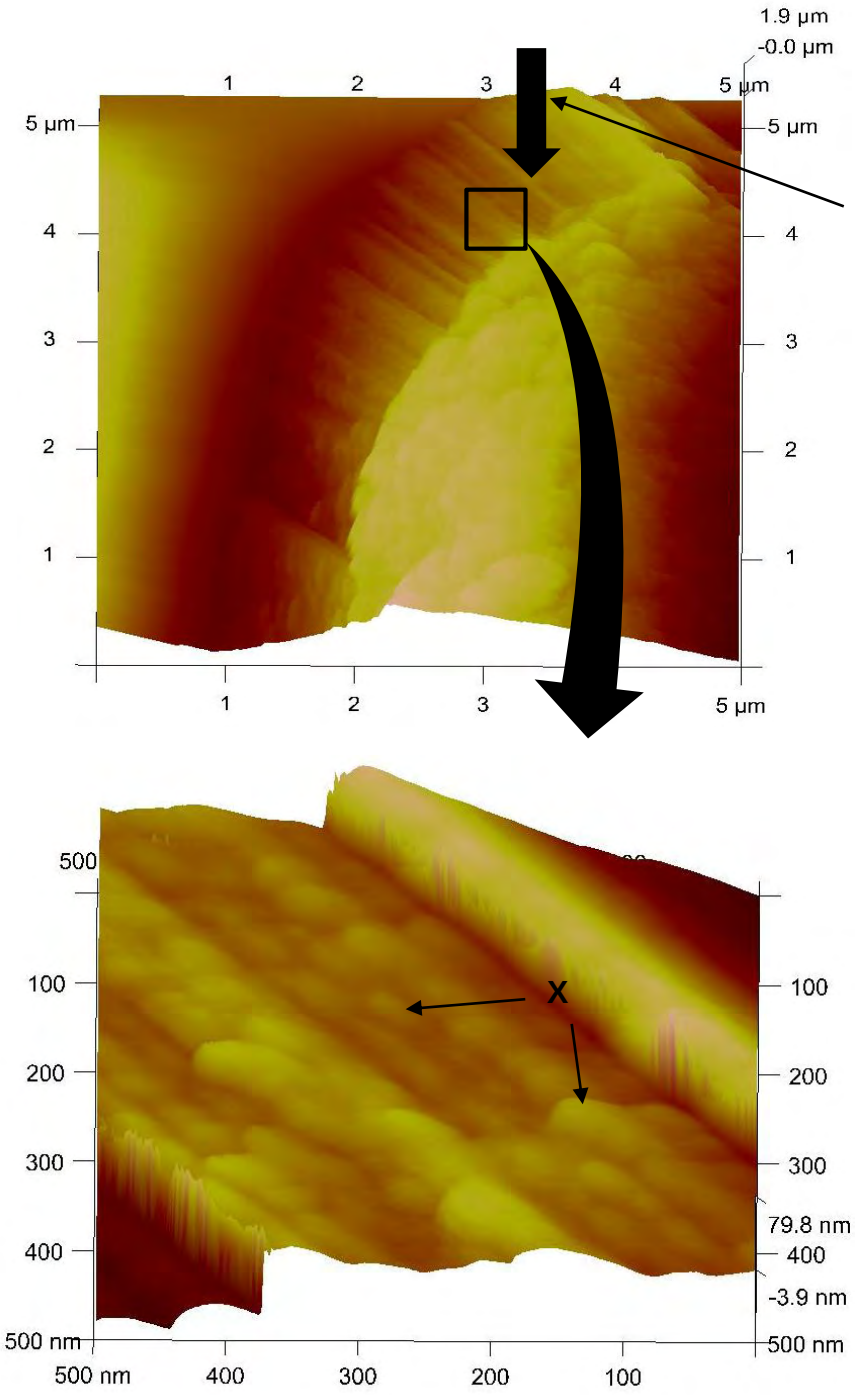

4.1.4.2 *Protein structure of treated kafirin microparticles*

SDS-PAGE of treated kafirin microparticles

SDS-PAGE under non-reducing conditions, of the wet heat-treated kafirin microparticles showed no change in band pattern compared with the control until the severity of the treatment was at 96^{o}C (Figure 4.11A). The highest band intensity was at 16–27 kDa with SDS-PAGE under both non-reducing and reducing conditions, which are the monomeric α-, β- and γ-kafirins (Shull et al., 1991). Bands 44–53 kDa and 78–93 kDa, probably dimers and trimers, respectively, based on classification by El Nour et al. (1998), were seen showing the occurrence of polymerized kafirin. The 96^{o}C heat treatment, under non-reducing conditions, however, showed a fainter trimer band and disappearance of an oligomer band (Figure 4.11A, arrows in Lane 4). This is considered indicative of polymerization of the different kafirin species, which then become too large to enter the separating gel (Ezeogu, Duodu and Taylor, 2005). The absence of visible change in band pattern at lower treatment temperatures may be due to the electrophoresis technique not being sufficiently sensitive to show a lower degree of polymerization. Under reducing conditions, all the treatments showed similar band patterns with very low levels of kafirin trimers and oligomers. This indicated that the kafirin polymers formed by heat treatment were the result of disulphide cross-linking, and that the linkages were broken on reduction, as demonstrated by the high level of kafirin monomers, as described by (Emmambux and Taylor, 2009).

Despite the changes in the physical appearance of the kafirin microparticles with transglutaminase treatment, there was no evidence of polymerization with SDS-PAGE (Figure 4.11B). However, with very high enzyme concentration (9.4% transglutaminase), which was over 15 fold the levels transglutaminase treatment used by other workers (Autio, Kruus, Knaapila, Gerber, Flander and Buchert, 2005; Bruno et al., 2008), a band approximately 39 kDa, probably a monomeric transglutaminase (Motoki and Seguro, 1998), was detected (Figure 4.11B, Lane 6). In addition, with the 9.4% transglutaminase treatment, faint 63 kDa and 118 kDa bands were detected using SDS-PAGE under reducing conditions, indicative of presence of kafirin trimers and oligomers, possibly formed by transglutaminase catalysed cross-linking of kafirin proteins. This suggested a low reactivity of kafirin with transglutaminase enzyme.

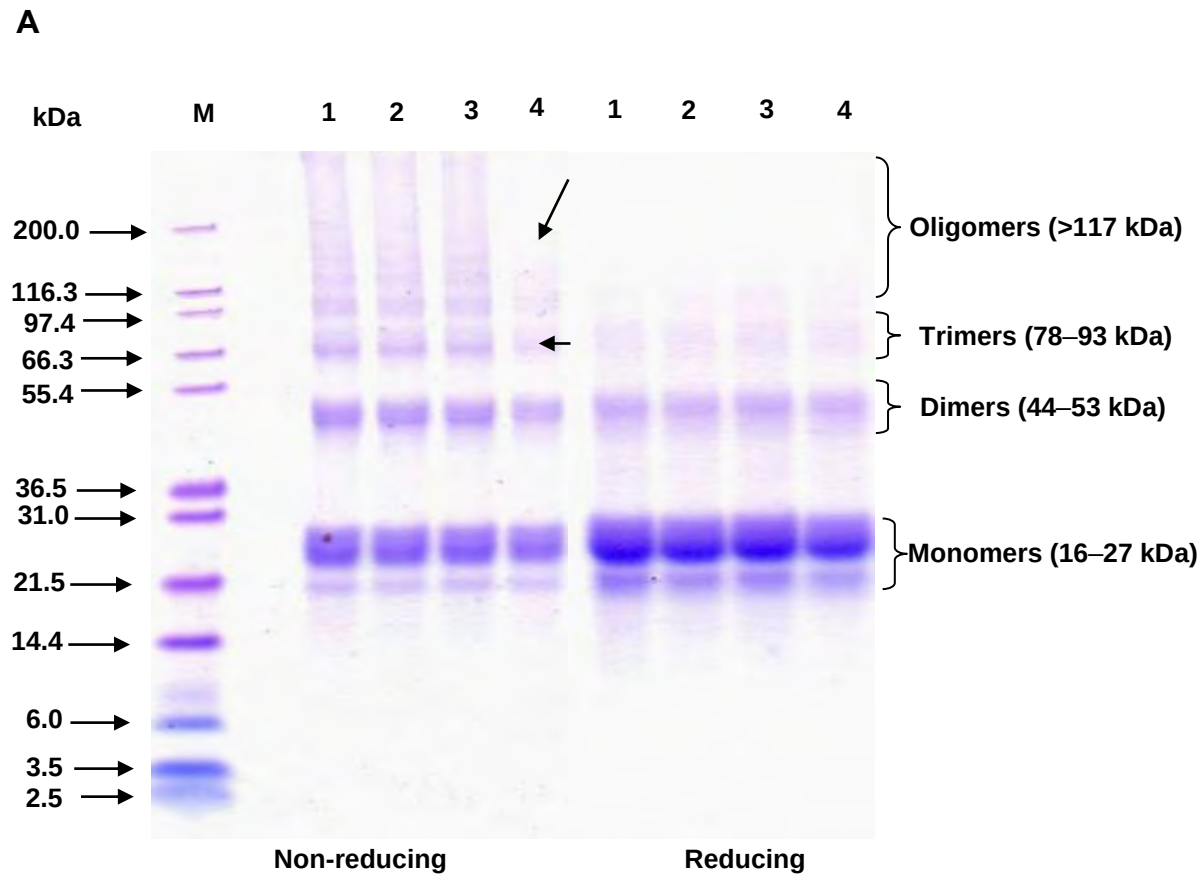

Figure 4.11 SDS-PAGE of treated kafirin microparticles. Protein loading, 10 µg.

A. Heat treatment. Lanes M: Molecular markers; 1: Control (22ºC); 2: 50ºC; 3: 75ºC; 4: 96ºC. Arrows in Lane 4 under non-reducing conditions show fading and disappearance of bands.

B. Transglutaminase (TG) treatment. Lanes M: Molecular markers; 1: TG; 2: Maltodextrin 3: 0.1% TG + maltodextrin; 4: 0.3% TG + maltodextrin; 5: 0.6% TG + maltodextrin; 6: 9.4% TG + maltodextrin*.

C. Glutaraldehyde treatment. Lanes M: Molecular markers; 1: Control; 2: 10%; 3: 20%; 4: 30%.

*The very high enzyme concentration (9.4% transglutaminase), which was over 15-fold the level of transglutaminase treatment in literature was tested only for SDS-PAGE to check whether it could have a cross-linking effect on the kafirin microparticles.

B

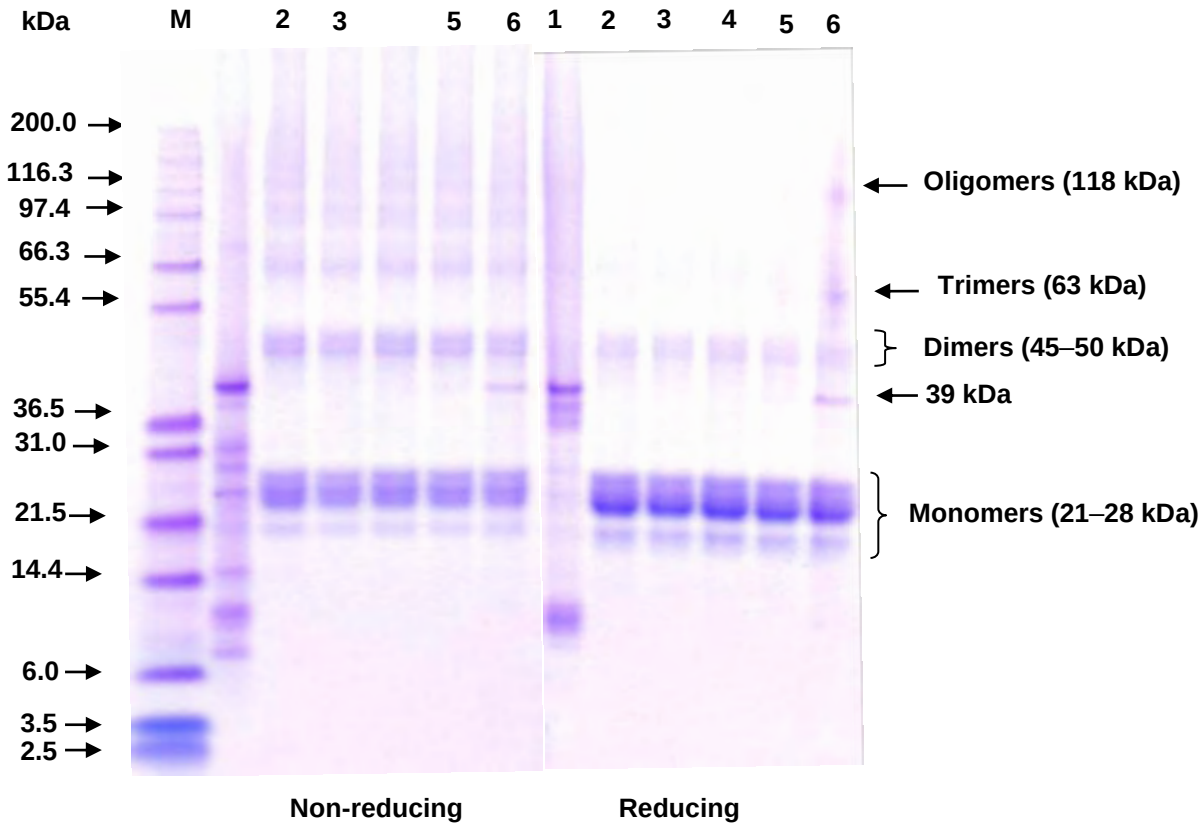
kDa
M
2
3
5
6
1
2
3
4
5
6
200.0
116.3
97.4
66.3
55.4
36.5
31.0
21.5
14.4
6.0
3.5
2.5
Oligomers (118 kDa)
Trimers (63 kDa)
Dimers (45–50 kDa)
39 kDa
Monomers (21–28 kDa)
Non-reducing
Reducing

C

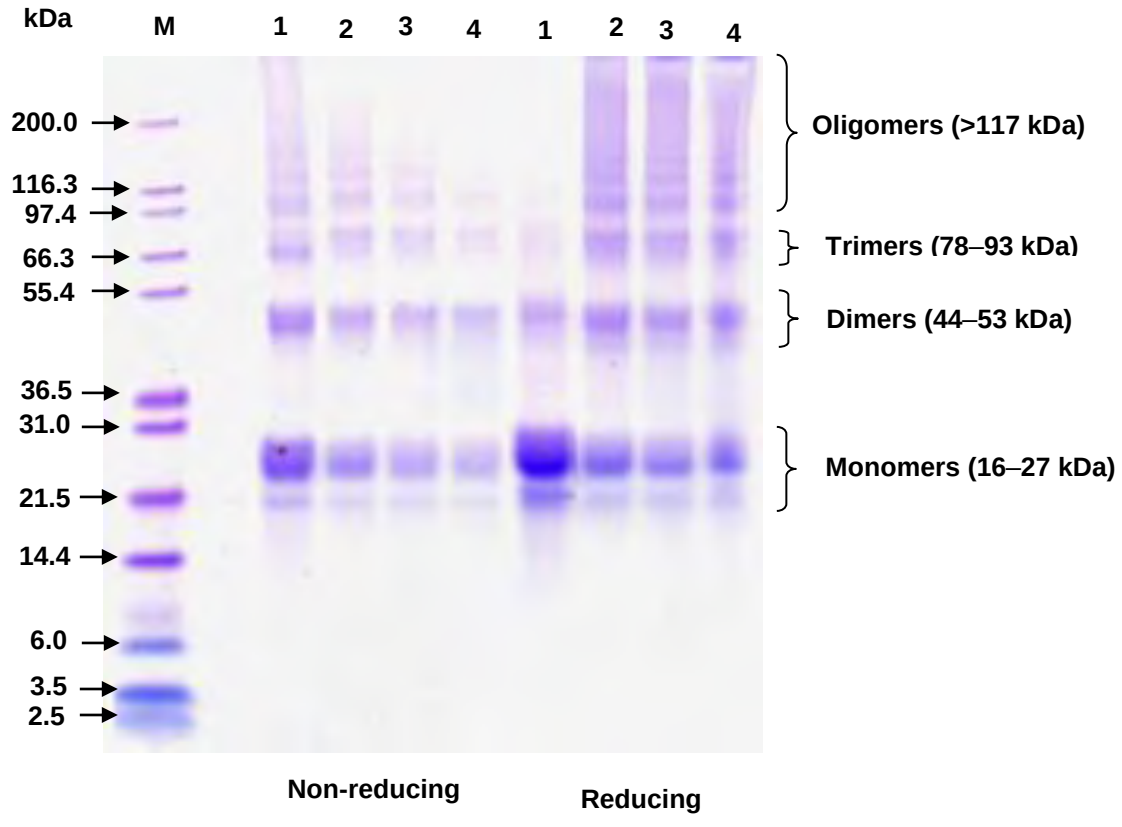
kDa
M
1
2
3
4
1
2
3
4
200.0
116.3
97.4
66.3
55.4
36.5
31.0
21.5
14.4
6.0
3.5
2.5
Oligomers (>117 kDa)
Trimers (78–93 kDa)
Dimers (44–53 kDa)
Monomers (16–27 kDa)
Non-reducing
Reducing

As stated, this is probably because of kafirin's very low lysine content (Belton et al., 2006). A similar poor cross-linking reaction was reported when wheat gliadin and the low molecular weight (LMW) glutenin subunits, which are also low in lysine, were cross-linked with transglutaminase (Autio et al., 2005).

In contrast, glutaraldehyde treatment of kafirin microparticles resulted in a progressive reduction of monomer (16–27 kDa), dimer (44–53 kDa), trimer (78–93 kDa) and oligomer (>117 kDa) bands under non-reducing conditions (Figure 4.11C). This is indicative of an increase in kafirin polymerization with increase in glutaraldehyde concentration, hence a reduction in the proportion of kafirin that could migrate into the separating gel. With SDS-PAGE under reducing conditions, the intensity of the kafirin monomer bands was much higher in the control than with the glutaraldehyde treatments. This indicated that the glutaraldehyde cross-linked the kafirin in such a way that breaking of the intermolecular disulphide bonds did not depolymerize it. Thus, the major cause of kafirin cross-linking with glutaraldehyde was not by disulphide bonding. It has been shown that cross-linking proteins with glutaraldehyde involves free amino groups of peptide chains and the carbonyl groups of the aldehyde (Rayment, 1997; Gerrard, Brown and Fayle, 2003) to form non-disulphide covalent bonds.

FTIR of heat, transglutaminase and glutaraldehyde treated kafirin microparticles

The kafirin microparticle secondary structure as analysed by FTIR showed a α-helical component of 48.7% for the control (Table 4.1) as determined at the Amide I band (≈1650–1620 cm^{-1}) based on the work by Duodu et al. (2001). Native kafirin is about 60% α-helical (reviewed by Belton et al., 2006), whereas Taylor et al. (2009a) found the secondary structure of kafirin microparticles between 50–56% α-helical conformation. These authors attributed the reduction in the proportion of α-helical conformation to protein aggregation during the formation of kafirin microparticles by self-assembly. The difference in the proportion of α-helical conformation in the control kafirin microparticles found in the present study compared to that reported by Taylor et al. (2009a) may be attributed to a number of factors, including differences in kafirin batches, method of kafirin extraction and drying effect on secondary structure measurements, as was suggested by Gao et al. (2005). Heat treatment of kafirin microparticles reduced further the relative proportion of α-helical conformation by up to about 17% compared to the control. The other amine bands (II and III) were not elaborated,

in this study, as they are less sensitive with FTIR spectroscopy in determining of protein secondary structure (reviewed by Jackson and Mantsch, 1995).

Table 4.1 Effects of heat, transglutaminase and glutaraldehyde treatments on the protein secondary structure of kafirin microparticles determined by FTIR

Treatment		Relative proportion of α-helical conformation at Amide I band (%)
Control	22°C	48.7 e (0.6)
Heat		
	50°C	45.5 d (0.3)
	75°C	40.9 ab (0.2)
	96°C	40.6 a (0.5)
Transglutaminase		
	Maltodextrin	41.9 b (0.8)
	0.1% TG + Maltodextrin	41.2 ab (0.8)
	0.3% TG + Maltodextrin	41.9 b (1.1)
	0.6% TG + Maltodextrin	43.3 c (0.8)
Glutaraldehyde		
	10%	44.5 d (0.6)
	20%	45.1 d (0.2)
	30%	45.1 d (0.8)

Values followed by different letters are significantly different ($p<0.05$). Values in the brackets are standard deviations (n=3). Control (22°C) is the same for heat and glutaraldehyde treatments. Amide I band ≈ 1650–1620 cm^{-1}.

The change in protein secondary structure with heat treatment has been related to the kafirin polymerization (Duodu et al., 2001; Byaruhanga et al., 2006). It has been suggested that thermal treatment disrupts the hydrogen bonds that stabilize the protein conformation, causing loss of the α-helix and β-sheet structures and creating new β-sheet arrangements (Emmambux and Taylor, 2009). Thus, it appears that the increase in size of the kafirin microparticles with increasing heat treatment was as a result of a further process of assisted-assembly caused by wet heat-induced kafirin disulphide-bonded polymerization, as described by Emmambux and Taylor (2009).

Treatment of the kafirin microparticles with transglutaminase appeared to result in slight changes to the protein secondary structure in comparison with microparticles to which only maltodextrin had been added. Similar observations were made by Eissa, Puhl, Kadla and

Khan (2006) studying the conformational changes of β-lactoglobulin treated with transglutaminase. These authors noted changes in microstructural properties, which were not reflected to the same extent in the molecular structure (protein secondary structure). In the present study, the essential absence of lysine in kafirin may have been a reason for the very small change in secondary structure. In addition, it has been proposed by Eissa et al. (2006) that there may be little effect of transglutaminase treatment on C=O stretching mode, probably due to the low number of the bonds created by the activity of the enzyme in comparison to the backbone bonds in the protein. When kafirin microparticles treated with transglutaminase and/or maltodextrin are compared to control without any treatment (control at 22^{o}C), it appears that there is a substantial difference in protein structure with about an 11–15% reduction in the relative proportion of α-helical conformation. This was probably because of the effect of maltodextrin, which constitutes the largest proportion of the transglutaminase enzyme mixture. A similar change in protein secondary structure as a result of reaction between dextrin and gliadin has been reported (Secundo and Guerrieri, 2005), which presumably was Maillard reaction. Maillard reaction has been shown to reduce the α-helical conformation of protein (Sun, Hayakawa and Izumori, 2004).

Despite the SDS-PAGE evidence of kafirin polymerization with glutaraldehyde treatment, FTIR indicated that it caused only a small reduction in the relative proportion of α-helical conformation (7–9%) (Table 4.1). There was no change in the protein secondary structure with increase in glutaraldehyde concentration. As stated, cross-linking protein with glutaraldehyde involves the free amino groups of the proteins and carbonyl groups of the aldehyde (Rayment, 1997). However, N–H bending contributes only less than 20% to Amide I band (Pelton and McLean, 2000; Surewicz et al., 1993). This is probably the reason for the small change in protein secondary structure with glutaraldehyde treatment. The present findings are consistent with a report by Caillard, Remondetto and Subirade (2009) on soy protein hydrogels, which showed little alteration in protein secondary structure with glutaraldehyde treatment despite a large effect on gel physical appearance and functional properties.

4.1.4.3 *Protein digestibility of heat, transglutaminase and glutaraldehyde treated kafirin microparticles*

Heat treatment resulted in up to 39% reduction in the IVPD of kafirin microparticles (Table 4.2). The reduction in IVPD with wet heat treatment is a characteristic of kafirin proteins and is due to disulphide cross-linking of these proteins (Hamaker et al., 1987; Duodu et al., 2003). Reduction in the IVPD of kafirin has been associated with reduction in proportion α-helical conformation at the amide I band (Emmambux and Taylor, 2009). The reduction in IVPD of kafirin microparticles with heat treatment agrees with the data on the protein secondary structure (Table 4.1).

Table 4.2 Effects of kafirin microparticle treatment with heat, transglutaminase and glutaraldehyde on their *in vitro* protein digestibility (IVPD)

Treatment		IVPD (%)
Control	22°C	92.2 e (0.4)
Heat		
	50°C	90.2 de (1.8)
	75°C	73.5 b (0.7)
	96°C	57.3 a (1.5)
Transglutaminase		
	Maltodextrin	90.0 de (0.1)
	0.1% TG + Maltodextrin	85.2 c (0.4)
	0.3% TG + Maltodextrin	86.3 cd (4.3)
	0.6% TG + Maltodextrin	88.7 cde (0.0)
Glutaraldehyde		
	10%	91.3 e (1.8)
	20%	91.9 e (2.8)
	30%	92.5 e (0.3)

Values followed by different letters are significantly different ($p<0.05$). Values in the brackets are standard deviations (n=3). Control (22°C) is the same for heat and glutaraldehyde treatments.

Transglutaminase treatment had little effect on IVPD of the kafirin microparticles, with a reduction of only about 1–5%, compared to their control kafirin microparticles to which only

maltodextrin was added. Similar findings were reported by Seguro, Kumazawa, Kuraishi, Sakamoto and Motoki (1996) and Roos, Lorenzen, Sick, Schrezenmeir and Schlimme (2003) working on transglutaminase-treated casein. This small effect of transglutaminase on IVPD of kafirin microparticles was probably due to the very low kafirin lysine content as discussed. Additionally, it has been suggested by Lundin, Golding and Wooster (2008) that the little effect of transglutaminase on protein digestibility may be because the cross-linked regions of the protein molecules are probably are not involved in the proteolytic reaction. However, the reduction in IVPD of transglutaminase-treated microparticles was slightly higher (4–8%) when compared with the control microparticles held at 22^{o}C. This was probably because the transglutaminase enzyme is prepared in maltodextrin (sugar) carrier base constituting 99%, which may participate in Maillard reaction with the proteins. Maillard reaction has been shown to inhibit protein digestibility (Friedman, 1996).

Despite the glutaraldehyde treatment causing kafirin polymerization, it did not significantly affect kafirin microparticle IVPD. This is consistent with the lack of change in protein secondary structure and is probably a result of an increase in protein void volume caused by the glutaraldehyde cross-linking. It has been suggested that polymeric forms of glutaraldehyde are involved in the cross-linking with protein (Migneault et al., 2004; Wine, Cohen-Hadar, Freeman and Frolow, 2007). These glutaraldehyde polymers may create long methylene bridges between peptides (Farris et al., 2010). Hence, the protein polymer chains may be kept far apart in a glutaraldehyde-protein complex, thereby allowing easier accessibility of pepsin enzyme to hydrolyse internal peptide bonds.

4.1.4.4 *Mechanical properties of heat, transglutaminase and glutaraldehyde treated kafirin microparticles*

These treatments reduced the slope of force-deformation curves obtained with AFM of kafirin microparticles (Figure 4.12, Table 4.3). Heat and glutaraldehyde treatments resulted in the greatest decrease in slope. The slope of a force-deformation curve is a measure of the elastic stiffness of the material (Lee, Wei, Kysar and Hone, 2008) and has been shown to directly correspond to the surface elastic modulus of nanoparticles (Krake and Damasche, 2000; Safanama, Marashi, Hesari, Firoozi, Aboutalebi and Jalilzadeh, 2012).

Various reasons may account for the differences in the elastic moduli of the kafirin microparticles with different treatments. In the case of glutaraldehyde treatment, it has been

suggested that molecular structure of the long methylene bridges formed between the glutaraldehyde cross-linked proteins may lead to a decrease in the intermolecular forces between polymer chains causing a plasticizer effect (Marquié, Tessier, Aymard and Guilbert, 1997).

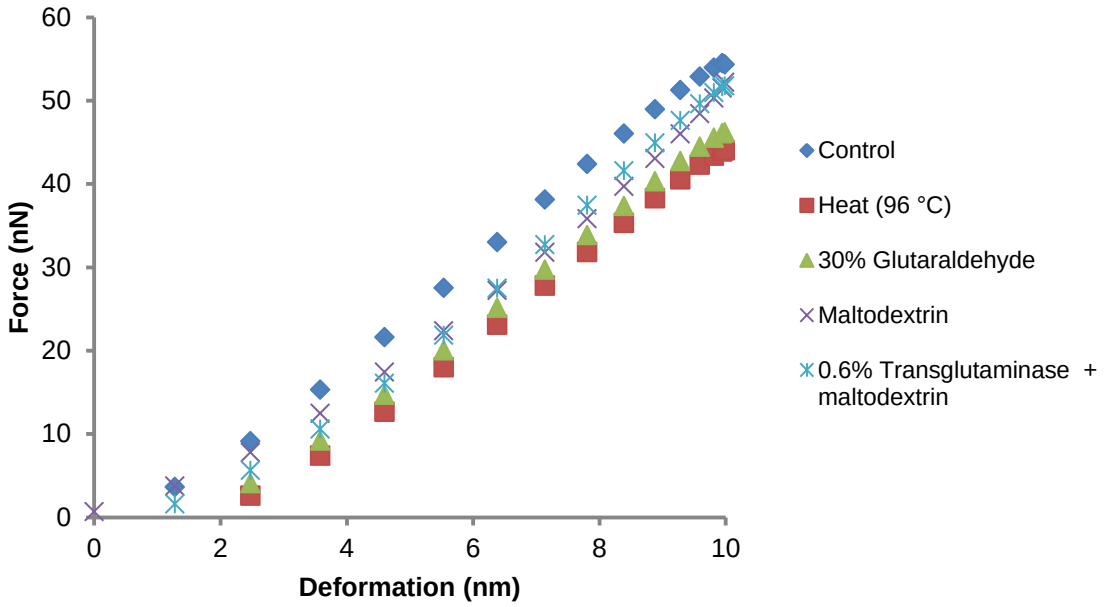

Figure 4.12 Representative linear portion of the force-deformation curves for heat, transglutaminase and glutaraldehyde treated kafirin microparticles, determined by AFM.

Table 4.3 Slope of linear portion of force-deformation curves of heat, transglutaminase and glutaraldehyde treated kafirin microparticles determined by AFM

Treatment		Slope (nN/nm)
Control	22 °C	6.18 c (0.27)
Heat	96°C	4.81 a (0.11)
Transglutaminase		
	Maltodextrin	5.42 b (0.23)
	0.6% TG + Maltodextrin	5.12 ab (0.30)
Glutaraldehyde	30%	4.83 a (0.32)

Values are mean slopes of curves for each treatment. Values followed by different letters are significantly different ($p<0.05$). Figures in the brackets are standard deviations (n=3)

In addition, non-linear protein aggregation is characterized by less elastic behaviour (Chen et al., 2006), which probably accounted for the higher elastic modulus of the control and the transglutaminase-treated kafirin microparticles compared to glutaraldehyde. With heat

treatment, the reduction in the elastic stiffness was probably due to the increase in the microparticle vacuole size. It is known that the elastic modulus of particles decreases with increase in their porosity (Phani and Niyogi, 1987). However, it is important to note that this AFM technique measures only a very small portion of the microparticles (reviewed by Kim, Cheng, Liu, Wu and Sun, 2010), hence the results have to be treated with caution.

4.1.4.5 *Kafirin microparticle further self-assembly*

This study shows that modification of kafirin microparticles with wet heat or glutaraldehyde treatment result in two structures that while similar in size and external morphology, are formed by significantly different mechanisms. It is also apparent that in both cases the larger kafirin microparticle structures had undergone some form of further assisted-assembly during the treatments and were not just formed as a result of 'gluing' the original microparticles together. The 'gluing together' of microparticles was observed when sorghum condensed tannins were encapsulated using kafirin microparticles (Taylor et al., 2009b). Furthermore, with both the heat and glutaraldehyde treatments, there was kafirin polymerization and although the treatments only resulted in a small changes in secondary structure from α-helical to β-sheet as shown by FTIR, there was a considerable proportion of β-sheet present, 59.4% and 54.9% for the most rigorous heat treatment and glutaraldehyde treatment, respectively (Table 4.1). A large proportion of β-sheet presence is considered indicative of protein aggregation (Mizutani et al., 2003) and the universal energetic minimum for aggregated protein (reviewed by Gorbenko and Kinnunen, 2006). Zein can self-assemble into aggregates as globules (Guo et al., 2005), fibrils (Erickson, Campanella and Hamaker, 2012), and spherical micro- and nano-particles (Wang and Padua, 2010) depending on the conditions of formation, all of which have a large proportion of β-sheet structure.

Wang and Padua (2010) working with zein dissolved in 70% ethanol showed that at low mass fraction zein formed spheres. With increasing zein concentration, they noted various different geometries formed by connecting, melting or deformation of spheres. They concluded that spheres were the basis of all other microphases. In this study, the heat-treated microparticles appeared to be formed by coalescence of spherical nanoparticles, in agreement with Wang and Padua (2010). Further work by Wang and Padua (2012) showed that at nanoscale, zein formed stripes, rings and discs with a periodicity characteristic of β-sheet. They indicated that these β-sheets self-assembled into stripes, which curled into rings and then the rings stacked into spheres. However, in this study AFM indicated the glutaraldehyde-treated microparticles

were formed from spindle-shaped nanostructures with little change in secondary structure but with a large proportion of β-sheet structure present. It appears unlikely that these structures formed from spheres. Further work is needed in order to understand the kafirin self-assembly process at a molecular level, under the different conditions used in this study so that the self-assembly process can be further manipulated to enable the formation of different structures.

4.1.5 Conclusions

Heat treatment increases the size of kafirin microparticles and enlarges the pores within these microstructures. While glutaraldehyde treatment, as with heat increases the size of the microparticles, it also results in the formation of presumed kafirin nanostructures with generally spindle shapes, probably due to formation of a linear kafirin-glutaraldehyde linkage. On the contrary, transglutaminase treatment has little effect on the size of individual microparticles but results in agglomeration of kafirin microparticles into large lumps. Cross-linking the formed kafirin microparticles using wet heat or glutaraldehyde treatment apparently causes further assisted-assembly by two significantly different mechanisms. Heat treatment, involves kafirin polymerization by disulphide bonding with the microparticles being formed from round, coalesced nanostructures. Kafirin polymerization in glutaraldehyde treated microparticles is not by disulphide bonding and the nanostructures are spindle-shaped.

4.1.6 References

American Association of Cereal Chemists (AACC International), 2000. Crude protein-combustion, Standard Method 46-30. Approved Methods of the AACC (10th ed.). The Association: St Paul, MN.

Autio, K., Kruus, K., Knaapila, A., Gerber, N., Flander, L., Buchert, J., 2005. Kinetics of transglutaminase-induced cross-linking of wheat proteins in dough. Journal of Agricultural and Food Chemistry 53, 1039–1045.

Belton, P.S., Delgadillo, I., Halford, N.G., Shewry, P.R., 2006. Kafirin structure and functionality. Journal of Cereal Science 44, 272–286.

Bruno, M., Giancone, T., Torrieri, E., Masi, P., Moresi, M., 2008. Engineering properties of edible transglutaminase cross-linked caseinate-based films. Food Bioprocess Technology 1, 393–404.

Byaruhanga, Y.B., Emmambux, M.N., Belton, P.S., Wellner, N., Ng, K.G., Taylor, J.R.N., 2006. Alteration of kafirin film structure by heating with microwave energy and tannin complexation. Journal of Agricultural and Food Chemistry 54, 4198–4207.

Caillard, R., Remondetto, G.E., Subirade, M., 2009. Physicochemical properties and microstructure of soy protein hydrogels co-induced by Maillard type cross-linking and salts. Food Research International 42, 98–106.

Duodu, K.G., Taylor, J.R.N., Belton, P.S., Hamaker, B.R., 2003. Factors affecting sorghum protein digestibility. Journal of Cereal Science 38, 117–131.

Eissa, A.S., Puhl, C., Kadla, J.F., Khan, S.A., 2006. Enzymatic cross-linking of β-lactoglobulin: conformational properties using FTIR spectroscopy. Biomacromolecules 7, 1707−1713.

El Nour, N.A., Peruffo, A.D.B., Curioni, A., 1998. Characterisation of sorghum kafirins in relations to their cross-linking behaviour. Journal of Cereal Science 28, 197–207.

Emmambux, N. M., Taylor, J.R.N., 2003. Sorghum kafirin interaction with various phenolic compounds. Journal of the Science of Food and Agriculture 83, 402–407.

Emmambux, N.M., Taylor, J.R.N., 2009. Properties of heat-treated sorghum and maize meal and their prolamin proteins. Journal of Agricultural and Food Chemistry 57, 1045–1050.

Erickson, D.P., Campanella, O.H., Hamaker, B.R., 2012. Functionalizing maize zein in viscoelastic dough systems through fibrous, β-sheet-rich protein networks: An alternative, physiochemical approach to gluten-free breadmaking. Trends in Food Science and Technology 24, 74–81.

Ezeogu, L.I., Duodu, K.G., Taylor, J.R.N., 2005. Effects of endosperm texture and cooking on the in vitro starch digestibility of sorghum and maize flours. Journal of Cereal Science 42, 33–44.

Ezpeleta, I., Rache, J.M., Gueguen, J., Orecchioni, A.M., 1997. Properties of glutaraldehyde cross-linked vicilin nano- and microparticles. Journal of Microencapsulation 14, 557–565.

Farris, S., Song, J., Huang, Q., 2010. Alternative reaction mechanism for the cross-linking of gelatin with glutaraldehyde. Journal of Agricultural and Food Chemistry 58, 998–1003.

Friedman, M., 1996. Food browning and its prevention: an overview. Journal of Agricultural and Food Chemistry 44, 631−653.

Gan, C.-Y., Cheng, L.-H., Easa, A.M., 2008. Evaluation of microbial transglutaminase and ribose cross-linked soy protein isolate-based microcapsules containing fish oil. Innovative Food Science and Emerging Technologies 9, 563–569.

Gao, C., Taylor, J., Wellner, N., Byaruhanga, Y.B., Parker, M.L., Mills, E.N.C., Belton, P.S., 2005. Effect of preparation conditions on protein secondary structure and biofilm formation of kafirin. Journal of Agricultural and Food Chemistry 53, 306–312.

Gerrard, J.A., Brown, P.K., Fayle, S.E., 2003. Maillard crosslinking of food proteins II: the reactions of glutaraldehyde, formaldehyde and glyceraldehyde with wheat proteins in vitro and in situ. Food Chemistry 80, 35–43.

Gong, S., Wang, H., Sun, Q., Xue, S.-T., Wang, J.-Y., 2006. Mechanical properties and in vitro biocompatibility of porous zein scaffolds. Biomaterials 27, 3793–3799.

Gorbenko, G.P., Kinnunen, P.K.J., 2006. The role of lipid-protein interactions in amyloid-type protein fibril formation. Chemistry and Physics of Lipids 141, 72–82.

Guo, Y., Liu, Z., An, H., Li, M., Hu, J., 2005. Nano-structure and properties of maize zein studied by atomic force microscopy. Journal of Cereal Science 41, 277–281.

Hamaker, B.R., Kirleis, A.W., Mertz, E.T., Axtell, J.D., 1986. Effect of cooking on the protein profiles and in vitro digestibility of sorghum and maize. Journal of Agricultural and Food Chemistry 34, 647−649.

Hamaker, B.R., Kirleis, A.W., Butler, L.G., Axtell, J.D., Mertz, E.T., 1987. Improving the in vitro protein digestibility of sorghum with reducing agents. Proceedings of the National Academy of Sciences of the United States of America 84, 626–628.

Hou, Q., De Bank, P.A., Shakesheff, K.M., 2004. Injectable scaffolds for tissue regeneration. Journal of Materials Chemistry 14, 1915–1935.

Jackson, M., Mantsch, H.H., 1995. The use and misuse of FTIR spectroscopy in the determination of protein structure. Critical Reviews in Biochemistry and Molecular Biology 30, 95–120.

Kim, K., Cheng, J., Liu, Q., Wu, X.Y., Sun, Y., 2010. Investigation of mechanical properties of soft hydrogel microcapsules in relation to protein delivery using a MEMS force sensor. Journal of Biomedical Materials Research Part A 92, 103–113.

Kim, S., Kang, Y., Krueger, C.H., Sen, M., Holcomb, J.B., Chen, D., Wenke, J.C., Yang, Y., 2012. Sequential delivery of BMP-2 and IFG-1 using a chitosan gel with gelatin microspheres enhances early osteoblastic differentiation. Acta Biomaterialia 8, 1768–1777.

Krake, B., Damasche, B., 2000. Measurement of nanohardness and nanoelasticity of thin gold films with scanning force microscope. Applied Physics Letters 77, 361–363.

Krebs, M.R.H., Devlin, G.L., Donald, A.M., 2007. Protein particulates: another generic form of protein aggregation? Biophysical Journal 92, 1336–1342.

Lee, C., Wei, X., Kysar, J.W., Hone, J., 2008. Measurement of the elastic properties and intrinsic strength of monolayer graphene. Science 321, 385–388.

Lehtinen, K.E.J., Zachariah, M.R., 2001. Effect of coalescence energy release on the temporal shape evolution of nanoparticles. Physical Review B 63 205402-1–205402-7.

Lundin, L., Golding, M., Wooster, T.J., 2008. Understanding food structure and function in developing food for appetite control. Nutrition and Dietetics 65 (Suppl. 3), S79–S85.

Marquié, C., Tessier, A.-M., Aymard, C., Guilbert, S., 1997. HPLC determination of the reactive lysine content of cottonseed protein films to monitor the extent of cross-linking by formaldehyde, glutaraldehyde, and glyoxal. Journal of Agricultural and Food Chemistry 45, 922–926.

Migneault, I., Dartiguenave, C., Bertrand, M.J., Waldron, K.C., 2004. Glutaraldehyde: behavior in aqueous solution, reaction with proteins, and application to enzyme crosslinking. BioTechniques 37, 790−802.

Mizutani, Y., Matsumura, Y., Imamura, K., Nakanishi, K., Mori, T., 2003. Effects of water activity and lipid addition on secondary structure of zein in powder systems. Journal of Agricultural and Food Chemistry 51, 229–235.

Motoki, M., Seguro, K., 1998. Transglutaminase and its use for food processing. Trends in Food Science and Technology 9, 204–210.

Muthuselvi, L., Dhathathreyan, A., 2006. Simple coacervates of zein to encapsulate gitoxin. Colloids and Surfaces B: Biointerfaces 51, 39–43.

Panchapakesan, C., Sozer, N., Dogan, H., Huang, Q., Kokini, J.L., 2012. Effect of different fractions of xeon on the mechanical and phase properties of zein films at nano-scale. Journal of Cereal Science 55, 174–182.

Parris, N., Cooke, P.H., Hicks, K.B., 2005. Encapsulation of essential oils in zein nanospherical particles. Journal of Agricultural and Food Chemistry 53, 4788–4792.

Patel, A., Hu, Y., Tiwari, J.K., Velikov, K.P., 2010. Synthesis and characterisation of zein–curcumin colloidal particles. Soft Matter 6, 6192–6199.

Pelton, J.T., McLean, L.R., 2000. Spectroscopic methods for analysis of protein secondary structure. Analytical Biochemistry 277, 167–176.

Phani, K.K., Niyogi, S.K., 1987. Young's modulus of porous brittle solids. Journal of Materials Science 22, 257–263.

Rayment, I., 1997. Reductive alkylation of lysine residues to alter crystallization properties of properties. Methods in Enzymology 276, 171–179.

Reddy, N., Yang, Y., 2011. Potential of plant proteins for medical applications. Trends in Biotechnology 29, 490–498.

Roos, N., Lorenzen, P.C., Sick, H., Schrezenmeir, J., Schlimme, E., 2003. Cross-linking by transglutaminase changes neither the in vitro proteolysis nor the in vivo digestibility of caseinate. Kieler Milchwirtschaftliche Forschungsberichte 55, 261–276.

Safanama, D.S., Marashi, P., Hesari, A.Z., Firoozi, S., Aboutalebi, S.H., Jalilzadeh, S., 2012. Elastic modulus measurement of nanocomposite materials by atomic force microscopy. International Journal of Modern Physics: Conference Series 5, 502–509.

Secundo, F., Guerrieri, N., 2005. ATR-FT/IR study on the interactions between gliadins and dextrin and their effects on protein secondary structure. Journal of Agricultural and Food Chemistry 53, 1757−1764.

Seguro, K., Kumazawa, Y., Kuraishi, C., Sakamoto, H., Motoki, M., 1996. The ε-(γ-glutamyl)lysine moiety in crosslinked casein is an available source of lysine for rats. Journal of Nutrition 126, 2557–2562.

Shakesheff, K.M., Davies, M.C., Jackson, D.E., Roberts, C.J., Tendler, S.J.B., Brown, V.A., Watson, R.C., Barrett, D.A., Shaw, P.N., 1994. Imaging the surface of silica microparticles with the atomic force microscope: a novel sample preparation method. Surface Science Letters 304, L393–L399.

Shull, J.M., Watterson, J.J., Kirleis, A.W., 1991. Proposed nomenclature for the alcohol-soluble proteins (kafirins) of *Sorghum bicolor* (L. Moench) based on molecular weight, solubility and structure. Journal of Agricultural and Food Chemistry 39, 83–87.

Sun, Y., Hayakawa, S., Izumori, K., 2004. Modification of ovalbumin with a rare ketohexose through the Maillard reaction: effect on protein structure and gel properties. Journal of Agricultural and Food Chemistry 52, 1293–1299.

Surewicz, W.K., Mantsch, H.H., Chapman, D., 1993. Determination of protein secondary structure by Fourier transform infrared spectroscopy: a critical assessment. Biochemistry 32, 389−394.

Taylor, J., Taylor, J.R.N., 2002. Alleviation of the adverse effects of cooking on sorghum protein digestibility through fermentation in traditional African porridges. International Journal of Food Science and Technology 37, 129–137.

Taylor, J., Taylor, J.R.N., Belton, P.S., Minnaar, A., 2009a. Formation of kafirin microparticles by phase separation from an organic acid and their characterization. Journal of Cereal Science 50, 90–105.

Taylor, J., Taylor, J.R.N., Belton, P.S., Minnaar, A., 2009b. Kafirin Microparticle encapsulation of catechin and sorghum condensed tannins. Journal of Agricultural and Food Chemistry 57, 7523–7528.

Wang, H.-J., Lin, Z.-X., Liu, X.-M., Sheng, S.-Y., Wang, J.-Y., 2005. Heparin-loaded zein microsphere film and hemocompatibility. Journal of Controlled Release 105, 120–131.

Wang, Y., Padua, G.W., 2010. Formation of zein microphases in ethanol-water. Langmuir 26, 12897–12901.

Wang, Y., Padua, G.W., 2012. Nanoscale characterization of zein self-assembly. Langmuir 28, 2429−2435.

Weiss, P., Layrolle, P., Clergeau, L.P., Enckel, B., Pilet, P., Amouriq, Y., Daculsi, G., Giumelli, B., 2007. The safety and efficacy of an injectable bone substitute in dental sockets demonstrated in a human clinical trial. Biomaterials 28, 3295−3305.

Wine, Y., Cohen-Hadar, N., Freeman, A., Frolow, F., 2007. Elucidation of the mechanism and end products of glutaraldehyde crosslinking reaction by x-ray structure analysis. Biotechnology and Bioengineering 98, 711–718.

Xiao, D., Davidson, P.M., Zhong, Q., 2011. Spray dried zein capsules with coencapsulated nisin and thymol as antimicrobial delivery system for enhanced antilisterial properties. Journal of Agricultural and Food Chemistry 59, 7393–7404.

Xu, H., Jiang, Q., Reddy, N., Yang, Y., 2011. Hollow nanoparticles from zein for potential medical applications. Journal of Materials Chemistry 21, 18227–18235.

Zhang, W., Zhong, Q., 2009. Microemulsions as nanoreactors to produce whey protein nanoparticles with enhanced heat stability by sequential enzymic cross-linking and thermal pretreatments. Journal of Agricultural and Food Chemistry 57, 9181–9189.

CHAPTER 2

4.2 IMPROVEMENT IN WATER STABILITY AND OTHER RELATED FUNCTIONAL PROPERTIES OF THIN CAST KAFIRIN PROTEIN FILMS

4.2.1 Abstract

Improvement in the water stability and other related functional properties of thin (<50 µm) kafirin protein films was investigated. Thin conventional kafirin films and kafirin microparticle films were prepared by casting in acetic acid solution. Thin kafirin films cast from microparticles were more stable in water than conventional cast kafirin films. Treatment of kafirin microparticles with heat and transglutaminase resulted in slightly thicker films with reduced tensile strength. In contrast, glutaraldehyde treatment resulted in up to 43% increase in film tensile strength. The films prepared from microparticles treated with glutaraldehyde were quite stable in ambient temperature water, despite the loss of plasticizer. This was probably due to the formation of covalent cross-linking between free amino groups of the kafirin polypeptides and carbonyl groups of the aldehyde. Thus, such thin glutaraldehyde-treated kafirin microparticle films appear to have good potential for use as biomaterials in aqueous applications.

4.2.2 Introduction

Films and other biomaterials made from proteins draw much interest as a consumer- and environment-friendly option to synthetic polymer products (Poole, Church and Huson, 2008; Bourtoom, 2009). Some of the applications or potential uses of protein biomaterials include packaging materials and food coatings (Krochta, 2002), carriers of antimicrobial agents (Pérez-Pérez, Regalado-González, Rodríguez-Rodríguez, Barbosa-Rodríguez, and Villaseñor-Ortega, 2006) and drug-eluting coating film for cardiovascular devices (Wang et al., 2005). However, with respect to films made from cereal proteins such as zein, their poor mechanical properties and water stability compared to similar materials made from synthetic polymers are major limitations (Lawton, 2002; Reddy et al., 2008).

Protein film functional properties can be modified by physical treatments such as heat (Byaruhanga et al., 2005), γ-irradiation (Soliman, Eldin and Furuta, 2009), chemicals such as aldehydes (Sessa et al., 2007) or enzymes such as transglutaminase (Chambi and Grosso, 2006). Most of these modifications have been done on films with >50 μm thickness. For example, Sessa et al. (2007) worked on 700 to 900 μm thick zein films, Chambi and Grosso (2006) worked on 750 μm thick gelatin and casein films, while Hernández-Muñoz, Kanavouras, Lagaron and Gavara (2005) study was on 55 μm thick gliadin films.

Kafirin, the storage prolamin protein in sorghum, is relatively hydrophobic compared to other cereal proteins such as zein (Duodu et al., 2003; Belton et al., 2006). Thus, kafirin has a potential for use in biomaterials that are stable in water. Research has shown that thin cast kafirin films (<50 μm) produced from kafirin microparticles have some superior functional properties such as better film surface characteristics and lower water vapour permeability, than the conventional cast films from kafirin protein (Taylor et al., 2009c). The objective of this study was to investigate various treatments to improve the water stability and other related functional properties of thin kafirin films. Specifically, the use of heat, transglutaminase and glutaraldehyde treated kafirin microparticles to produce films was explored.

4.2.3 Materials and methods

4.2.3.1 *Materials*

Kafirin was extracted from mixture of two very similar white, tan-plant non-tannin sorghum cultivars PANNAR PEX 202/606, as described (Emmambux and Taylor, 2003). Briefly, whole milled sorghum grain was mixed with 70% (w/w) aqueous ethanol containing 3.5% (w/w) sodium metabisulphite and 5% (w/w) sodium hydroxide and then heated at 70^{o}C for 1 h with vigorous stirring. The clear supernatant was recovered by centrifugation and the ethanol evaporated. Kafirin was precipitated by adjusting the pH of the protein suspension to 5.0. The precipitated kafirin was recovered by vacuum filtration, freeze-drying, defatting with hexane at ambient temperature and air-drying.

4.2.3.2 *Preparation of conventional cast kafirin films*

Conventional kafirin films were prepared by the casting method described by Taylor et al. (2005b) from a 2% (w/w protein basis) kafirin solution in glacial acetic acid, containing 40% (w/w with respect to protein) plasticizer (a 1:1:1 w/w mixture of glycerol: polyethylene glycol 400: lactic acid). It has been shown that this plasticizer combination is effective in kafirin films (Taylor et al., 2009c). Films were dried overnight at 50°C in an oven (not forced draft) on a level surface.

4.2.3.3 *Preparation of kafirin microparticle films*

To prepare kafirin microparticle films, firstly, kafirin microparticles were prepared using acetic acid solvent according to Taylor et al. (2009c) with some modification. Plasticizer (0.66 g) was mixed with glacial acetic acid (4.34 g) and added to kafirin (1.9 g, 84% protein) with gentle stirring until fully dissolved. The kafirin solution was held at ambient temperature (22°C) for 16 h to equilibrate. Then, kafirin microparticles were prepared by adding 73.1 g distilled water to 6.9 g kafirin solution at a rate of 1.4 mL/min using a Watson-Marlow Bredel peristaltic pump (Falmouth, U.K.), while mixing using a magnetic stirrer at 600 rpm at ambient temperature. This suspension contained 2% (w/w) kafirin protein and 5.4% (w/w) (0.9 M) acetic acid.

To cast the films, 4.0 g suspensions of kafirin microparticles were centrifuged at 3150 *g* for 10 min. The clear supernatants were carefully removed and replaced by 25% (w/w) (4.2 M)

acetic acid and then left to equilibrate at ambient temperature for 12 h. Then, 32 mg plasticizer (40% w/w on kafirin protein basis) was added and films cast in the bottom dishes (90 mm diameter) of 100 mm × 15 mm borosilicate glass Petri dishes (Schott Glas, Mainz, Germany) by drying overnight at 50°C in an oven (not forced draught). All the films were assessed visually and photographed using a flatbed scanner.

Preparation of films from heat-treated kafirin microparticles

Kafirin microparticle film preparation suspension (4.0 g), described above, was washed with distilled water three times to remove the acetic acid. Treatment of kafirin microparticles with heat was done by heating the microparticles suspended in water, at 50°C, 75°C and 96°C for 1 h. A control film preparation mixture was maintained at ambient temperature for the same period. Then, supernatants were replaced with 25% acetic acid, plasticizer added and films were cast as described.

Preparation of films from transglutaminase-treated kafirin microparticles

The supernatants in the 4.0 g kafirin microparticle suspensions were removed by centrifugation and washed with distilled water as described above. The supernatants were replaced with 0.1%, 0.3% and 0.6% (w/w) microbial transglutaminase (Activa WM), activity 100 U/g (Ajinomoto Foods Europe, S.A.S., France) (on protein basis) in 0.02 M Tris–HCl buffer (pH 7.0). The buffer had been pre-heated to 50°C prior to dissolving the enzyme. For control films, 25% pure maltodextrin in 0.02 M Tris–HCl buffer, pH 7.0 was used as the transglutaminase enzyme is supplied in a 99% maltodextrin carrier base. Transglutaminase reaction was carried out at 30°C for 12 h. Optimal transglutaminase reaction temperature is 50°C (Ando, Adashi, Umeda, Matsuura, Nonaka, Uchio, Tanaka and Motoki, 1989) but complete films could not be formed when this temperature was used, probably because of heat induced cross-linking of the kafirin proteins. The films were cast as described.

Preparation of films from glutaraldehyde-treated kafirin microparticles

These were prepared by adding 10%, 20% and 30% (w/w) glutaraldehyde (Saarchem, Krugersdorp, South Africa) (as a proportion of protein) to 4.0 g film preparation mixtures in 25% acetic acid (pH 2.0). Reaction with glutaraldehyde was carried out at ambient temperature for 12 h and the films cast as described.

4.2.3.4 *SEM*

The film surfaces were examined using SEM as described (Taylor et al., 2009c). Strips of the films were mounted on an aluminium stub using a double-sided transparent tape, sputter-coated with gold and viewed using a Jeol JSM-840 Scanning Electron Microscope (Tokyo, Japan).

4.2.3.5 *SDS-PAGE*

Films were characterized by SDS-PAGE under reducing and non-reducing conditions. An X Cell SureLock™ Mini-Cell electrophoresis unit (Invitrogen Life Technologies, Carlsbad, CA, USA) was used with 15-well 1 mm thick pre-prepared Invitrogen NuPAGE® 4–12% Bis-Tris gradient gels. The loading was ≈10 µg protein. Invitrogen Mark12™ Unstained Standard was used. Proteins were stained with Coomassie® Brilliant Blue R250 overnight, destained and photographed.

4.2.3.6 *FTIR spectroscopy*

FTIR spectroscopy was performed as described (Taylor et al., 2009c). Briefly, the films were dried for a week in a desiccator. Then small pieces of the films were scanned in a Vertex 70v FT-IR spectrophotometer (Bruker Optik, Ettlingen, Germany), using 64 scans, 8 cm^{-1} band and an interval of 1 cm^{-1} in the Attenuated Total Reflectance (ATR) mode at wavenumber 600–4000 cm^{-1}. At least four replicates were performed for each treatment. The FTIR spectra were Fourier-deconvoluted with a resolution enhancement factor of 2 and a bandwidth of 12 cm^{-1}. The proportions of the α-helical conformations (≈1650 cm^{-1}) and the β-sheet structures (≈1620 cm^{-1}) were calculated by measuring the heights of the peaks assigned to the secondary structures on the FTIR spectra. The relative proportions of the α-helical conformations were calculated as described (section 4.1.3.9).

4.2.3.7 *Water vapour transmission (WVT) and water vapour permeability (WVP)*

These were measured using a modified method based on ASTM E96-97 method (American Society for Testing & Materials, 1997b) as described by Taylor et al. (2005b). Briefly, the thicknesses of the films were measured in five different places using the micrometer gauge (Braive Instruments) and the average calculated after conditioning the films for 72 h in a 50% relative humidity (RH) chamber. Cast films (31 mm diameter) were mounted on top of

modified Schott bottles containing distilled water to a level where the bottle neck had a constant diameter. The bottles with films secured at the top were placed in a forced draught incubator at 29^{o}C with an average RH of 16% over the period of the test. Weight loss was recorded daily for 12 days. Three replicate measurements were performed for each treatment. Graphs of water loss against time were plotted for each treatment and gradients of the best-lines-of-fit recorded. WVT was calculated by dividing the gradient of the line with the area of the film. The WVP was calculated thus:

$$\text{WVP} = \frac{(\text{gradient (g/h)} \times \text{thickness of film (mm)})}{\text{Area (m}^2) \times P_o \text{ (kPa)} \times (RH_1\text{-}RH_2)/100}$$

Where:

P_o = saturated vapour pressure at 25^{o}C = 3.17 kPa

RH_1 = Relative humidity inside the bottle (i.e. 100%)

RH_2 = Relative humidity outside the bottle

4.2.3.8 *Water stability*

Complete conventional cast kafirin films and kafirin microparticle films were immersed in water (22^{o}C) containing 0.02% (w/v) sodium azide in separate transparent plastic containers then mounted on an orbital shaker set at a gentle speed of 70 rpm and monitored over a period of 48 h. To determine the extent to which the films would maintain their physical integrity in water under vigorous shaking, complete films were immersed in distilled water containing sodium azide at 22°C, and then mounted on an orbital shaker set at speed of 300 rpm for 72 h. At the end of the shaking period, the films were visually assessed and photographed using a flatbed scanner in the plastic containers.

4.2.3.9 *Water uptake and weight loss of films in water*

These were measured according to Soliman et al. (2009) with some modification. Films (90 mm diameter) were dried in a desiccator for 72 h and then weighed. The dried films were immersed in distilled water for 24 h at 22^{o}C with gentle agitation on a rocking platform set at 30 rpm. The water on the film surfaces was removed by placing the films between paper towels and then weighed. The films were then dried in a desiccator as before and weighed again. The film water uptake and weight loss in water were calculated thus:

$$\% \text{ Water uptake} = \frac{(\text{Mass after immersion} - \text{Initial dry mass})}{\text{Initial dry mass}} \times 100$$

$$\% \text{ Weight loss in water} = \frac{(\text{Initial dry mass} - \text{Mass after immersion and drying})}{\text{Mass after immersion and drying}} \times 100$$

4.2.3.10 *Surface density*

Film surface density was measured based on the procedure of Soliman et al. (2009). Films (90 mm diameter) were weighed. The weight of each film was divided by its area to calculate the surface density (mg/cm^2).

4.2.3.11 *Tensile properties*

The films were conditioned at 50% relative humidity and 25°C for 72 h in a desiccator maintained using 4.99 M calcium chloride (Stokes and Robinson, 1949). Then the film strips 60 mm x 10 mm were cut. The thicknesses of the films were measured in five different places using a micrometer gauge (Braive Instruments, Hermalle-sous-Argenteau, Belgium) and the average calculated. Tensile properties of the films were studied as described (Taylor et al., 2005b), based on ASTM D882–97 method (American Society for Testing and Materials (ASTM), 1997a), using a TA-XT2 Texture Analyser (Stable Micro Systems, Goldalming, U.K.). For soaked films, the films were air-dried at ambient temperature for 30 min before measuring tensile properties.

4.2.3.12 *IVPD*

This was performed by a pepsin digestion procedure based on that of Hamaker et al. (1986). Prior to IVPD assay, the films were freeze-fractured in liquid nitrogen and ground into powder using a mortar and pestle. Accurately weighed film powder (10 mg) was digested with a P7000-100G pepsin (Sigma, Johannesburg, South Africa), activity 863 units/mg protein for 2 h at 37^{o}C and the products of the digestion were pippeted off. The residue was washed with distilled water and dried at 100^{o}C overnight. The residual protein was determined by Dumas nitrogen combustion method (AACC International, 2000) method 46-30. IVPD was calculated by the difference between the total protein and the residual protein after pepsin digestion divided by the total protein and expressed as a percentage.

4.2.3.13 *Statistical analyses*

All the experiments were repeated at least twice. The film FTIR, thickness, water vapour WVT, WVP, tensile properties, water uptake, weight loss in water, IVPD data were analysed by one-way analysis of variance (ANOVA). These measured parameters were the dependent variables while and heat, transglutaminase and glutaraldehyde treatments were the independent variables. Significant differences among the means were determined by Fischer's least significant difference (LSD) test. The calculations were performed using Statistica software version 10 (StatSoft, Tulsa, OK).

4.2.4 Results and discussion

4.2.4.1 *Water stability of conventional cast kafirin films and cast kafirin microparticle films*

Conventional cast kafirin films disintegrated into many small fragments in water, while the cast kafirin microparticle films remained largely intact (Figure 4.13). The better stability of kafirin microparticle films in water was probably due to changes in kafirin protein secondary structure during microparticle preparation. During the formation of kafirin microparticles, there is a reduction in the proportion of protein α-helical conformation, probably with corresponding increase in β-sheet conformation (Taylor et al., 2009a). Subirade, Kelly, Guéguen and Pézolet (1998) suggested that β-sheet conformation may be essential for protein-protein interactions and network formation in protein films from plant origins, whereby intermolecular H-bonding between β-sheets probably act as junction zones that stabilize the film network. Additionally, the characteristic presence of large voids within the kafirin microparticles, when prepared by coacervation (Taylor et al., 2009a) enhances protein solubility in the casting solution, probably thereby improving the film matrix cohesion. Because of the better water stability of cast kafirin films prepared from microparticles they were investigated further using various treatments: heat, transglutaminase and glutaraldehyde, to enhance this and other related film functional properties

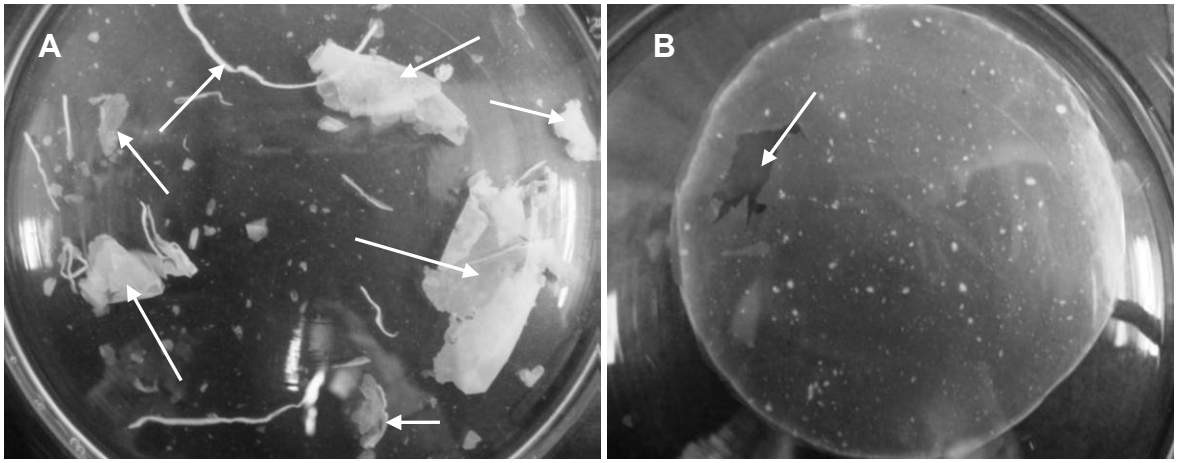

Figure 4.13 Appearance of kafirin films cast in acetic acid, after immersion in water for 48 h at room temperature with gentle shaking (70 rpm). Films photographed in transparent plastic tubs while immersed in water. **A**. Conventional kafirin film. Arrows point to film fragments. **B.** Kafirin microparticle film. Arrow points to torn section of film. (Pictures taken by Miss Amy J. Taylor on behalf of the candidate).

4.2.4.2 *Film physical appearance*

Treating kafirin microparticles with heat at moderate temperature (50^{o}C) did not change the clarity of the films made from them (Figure 4.14A- b). However, when viewed by SEM the film surfaces were rough (Figure 4.14A- f). Higher temperature treatment (75^{o}C and 96^{o}C) resulted in the formation of opaque and incomplete films (arrows, Figure 4.14A- c, d). These films had a rough surface and the microparticles were poorly fused. The outline of individual microparticle shapes was clearly visible with gaps in between them (arrows, Figure 4.14A-g, h), which was similar to the appearance of biomaterials made from zein microparticles such as films (Dong et al., 2004) and sponges (Wang et al., 2008). Byaruhanga et al. (2005) working on cast films prepared from microwave-heated kafirin reported formation of films with rough surface and, attributed this to undissolved lumps of kafirin. Likewise, in the present study the poor fusion of the heated kafirin microparticles was probably due to reduction in their solubility in the aqueous acetic acid casting solution. Hamaker et al. (1986) suggested that the reduction in solubility of kafirin proteins as a result of thermal treatment is probably due to disulphide cross-linking of kafirin proteins.

In contrast, transglutaminase-treated kafirin microparticle films were as clear as their control (Figure 4.14B, i–l). However, these films had a rough surface when viewed by SEM (Figure 4.14B, m–p), indicating poor fusion of the microparticles.

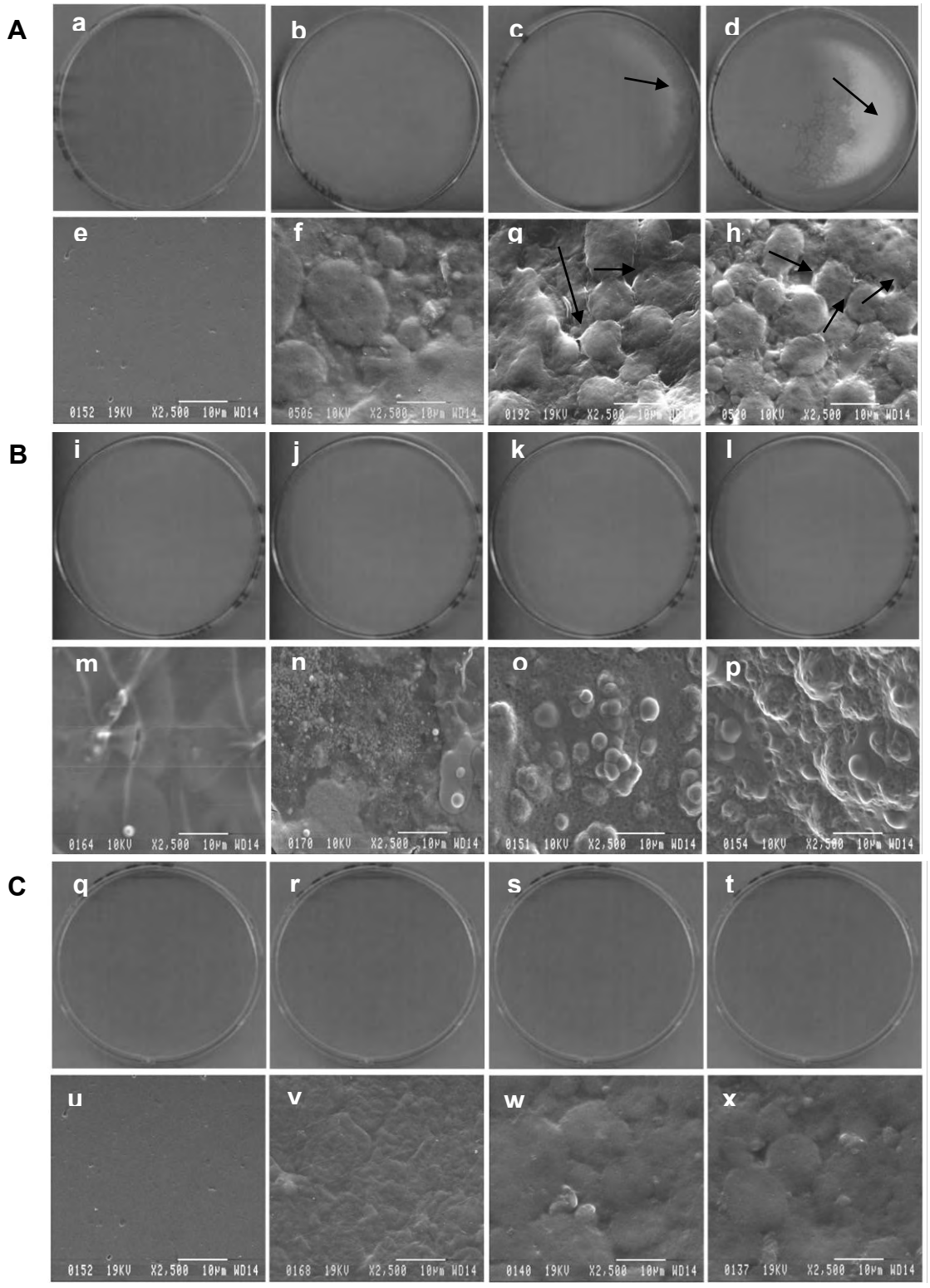

Figure 4.14 Physical appearance of films prepared from treated kafirin microparticles. **A.** Heat treatment. a-d: photographs, e-h: SEM. **a, e** - control; **b, f** - 50°C; **c, g** - 75°C; **d, h** - 96°C. Arrows: **c, d**- opaque incomplete sections; **g, h** –gaps. **B.** Transglutaminase (TG) treatment. i-l: photographs; m-p: SEM. **i, m** - Maltodextrin; **j, n** - 0.1% TG + Maltodextrin; **k, o** - 0.3% + Maltodextrin; **l, p** - 0.6% TG + Maltodextrin. **C.** Glutaraldehyde treatment. q-t: photographs, u-x: SEM. **q, u** - control; **r, v** - 10%; **s, w** - 20%; **t, x** - 30%.

Tang, Jiang, Wen, Yang (2005) also reported a rough and uneven surface of films prepared from transglutaminase-treated SPI. In the present study, Maillard reaction due to the presence of maltodextrin may have caused poor solubility of the microparticles, thereby resulting in the uneven film surface.

Treating kafirin microparticles with glutaraldehyde did not change the clarity of the films, irrespective of the concentration of glutaraldehyde (Figure 4.14C, q–t). However, these glutaraldehyde-treated kafirin microparticle films were slightly rough (Figure 4.14C, v–x), probably due to reduction in solubility of the kafirin microparticles as a result of glutaraldehyde cross-linking of the kafirin proteins. Notwithstanding this, the glutaraldehyde-treated kafirin microparticles were clearly better fused than the heat-treated and transglutaminase-treated microparticles.

4.2.4.3 *Film chemical structure*

SDS-PAGE under non-reducing and reducing conditions of films prepared from heat-treated kafirin microparticles and untreated control had highest band intensity at 16–28 kDa (Figure 4.15A), which are the monomeric α-, β- and γ- kafirins (Shull et al., 1991). In addition, bands of approximately 42–58 kDa and 61–88 kDa, identified as dimers and trimers, respectively (El Nour et al., 1998), were present in all the films, indicative of kafirin polymerization. Treating kafirin microparticles with heat did not result in any change in band pattern with SDS-PAGE under non-reducing conditions. This was probably because despite the differences in heat treatment temperatures, all the film-forming mixtures were subjected to 50^{o}C for a long time (12 h) during evaporation to prepare the films. With heat treatment at 96^{o}C some oligomers (≈94–183 kDa) (arrow in Figure 4.15A, lane 4 under reducing conditions) resistant to reduction by mercaptoethanol remained. These may be attributed to concealed covalent cross-links induced by heat that are inaccessible to the reducing agent, as suggested by Duodu et al. (2003).

Despite changes in the physical appearance of films, there was no evidence of transglutaminase-induced kafirin polymerization (Figure 4.15B). This was probably because kafirin has very low lysine content (Belton et al., 2006), which renders it a poor substrate for the transglutaminase reaction that produces ε-(γ-glutamyl)-lysine bridges. For a lysine-poor protein, the transglutaminase-catalysed protein reaction may progress through deamidation, an alternative reaction pathway (Larré, Chiarello, Blanloeil, Chenu and Gueguen, 1993).

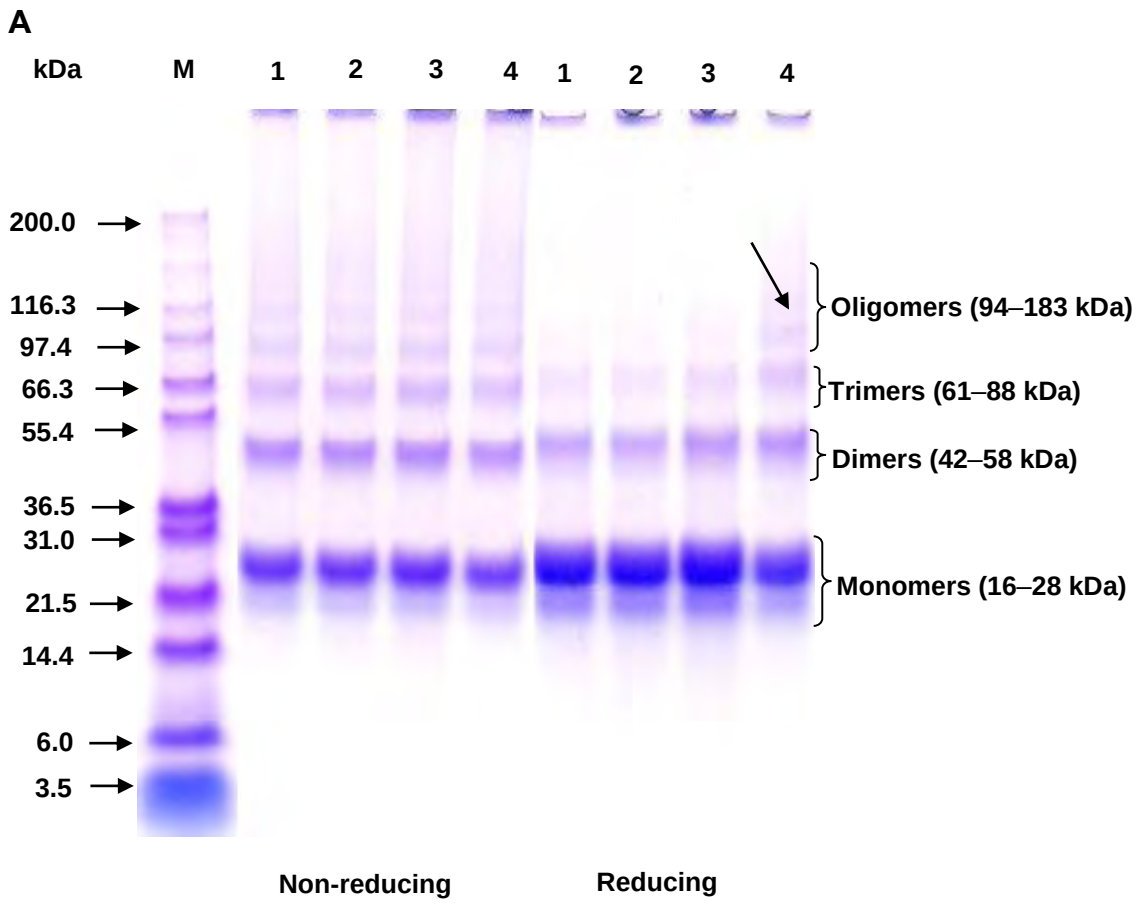

Figure 4.15 SDS-PAGE of films prepared from treated kafirin microparticles. Protein loading, 10 µg.

A. Heat treatment. Lanes M: Molecular markers; 1: Control (22ºC); 2: 50ºC; 3: 75ºC; 4: 96ºC. Arrow: reduction-resistant oligomers.

B. Transglutaminase (TG) treatment. Lanes M: Molecular markers; 1: Maltodextrin; 2: 0.1% TG + Maltodextrin; 3: 0.3% TG + Maltodextrin; 4: 0.6% TG + Maltodextrin.

C. Glutaraldehyde treatment. Lanes M: Molecular markers; 1: Control; 2: 10%; 3: 20%; 4: 30%.

B

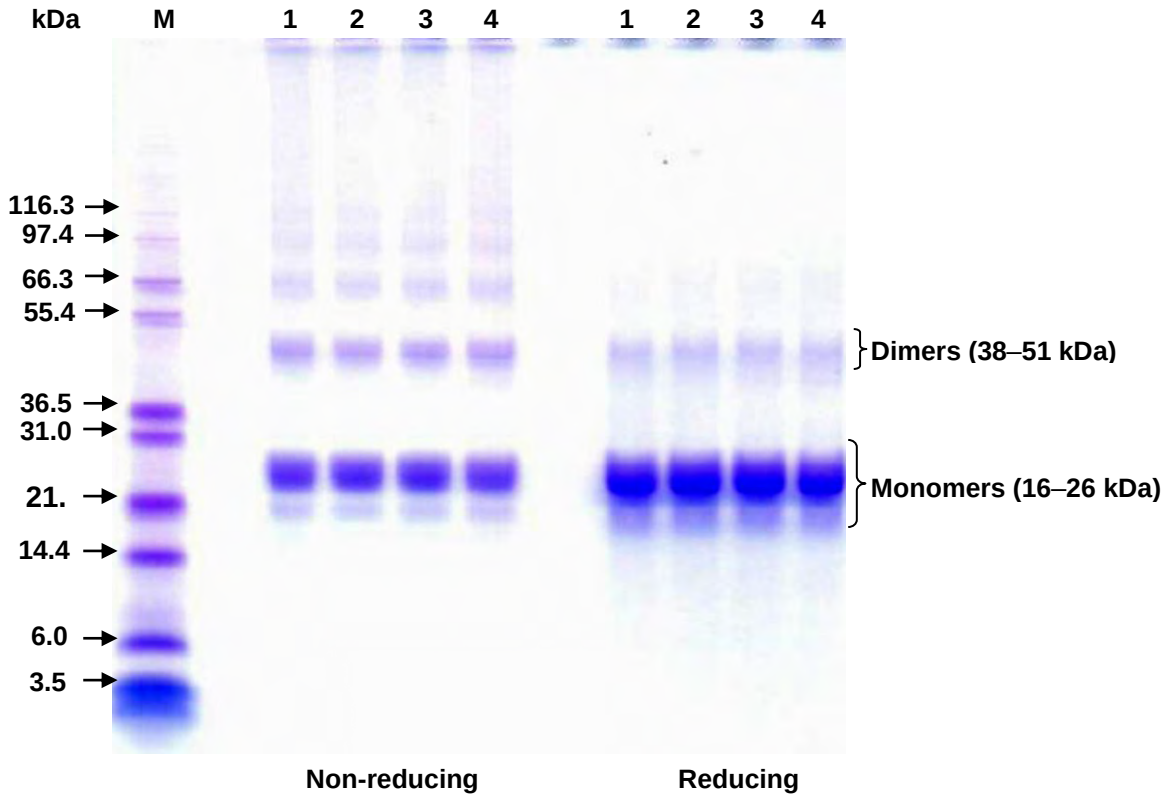
kDa
M
1
2
3
4
1
2
3
4
116.3
97.4
66.3
55.4
36.5
31.0
21.
14.4
6.0
3.5
Dimers (38–51 kDa)
Monomers (16–26 kDa)
Non-reducing
Reducing

C

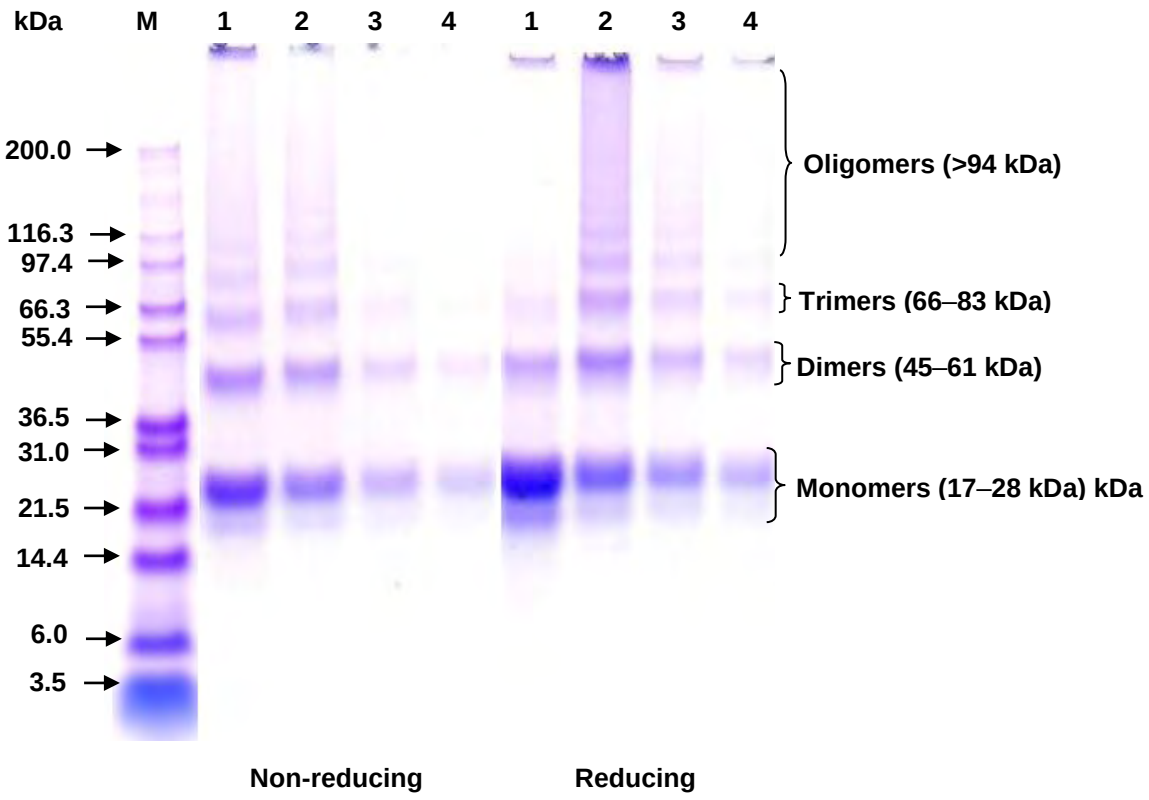
kDa
M
1
2
3
4
1
2
3
4
200.0
116.3
97.4
66.3
55.4
36.5
31.0
21.5
14.4
6.0
3.5
Oligomers (>94 kDa)
Trimers (66–83 kDa)
Dimers (45–61 kDa)
Monomers (17–28 kDa) kDa
Non-reducing
Reducing

The results in the present study are consistent with those of Motoki, Seguro, Nio and Takinami (1986) working on glutamine-specific deamidation of α_{s1}-casein by transglutaminase, who found no changes in molecular weights. Similarly, Flores, Cabra, Quirasco, Farres and Galvez (2010) working on maize protein isolate emulsions found a similar electrophoretic band pattern for deamidated and non-deamidated emulsions, despite their difference in emulsion stability. The fact that films prepared from transglutaminase-treated kafirin microparticles were rough (Figure 4.14B, n–p) may be attributed to an increase in negative charges in the kafirin due to deamidation, probably making the microparticles less soluble in the acetic acid casting solution.

Glutaraldehyde treatment of the kafirin microparticles resulted in the reduction in monomer (17–28 kDa), dimer (45–61 kDa), trimer (66–83 kDa) and oligomer (>94 kDa) band intensities with the SDS-PAGE under non-reducing conditions (Figure 4.15C). With SDS-PAGE under reducing conditions, there was an increase in intensities of dimer, trimer and oligomer bands for 10% glutaraldehyde treatment (Figure 4.15C, lane 2), indicating the presence of polymerized kafirin proteins. The presence of polymerized kafirin under reducing conditions was expected as cross-links with glutaraldehyde are formed between free amino groups of peptide chains and the carbonyl groups of the aldehyde (Migneault et al., 2004) and not disulphide linkages. Similar protein polymerization through non-disulphide bonding was reported by Sessa, Mohamed and Byars (2008) working on zein films treated with glutaraldehyde. Treatments with higher glutaraldehyde concentrations (20% and 30%) resulted in the monomer, dimer and trimer bands being much fainter and an almost complete absence of oligomer bands. These observations indicate the formation of highly polymerized kafirin polymers of MW > 200 kDa at higher glutaraldehyde concentrations, which were too large to migrate into the separating gel. A similar result was reported by Reddy et al. (2008) who found disappearance of molecular weight bands, when they cross-linked pre-formed wheat gluten fibres with high concentration of glutaraldehyde.

With regard to protein secondary structure, treating the kafirin microparticles with heat decreased the relative proportion of α-helical conformation in the films by up to 11%, at the Amide I band (wavenumber ≈1650–1620 cm^{-1}) (Table 4.4), as determined by FTIR. There was a decrease in the relative proportion of α-helical conformation with increase in heating temperature. Byaruhanga et al. (2006) reported a similar decrease in proportion of α-helical conformation with concomitant increase in β-sheet conformation when they heated kafirin

and kafirin film with microwave energy. Similarly, Emmambux and Taylor (2009) reported a reduction in α-helical conformation when they studied the protein secondary structure of cooked kafirin. It has been suggested that during thermal treatment the hydrogen bonds stabilizing protein structure are disrupted, causing loss of the α-helical and β-sheet conformation and creating new β-sheet arrangements (Duodu et al., 2001). Loss of α-helical conformation can be indicative of protein aggregation (Mizutani et al., 2003). In the present study, the relative proportion of α-helical conformation in the Amide I band for control films was 53.9%. Taylor et al. (2009c) reported a lower percentage (50.5%) for similar kafirin microparticle films. These differences can be attributed to the kafirin batch variations. Such differences have been reported previously by Taylor et al. (2009a), when they compared the proportion of α-helical conformation in their study with the data by Gao et al. (2005) on kafirin extracted and dried under similar conditions.

Table 4.4 Effects of treating kafirin microparticles with heat, transglutaminase and glutaraldehyde on the protein secondary structure of films prepared from them, as determined by FTIR

Treatment		Relative proportion of α-helical conformation at Amide I band (%)
Control	22ºC	53.9 e (0.1)
Heat		
	50ºC	52.2 d (0.9)
	75ºC	50.7 c (0.1)
	96ºC	48.0 a (0.6)
Transglutaminase		
	Maltodextrin	50.8 c (0.7)
	0.1% TG + Maltodextrin	50.4 c (0.4)
	0.3% TG + Maltodextrin	49.3 b (0.3)
	0.6% TG + Maltodextrin	48.5 a (0.5)
Glutaraldehyde		
	10%	50.6 c (0.5)
	20%	51.0 c (0.9)
	30%	52.2 d (0.3)

Values followed by different superscript letters are significantly different ($p<0.05$). Numbers in the parentheses are standard deviations (n=4). Control for heat and glutaraldehyde treatments is the same. Amide I band (≈1650–1620 cm^{-1}). TG- Transglutaminase

Transglutaminase treatment of kafirin microparticles resulted in up to 5% reduction in the relative proportion of α-helical conformation with respect to control films with maltodextrin treatment. As with heat treatment, there was a progressive decrease in the relative proportion of α-helical conformation with increase in concentration of transglutaminase. This was probably due to transglutaminase-induced deamidation of kafirin proteins, as discussed. In a similar study using proteins from soymilk residue, Chan and Ma (1999) also found a reduction in the α-helical conformation with acid-induced deamidation. Similarly, working on gluten, Matsudomi, Kato and Kobayashi (1982) reported a decrease in α-helical conformation with increase in deamidation. Wagner and Gueguen (1995) proposed that a reduction in proportion of α-helical conformation as a result of deamidation may be caused mainly by the increased electrostatic repulsion and the decreased hydrogen bonding.

In contrast to the trend with heat and transglutaminase treatments, there was a progressive increase in the relative proportion of α-helical conformation with increase in glutaraldehyde concentration. Selling, Woods, Sessa and Biswas (2008) reported a similar increase in α-helical conformation of zein fibres treated with glutaraldehyde. As with transglutaminase treatment, the changes in the protein secondary structure due to treatment with glutaraldehyde were generally small compared to heat treatment. This is consistent with findings by Caillard et al. (2009) on soy protein hydrogels cross-linked using glutaraldehyde, which showed changes in gel physical appearance and functional properties that were not reflected to the same extent by alterations in the protein secondary structure.

4.2.4.4 *Film functional properties*

Film WVT and WVP

Heat treatment resulted in films 20–29% thicker than their control (Table 4.5). However, these films were still thinner than those reported in similar studies. For example, the films reported by Sessa et al. (2007) were about 30 times in thickness compared to the kafirin microparticle films in the present study. The WVT of the films prepared from all the treated kafirin microparticles was generally similar to that of the control. The WVT values were within the range reported for unmodified kafirin microparticle films (Taylor et al., 2009c) and whey proteins films (Kaya and Kaya, 2000). Treating kafirin microparticles with heat resulted in films that were 20–29% thicker than their control.

Table 4.5 Effects of treating kafirin microparticles with heat, transglutaminase glutaraldehyde on the thickness, water vapour transmission (WVT) and water vapour permeability (WVP) of films

Treatment		Thickness (μm)	WVT ($g\ h^{-1}\ m^{-2}$)	WVP ($g\ mm\ m^{-2}\ h^{-1}\ kPa^{-1}$)
Control	22°C	16.3 ab (1.0)	33.0 a (3.2)	0.17 a (0.01)
Heat				
	50°C	20.3 c (0.9)	34.9 ab (1.3)	0.22 b (0.01)
	75°C	19.6 bc (0.3)	38.4 b (0.8)	0.24 b (0.00)
	96°C	21.0 c (0.4)	34.5 ab (2.9)	0.23 b (0.02)
Transglutaminase				
	Maltodextrin	22.7 cd (3.3)	34.0 ab (3.9)	0.24 b (0.01)
	0.1% TG + Maltodextrin	25.3 de (0.3)	37.9 b (1.6)	0.30 c (0.01)
	0.3% TG + Maltodextrin	28.0 e (1.1)	34.5 ab (0.0)	0.30 c (0.01)
	0.6% TG + Maltodextrin	26.5 e (0.6)	34.5 ab (0.1)	0.29 c (0.01)
Glutaraldehyde				
	10%	16.3 ab (2.4)	31.5 a (1.3)	0.16 a (0.03)
	20%	15.8 a (1.7)	33.0 a (3.2)	0.16 a (0.01)
	30%	16.1 ab (3.6)	33.0 a (1.3)	0.17 a (0.03)

Values in the same column but with different letters are significantly different ($p<0.05$). Numbers in parentheses are standard deviations (n=3). Control for heat and glutaraldehyde treatments is the same. TG- Transglutaminase

These differences in thickness were reflected by the roughness of the film surfaces noted using SEM (Figure 4.14). The WVP of the heat-treated kafirin microparticle films was higher by 29–41% compared to the control, probably because these films were thicker, therefore they probably had more pinholes. A linear increase in WVP with film thickness has been reported by Park and Chinnan (1995), which may be attributed to changes in film structure due to thickness as well as swelling of hydrophobic films, which may alter their structure too. Similar results were reported by Taylor et al. (2009c) who found that thicker kafirin films had higher WVP than thinner kafirin microparticle films. In addition, the fact that the heat treatment resulted in gaps especially at higher temperature (Figure 4.14A- g, h) may have led to increase in WVP.

As with heat treatment, treating the kafirin microparticles with transglutaminase increased the thickness of the films, probably because the films were rough as result of the poor fusion of the microparticles with transglutaminase. The WVP of the films increased by 11–23% as a result of transglutaminase treatment. As with the heat treatment, the poor fusion of the

transglutaminase-treated kafirin microparticles may have resulted in the increase in film WVP. When compared to the other treatments, the WVP for films prepared from transglutaminase-treated kafirin microparticles were 25–88% higher. This is probably because the suggested excess negative charges resulting from transglutaminase-induced deamidation of kafirin may have caused electrostatic repulsion within the film matrix leading to greater interstitial spacing than with the other treatments, thereby resulting in higher WVP.

Glutaraldehyde treatment did not change the thickness or the WVP of the films, despite the fact that the films were rougher than the control as observed by SEM (Figure 4.14). Micard, Belamri, Morel and Guilbert (2000) also found no change in the WVP of gluten films treated with formaldehyde. In the present study, formation of additional non-disulphide covalent cross-links as result of the treatment with the glutaraldehyde may be a reason for the similarity in WVP. Chambi and Grosso (2006) proposed that bonding at molecular level, which stabilizes the protein network, could compensate for morphological differences in influencing the film functional properties.

Film water stability, water uptake and weight loss in water

Treating the kafirin microparticles with transglutaminase resulted in poor water stability of the kafirin microparticle films (Figure 4.16A), probably due to the poor fusion of the kafirin microparticles (Figure 4.14B). In addition, the poor water stability of the films prepared from transglutaminase-treated kafirin microparticles was also probably due to transglutaminase-induced deamidation. In contrast, treating kafirin microparticles with glutaraldehyde resulted in films that were resistant to disintegration in water (Figure 4.16B). SEM of the films after soaking in water for 72 h with vigorous agitation (Figure 4.17) showed the presence of fewer holes (arrows in Figure 4.17) in the films prepared from glutaraldehyde-treated kafirin microparticles, indicating that less physical damage occurred. There was an increase in film stability in water with increasing glutaraldehyde concentration. Increase in water stability has been reported when glutaraldehyde is used to modify a number of similar protein biomaterials such as zein films (Sessa et al., 2007), gliadin films (Hernández-Muñoz et al., 2005), zein fibres (Selling et al., 2008) and gluten fibres (Reddy et al., 2008).

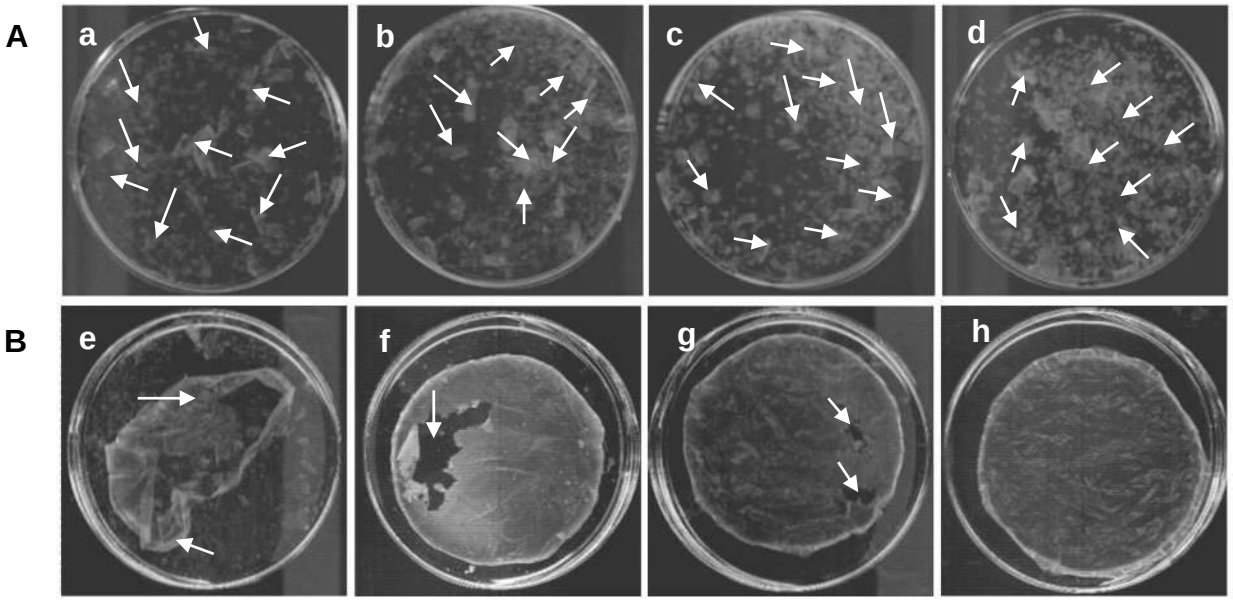

Figure 4.16 Water stability of films prepared from treated kafirin microparticles. The films were photographed in Petri dishes in water: **A.** Transglutaminase (TG) treatment (a–d). **a**: Maltodextrin; **b**: 0.1% TG + Maltodextrin; **c**: 0.3% TG + Maltodextrin; **d**: 0.6% TG + Maltodextrin. Arrows: film fragments. **B.** Glutaraldehyde treatment (e–h). **e**: Control; f: 10%; **g**: 20%; **h**: 30%; Arrows- **e**: fragmented film; **f, g**: disintegrated section of film. Heat treatment resulted in incomplete films hence no data was obtained as complete films were required for a meaningful comparison.

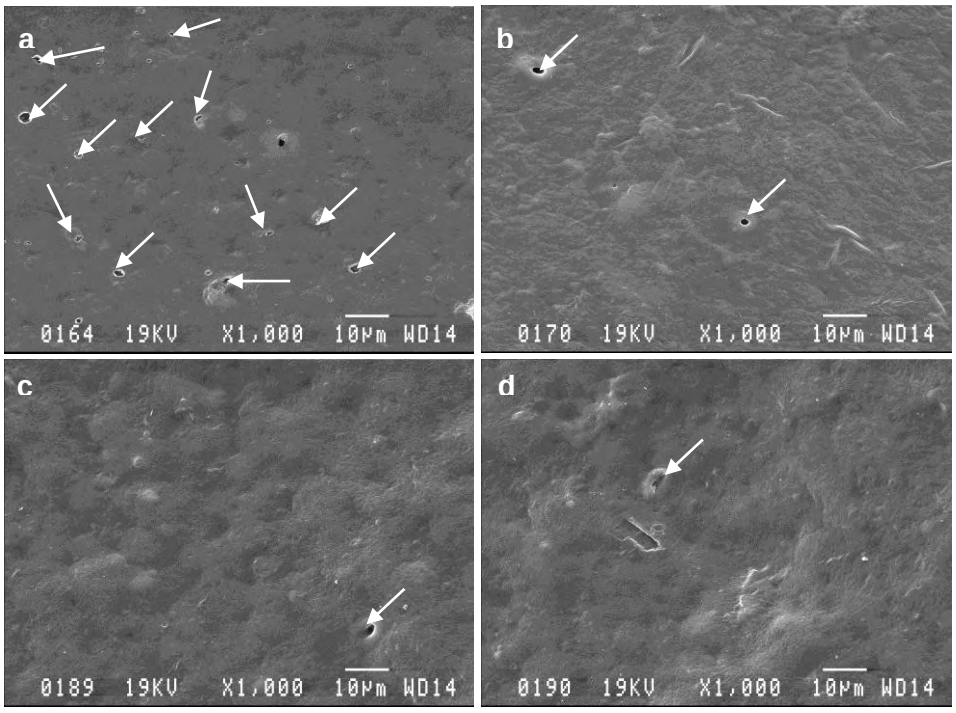

Figure 4.17 SEM of kafirin microparticle films after vigorous agitation in water for 72 h at 22^{o}C: **a**: Control; **b**: 10% GTA; **c**: 20% GTA; **d**: 30% GTA. Arrows point to the holes probably caused by physical damage by water agitation. GTA- Glutaraldehyde.

An interesting finding in the present study was that the glutaraldehyde-treated microparticle films maintained their integrity in water. This was despite the fact that they were several magnitudes thinner than the biomaterials reported in these previous studies. Glutaraldehyde treatment resulted in reduction of both film water uptake and film weight loss in water (Table 4.6). Similar reductions in film water uptake and weight loss in water as result of glutaraldehyde treatment has been reported by Orliac, Rouilly, Silvestre and Rigal (2002) working on sunflower protein isolate films. Likewise, glutaraldehyde treatment has been shown to cause reductions in weight loss in water with gliadin films (Hernández-Muñoz et al., 2005). As kafirin is a relatively hydrophobic protein (Duodu et al., 2003), the weight loss in water of the kafirin microparticle films was mainly due to loss of plasticizer through diffusion into the water. This is consistent with the fact that the film weight loss in water was equivalent to 88–95% of the plasticizer content. It has been shown that protein film weight loss in water corresponds to hydrophilic plasticizer content (Hernández-Muñoz et al., 2005). The reduction in film water uptake or weight loss in water as a result of glutaraldehyde treatment is probably due to the covalent bonding leading to the formation of a more stable cross-linked network resistant to water. Reddy et al. (2008) proposed two reasons for improvement in film water stability after treatment with glutaraldehyde. First, treatment with glutaraldehyde may result in fewer hydrophilic groups. This is because there is preferential reaction of the aldehydes with the free amino groups of the basic amino acids, which are the primary water-bonding sites on proteins. Second, the formation of higher molecular weight proteins by glutaraldehyde treatment may result in better water resistance. This latter explanation concurs with SDS-PAGE findings (Figure 4.15C), which showed presence of polymerized proteins in glutaraldehyde-treated kafirin microparticle films.

Table 4.6 Effects of glutaraldehyde treatment on the water uptake and weight loss in water of kafirin microparticle films

Glutaraldehyde treatment	Water Uptake of film (g/100 g dry film)	Film Weight Loss in water (g/100 g dry film)
Control	29.2 c (0.4)	31.8 b (0.6)
10%	27.0 b (1.2)	29.9 a (0.9)
20%	26.0 b (0.9)	29.3 a (0.4)
30%	23.4 a (1.4)	29.1 a (0.3)

Values in the same column but with different letters are significantly different ($p<0.05$). Numbers in parentheses are standard deviations (n=3).

As shown (Figure 4.14A), treating kafirin microparticles with heat resulted in formation of incomplete films, especially when subjected to higher temperature treatments. Therefore, no data was obtained from water resistance tests for heat cross-linked films, as complete films were required for a meaningful comparison. In addition, as transglutaminase treatment resulted in poor water stability of the films (Figure 4.16A), the determination of water uptake and weight loss in water was not feasible for these films.

Film tensile properties before and after soaking

There was a progressive reduction in maximum stress with increase in treatment temperature (Figure 4.18A; Table 4.7). The reduction in film maximum stress was probably because, as noted by SEM (Figure 4.14A), these films had poorly fused microparticles, indicating poor structural cohesion of film matrix. Similarly, transglutaminase treatment resulted in a 24-53% reduction in film maximum stress, with respect to control films with maltodextrin treatment (Figure 4.18B, Table 4.7). As with heat treatment, the poor fusion of the microparticles due to treatment with transglutaminase (Figure 4.14B) could probably be a reason for weakness of these films. In addition, transglutaminase induced deamidation may have been a contributing factor.

Surface density was determined for glutaraldehyde-treated kafirin microparticle films, as they showed evidence of stability in water. Glutaraldehyde treatment slightly increased the film surface density, while it resulted in varied effects on film tensile strength, depending on concentration of glutaraldehyde (Table 4.7; Figure 4.18C). With 10% glutaraldehyde treatment, there was a 43% increase in film maximum tensile stress, and 58% increase in maximum strain. However, at higher glutaraldehyde concentration (20% and 30%), there was a 42–43% reduction in film breaking stress. This was accompanied by about four-fold increase in maximum strain. Increase in the film maximum stress as a result of glutaraldehyde treatment is presumably due to formation of additional cross-links, as discussed. Similar increases in protein film tensile strength have been reported when glutaraldehyde is used to cross-link many proteins, such as gliadin (Hernández-Muñoz et al., 2005), zein (Parris and Coffin, 1997; Sessa et al., 2007) and sunflower protein isolate (Orliac et al., 2002). On the other hand, the fact that there was a reduction in maximum stress accompanied by increase in maximum strain at higher glutaraldehyde concentration was probably due to a plasticizing effect of excess glutaraldehyde molecules in the protein network.

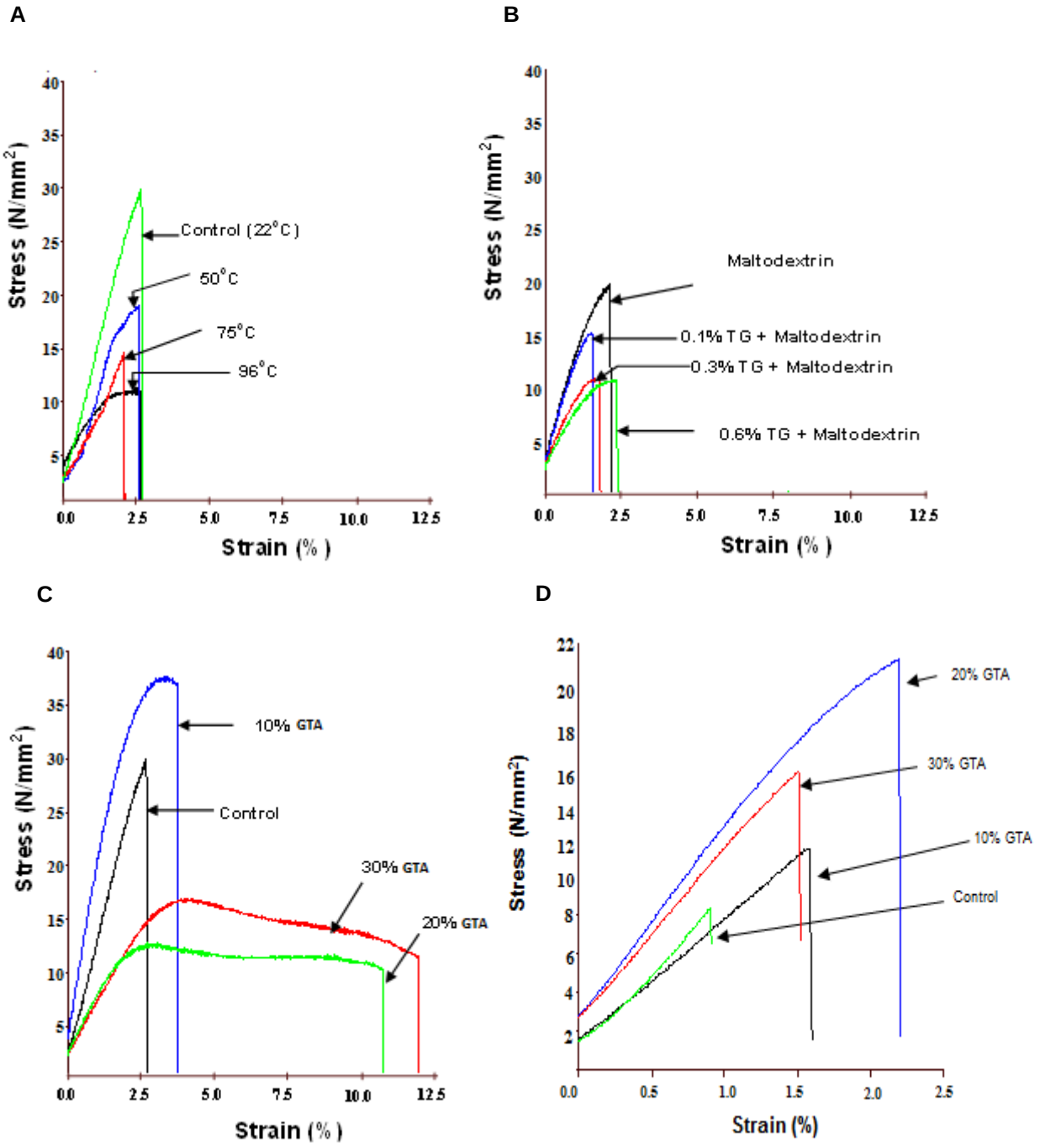

Figure 4.18 Typical stress-strain curves of films prepared from treated kafirin microparticles determined by a TA-XT2 Texture Analyser. **A**. Heat treatment. **B**. Transglutaminase (TG) treatment. **C.** Glutaraldehyde (GTA) treatment. **D**. Effect of glutaraldehyde treatment on tensile properties of kafirin microparticle films after soaking in water.

Table 4.7 Effects of treating kafirin microparticles with heat, transglutaminase and glutaraldehyde on the surface density, tensile properties and *in vitro* protein digestibility (IVPD) of films made from them

Treatment		Surface Density (mg/cm^2)	Maximum Stress (N/mm^2)	Maximum Strain (%)	IVPD (%)	IVPD* (Percentage of control)
	Before soaking in water					
Control	22°C	3.42 a (0.01)	24.3 e (5.2)	2.6 a (0.2)	37.7 e (0.8)	
Heat						
	50°C		18.6 cd (0.7)	3.5 ab (1.1)	37.1 e (0.3)	98.4
	75°C		13.5 ab (0.5)	2.6 ab (0.6)	36.6 de (0.2)	97.1
	96°C		10.7 a (1.4)	3.0 ab (0.4)	35.0 cd (0.8)	92.8
Transglutaminase						
	Maltodextrin		19.7 d (1.1)	2.5 a (0.5)	34.0 bc (0.6)	90.2
	0.1% TG + Maltodextrin		15.0 bc (0.5)	2.1 a (0.6)	32.8 b (1.2)	87.0
	0.3% TG + Maltodextrin		10.2 a (1.2)	2.1 a (0.4)	31.0 a (1.0)	82.2
	0.6% TG + Maltodextrin		9.3 a (0.2)	2.0 a (0.6)	30.3 a (0.4)	80.4
Glutaraldehyde						
	10%	3.45 ab (0.02)	34.8 f (3.7)	4.1 b (0.4)	39.7 f (0.9)	105.3
	20%	3.49 b (0.02)	13.9 b (2.1)	12.2 c (0.4)	40.7 fg (1.2)	108.0
	30%	3.56 c (0.04)	14.2 b (2.6)	13.9 d (2.1)	42.2 h (0.2)	111.9
	After soaking films in water for 24 h and drying in air at room temperature for 30 min					
Glutaraldehyde						
	Control		6.6 a (2.2)	0.8 a (0.2)		
	10%		11.8 b (1.1)	1.6 b (0.2)		
	20%		16.2 b (4.4)	1.7 b (0.5)		
	30%		12.7 b (4.2)	1.7 b (0.4)		

Values in a column followed by different letters are significantly different ($p<0.05$). Numbers in the parentheses are standard deviations (n=3). Control for heat and glutaraldehyde treatments is the same. TG- Transglutaminase. * Values calculated from the mean IVPD values expressed as per cent of IVPD of control 22°C.

Similar results were reported by Marquié et al. (1997) working on cottonseed protein films who noted a decrease in film maximum puncture force. Likewise, increase in elongation at break has been reported for other protein films cross-linked using glutaraldehyde such as zein films (Parris and Coffin, 1997). Marquié et al. (1997) proposed that molecular structure of the long methylene bridges formed between the glutaraldehyde cross-linked proteins may lead to a decrease in the intermolecular forces between polypeptide chains.

Concerning the tensile properties of films that had been soaked for 24 h in water, glutaraldehyde treatment resulted in retention of far higher tensile strength than the control (Table 4.7; Figure 4.18D). This agrees with the data on film water stability (Figures 4.16B and 4.17), water uptake and weight loss in water (Table 4.6), which showed that glutaraldehyde treatment resulted in kafirin microparticle films with better integrity even after soaking in water. These data on tensile strength retention compare favourably with published data for similar glutaraldehyde treatments, despite the differences in type of protein from which the film is prepared and film thickness. For example, in the study by Sessa et al. (2007) tensile strength of soaked zein films was ≈31% of the pre-soaked film tensile strength with 8% glutaraldehyde treatment, which compares closely with 34% obtained with 10% glutaraldehyde treatment in the present study. Better retention of tensile strength after soaking in water has also been reported for other glutaraldehyde-treated biomaterials such as gluten fibres (Reddy et al., 2008). The tensile strain of kafirin microparticle films was reduced after soaking in water, probably due to the washing out of the plasticizer. No data were obtained for heat and transglutaminase treatments as they produced films that were not useful for tensile test after soaking.

Film IVPD

Heat treatment of kafirin microparticles slightly reduced the IVPD of the films made from them (Table 4.7). Byaruhanga et al. (2005) reported a reduction in IVPD of cast kafirin films as a result of heat treatment. Reduction in IVPD of wet heated-kafirin is a known phenomenon, which is attributed to disulphide cross-linking (Duodu et al., 2003). However, in the present study, the small IVPD reduction may be attributed the prolonged heat treatment for all the films as discussed. As with heat treatment, treating kafirin microparticles with transglutaminase reduced film IVPD. A reduction in protein digestibility has been reported for soy protein isolate treated with transglutaminase (Tang, Li, Yang, 2006). The film IVPD

was lower with transglutaminase treatment than with heat treatment. This is probably due to the fact maltodextrin (a carbohydrate), which is the transglutaminase enzyme carrier base constituting 99% of the enzyme material, may interact with kafirin (a protein) through Maillard reaction, thereby reducing further the IVPD.

On the contrary, treatment with glutaraldehyde increased the IVPD of the kafirin microparticle films by up to some 12%. The increase in protein digestibility as a result of glutaraldehyde treatment may probably be due to an increase in void volume. Migneault et al. (2004) suggested that it is polymeric forms of glutaraldehyde (polyglutaraldehydes) that are involved in the cross-linking of proteins. These glutaraldehyde polymers may form long distance methylene bridges between protein chains, probably creating easier access of the pepsin enzyme to the peptide bonds in the kafirin. Overall, the changes in IVPD of the kafirin microparticle films as a result of all the three treatments were not large compared to the control (maximum of 20% change). This was probably because irrespective of the treatments, all the film-forming mixtures were subjected to the same relatively high temperature (50^{o}C) for a long time (12 h) during solvent evaporation.

4.2.5 Conclusions

Thin kafirin films cast from microparticles are more stable in water than conventional cast kafirin films. Glutaraldehyde treatment of the thin kafirin microparticle films renders them quite stable in ambient temperature water, despite the loss of plasticizer. Thus, glutaraldehyde-treated kafirin microparticle films appear to have good potential for use as thin biomaterials in aqueous applications.

4.2.6 References

American Association of Cereal Chemists (AACC International), 2000. Crude protein-combustion, Standard Method 46-30. Approved Methods of the AACC (10th ed.). The Association: St Paul, MN.

American Society for Testing and Materials (ASTM), 1997a. Annual Book of the ASTM Standards. ASTM D882-97: Standard method for tensile properties of thin plastic sheeting. The Society: West Conshohocken, PA.

American Society for Testing and Materials (ASTM), 1997b. Annual Book of the ASTM Standards. ASTM E96-97: Standard test methods for water vapor transmission of materials. The Society: West Conshohocken, PA.

Ando, H., Adashi, M., Umeda, K., Matsuura, A., Nonaka, M., Uchio, R., Tanaka, H., Motoki, M., 1989. Purification and characteristics of a novel transglutaminase derived from microorganisms. Agricultural and Biological Chemistry 53, 2613−2617.

Belton, P.S., Delgadillo, I., Halford, N.G., Shewry, P.R., 2006. Kafirin structure and functionality. Journal of Cereal Science 44, 272–286.

Bourtoom, T., 2009. Edible protein films: properties enhancement. International Food Research Journal 16, 1−9.

Byaruhanga, Y.B., Erasmus, C., Taylor, J.R.N., 2005. Effect of microwave heating of kafirin on the functional properties of kafirin films. Cereal Chemistry 82, 565−573.

Byaruhanga, Y.B., Emmambux, M.N., Belton, P.S., Wellner, N., Ng, K.G., Taylor, J.R.N., 2006. Alteration of kafirin film structure by heating with microwave energy and tannin complexation. Journal of Agricultural and Food Chemistry 54, 4198−4207.

Caillard, R., Remondetto, G.E., Subirade, M., 2009. Physicochemical properties and microstructure of soy protein hydrogels co-induced by Maillard type cross-linking and salts. Food Research International 42, 98–106.

Chambi, H., Grosso, C., 2006. Edible films produced with gelatin and casein cross-linked with transglutaminase. Food Research International 39, 458–466.

Chan, W.-M., Ma, C.-Y., 1999. Acid modification of proteins from soymilk residue (okara). Food Research International 32, 119−127.

Dong, J., Sun, Q., Wang, J.Y., 2004. Basic study of corn protein, zein, as a biomaterial in tissue engineering, surface morphology and biocompatibility. Biomaterials 25, 4691–4697.

Duodu, K.G., Taylor, J.R.N., Belton, P.S., Hamaker, B.R., 2003. Factors affecting sorghum protein digestibility. Journal of Cereal Science 38, 117−131.

Duodu, K.G., Tang, H., Wellner, N., Belton, P.S., Taylor, J.R.N., 2001. FTIR and solid state ^{13}C NMR spectroscopy of proteins of wet cooked and popped sorghum and maize. Journal of Cereal Science 33, 261−269.

El Nour, N.A., Peruffo, A.D.B., Curioni, A., 1998. Characterisation of sorghum kafirins in relations to their cross-linking behaviour. Journal of Cereal Science 28, 197−207.

Emmambux, N.M., Taylor, J.R.N., 2003. Sorghum kafirin interaction with various phenolic compounds. Journal of the Science of Food and Agriculture 83, 402–407.

Emmambux, N.M., Taylor, J.R.N., 2009. Properties of heat-treated sorghum and maize meal and their prolamin proteins. Journal of Agricultural and Food Chemistry 57, 1045–1050.

Flores, I., Cabra, V., Quirasco, M.C., Farres, A., Galvez, A., 2010. Emulsifying properties of chemically deamidated corn (*Zea mays*) gluten meal. Food Science and Technology International 16, 241–250.

Gao, C., Taylor, J., Wellner, N., Byaruhanga, Y.B., Parker, M.L., Mills, E.N.C., Belton, P.S., 2005. Effect of preparation conditions on protein secondary structure and biofilm formation of kafirin. Journal of Agricultural and Food Chemistry 53, 306–312.

Hamaker, B.R., Kirleis, A.W., Mertz, E.T., Axtell, J.D., 1986. Effect of cooking on the protein profiles and in vitro digestibility of sorghum and maize. Journal of Agricultural and Food Chemistry 34, 647−649.

Hernández-Muñoz, P., Kanavouras, A., Lagaron, J.M., Gavara, R., 2005. Development and characterization of films based on chemically cross-linked gliadins. Journal of Agricultural and Food Chemistry 53, 8216−8223.

Kaya, S., Kaya, A., 2000. Microwave drying effects on properties of whey protein isolate edible films. Journal of Food Engineering 43, 91–96.

Krochta, J.M., 2002. Proteins as raw materials for films and coatings: definitions, current status, and opportunities. In: Gennadios, A. (Ed.), Protein-Based Films and Coatings. CRC Press: Boca Raton, FL, pp. 1−41.

Larré, C., Chiarello, M., Blanloeil, Y., Chenu, M., Gueguen, J., 1993. Gliadin modifications catalyzed by guinea pig liver transglutaminase. Journal of Food Biochemistry 17, 267–282.

Lawton, J.W., 2002. Zein: a history of processing and use. Cereal Chemistry 79, 1–18.

Marquié, C., Tessier, A.-M., Aymard, C., Guilbert, S., 1997. HPLC determination of the reactive lysine content of cottonseed protein films to monitor the extent of cross-linking by formaldehyde, glutaraldehyde, and glyoxal. Journal of Agricultural and Food Chemistry 45, 922–926.

Matsudomi, N., Kato, A., Kobayashi, K., 1982. Conformation and surface properties of deamidated gluten. Agricultural and Biological Chemistry 46, 1583−1586.

Micard, V., Belamri, R., Morel, M.-H., Guilbert, S., 2000. Properties of chemically and physically treated wheat gluten films. Journal of Agricultural and Food Chemistry 48, 2948–2953.

Migneault, I., Dartiguenave, C., Bertrand, M.J., Waldron, K.C., 2004. Glutaraldehyde: behavior in aqueous solution, reaction with proteins, and application to enzyme crosslinking. BioTechniques 37, 790−802.

Mizutani, Y., Matsumura, Y., Imamura, K., Nakanishi, K., Mori, T., 2003. Effects of water activity and lipid addition on secondary structure of zein in powder systems. Journal of Agricultural and Food Chemistry 51, 229–235.

Motoki, M., Seguro, K., Nio, N., Takinami, K., 1986. Glutamine-specific deamidation of α_{sl}-casein by transglutaminase. Agricultural and Biological Chemistry 50, 3025−3030.

Orliac, O., Rouilly, A., Silvestre, F., Rigal, L., 2002. Effects of additives on the mechanical properties, hydrophobicity and water uptake of thermomoulded films produced from sunflower protein isolate. Polymer 43, 5417–5425.

Park, H.J., Chinnan, M.S., 1995. Gas and water vapor barrier properties of edible films from protein and cellulosic materials. Journal of Food Engineering 25, 497–507.

Parris, N., Coffin, D.R., 1997. Composition factors affecting the water vapor permeability and tensile properties of hydrophilic zein films. Journal of Agricultural and Food Chemistry 45, 1596−1599.

Pérez-Pérez, C., Regalado-González, C., Rodríguez-Rodríguez, C.A., Barbosa-Rodríguez, J.R., Villaseñor-Ortega, F., 2006. Incorporation of antimicrobial agents in food packaging films and coatings. In: Guevara-González, R.G., and Torres-Pacheco, I. (Eds.), Advances in Agricultural and Food Biotechnology. Research Signpost: Trivandrum, India, pp. 193−216.

Poole, A.J., Church, J.S., Huson, M.G., 2008. Environmentally sustainable fibers from regenerated protein. Biomacromolecules 10, 1−8.

Reddy, N., Tan, Y., Li, Y., Yang, Y., 2008. Effect of glutaraldehyde crosslinking conditions on the strength and water stability of wheat gluten fibers. Macromolecular Materials and Engineering 293, 614–620.

Selling, G.W., Woods, K.K., Sessa, D., Biswas, A., 2008. Electrospun zein fibers using glutaraldehyde as the crosslinking reagent: effect of time and temperature. Macromolecular Chemistry and Physics 209, 1003–1011.

Sessa, D.J., Mohamed, A., Byars, J.A., 2008. Chemistry and physical properties of melt-processed and solution-cross-linked corn zein. Journal of Agricultural and Food Chemistry 56, 7067–7075.

Sessa, D.J., Mohamed, A., Byars, J.A., Hamaker, S.A., Selling, G.W., 2007. Properties of films from corn zein reacted with glutaraldehyde. Journal of Applied Polymer Science 105, 2877–2883.

Shull, J.M., Watterson, J.J., Kirleis, A.W., 1991. Proposed nomenclature for the alcohol-soluble proteins (kafirins) of *Sorghum bicolor* (L. Moench) based on molecular weight, solubility and structure. Journal of Agricultural and Food Chemistry 39, 83–87.

Soliman, E.A., Eldin, M.S.M., Furuta, M., 2009. Biodegradable zein-based films: influence of γ-irradiation on structural and functional properties. Journal of Agricultural and Food Chemistry 57, 2529–2535.

Stokes, R.H., Robinson, R.A., 1949. Standard solutions for humidity control at 25°C. Industrial and Engineering Chemistry 41, 2013.

Subirade, M., Kelly, I., Guéguen, J., Pézolet, M., 1998. Molecular basis of film formation from a soybean protein: comparison between the conformation of glycinin in aqueous solution and in films. International Journal of Biological Macromolecules 23, 241–249.

Tang, C.-H., Jiang, Y., Wen, Q.-B., Yang, X.-Q., 2005. Effect of transglutaminase treatment on the properties of cast films of soy protein isolates. Journal of Biotechnology 120, 296–307.

Tang, C.-H., Li, L., Yang, X.-Q., 2006. Influence of transglutaminase-induced cross-linking on *in vitro* digestibility of soy protein isolate. Journal of Food Biochemistry 30, 718–731.

Taylor, J., Taylor, J.R.N., Belton, P.S., Minnaar, A., 2009c. Preparation of free-standing films from kafirin protein microparticles: mechanism of formation and functional properties. Journal of Agricultural and Food Chemistry 57, 6729–6735.

Taylor, J., Taylor, J.R.N., Dutton, M.F., De Kock, S., 2005b. Identification of kafirin film casting solvents. Food Chemistry 32, 149−154.

Wagner, J.R., Gueguen, J., 1995. Effects of dissociation, deamidation, and reducing treatment on structural and surface active properties of soy glycinin. Journal of Food Biochemistry 43, 1993−2000.

Wang, H.-J., Lin, Z.-X., Liu, X.-M., Sheng, S.-Y., Wang, J.-Y., 2005. Heparin-loaded zein microsphere film and hemocompatibility. Journal of Controlled Release 105, 120–131.

Wang, Q., Yin, L., Padua, G.W., 2008. Effect of hydrophilic and lipophilic compounds on zein microstructures. Food Biophysics 3, 174–181.

CHAPTER 3

4.3 *IN VITRO* BMP-2 BINDING TO KAFIRIN MICROSTRUCTURES, RAT MODEL ASSESSMENT OF KAFIRIN MICROPARTICLE FILM-BMP-2 SYSTEM SAFETY, EVALUATION OF BIODEGRADABILITY OF KAFIRIN MICROPARTICLE FILM IMPLANT AND ASSESSMENT OF KAFIRIN MICROPARTICLE FILM-BMP-2 INDUCED ECTOPIC BONE FORMATION

4.3.1 Abstract

Mammalian collagen, a standard carrier used to enhance the osteoinductive effect of BMP-2, may induce immune response and has a risk of transmitting diseases. The potential of kafirin microstructures as biomaterials for replacement of collagen was investigated. The ability of kafirin microstructures to bind BMP-2 *in vitro* was evaluated. A rat model assessment of glutaraldehyde- and polyphenol-treated kafirin microparticle films, and kafirin microparticle film-BMP-2 system safety was performed. In addition, the biodegradability of these kafirin microparticle film implants and the ability of kafirin microparticle film-BMP-2 system to induce ectopic bone formation were investigated. Compared to collagen standard, the BMP-2 binding capacities of control, heat-treated, transglutaminase-treated and glutaraldehyde-treated kafirin microparticles were 7%, 18%, 34% and 22% higher, respectively, after 24 h binding, probably due mainly to the vacuoles creating a greater surface area in the microparticles. The glutaraldehyde- and polyphenol-treated films, and kafirin microparticle film-BMP-2 system were non-irritant to the animals, probably because kafirin is non-allergenic. Kafirin microparticle film implants degraded slowly, probably because of the low susceptibility of kafirin to mammalian proteolytic enzymes. Kafirin microparticle film-BMP-2 system did not induce ectopic bone morphogenesis, probably mainly due to low BMP-2 dosage and short study duration. These kafirin microstructures could have application as natural, non-animal protein biomaterials such as bioactive scaffolds for hard or soft tissue repair. However, at low BMP-2 levels (107–2140 ng/g) and a short implantation period (28 days), the kafirin microparticle film-BMP-2 system does not induce bone morphogenesis in the rat. Therefore more work needs to be done to optimize BMP-2 loading and release profile with kafirin microstructures.

4.3.2 Introduction

In the previous research chapters, it was established that treatment of kafirin microparticles with heat, transglutaminase and glutaraldehyde modified the functional properties of the kafirin microstructures. It was found that heat and glutaraldehyde cross-linking treatments both increased the microparticle size (Chapter 1). Additionally heat treatment increased the microparticle vacuole size, thereby increasing their internal surface area enabling their potential application for binding to delay or control the release of the encapsulated bioactives. In Chapter 2, it was shown that the thin kafirin microparticle films were relatively stable in ambient temperature water, which was enhanced by treatment with glutaraldehyde, indicating their potential stability in aqueous physiological environment.

Several workers have shown the potential of cereal protein microstructures to bind or carry bioactives or as scaffolds. For example, Taylor et al. (2009b) found that the vacuolated kafirin microparticles could encapsulate antioxidants, probably because of the presence of the holes, which increased the internal surface area for binding these bioactives. Similarly, in a study by Wang et al. (2005), they reported a heparin-loaded zein microsphere films with potential for application as drug-eluting coating film for cardiovascular devices. Likewise, Tu, Wang, Li, Dai, Wang and Zhang (2009) showed that the complexes of zein scaffolds and rabbit mesenchymal stem cells could undergo ectopic bone formation in the thigh muscle pouches of nude mice. To determine whether the kafirin microstructures could be used as biomaterial scaffolds or *in vivo* carriers for other bioactives, such as bone morphogenetic proteins (BMPs), stem cells, heparin among others, it is necessary first to establish their safety. It is also important to determine the binding of the kafirin microstructures with these bioactives.

Safe, slowly biodegradable and effective implantable medical devices are needed in order to promote regeneration of bone tissue. Many conditions occur where bone regeneration is necessary, such as periodontitis, bone tooth cavities, degenerative spinal conditions and severe fractures (reviewed by Bessa et al., 2008). One of the major concerns with medical devices is immune reaction and implant rejection by the body (reviewed by Nag and Banerjee, 2012). There is also a requirement that medical devices have to last for sufficient time in order for complete tissue regeneration to take place (reviewed by Bessa et al., 2008). The thin, water stable kafirin microparticle films (Chapter 2) may have good functional properties for this type of application.

BMPs are multi-functional growth factors that belong to the transforming growth factor β (TGF-β) superfamily (Chen, Zhao and Mundy, 2004), which induce cartilage and bone formation in addition to non-osteogenic developmental processes such as in neural induction (reviewed by Shah, Keppler, and Rutkowski, 2011). According to Shah et al. (2011), there are 23 different members of TGF-β family of which 17 are BMPs. BMP-2 plays a critical role in bone formation and regeneration. While BMP-2 by itself is sufficient to induce bone formation, its rapid distribution from implant site reduces its inductive effect (reviewed by Kim, Kim, Kim, Choi, Chai, Kim and Cho, 2005). Other factors that affect the therapeutic outcome of BMP-2 are its quantity, concentration and time of application (reviewed by King and Cochran, 2002; La, Kang, Yang, Bhang, Lee, Park and Kim, 2010). The ability to immobilize this molecule in certain matrices can be crucial in bone tissue engineering. While mammalian collagen is the current standard carrier for BMP-2 (reviewed by Gautschi, Frey and Zellweger, 2007), it has the potential to induce an immune response due to its xenobiotic origin as well as having a high risk of transmitting Creutzfeldt–Jakob disease (CJD) (reviewed by Bessa et al., 2008, 2010; Silva, Ducheyne and Reis, 2007; Haidar et al., 2009). Therefore, delivery systems that do not elicit an immune response need to be sought.

Kafirin microstructures may be highly suitable for a number of reasons. Firstly, kafirin is a relatively hydrophobic protein (Duodu et al., 2003). This may enhance its ability to bind BMP-2, which has been shown to have a strong affinity for hydrophobic surfaces (Utesch, Daminelli and Mroginski, 2011). Secondly, the fact that kafirin microparticles are vacuolated (Taylor et al., 2009a) may provide a large surface area for BMP-2 binding. Additionally, kafirin is slowly biodegraded by mammalian proteolytic enzymes (Emmambux and Taylor, 2009) attributed to kafirin hydrophobicity as enzymes function in an aqueous environment (Duodu et al., 2003), which might prolong the degradation period of the kafirin microstructures in the body. Most importantly, kafirin is non-allergenic (Ciacci et al., 2007).

The present study investigated the potential of modified kafirin microstructures to bind BMP-2. A rat model assessment of the safety of kafirin microparticle film implants and kafirin microparticle film-BMP-2 system was performed. In addition, the biodegradability of kafirin microparticle film implants in the rat model was evaluated. Also, the ability of kafirin microparticle film-BMP-2 to induce ectopic bone formation in the rodent model was investigated.

4.3.3 Materials and methods

4.3.3.1 *Materials*

Kafirin was extracted from a mixture of two similar white, tan-plant non-tannin sorghum cultivars PANNAR PEX 202 and 606 and used to prepare kafirin microparticles as described in Chapter 1. All the other materials used in the study are specified in the relevant sections of the text.

4.3.3.2 *Binding BMP-2 with kafirin microparticles*

The BMP-2 binding study was performed by the candidate under the guidance of Dr Nicolaas Duneas of Altis Biologics.

Medium exchange for kafirin microparticles

As kafirin microparticles were stored in 0.9 M acetic acid, the carrier medium was exchanged to 20 mM acetic acid. The kafirin microparticle suspensions were centrifuged at 3150 *g* for 20 min. Then the supernatants were carefully decanted off, replaced with 20 mM acetic acid (pH 3.3), re-suspended for 15 min on a rocking platform, and centrifuged as before. The supernatant were replaced with fresh 20 mM acetic acid. This process was repeated three times. Then, the volume of 20 mM acetic acid was adjusted to give a solids content of at least 6% (w/w).

Binding BMP-2 with kafirin microparticles

Kafirin microparticle suspensions containing 100 mg protein were weighed into 5 mL cryovials. Then, 0.5 mL 1000 ppm Tween® 20 (polyoxyethylene sorbitan monolaurate) (Merck-Schuchardt, Munich, Germany) was added and vortex-mixed. Similarly, 100 mg porcine collagen standard (Altis Biologics, Pretoria, South Africa) was weighed and treated the same way as the kafirin microparticles. Porcine BMP complex (0.778 mg/mL) (pH 3.3) with BMP-2 abundance of 0.00085% (w/w) as a proportion of BMP complex (Altis Biologics) (1.5 mL) was added to kafirin microparticles or collagen standard and vortex-mixed to give a BMP complex to carrier protein ratio of approximately 1:100. The reaction volumes of the mixtures were adjusted to 4.5 mL using 20 mM acetic acid and the contents mixed well. Samples were drawn from clear supernatants after centrifugation at 3150 *g* for 20 min. An initial 50 µL sample was drawn from unbound sample and transferred into

microwells of a microplate (Greiner Bio-One, Frickenhausen, Germany) to account for time 0. Then, the cryovials were placed on a rocking platform set at 50 rpm and 50 µL sample material was subsequently drawn from clear supernatants of each sample treatment after 5, 10, 30, 60, 120 and 1440 min intervals. Controls containing kafirin microparticles, collagen without BMP complex and BMP complex without binding material (kafirin microparticle or collagen) were included. The reaction mixture had pH 3.0. and ionic strength of 20 mM.

4.3.3.3 *SDS-PAGE*

To characterize the proteins BMP binding residues (kafirin microparticles or collagen loaded with BMP complex), SDS-PAGE under reducing and non-reducing conditions was performed as described in Chapter 1. Then silver-stain was used after destaining the gels according to the protocol provided for PlusOne Silver Staining kit, Protein (GE Healthcare Bio-Sciences AB, Uppsala, Sweden).

4.3.3.4 *SEM*

Suspensions of kafirin microparticles and collagen standard loaded with BMP complex were prepared for SEM and analysed as described in Chapter 1.

4.3.3.5 *Lowry protein assay*

The concentration of protein in the clear supernatants was measured by the Lowry protein assay (Lowry, Rosebrough, Farr and Randall, 1951) using a Bio-Rad DC Protein Assay kit (Bio-Rad Laboratories, Hercules, CA) to establish evidence of kafirin microparticle binding to BMP-2. The Lowry protein assay was used to measure free protein in the clear supernatants to give an inverse indication of BMP-2 binding. Controls containing kafirin microparticles or collagen without BMP complex were included. The protein concentrations of the supernatants were obtained by subtracting the protein concentration in supernatant of controls from the treatments with BMP complex.

4.3.3.6 *Enzyme-linked immunosorbant assay (ELISA)*

For confirmation of kafirin microparticle binding to BMP-2, BMP-2 ELISA was used to measure the amount of BMP-2 in the clear supernatants of treatments, which with Lowry protein assay, showed BMP binding profiles that were closely similar to collagen standard. A

Quantikine® BMP-2 Immunoassay kit (R&D Systems, Minneapolis, MN) was used. This is a quantitative sandwich enzyme immunoassay technique, whereby a monoclonal antibody specific for BMP-2 is pre-coated onto a microplate. The standards and samples are pipetted into the wells and the immobilized antibody binds any BMP-2 present. Any unbound substances are washed out from the wells and then an enzyme-linked monoclonal antibody specific for BMP-2 is added to the wells. Then the unbound antibody-enzyme reagent is removed by washing and a colour reagent solution containing a mixture of hydrogen peroxide and tetramethylbenzidine (a chromogen) is added to the wells. Colour develops in proportion to the amount of BMP-2 bound in the initial step. The absorbances were read at 450 nm with correction readings at 570 nm. The BMP-2 concentration in the supernatants was inversely related to binding.

4.3.3.7 *Subcutaneous bioassay using rat model*

The subcutaneous bioassay using rat model was performed to accomplish three objectives. First, was to assess the safety of kafirin microparticle film implants and kafirin microparticle film-BMP-2 system in the rat model. The second objective was to evaluate the biodegradability of kafirin microparticle film implants in the rat tissue. The third was to establish whether the kafirin microparticle film-BMP-2 system was capable of promoting ectopic bone morphogenesis in the rat model. Collagen was used as standard. Because of their good water stability, kafirin microparticle film implants were used in the rat study. In addition, recombinant human BMP-2 (rhBMP-2) was used in the animal study to preclude possible infection from the porcine BMP complex, which contained unpurified BMP-2.

Kafirin microparticle film preparation

Control kafirin microparticle films and a 20% glutaraldehyde-treated kafirin microparticle films were prepared as described in Chapter 2. Kafirin microparticle films treated with polyphenols were prepared as described below. The work on the polyphenol-treated kafirin microparticle films was performed as a previous study by Taylor et al. (2009b) had shown that kafirin microparticles could bind polyphenol but information on the safety and biodegradability of kafirin microstructure-polyphenol system in an animal model was lacking.

Treatment of kafirin microparticle films with polyphenol extract

Polyphenol extract was obtained from Black non-tannin sorghum grain bran. To obtain the bran, the sorghum grains were hand cleaned and sorted to remove foreign objects, damaged and diseased grain. Dehulling was performed using a Tangential Abrasive Dehulling Device (TADD) Model 4E-115 (Venables Machine Works, Saskatoon, SK, Canada). Equal amounts of the sorghum grain (approximately 75 g) were placed into each of the eight compartments of the equipment's chamber holding disc and dehulled for at least 2 min to remove the bran that collected into the holding bag. The collected sorghum brans were then sieved through a 1000 µm aperture test sieve respectively and ground into a powder using a coffee mill (IKA A11, Staufen, Germany). These were further passed through a 500 µm aperture test sieve, packed under vacuum and then stored at 4^{o}C until required for extraction. Then the polyphenols were extracted from the Black sorghum bran according to a protocol by Emmambux and Taylor (2003). Briefly, Black sorghum bran (10 g) was mixed with 150 mL distilled water and stirred for 30 min before adjusting to pH 2.0 using 1.0 M HCl. The mixture was then incubated for 30 min in a shaking water bath at 37^{o}C. Then, the pH was further adjusted to pH 6.0 using 1.0 M NaOH and the incubation continued in the shaking water bath for 30 min. The sample was centrifuged at 7500 *g* for 15 min. Total polyphenol content of the extract was determined using the Folin-Ciocalteu method (Singleton and Rossi, 1965). Polyphenol-treated kafirin microparticle films were prepared by soaking the films in an aqueous extract of polyphenols for 12 h at room temperature.

Washing out plasticizer from kafirin microparticle film

Plasticizer was washed out of the kafirin microparticle films to create a porous matrix for diffusion of BMP-2 molecules to enhance binding and to reduce impurities due to plasticizer content. This is based on the knowledge that a plasticiser acts by disrupting intermolecular chain forces and increasing the free volume of the polymer network (reviewed by Cuq et al., 1998). Hence, when the plasticizer is washed off the film would be expected to become porous due to the voids left at molecular level. The plasticizer in the films was washed out by soaking in distilled water as described in Chapter 2. To decide on whether use of wet or dried kafirin microparticle films would be more suitable for binding rhBMP-2 for the animal study, both wet and dry kafirin microparticle films were prepared. For the wet kafirin microparticle films, the water on the film surfaces after soaking was removed by placing the films in between a paper towel before using the films for binding rhBMP-2 without drying. The dry

kafirin microparticle films were prepared by further drying the films in a desiccator for 72 h before use. The wet kafirin microparticle films were eventually used for rhBMP-2 binding for the rat study based on the rhBMP-2 binding data.

Preparation of rhBMP-2 loaded kafirin microparticle films and collagen

The rhBMP-2 (Invitrogen, Carlsbad, CA) was dissolved in 0.01 M phosphate buffered saline (pH 7.4) (Sigma-Aldrich, St. Louis, MO) to make a 400 ng/mL rhBMP-2 solution. Two doses, a low rhBMP-2 dose (106.7 ng rhBMP-2/g kafirin microparticle film or collagen) and high dose (2140 ng rhBMP-2/g kafirin microparticle film or collagen) were prepared by diffusion loading according to the protocol of Patel et al. (2008), whereby the rhBMP-2 was dripped onto 75 mg kafirin microparticle film or collagen using a micropipette. These loadings were equivalent to 8 ng and 160 ng rhBMP-2 per implant for low dose and high dose, respectively. Then, the implants were incubated at 4^{o}C for 24 h and then dried in air. Kafirin microparticle films and collagen without rhBMP-2 were used as controls.

4.3.3.8 *Sterilization of implant materials*

The dried film dosages were folded into approximately 1 cm × 0.75 cm and placed into individual 2 mL Eppendorf tubes (one per dose). The collagen dosages were also placed in individual 2 mL Eppendorf tubes (one per dose). The Eppendorf tubes containing individual dosages were then packed into a cardboard box. Then, the implant materials were sterilised using γ-irradiation (25 kGry), performed by Synergy Sterilisation (Johannesburg, South Africa). Tables 4.8 and 4.9 provide summaries of the constituents of the treatments for assessment of safety, biodegradability and ectopic bone growth.

Table 4.8 Summary of the constituents of the BMP-2 loaded kafirin microparticle film or collagen and controls for safety and biodegradability assessment

Material	Treatment	Composition
Kafirin microparticle film	Control kafirin microparticle film	75 mg untreated kafirin microparticle film
	20% glutaraldehyde treated kafirin microparticle film	75 mg 20% glutaraldehyde treated kafirin microparticle film
	Polyphenol treated kafirin microparticle film	75 mg polyphenol treated kafirin microparticle film
	BMP-2 loaded control kafirin	75 mg kafirin microparticle film + 8 ng

Material	Treatment	Composition
	microparticle film Low loading	rhBMP-2
	BMP-2 loaded control kafirin microparticle film High loading	75 mg kafirin microparticle film + 160 ng rhBMP-2
Collagen	Control collagen	75 mg collagen without BMP-2
	BMP loaded collagen Low loading	75 mg collagen+ 8 ng rhBMP-2
	BMP loaded collagen High loading	75 mg collagen + 160 ng rhBMP-2

Table 4.9 Summary of the constituents of the BMP-2 loaded kafirin microparticle film or collagen and controls for assessment of biodegradability and ectopic bone growth

Material	Treatment	Composition
Kafirin microparticle film	Control kafirin microparticle film	75 mg kafirin microparticle film without BMP-2
	BMP-2 loaded kafirin microparticle film Low loading	75 mg kafirin microparticle film + 8 ng rhBMP-2
	BMP-2 loaded kafirin microparticle film High loading	75 mg kafirin microparticle film + 160 ng rhBMP-2
Collagen	Control collagen	75 mg collagen without BMP-2
	BMP-2 loaded collagen Low loading	75 mg collagen+ 8 ng rhBMP-2
	BMP-2 loaded collagen High loading	75 mg collagen + 160 ng rhBMP-2

4.3.3.9 *Implantation*

The implant materials were prepared by the candidate while implantation procedures were performed by Prof Vinny Naidoo who is a veterinarian. Sprague–Dawley rats (20) (SA Vaccine Producers, Johannesburg, South Africa) with a weight range of 155–223 g were used in the study. Rats were allowed autoclaved potable water and irradiated food (Rat Chow, Epol, Johannesburg, South Africa) *ad libitum*. This protocol was approved by the University of Pretoria Animal Use and Care Committee (approval number H016-11) (see Annex 1) prior to commencement of the study, according to the South African national standard for the use and care of laboratory animals. The rats were pair-housed in the Biomedical Research Centre

of the University of Pretoria in Eurostandard type III cages (Techniplast, Buguggiate, Italy). Animals were housed on wood shaving and had access to cardboard cartons and tissue paper for enrichment. Four paravertebral skin incisions of 1.5 cm were made with a scalpel blade just caudal to the point of the scapula by a veterinarian. A blind pouch was created subcutaneously by blunt dissection with scissors. After insertion of the implants, the incisions were closed with cyanoacrylate. Treatments were randomised to the available sites by numbering the wound sites 1 to 4 starting on the top left of the dorsum moving in a clockwise direction and subsequently allocating the treatments to a site using a table of random numbers.

4.3.3.10 *Examination of appearance of implants*

The appearances of skin at the sites of the implants were visually assessed by the candidate over the period of the animal experiment.

4.3.3.11 *Histological evaluations*

Independent histological examinations were performed by Idexx Laboratories (Pretoria, South Africa), which is an independent international laboratory. Idexx Laboratories deals in services that include pet-side diagnostic tests, reference laboratory services, digital radiography among other services (http://www.idexxsa.co.za/AboutIDEXX/tabid/103/Default.aspx). The implant treatment identities were coded by the candidate to ensure a blind independent evaluation by Idexx Laboratories.

4.3.3.12 *Safety assessment*

On Day 7, eight animals were euthanized by a veterinarian using isoflurane overdose in a saturated glass chamber and the implants removed for examination by Idexx Laboratories for further evaluation. Animals were also submitted for full necropsy and histopathological evaluation of the major organs (adrenal, brain, gonad, heart, intestines, kidney, liver, lung, pancreas, spleen, stomach, thymus and urinary bladder) by Idexx Laboratories.

4.3.3.13 *Assessment for ectopic bone growth*

On Day 28, the remaining 12 animals were euthanized as above and subjected to radiology to determine whether bone morphogenesis had taken place. Following implant removal by Idexx Laboratories, the implants were sectioned so that half the implants per treatment could be frozen for quantification of alkaline phosphatase enzyme activity. In addition, the gross appearance of the dissected implants was examined using a Zeiss Discovery V20 stereo microscope (Jena, Germany). The alkaline phosphatase enzyme activity test and the gross appearance of the implants were analysed by the candidate. The other half of the implants were placed in 10% buffered formalin for independent histological examination, which was performed by Idexx Laboratories.

Histopathology

This was performed by Idexx Laboratories. After fixation for 2 days, selected blocks of tissue as well as a cross-section of the implantation site were sectioned and processed in an automatic histological tissue processor (Pathcentre Enclosed Tissue Processor, Thermo Scientific, Johannesburg, South Africa). After overnight tissue processing, wax blocks were produced and histological sections of 6 µm were cut on a HM450 Sliding Microtome (Thermo Scientific). The slides were then stained with haematoxylin and eosin staining using a Shandon Varistain Gemini ES automatic slide stainer (Thermo Scientific). Status of the implant materials was examined. Additionally, the implant sites were evaluated for foreign body reaction, granulomatous reaction, osteolysis, osteogenesis (bone morphogenesis) and skin ulceration. Standard histopathology was performed on the animal organs. Photographs of specific morphological findings were taken and histological scoring for tissue response to the implants was recorded according to similar studies (Babensee, 1990; Bensaid, Triffitt, Blanchat, Oudina, Sedel and Petite, 2003). Results were graded as follows: negative/none (-), mild (+), moderate (++), severe (+++).

Alkaline phosphatase activity

Alkaline phosphatase (ALP) activity of cells on the implants was assayed by the candidate using an adenosine 3',5'-cyclic monophosphate (cAMP) direct enzyme immunoassay kit (Catalogue number CA200, Sigma, St. Louis, MO). This assay is based on the competitive binding technique in which cAMP present in a sample competes with a fixed amount of

alkaline phosphatase-labelled cAMP for sites on a rabbit polyclonal antibody. During the incubation, the polyclonal antibody becomes bound to the goat anti-rabbit antibody coated onto the microplate. Following a wash to remove excess conjugate and unbound sample, a substrate solution (a solution of *p*-nitrophenyl phosphate in buffer) is added to the wells to determine the bound enzyme activity. The colour development is stopped and the absorbance is determined. The intensity of the colour is inversely proportional to the concentration of cAMP in the sample, which is used as measure of ALP activity. The ALP assay was performed according to the manufacturer's instructions. Briefly, the implants were frozen in liquid nitrogen and ground using a mortar and pestle. The ground implant were weighed and homogenized in 0.1 M HCl to stop endogenous phosphodiesterase activity. The ALP activity test was performed on the homogenised samples. The absorbance readings were done at 405 nm with a correction at 570 nm using a microplate reader.

4.3.3.14 *Statistical analyses*

One-way analysis of variance (ANOVA) was used to analyse numerical data with Statistica software version 10 (StatSoft, Tulsa, OK). The dependent variables were the BMP-2 binding capacity and the ALP activity while the independent variables were the BMP-2 carrier materials i.e. collagen standard and kafirin microparticles or kafirin microparticle films. With Lowry protein assay, BMP-2 ELISA and ALP activity tests, four microwells were used per treatment for at least two replicate experiments. The mean differences were assessed by Fischer's Least Significant Difference (LSD) test. Histopathology data were obtained by the histological scoring system for tissue response in four replicate implant sites, by the Idexx Laboratories.

4.3.4 Results and discussion

4.3.4.1 *Binding BMP-2 with kafirin microparticles*

With the Lowry protein assay, there was an increase in protein concentration in the clear supernatant with time (Figure 4.19), which seems counter intuitive. It was expected that if the collagen or kafirin microparticles were to bind the BMP, the concentration of free proteins in the clear supernatant after centrifugation would decrease. Otherwise, in case of no BMP binding, the free protein concentration in the supernatant was expected to be unchanged. The inconsistent result was probably because the Lowry protein assay is based on the reaction of

protein with an alkaline copper tartrate solution and Folin reagent (Lowry et al., 1951). Hence, it is not specific for the BMP. However, Lowry protein assay can be used as indication of collagen binding to BMP (Dr Nicolaas Duneas, Altis Biologics, personal communication). The assay has also been used in other studies such as in the investigation of the synergy between recombinant TGF-β1 and BMP-7 in inducing endocrine bone formation in a baboon (Ripamonti, Duneas, Van Den Heever, Bosch and Crooks, 1997) as part of biochemical analyses. Kafirin microparticles heat-treated at 75^{o}C had binding profile closely following the trend obtained with collagen, suggesting that the ability of these kafirin microparticles to bind BMP-2 was probably similar to the collagen standard.

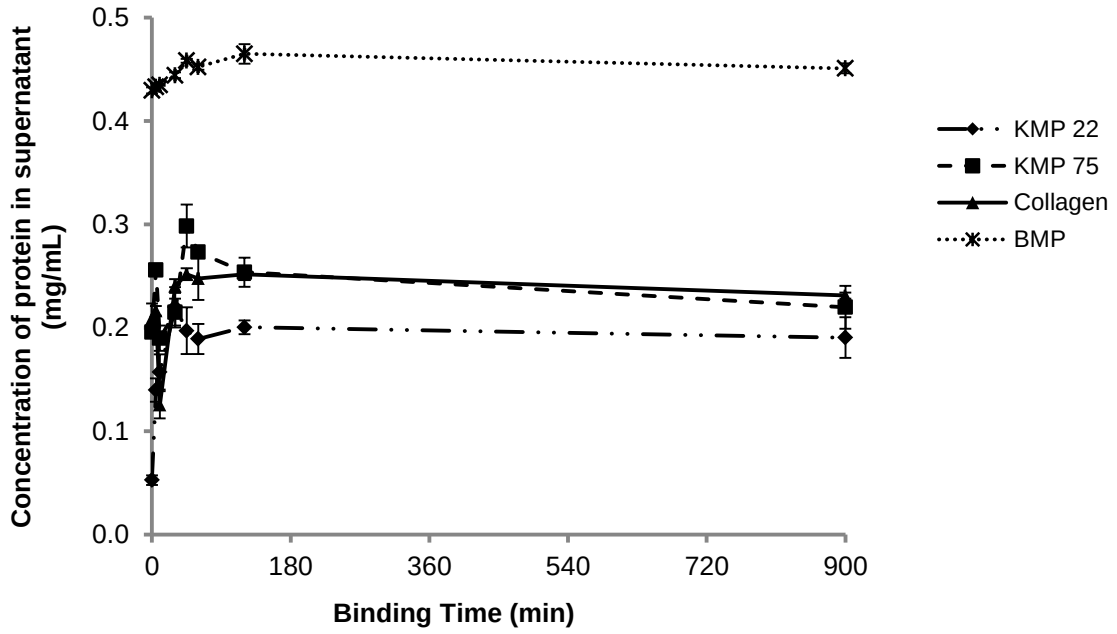

Figure 4.19 Effect of binding of kafirin microparticles (KMP) and collagen standard with BMP on concentration of "BMP complex" in the clear supernatants (free unbound protein), determined by Lowry protein assay. Error bars are standard deviations (n=2). KMP 22– KMP held at ambient temperature (22°C) for 1 h KMP 75– KMP heated at 75°C for 1 h; BMP– bone morphogenetic protein complex without binding material.

SEM showed no changes in the morphology of the kafirin microparticles or collagen particles after binding with BMP (Figure 4.20). These findings are in apparent contrast with the reports in literature such as the work by Balmayor et al. (2009), which showed increase in size of microspheres when bound to BMP-2. It seems the very low concentration of BMP-2 with

respect to the protein in the binding material (kafirin microparticles or collagen), less than one part per million, probably made it impractical to detect any possible changes to the morphology of kafirin microparticles or collagen after binding with BMP.

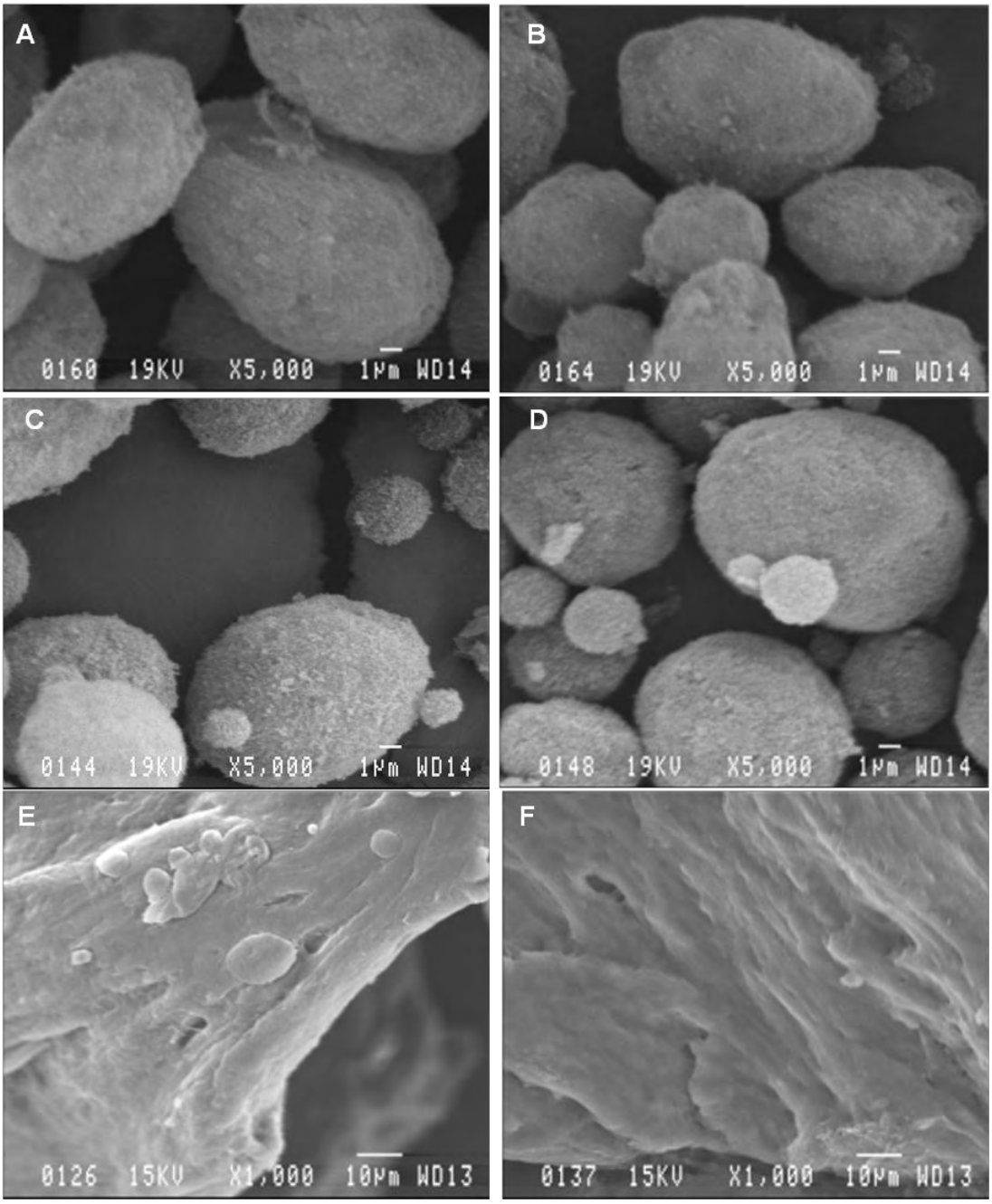

Figure 4.20 SEM of kafirin microparticles (KMP) and collagen standard at the end of binding period with BMP. **A**: KMP 22 (control); **B**: KMP 22 + BMP; **C**: KMP 75; **D**: KMP 75 + BMP; **E**: Collagen; **F**: Collagen + BMP. KMP 22– KMP held at ambient temperature (22°C) for 1 h KMP 75– KMP heated at 75°C for 1 h; BMP– bone morphogenetic protein.

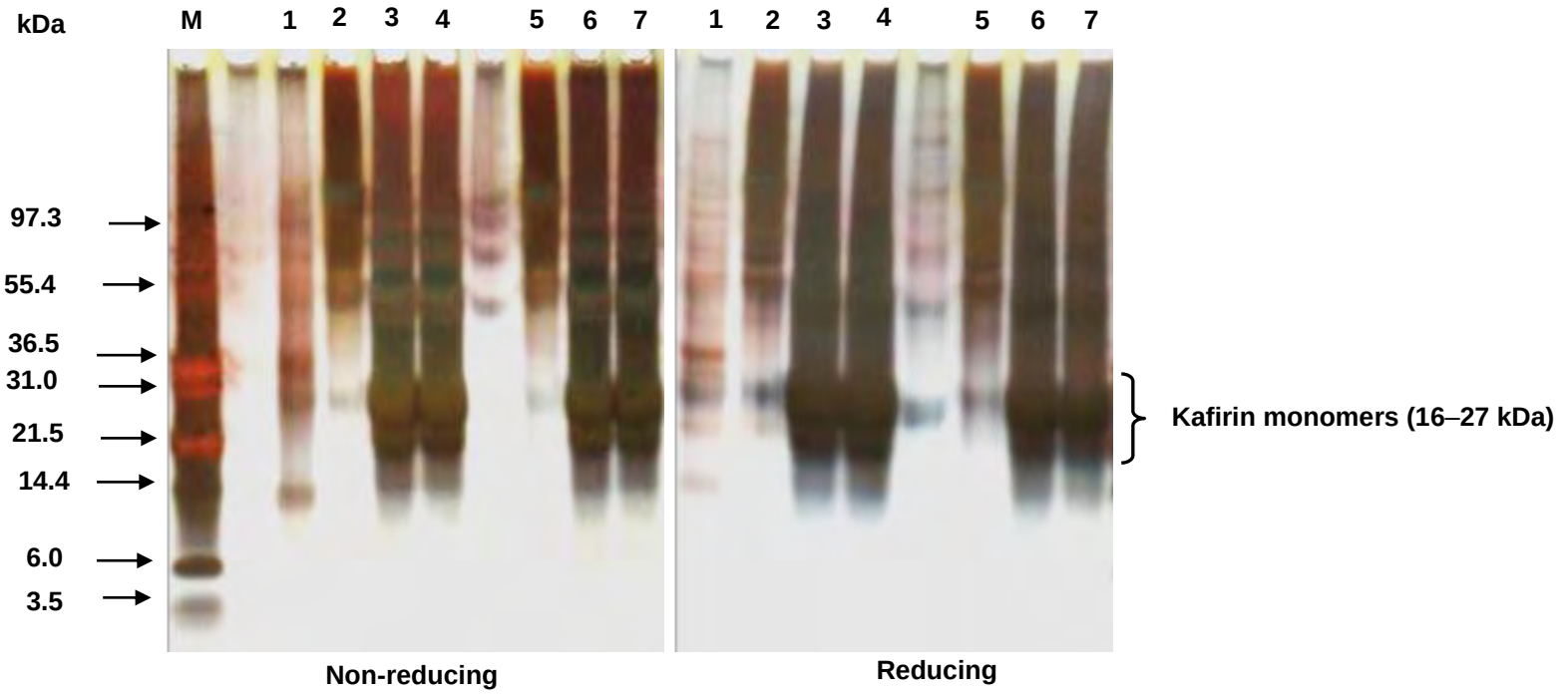

Figure 4.21 SDS-PAGE with silver staining of kafirin microparticles (KMP) and collagen standard after binding with BMP. Protein loading, 10 µg. Lanes M: Molecular markers; 1: BMP; 2: Collagen + BMP; 3: KMP 75 + BMP; 4: KMP 22 + BMP; 5: Collagen; 6: KMP 75; 7: KMP 22.

KMP 22– KMP held at ambient temperature (22°C) for 1 h; KMP 75– KMP heated at 75°C for 1 h; BMP– bone morphogenetic protein.

However, it is important to note that a minimum of 20 ng BMP-2/g binding material is acceptable (Dr Nicolaas Duneas, personal communication), which is a very low concentration. SDS-PAGE with Coomassie Brilliant Blue staining showed no changes in bands after BMP-2 binding (data not shown). Because silver stain has better sensitivity than Coomassie Brilliant Blue (Chevallet, Luche and Rabilloud, 2006), silver staining was used on the same gels previously stained with Coomassie Brilliant Blue after complete destaining in an attempt to detect any possible changes in molecular bands. No clear differences were found in the molecular weight distributions of the kafirin microparticles and collagen standard bound to BMP, compared to their controls using SDS-PAGE with silver staining (Figure 4.21). As with the SEM, it seems that the extremely low BMP complex concentration compared to the kafirin microparticles and collagen, probably made it unfeasible to detect any possible changes in molecular weight. Additionally, the very high sensitivity of silver staining made it difficult to see any differences due to the presence of ghost bands.

BMP-2 ELISA

As indicated, initially kafirin microparticles heat-treated at 75^{o}C was used along with collagen standard to confirm BMP-2 binding. This was because the Lowry protein assay showed closely similar binding profiles for the two binding materials (Figure 4.19). Preliminary ELISA confirmed that kafirin microparticles could bind the BMP-2 (Figure 4.22). Unlike the Lowry assay, ELISA showed reductions in BMP-2 concentration in supernatants with time. After 2 h reaction, the BMP-2 binding capacity of kafirin microparticles was about 15% higher than that of collagen standard. The binding between kafirin microparticles and BMP-2 was probably greater because of the presence of the pores within the kafirin microparticles in which the BMP-2 could diffuse during incubation. Also, as the interaction between BMP-2 and collagen probably involves electrostatic attraction (Patel et al., 2008), a similar but probably stronger interaction may have occurred between kafirin, pI 6 (Csonka et al., 1926) and BMP-2, pI 9 (Geiger, Li and Friess, 2003) given the higher pI of collagen (7.8) (Higberger, 1939). In fact, collagen has a relatively low affinity for BMP-2 (Ishikawa, Terai and Kitajima, 2001; Visser, Arrabal, Becerra, Rinas and Cifuentes, 2009). In addition, kafirin is very hydrophobic for a protein (Duodu et al., 2003). Hence, kafirin may have a better potential to bind to BMP-2, which has been shown to have a stronger attraction to hydrophobic surfaces (Utesch et al., 2011), probably due to the hydrophobic pockets formed by BMP-2 monomer residues (Nickel, Dreyer, Kirsch and

Sebald, 2001). As explained by Scheufler, Sebald and Hülsmeyer (1999), the isolated BMP-2 monomer by itself has no hydrophobic core, whereas a stable BMP-2 structure is achieved by homodimerization. Through interactions of helix α3 in a subunit with the β-sheets of the adjacent subunit, two tightly packed hydrophobic cores are generated, with hydrophobic packing being the most abundant form of subunit interactions in the BMP-2 homodimer.

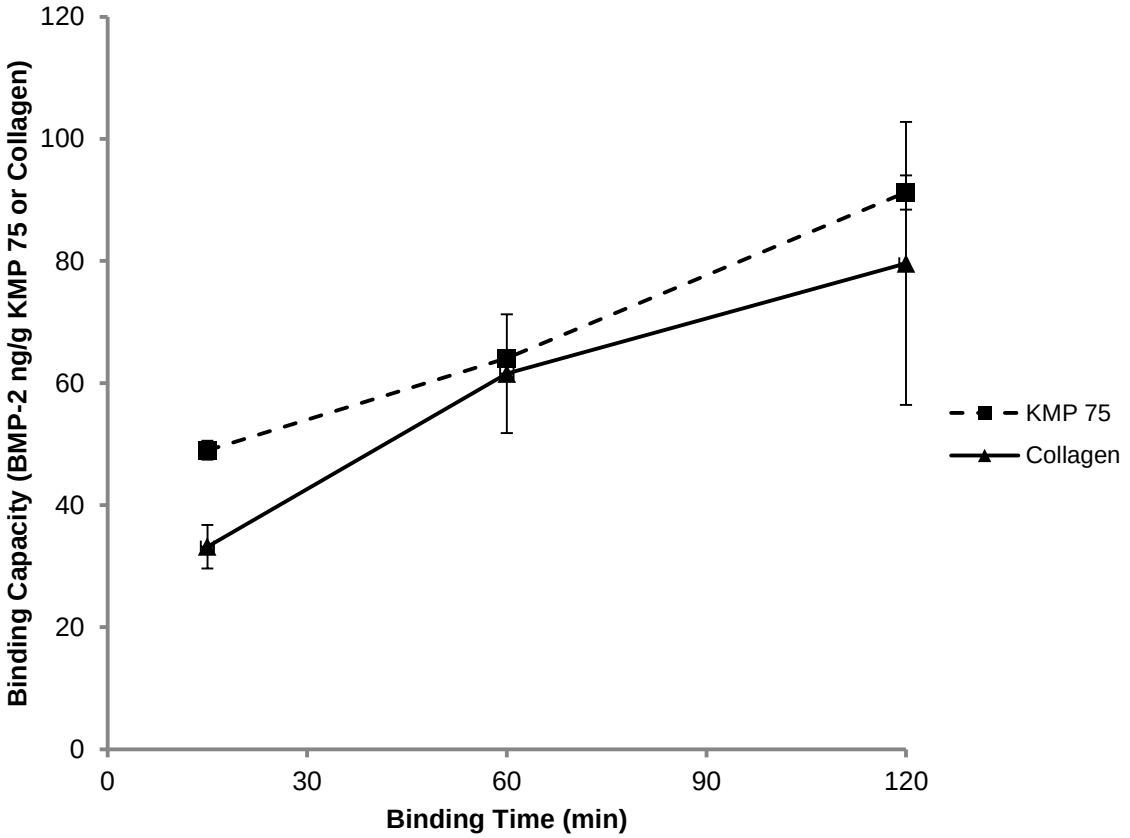

Figure 4.22 Preliminary BMP-2 binding capacity of kafirin microparticles (KMP) heat-treated at 75°C (KMP 75) compared to collagen standard during the first 120 min reaction period, determined by BMP-2 ELISA. The preliminary amounts of bound BMP-2 were calculated by determining the difference in amount of BMP-2 in solution at the beginning (first 2 min as reference point) and after binding for 15, 60 and 120 min time intervals. Error bars are standard deviations (n=2).

Having established from the preliminary binding assay that kafirin microparticles could bind BMP-2 within the first 120 min, a more comprehensive assessment was performed to determine the effects of treating kafirin microparticles with heat, transglutaminase and glutaraldehyde on BMP-2 binding capacity over a longer reaction period (24 h). Heat treatment of kafirin microparticles increased the BMP-2 binding capacity by up to 10%

(Figure 4.23 and Table 4.10), probably as a result of the increase in microparticle and vacuole size in the microparticles (Chapter 1). Ruhé, Boerman, Russel, Spauwen, Mikos and Jansen (2005) working with PLGA also in the form of microparticles reported an increase in BMP-2 entrapment efficiency with increase in particle size. Compared to the collagen standard, control and heat-treated kafirin microparticles had 7% and 18% higher BMP-2 binding capacity, respectively. Transglutaminase treatment of kafirin microparticles resulted in BMP-2 binding capacity 35% higher than collagen standard and an increase of 21% compared to control. As the transglutaminase reaction with kafirin probably occurred through deamidation due to the kafirin's very low lysine content, the excess negative charge may have enhanced electrostatic attraction with BMP-2, thereby resulting in the apparent higher BMP-2 binding capacity. Glutaraldehyde treatment of kafirin microparticles resulted in a BMP-2 binding capacity up to 14% higher than the control. This is probably because of increase in microparticle size, similar to heat treatment. Overall, transglutaminase treatment resulted in microparticles with the highest BMP-2 binding capacity after 1440 min reaction period. This corroborates the suggestion that the interaction between BMP-2 and carrier protein occurs through electrostatic attraction.

The BMP-2 binding obtained were in the range of 86–184 ng BMP-2/g kafirin microparticles and 102–137 ng BMP-2/g collagen depending on the treatment and incubation time. The literature gives both lower and higher BMP-2 binding capacity values compared to the figures in the present study. For example, a study by Friess, Uludag, Foskett, Biron and Sargeant (1999) showed that rhBMP-2 binding to collagen sponge was negligible at pH 3.0 and 4.0, while amounts of rhBMP-2 bound were up to 100000–200000 ng rhBMP-2 per mg collagen at pH 5.2 and pH 6.5. On the other hand, using PLGA microparticles, Ruhé et al. (2005) reported binding capacity values of 6000–7000 ng rhBMP-2 per mg PLGA microparticles. It has been found that apart from pH, many factors may influence the BMP-2 binding capacity, including concentration of the BMP-2 used in the binding process (Schrier and DeLuca, 1999), isoelectric point of the binding protein (Patel et al., 2008), ionic strength of the reaction medium (Geiger et al., 2003) and the method of loading of the BMP-2 to the carrier material (Ruhé et al., 2005). Therefore, these factors may explain the differences seen between BMP-2 binding capacity in the present study and literature values.

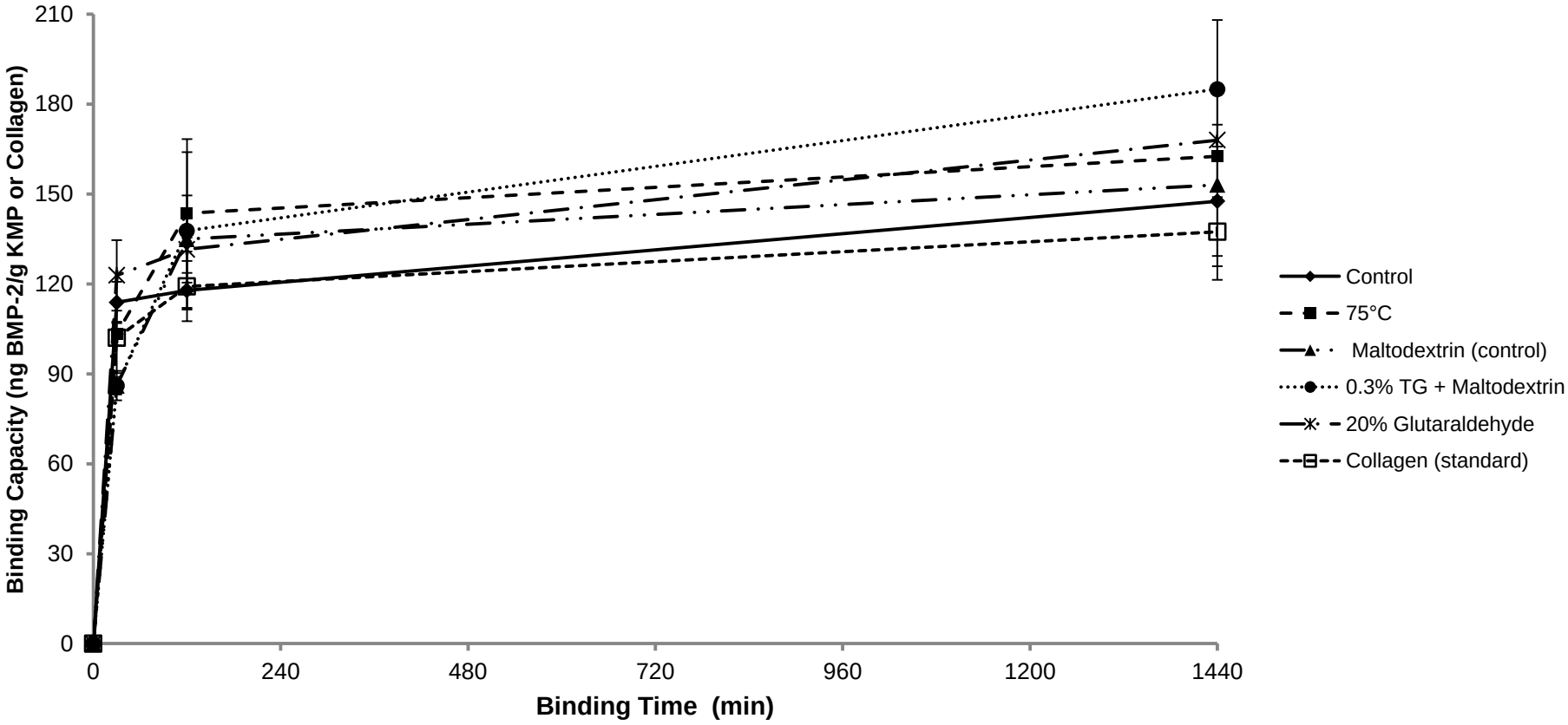

Figure 4.23 BMP-2 binding capacity of kafirin microparticles (KMP) treated with heat, transglutaminase and glutaraldehyde compared with collagen standard over a 24 h reaction period, determined by BMP-2 ELISA. Curves are plotted using mean relative BMP-2 binding capacity at the set time intervals. Error bars are standard deviations (n=2).

Table 4.10 Effects of treating kafirin microparticles with heat, transglutaminase (TG) and glutaraldehyde on their BMP-2 binding capacity (ng BMP-2/g binding material) compared with collagen standard over a 24 h reaction period, determined by BMP-2 ELISA (the data presented here show a statistical analysis of data in Figure 4.23)

Binding material	Treatment		Binding Time (min)		
			30	120	1440
Kafirin microparticles					
	Control	22°C	113.8 bc (6.9) [112]	117.8 a (5.8) [99]	147.6 ab (18.2) [107]
	Heat	75°C	103.4 b (3.9) [101]	143.5 a (24.8) [120]	162.5 ab (10.6) [118]
	Transglutaminase				
		Maltodextrin	86.0 a (2.9) [84]	135.0 a (14.6) [113]	153.0 ab (31.7) [111]
		0.3% TG + Maltodextrin	86.0 a (4.9) [84]	137.7 a (26.2) [116]	184.9 b (23.0) [135]
	Glutaraldehyde	20%	122.8 c (11.8) [120]	131.5 a (3.9) [110]	168.0 ab (16.3) [122]
Collagen standard			102.0 b (11.8)	119.2 a (11.7)	137.4 a (11.5)

Values in a column followed by different letters are significantly different ($p<0.1$). Numbers in ( ) brackets are standard deviations (n=2). Numbers in [ ] brackets are BMP-2 binding capacity of kafirin microparticles as percentage of corresponding binding capacity of collagen standard. Control for heat and glutaraldehyde treatments is the same

Having established that kafirin microparticles could bind BMP-2 in the BMP complex to similar or larger extent compared to collagen standard, the safety, biodegradability and efficacy of kafirin microparticle film-BMP-2 system in bone regeneration was assessed in the animal study. The purified rhBMP-2 was used in the ectopic rat study to preclude possible infection from the porcine BMP complex and to improve the chance of ectopic bone growth as rhBMP-2 appears to be about 10000 times more potent than partially purified BMP-2 for regenerating bone in rats as reviewed by Hollinger et al. (1998). The binding capacities (after 24 h reaction period) of the wet kafirin microparticle films and dry kafirin microparticle films to rhBMP-2 compared to the binding capacity of kafirin microparticles with the BMP-2 in the BMP complex, were approximately three-fold and five-fold lower, respectively (Table 4.11). Similarly, for the same reaction period, the binding capacity of collagen with the rhBMP-2 was about three-fold lower than that obtained with the BMP-2 in the BMP complex. With regard to the kafirin microstructures binding with BMP-2, the formation of kafirin microparticle film from the kafirin microparticles probably changed the morphology of the individual kafirin microparticles, thereby affecting their rhBMP-2 binding capacity. Formation of cast kafirin microparticle films is very similar to an evaporation-induced self-assembly (EISA), which as explained by Wang and Padua (2012), involves binary or tertiary solvents where preferential evaporation of one of the solvents changes the polarity of the solution, which drives the self-assembly of solutes. EISA has been found to result in alteration of the morphology of similar protein microstructures such as zein microspheres (Wang and Padua, 2010). As reported by these authors, the EISA-transformed structures may range from sponges to continuous films, which could have different physical properties compared to the microspheres. For example, Wang et al. (2008) reported a collapse of zein microspheres by EISA as a result of evaporation of methanol trapped within the microspheres. Therefore, in the present study, a similar scenario may have occurred in which the vacuoles within the kafirin microparticles could have collapsed during solvent evaporation to prepare the films, thereby reducing the capacity of the kafirin microparticle films to bind rhBMP-2. This probably resulted in most binding of kafirin microparticle films with rhBMP-2 occurring at the surface as well as in the pores probably created by the soaking and washing out of the plasticizer. In addition, the fact rhBMP-2 and the BMP complex are from different sources suggests that they are innately different. Hence, they may have had different physical and chemical properties, thereby causing differences in their affinity for collagen and kafirin microstructures. The binding data also showed that the wet kafirin

microparticle film had a similar rhBMP-2 binding capacity compared with collagen standard, which was higher than that of the dry kafirin microparticle film. However, these rhBMP-2 binding capacities were not statistically significantly different ($p>0.1$). Therefore, the wet kafirin microparticle film was used as carrier for the rhBMP-2 for ectopic rat bioassay due to its relatively higher mean rhBMP-2 binding capacity compared to dry kafirin microparticle film.

Table 4.11 RhBMP-2 binding capacity of kafirin microparticle films compared with collagen standard after a 24 h reaction period, determined by BMP-2 ELISA

Binding material		rhBMP-2 binding capacity (ng rhBMP-2/g binding material)
Wet kafirin microparticle film	soaked and surface water removed by placing film between paper towels	32.9 a (8.8)
Dry kafirin microparticle film	soaked and dried in a desiccator for 72 h	22.2 a (4.8)
Collagen	standard	31.5 a (1.2)

Values in a column followed by same letter are not significantly different ($p>0.1$). Numbers in the brackets are standard deviations (n=2).

4.3.4.2 *Implant safety assessment*

Evidence of toxicity was sought to assess the safety of the kafirin microparticle film implants when used to deliver BMP-2 to stimulate bone regeneration in a rat. By Day 7 post implantation, there was visible wound healing progress, indicated by the formation of scabs on the implant sites (Figure 4.24). By Day 28 post implantation, there was a complete healing of most of the wounds as evidenced by the faint marks at the external surface of the implant sites. Such observations indicate that the rats reacted normally to the trauma resulting from the skin surgery (Babensee et al., 1998).

The gross appearance of the implants by Day 28 post implantation was also examined. All the implants were surrounded by tissue capsules (Figure 4.25). There was some infiltration of blood vessels within the encapsulated collagen implants**.** There was no difference in gross appearance between collagen control and the rhBMP-2 loaded collagen. There was more prominent infiltration of blood vessels within the encapsulated kafirin microparticle film implants than with collagen.

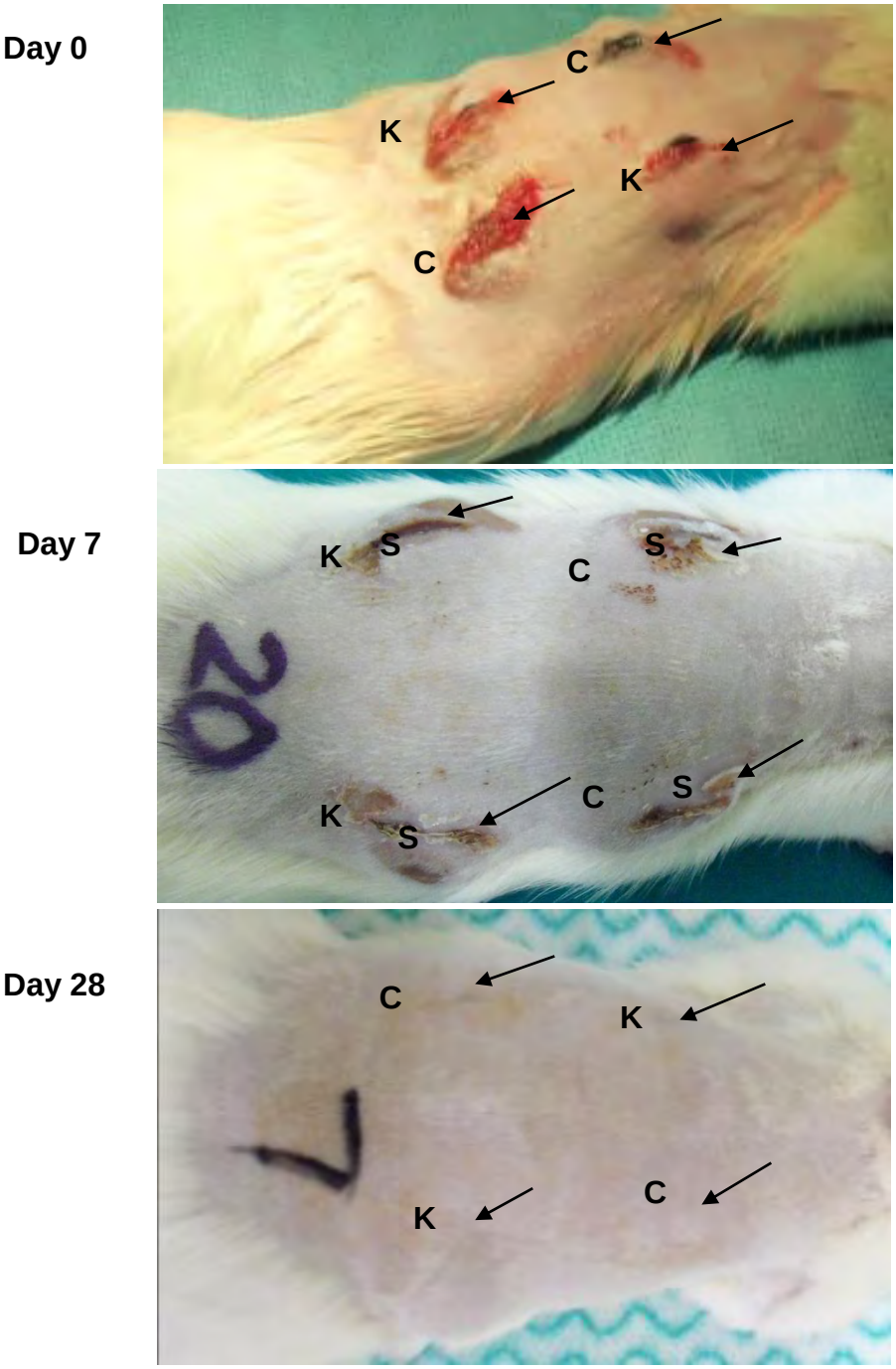

Figure 4.24 Typical appearance of implant sites by Day 0, 7, and 28 post implantation. Arrows point to implant sites. Note the occurrence of scabs denoted by 'S' by Day 7 post implantation and the healing by Day 28 post implantation. C-Collagen implant; K-kafirin microparticle film implant.

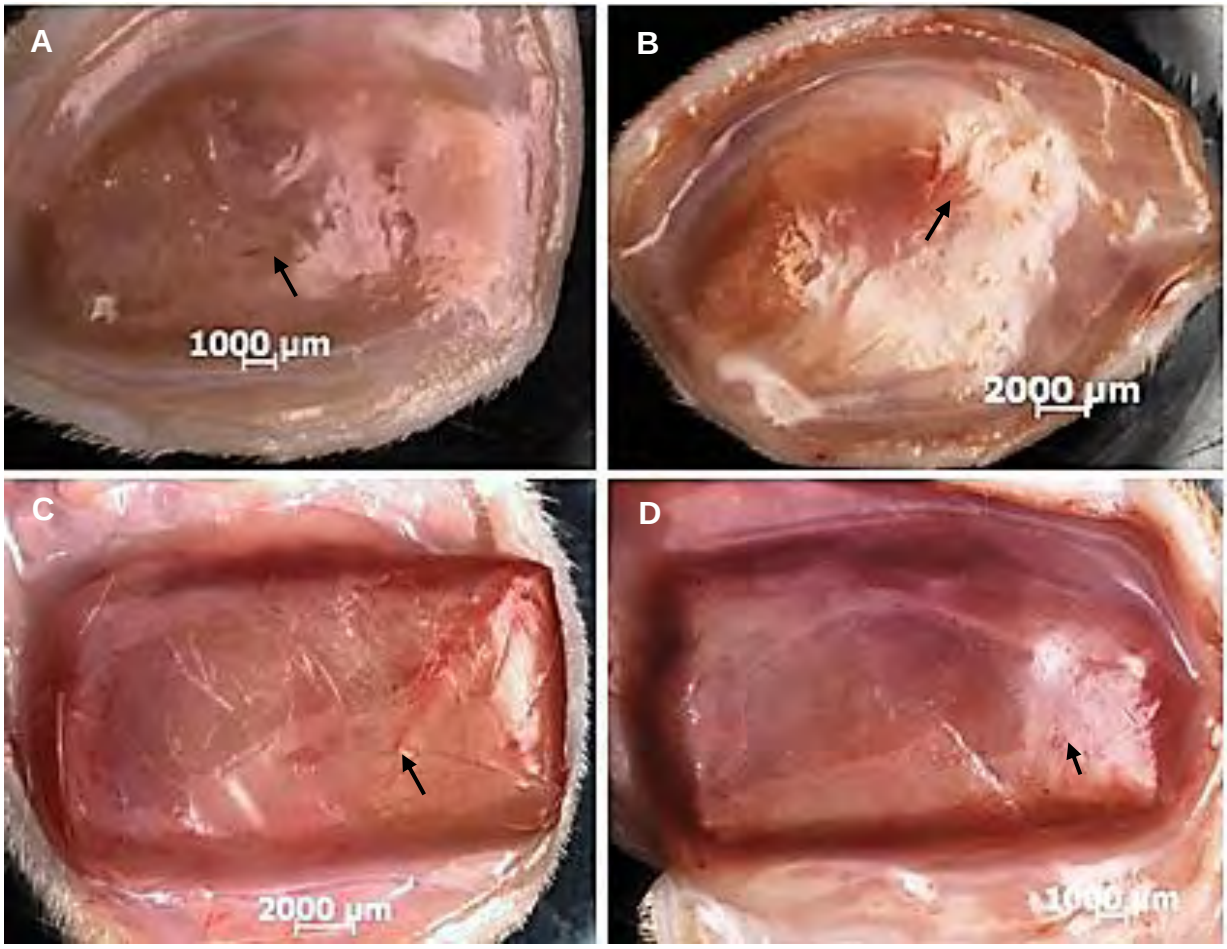

(i)

Figure 4.25 Gross appearance of encapsulated implants by Day 28 post implantation

(i) Plane view. **A**. Collagen control; **B**. Collagen+ rhBMP-2; **C**. Kafirin microparticle film control; **D**. Kafirin microparticle film+ rhBMP-2. Arrows point to blood vessels.

(ii) Cross-sectional view. **A**. Collagen control; **B**. Collagen+ rhBMP-2; **C** Kafirin microparticle film control; **D** Kafirin microparticle film+ rhBMP-2. Arrows are pointing at the encapsulated implant material.

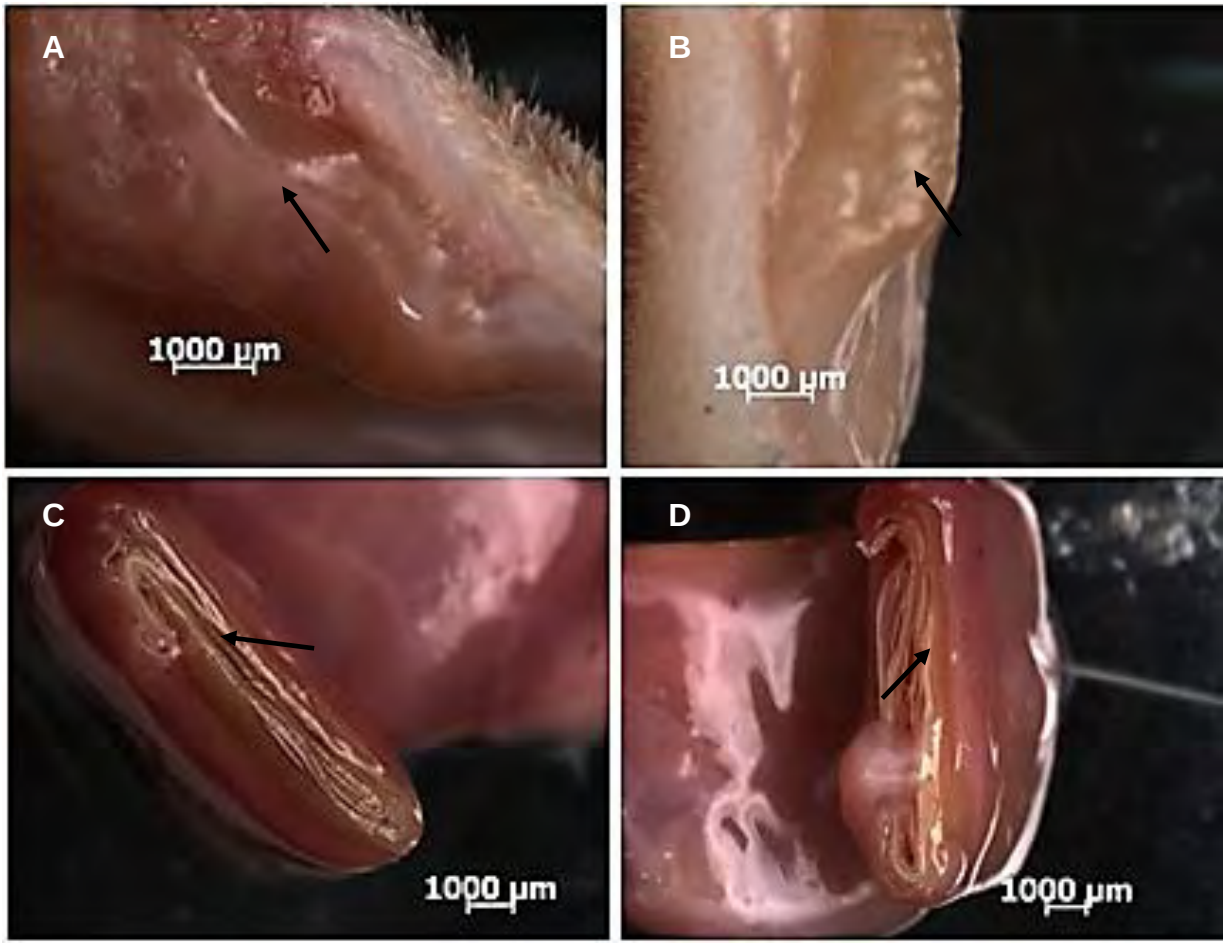

(ii)

As with the collagen standard, no difference in gross appearance was observed between the control and the rhBMP-2 loaded kafirin microparticle film implants. According to Nag and Banerjee (2012) there are four different types of tissue responses to the biomaterial implants concerning toxicity. Firstly, if the implant is toxic the surrounding tissue dies. Secondly, for a nontoxic and biologically inactive biomaterial, a fibrous tissue forms. Thirdly, if the biomaterial is nontoxic and active, the tissue bonds with it. Lastly, for a non-toxic and dissolving biomaterial implant, it is replaced by the surrounding tissue. According to the Idexx Laboratories report (Annex 2), macroscopic and histological evaluation did not show abnormal pathology for both rhBMP-2 loaded and unloaded kafirin microparticle film and collagen implants. As a measure of toxicity, tissue inflammatory response to the implants was examined. According to the Idexx Laboratories report (Annex 2), by Day 7 post implantation small microgranulomas were observed around all the implants, typical for a foreign body inflammatory reaction, with the response being more prominent for the collagen implant

compared to kafirin microparticle film implant (Table 4.12). The greater foreign body inflammatory reaction initially seen for the collagen implants possibly occurred as collagen was in a particulate matrix form while the kafirin microstructure was a film. According to Weiler, Helling, Kirch, Zirbes and Rehn (1996), the level of inflammatory cells present at the implant site is dependent on the amount of particles available for phagocytosis. In the case of the collagen implant with its granular form a large surface area would be available for phagocytosis with the result that more cells would migrate into the area of inflammation. In contrast, for the kafirin microparticle film the slow rate of biomaterial degradation meant that the surface area available to cells was much lower, hence resulting in a smaller degree of cellular attraction to the area. Further support for this theory can be seen by the presence of the multinucleated giant cells (Figure A3 in Annex 2). The presence of the giant cells is specific for the presence of poorly soluble, indigestible material in the tissue, as the smaller macrophages or epithelioid cells fuse (forming the giant cells) to enhance total phagocytic activity (reviewed by Rippey, 1994). By Day 28 post implantation, foreign body reaction was evident in all of the implantation sites. By this point post implantation, foreign body reaction varied from mild to severe with little difference between the collagen implants and the kafirin microparticle film implants.

Skin ulceration was examined as part of safety assessment. According to the Idexx Laboratories report (Annex 2), the areas of ulceration were small and microscopically confirmed at the implantation site on the surface of the skin that showed superficial exudative crusts and some areas of full-thickness epithelial necrosis. Mild inflammation was present in the dermis underneath the ulcerated skin. At Day 7 post implantation, these superficial ulcerations were found at both collagen and kafirin microparticle film implant sites. However, at Day 28 post implantation, superficial ulceration in the epidermis was found in only three collagen implantation sites (Table 4.12). As explained in the Idexx Laboratories report, the superficial skin ulceration was probably due to external irritation from animal scratching. The Idexx Laboratories report also indicated that dermal scarring due to the implantation was present underneath these ulcers and in some of the non-ulcerated sites. This was attributed to be probably part of the normal healing process. The fact that ulceration was found in only a few collagen implantation sites is possibly an indication of interspecies variation, which is an issue in toxicity testing using animal models (reviewed by Smart, Nicholls, Green, Rogers and Cook, 1999).

Table 4.12 Summary of Idexx Laboratories report on the histological scoring for inflammatory and osteogenic response of rat tissue to kafirin microparticle (KMP) film and collagen loaded with BMP-2 and polyphenol and glutaraldehyde treated KMP film implants by Day 7 and Day 28 post implantation

Day 7 post implantation

Carrier material	Treatment	Foreign body reaction	Granulomatous reaction	Ulcerated skin	Osteolysis[#]	Osteogenesis
Collagen						
	Control	+++ (1), ++ (3)	+++ (4)	++ (1), + (2), - (1)	+++ (2), ++ (2)	- (4)
	Low rhBMP-2*	+++ (1), ++ (2)	+++ (3)	+ (2), - (1)	+++ (1), ++ (2)	- (3)
	High rhBMP-2	+++(1), ++ (3)	+++ (4)	+ (3), - (1)	+++ (1), ++ (2), + (1)	- (4)
KMP film						
	Control	+ (1), - (3)	++ (1), + (3)	++ (1), + (2), - (1)	- (4)	- (4)
	Low rhBMP-2	++ (1), + (1), - (2)	+++ (1), ++ (1), + (2)	++ (2), + (1), - (1)	- (4)	- (4)
	High rhBMP-2	+ (1), - (3)	+++ (1), ++ (1), + (2)	+++ (1), - (3)	- (4)	- (4)
	Glutaraldehyde	+ (1), - (3)	+ (4)	+ (3), - (1)	- (4)	- (4)
	Polyphenol	++ (1), + (1), - (2)	+++ (1), ++ (1), + (2)	++ (1), + (2), - (2)	- (4)	- (4)

(Continued over leaf)

Day 28 post implantation

Carrier material	Treatment	Foreign body reaction	Granulomatous reaction	Ulcerated skin	Osteolysis[#]	Osteogenesis
Collagen						
	Control	+++ (3), + (1)	+++ (3), ++ (1)	+ (1), - (3)	+++ (1), ++ (3)	- (4)
	Low rhBMP-2	++ (4)	+++ (2), ++ (1), + (1)	+ (1), - (3)	++ (2), + (2)	- (4)
	High rhBMP-2	+++(2), ++ (2)	+++ (1), ++ (2), + (1)	+ (1), - (3)	+++ (1), ++ (3)	+ (1), - (3)
KMP film						
	Control	++ (2), + (2)	+++ (1), ++ (2), + (1)	- (4)	+++ (1), ++ (2), - (1)	- (4)
	Low rhBMP-2	++ (3), + (1)	+++ (2), ++ (1), + (1)	- (4)	++ (2), + (1), - (1)	- (4)
	High rhBMP-2	++ (3), + (1)	+++ (1), ++ (2), + (1)	- (4)	++ (1), + (2), - (1)	- (4)

Results were graded as follows: negative/none (-), mild (+), moderate (++), severe (+++). The number of implants with the indicated score is in the brackets. Total number of implants per treatment =4. RhBMP-2 Dose: Control=0 µg/g, Low=0.107 µg/g; High=2.14 µg/g

* One implant sample lost

NB: The treatments were coded before evaluation by Idexx Laboratories.

[#] Osteolysis was used as measure of degradation of the implant material (Dr W.S. Botha, Idexx Laboratories, personal communication post submission of the Idexx report).

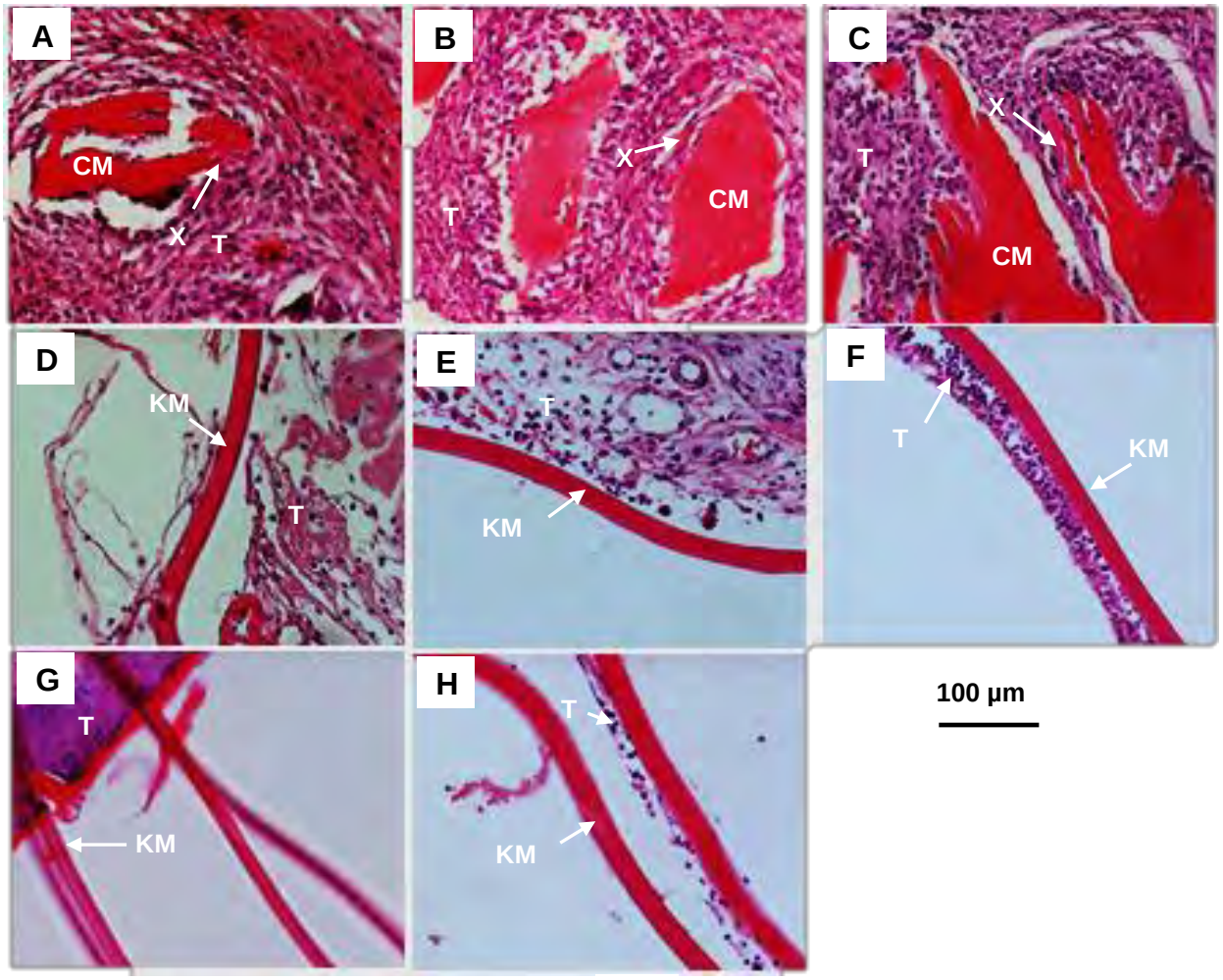

(i)

Figure 4.26 Images of haematoxylin–eosin stained sections of implants showing evidence of degradation of implants. The photographs were taken of slides prepared by Idexx Laboratories for the report (Annex 2).

(i) Day 7 post implantation. **A.** Collagen control. **B.** Collagen + low rhBMP-2 dose. **C.** Collagen + high rhBMP-2 dose. **D.** Kafirin microparticle film control. **E.** Kafirin microparticle film + low rhBMP-2 dose. **F.** Kafirin microparticle film + high rhBMP-2 dose. **G.** Glutaraldehyde-treated kafirin microparticle film. **H.** Polyphenol-treated kafirin microparticle film. KM-Kafirin microparticle film material; CM-Collagen material, T-Tissue. X-Degraded section of implant.

(ii) Day 28 post implantation. **A.** Collagen control. **B.** Collagen + low rhBMP-2 dose. **C.** Collagen + high rhBMP-2 dose. **D.** Kafirin microparticle film control. **E.** Kafirin microparticle film + low rhBMP-2 dose. **F.** Kafirin microparticle film + high rhBMP-2 dose. KM- Kafirin microparticle film material; CM-Collagen material, T-Tissue. NB. Glutaraldehyde-treated and polyphenol-treated kafirin microparticle film implants were only subjected to a 7-day implantation. X-Degraded section of implant.

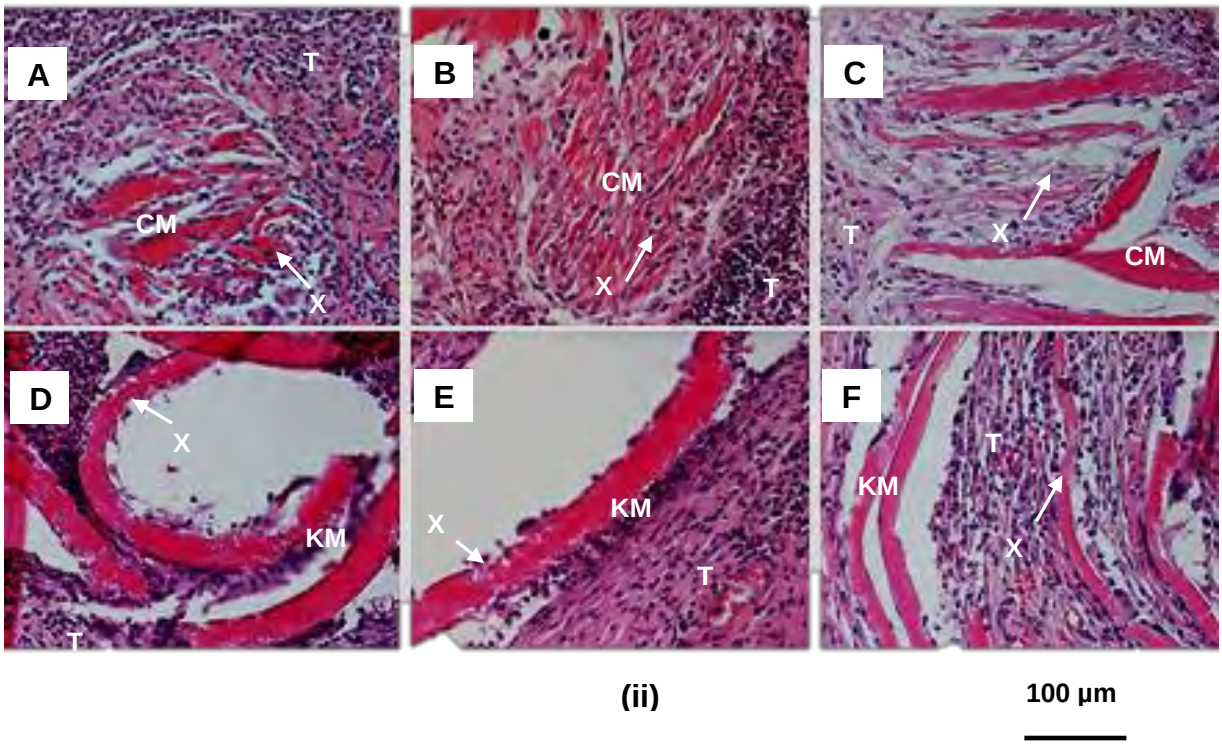

Overall, according to the Idexx report the safety assessment data showed that kafirin microparticle film implants were non-irritant to the animals. This is probably because kafirin is non-allergenic (Ciacci et al., 2007) as it does not contain the amino acid sequences known to be toxic (reviewed by Wieser and Koehler, 2008).

4.3.4.3 *Evidence of implant degradation*

Lysis of the implant was used as a measure of implant degradation (Dr W.S. Botha, Idexx Laboratories, personal communication post submission of the Idexx report). According to Idexx Laboratories report (Annex 2), by Day 7 post implantation, degradation of the collagen implants had started, as indicated by resorption of the implant material, while the kafirin microparticle film implants were all intact (Table 4.12 and Figure 4.26 (i)). By Day 28 post implantation, most of the collagen implants had completely degraded (Figure 4.26 (ii)). In contrast, the kafirin microparticle film implants showed signs of some degradation but a large proportion of these implants was still intact. Studies have found that collagen implants degrade relatively quickly as a result of proteolysis. For example, Brown, Li, Guda, Perrien, Guelcher and Wenke (2011) worked on biodegradable polyurethane microsphere scaffolds compared to collagen sponge delivery system for release of rhBMP-2 in a critical-sized rat segmental defect model. These authors reported in their histological evaluation of the tissues with scaffold implants that after four weeks post implantation the polyurethane scaffolds

were still visible, but the collagen carrier had been degraded. In the present study, the fact that kafirin microparticle film implants were still largely intact by Day 28 post implantation indicated that the kafirin microparticle films were biodegradable but at a slower rate, probably due to the low susceptibility of kafirin to proteolysis (Emmambux and Taylor, 2009), as result of its hydrophobicity, as discussed.

Another factor that may have contributed to the more rapid degradation of the collagen implants compared to kafirin microparticle film implants was probably the differences in size of the implants. Despite the fact that the implants were of the same weight, the collagen implants were smaller but with a large surface area due to its granulated form. On the other hand, kafirin microparticle films were folded which may have changed how they degraded.

4.3.4.4 *Evidence of ectopic bone morphogenesis*

Radiographs of the rats post-mortem showed no indication of new bone for any of the implants by Day 28 post implantation (Figure 4.27). This was confirmed by histological evaluation by Idexx Laboratories (Annex 2). By Day 7 post implantation, osteogenesis appeared to be absent in the implants sites (Table 4.12). Histological evaluation, however, did indicate mild osteogenesis by Day 28 post implantation in one of the collagen implant sites. Alkaline phosphatase (ALP) activity was evaluated as a chemical pathological marker of early osteoblast differentiation, because ALP activity is expected to be elevated in case of an increased osteoblastic activity as bone ALP is localised in the plasma membrane of osteoblastic cells (reviewed by Withhold, Schulte and Reinauer, 1996). No substantial change in the ALP activity was evident for either BMP-2 loaded collagen or the kafirin microparticle films (Table 4.13) in agreement with the findings from the radiographs and the histopathology. The collagen implants nonetheless seemed to have significantly higher ALP than the kafirin microparticle film implants ($p<0.05$), probably because collagenous implants have the ability to induce some bone morphogenesis (Hollinger et al., 1998). However, the results in the present study were confounded by the apparent reduction of physically visible collagen implant material, probably due to digestion by tissue enzymes, while the kafirin microparticle film implants maintained their integrity. Hence, the collagen implant samples used in ALP assay probably had a relatively higher content of animal tissue material obtained from the implant site than the kafirin microparticle film implant material. This greater amount of tissue material in the collagen implants may have resulted in the apparently higher ALP activity value, as a result of contribution from serum ALP.

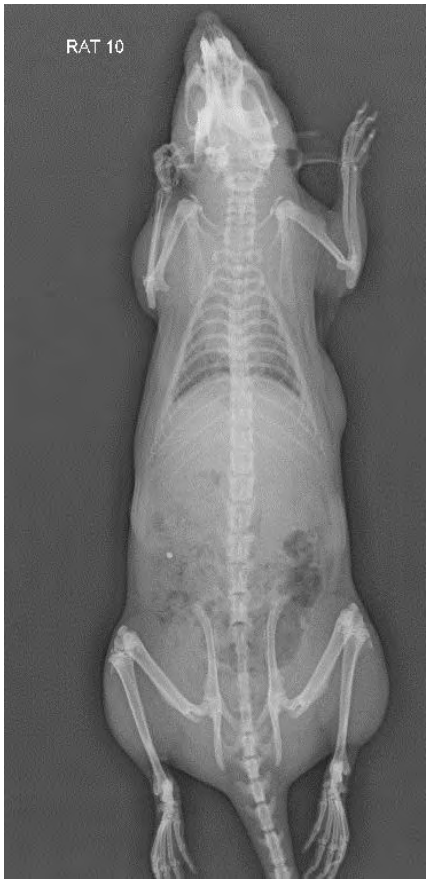

Figure 4.27 Representative radiograph of rat by Day 28 post implantation. All the radiographs of the rats with implantations were similar.

Table 4.13 Alkaline phosphatase (ALP) activity of capsule and kafirin microparticle film or collagen standard implants loaded with rhBMP-2 after 28 days of implantation

Carrier material	rhBMP-2 Dose	ALP concentration (pmol/g capsule + implant)	ALP concentration (pmol/g capsule*)
Collagen			
	Control	174.3 c (11.5)	
	Low	184.3 c (8.6)	
	High	244.3 d (7.4)	
Kafirin microparticle film			
	Control	111.0 b (3.8)	195.4 c (6.6)
	Low	72.4 a (8.2)	95.6 a (10.8)
	High	118.6 b (8.4)	130.1 b (9.2)

Values in a column followed by different letters are significantly different ($p<0.05$). Numbers in the brackets are standard deviations, (n=4)

*Collagen was digested by the tissue enzymes; hence, it was impractical to calculate concentration of the ALP in the tissue without collagen implant

RhBMP-2 Dose: Control=0 µg/g, Low=0.107 µg/g; High=2.14 µg/g

ALP activity is not specific for bone growth as other body organs such as the liver and intestines also form the enzyme (reviewed by Hoffmann et al., 1994). The radiology, histology and ALP data all indicated the absence of ectopic bone morphogenesis induced by kafirin microparticle film-rhBMP-2 or the collagen-rhBMP-2 system.

A patent of Duneas (2010) states that a collagen and BMP complex system can induce bone growth in rats, as measured by ALP activity, as early as 12 days post implantation. While it could not be ascertained why the implant failed to induced to osteogenesis, a number of reasons are plausible. First, the rhMBP-2 dose was possibly too low, particularly in comparison to the BMP complex applied in the work by Duneas (2010), which was 100000 ng per implant. Although low BMP-2 dosage levels in a carrier-BMP-2 system could induce bone growth (Dr Nicolaas Duneas, personal communication), the wide range of BMP-2/rhBMP-2 doses, the different animal models and the different implantation durations used in similar studies made it difficult to determine the appropriate BMP-2 dosage. For example, Bessa et al. (2010) working with silk fibroin microparticles reported bone morphogenesis measured by ALP activity in a rat model when they used 5 µg and 12.5 µg BMP-2 per implantation site. Similarly, Yasko, Lane, Fellinger, Rosen, Wozney and Wang (1992) working with demineralized rat-bone matrix as a carrier applied 1400000 ng and 11000000 ng rhBMP-2 per implant site and reported bone growth determined by radiology, histology and mechanical analysis. The BMP-2 levels used by these workers were greater than the 8 ng and 160 ng rhBMP-2 per implant that was used in the present study or the 1 ng BMP-2 per implant used by Fu, Nie, Ho, Wang and Wang (2008) in their study using a nude mice model. The choice of the relatively low rhBMP-2 dosage in the present study was motivated by the higher potency of rhBMP-2, which has been reported to be about 10000 times more than partially purified BMP-2 for regenerating bone in rats (reviewed by Hollinger et al, 1998).

Secondly, the duration of study was probably too short and therefore insufficient to induce osteogenesis. Although Wang, Rosen, D'Alessandro, Bauduy, Cordes, Harada, Israel, Hewick, Kerns, Lapan, Luxenberg, McQuaid, Moutsatsos, Nove and Wozney (1990) and Bessa et al. (2010) reported BMP-2 induced ectopic bone morphogenesis measured by ALP activity in rats within a month post implantation, many researchers have also found substantial subcutaneous bone morphogenesis induced by BMP-2 loaded biomaterials after a longer time post implantation, usually greater than three months (reviewed by Babensee et al., 1998; Kempen, Lu, Hefferan, Creemers, Maran, Classic, Dhert and Yaszemski, 2008).

Thirdly, immune sensitization may have occurred since the rhBMP-2 could have induced an immune reaction such as osteolysis of regenerated bone as the animals were immunocompetent. Other additional factors that may have also caused the disparity of results in the present study and those in literature include differences in placement site for the implants and differences in age of the animals (Prof Vinny Naidoo, University of Pretoria Biomedical Research Centre, personal communication). Therefore, it was difficult to make a direct comparison between the rat tissue response to kafirin microparticle film-BMP-2 system in the present study and data from the similar systems in the literature.

4.3.5 Conclusions

Kafirin microparticles can bind BMP-2. This binding is enhanced through modification by heat, transglutaminase or glutaraldehyde treatment. Also, kafirin microparticle film is non-toxic showing no abnormal inflammatory reactions when implanted subcutaneously in a rat. In addition, kafirin microparticle film shows a prolonged degradation when implanted in an animal tissue, which is a great advantage as the kafirin microparticle film implants can eventually degrade after their scheduled "task" is complete by the body's own metabolic process. The kafirin microstructures could therefore have application as biomaterials such as bioactive scaffolds for hard or soft tissue repair. However, at the low BMP-2 levels (107–2140 ng/g) and for the short implantation period (28 days), the kafirin microparticle film-BMP-2 does not induce bone morphogenesis in the rat model. Therefore more work needs to be done to optimize BMP-2 loading and release profile with kafirin microstructures.

4.3.6 References

Babensee, J.E., 1990. Morphological assessment of HEMA-MMA microcapsules for liver cell transplantation. PhD Thesis, University of Toronto, Toronto.

Babensee, J.E., Anderson, J.M., McIntire, L.V., Mikos, A.G., 1998. Host response to tissue engineered devices. Advanced Drug Delivery Reviews 33, 111–139.

Balmayor, E.R., Feichtinger, G.A., Azevedo, H.S., Van Griensven, M., Reis, R.L., 2009. Starch-poly-ε-caprolactone microparticles reduce the needed amount of BMP-2. Clinical Orthopaedics and Related Research 467, 3138–3148.

Bensaid, W., Triffitt, J.T., Blanchat, C., Oudina, K., Sedel, L., Petite, H., 2003. A biodegradable fibrin scaffold for mesenchymal stem cell transplantation. Biomaterials 24, 2497–2502.

Bessa, P.C., Balmayor, E.R., Hartinger, J., Zanoni, G., Dopler, D., Meinl, A., Banerjee, A., Casal, M., Redl, H., Reis, R.L., Van Griensven, M., 2010. Silk fibroin microparticles as carriers for delivery of human recombinant bone morphogenetic protein-2: in vitro and in vivo bioactivity. Tissue Engineering: Part C 16, 937–945.

Bessa, P.C., Casal, M., Reis, R.L., 2008. Bone morphogenetic proteins in tissue engineering: the road from laboratory to clinic, Part II (BMP delivery). Journal of Tissue Engineering and Regenerative Medicine 2, 81–96.

Brown, K.V., Li, B., Guda, T., Perrien, D.S., Guelcher, S.A., Wenke, J.C., 2011. Improving bone formation in a rat femur segmental defect by controlling bone morphogenetic protein-2 release. Tissue Engineering: Part A 17, 1735–1746.

Chen, D., Zhao, M., Mundy, G.R., 2004. Bone morphogenetic proteins. Growth Factors 22, 233–241.

Chevallet, M., Luche, S., Rabilloud, T., 2006. Silver staining of proteins in polyacrylamide gels. Nature Protocols 1, 1852–1858.

Ciacci, C., Maiuri, L., Caporaso, N., Bucci, C., Del Giudice, L., Massardo, D.R., Pontieri, P., Di Fonzo, N., Bean, S.R., Ioerger, B., Londei, M., 2007. Celiac disease: in vitro and in vivo safety and palatability of wheat-free sorghum food products. Clinical Nutrition 26, 799–805.

Csonka, F.A., Murphy, J.C., Jones, D.B., 1926. The iso-electric points of various proteins. Journal of the American Chemical Society 48, 763–768.

Cuq, B., Gontard, N., Guilbert, S., 1998. Proteins as agricultural polymers for packaging production. Cereal Chemistry 75, 1–9.

Duneas, N., 2010. Osteoinductive biomaterials. European Patent Office EP 1 539 812 B1.

Duodu, K.G., Taylor, J.R.N., Belton, P.S., Hamaker, B.R., 2003. Factors affecting sorghum protein digestibility. Journal of Cereal Science 38, 117–131.

Emmambux, N.M., Taylor, J.R.N., 2003. Sorghum kafirin interaction with various phenolic compounds. Journal of the Science of Food and Agriculture 83, 402–407.

Emmambux, N.M., Taylor, J.R.N., 2009. Properties of heat-treated sorghum and maize meal and their prolamin proteins. Journal of Agricultural and Food Chemistry 57, 1045–1050.

Friess, W., Uludag, H., Foskett, S., Biron, R., Sargeant, C., 1999. Characterization of absorbable collagen sponges as rhBMP-2 carriers. International Journal of Pharmaceutics 187, 91–99.

Fu, Y.-C., Nie, H., Ho, M.-L., Wang, C.-K., Wang, C.-H., 2008. Optimized bone regeneration based on sustained release from three-dimensional fibrous PLGA/Hap composite scaffolds loaded with BMP-2. Biotechnology and Bioengineering 99, 996–1006.

Gautschi, O.P., Frey, S.P., Zellweger, R., 2007. Bone morphogenetic proteins in clinical applications. ANZ Journal of Surgery 77, 626–631.

Geiger, M., Li, R.H., Friess, W., 2003. Collagen sponges for bone regeneration with rhBMP-2. Advanced Drug Delivery Reviews 55, 1613–1629.

Haidar, Z.S., Hamdy, R.C., Tabrizian, M., 2009. Delivery of recombinant bone morphogenetic proteins for bone regeneration and repair. Part B: Delivery systems for BMPs in orthopaedic and craniofacial tissue engineering. Biotechnology Letters 31, 1825–1835.

Higberger, J.H., 1939. The isoelectric point of collagen. Journal of the American Chemical Society 61, 2302-2303.

Hoffmann, W.E., Everds, N., Pignatello, M., Solter, P.F., 1994. Automated and semiautomated analysis of rat alkaline phosphatase isoenzymes. Toxicologic Pathology 22, 633–638.

Hollinger, J.O., Schmitt, J.M., Buck, D.C., Shannon, R., Joh, S.P., Zegzula, H.D., Wozney, J., 1998. Recombinant human bone morphogenetic protein-2 and collagen for bone regeneration. Journal of Biomedical Materials Research 43, 356–364.

Ishikawa, T., Terai, H., Kitajima, T., 2001. Production of a biologically active epidermal growth factor fusion protein with high collagen affinity. Journal of Biochemistry 129, 627–633.

Kempen, D.H.R., Lu, L., Hefferan, T.E., Creemers, L.B., Maran, A., Classic, K.L., Dhert, W.J.A., Yaszemski, M.J., 2008. Retention of in vitro and in vivo BMP-2 bioactivities in sustained delivery vehicles for bone tissue engineering. Biomaterials 29, 3245–3252.

Kiernan, J.A., 2000. Formaldehyde, formalin, paraformaldehyde and glutaraldehyde: What they are and what they do. Microscopy Today 00-1, 8–12.

Kim, C.-S., Kim, J.-I., Kim, J., Choi, S.-H., Chai, J.-K., Kim, C.-K., Cho, K.-S., 2005. Ectopic bone formation associated with recombinant human bone morphogenetic proteins-2 using absorbable collagen sponge and beta tricalcium phosphate as carriers. Biomaterials 26, 2501–2507.

King, G.N., Cochran, D.L., 2002. Factors that modulate the effects of bone morphogenetic protein-induced periodontal regeneration: a critical review. Journal of Periodontology 73, 925–936.

La, W.-G., Kang, S.-W., Yang, H.S., Bhang, S.H., Lee, S.H., Park, J.-H, Kim, B.-S., 2010. The efficacy of bone morphogenetic protein-2 depends on its mode of delivery. Artificial Organs 34, 1150–1153

Lowry, O.H., Rosebrough, N.J., Farr, A.L., Randall, R.J., 1951. Protein measurement with the Folin phenol reagent. Journal of Biological Chemistry 193, 265–275.

Nag, S., Banerjee, R., 2012. Fundamentals of medical implant materials. In: Narayan, R. (Ed.), ASM Handbook: Materials for Medical Devices. ASM International: Russell Township, OH, Vol. 23, pp. 6–17.

Nickel, J., Dreyer, M.K., Kirsch, T., Sebald, W., 2001. The crystal structure of the BMP-2:BMPR-IA complex and the generation of BMP-2 antagonists. Journal of Bone and Joint Surgery 83-A (Suppl. 1, Part 1), S7–S14.

Patel, Z.S., Yamamoto, M., Ueda, H., Tabata, Y., Mikos, A.G., 2008. Biodegradable gelatin microparticles as delivery systems for the controlled release of bone morphogenetic protein-2. Acta Biomaterialia 4, 1126–1138.

Ripamonti, U., Duneas, N., Van Den Heever, B., Bosch, C., Crooks, J., 1997. Recombinant transforming growth factor-β1 induces endochondral bone in the baboon and synergizes with recombinant osteogenic protein-1 (bone morphogenetic protein-7) to initiate rapid bone formation. Journal of Bone and Mineral Research 12, 1584–1595.

Rippey, J.J., 1994. General Pathology. Illustrated Lecture Notes. (2nd ed.), Wits University Press: Johannesburg, South Africa, pp. 151–152.

Ruhé, P.Q., Boerman, O.C., Russel, F.G.M., Spauwen, P.H.M., Mikos, A.G., Jansen, J.A., 2005. Controlled release of rhBMP-2 loaded poly(DL-lactic-co-glycolic acid)/calcium phosphate cement composites in vivo. Journal of Controlled Release 106, 162–171.

Scheufler, C., Sebald, W., Hülsmeyer, M., 1999. Crystal structure of human bone morphogenetic protein-2 at 2.7 Å resolution. Journal of Molecular Biology 287, 103–115.

Schrier, J.A., DeLuca, P.P., 1999. Recombinant human bone morphogenetic protein-2 binding and incorporation in PLGA microsphere delivery systems. Pharmaceutical Development and Technology 4, 611–621.

Shah, P, Keppler, L., Rutkowski, J., 2011. A review of bone morphogenic protein: an elixir for bone grafting. Journal of Oral Implantology (in press) DOI: http://0-dx.doi.org.innopac.up.ac.za/10.1563/AAID-JOI-D-10-00196.

Silva, G.A., Ducheyne, P., Reis, R.L., 2007. Materials in particulate form for tissue engineering. 1. Basic concepts. Journal of Tissue Engineering and Regenerative Medicine 1, 4–24.

Singleton, V.L., Rossi, J., 1965. Colorimetry of total phenolics with phosphomolybdic-phosphotungstic acid reagents. American Journal of Enology and Viticulture 16, 144–158.

Smart, J.D., Nicholls, T.J., Green, K.L., Rogers, D.J., Cook, J.D., 1999. Lectins in drug delivery: a study of the acute local irritancy of the lectins from *Solanum tuberosum* and *Helix pomatia*. European Journal of Pharmaceutical Sciences 9, 93–98.

Taylor, J., Taylor, J.R.N., Belton, P.S., Minnaar, A., 2009a. Formation of kafirin microparticles by phase separation from an organic acid and their characterisation. Journal of Cereal Science 50, 99–105.

Taylor, J., Taylor, J.R.N., Belton, P.S., Minnaar, A., 2009b. Kafirin microparticle encapsulation of catechin and sorghum condensed tannins. Journal of Agricultural and Food chemistry 57, 7523–7528.

Tu, J., Wang, H., Li, H., Dai, K., Wang, J., Zhang, X., 2009. The in vivo bone formation by mesenchymal stem cells in zein scaffolds. Biomaterials 30, 4369–4376.

Utesch, T., Daminelli, G., Mroginski, M.A., 2011. Molecular dynamics simulations of the adsorption of bone morphogenetic protein-2 on surfaces with medical relevance. Langmuir 27, 13144–13153.

Visser, R., Arrabal, P.M., Becerra, J., Rinas, U., Cifuentes, M., 2009. The effect of an rhBMP-2 absorbable collagen sponge-targeted system on bone formation in vivo. Biomaterials 30, 2032–2037.

Wang, E.A., Rosen, V., D'Alessandro, J.S., Bauduy, M., Cordes, P., Harada, T., Israel, D.I., Hewick, R.M., Kerns, K.M., Lapan, P., Luxenberg, D.P., McQuaid, D., Moutsatsos, I.K., Nove, J., Wozney, J.M., 1990. Recombinant human bone morphogenetic protein induces bone formation. Proceedings of the National Academy of Sciences of the United States of America 87, 2220–2224.

Wang, H.-J., Lin, Z.-X., Liu, X.-M., Sheng, S.-Y., Wang, J.-Y., 2005. Heparin-loaded zein microsphere film and hemocompatibility. Journal of Controlled Release 105, 120–131.

Wang, H.-J., Gong, S.-J., Lin, Z.-X., Fu, J.-X., Xue, S.-T., Huang, J.-C., Wang, J.-Y., 2007. In vivo biocompatibility and mechanical properties of porous zein scaffolds. Biomaterials 28, 3952–3964.

Wang, Q., Yin, L., Padua, G.W., 2008. Effect of hydrophilic and lipophilic compounds on zein microstructures. Food Biophysics 3, 174–181.

Wang, Y., Padua, G.W., 2010. Formation of zein microphases in ethanol-water. Langmuir 26, 12897–12901.

Wang, Y., Padua, G.W., 2012. Nanoscale characterization of zein self-assembly. Langmuir 28, 2429−2435.

Weiler, A., Helling, H.-J., Kirch, U., Zirbes, T.K., Rehn, K.E., 1996. Foreign-body reaction and the course of osteolysis after polyglycolide implants for fracture fixation. Journal of Bone and Joint Surgery [Br] 78-B, 369–376.

Wieser, H., Koehler, P., 2008. The biochemical basis of celiac disease. Cereal Chemistry 85, 1–13.

Yasko, A.W., Lane, J.M., Fellinger, E.J., Rosen, V., Wozney, J.M., Wang, E.A., 1992. The healing of segmental bone defects, induced by recombinant human bone morphogenetic protein (rhBMP-2). A radiographic, histological, and biomechanical study in rats. Journal of Bone and Joint Surgery 74-A, 659–670.

5 GENERAL DISCUSSION

The general discussion is divided into three subsections. The first is a critical review of the main methodologies as applied in this research, including cross-linking techniques, electron microscopy, AFM, SDS-PAGE, FTIR, ELISA and subcutaneous rat bioassay. Mechanisms responsible for cross-linking of the kafirin microparticles and how they relate the morphologies, especially the occurrence of spindle-shaped glutaraldehyde-treated kafirin nanostructures will be proposed. Lastly, there will be a brief discussion on the potential application of the modified kafirin microstructures and suggestions for future studies that might be required to optimize the application of these microstructures. Reviews of the methodologies used in the measurement of water vapour barrier and tensile properties were discussed by Emmambux (2004) and so will not be reviewed further here.

5.1 METHODOLOGY: CRITICAL REVIEW

Cross-linking treatments were performed on pre-formed kafirin microparticles. As discussed, an attempt to modify the microparticle structures with heat or glutaraldehyde while forming them produced only slightly larger microparticles compared to the control. In addition, there was absence of vacuoles within the microparticles cross-linked with heat during their preparation, while there was a reduction in vacuole size with glutaraldehyde treatment. However, when the treatments were applied on pre-formed microparticles, there was a significant change in particle morphology, hence this protocol was applied. Cross-linking the kafirin in solution in glacial acetic acid before preparation of the microparticles was considered but applying the cross-linking treatments directly to kafirin dissolved in glacial acetic acid would have been impractical. First, heating kafirin in high acid concentration could probably decompose the protein through acid hydrolysis, as has been reported with other proteins (reviewed by Tsugita and Scheffler, 1982; Fountoulakis and Lahm, 1998). Secondly, the glutaraldehyde cross-linking reaction would probably be less effective at high acid concentration due to instability of Schiff base (imine) formed by interaction of the aldehyde carbonyl group and amino group from the protein (reviewed by Migneault et al., 2004). Additionally, as the optimal pH for the transglutaminase enzyme reaction is 6–7 (Ando et al., 1989) a low pH would have inactivated the enzyme. Another challenge was that the temperature used in the present study for transglutaminase reaction was 30^{o}C, which is

well below the optimum of 50°C (Ando et al., 1989). This was necessary to preclude heat-induced disulphide cross-linking of the kafirin proteins as this would have confounded interpretation of data from the enzyme treatment, especially because 50°C was used as a temperature for heat treatment. But the application of the lower temperature may have compromised transglutaminase catalysed cross-linking reaction. However, the lower temperature did not affect the precision of the findings.

Conventional SEM was used to examine the surface properties of the microparticles and microparticle films. While conventional SEM protocol does not invalidate data, its main limitation is the potential introduction of artefacts due to sample preparation. As the microparticles were wet, they had to be dried before examination hence the images obtained were not necessarily of 'native' state kafirin microparticles. Therefore, the SEM images showing association (agglomeration) of particles may possibly have been a sample preparation artefact arising from removal of the acid. Drying would therefore probably result in sphere-to-sphere interfaces resulting into particle agglomeration. Therefore, no conclusive evidence could be drawn from such observations, especially with the transglutaminase-treated microparticles. In addition, there was poor image resolution at relatively high magnification (×10000). Thus, the magnification was limited to ×2500 for clarity of the SEM images. Lastly, using SEM in an attempt to investigate the effect of BMP-2 binding on the morphology of the kafirin microparticles did not show physical difference, probably because of the very low proportion of BMP-2 compared to the binding material, kafirin microparticle or collagen standard.

TEM was used to study the internal microstructure of the microparticles. A drawback in the use of TEM is also the potential occurrence of artefacts, which may result from specimen preparation, such as staining, drying and sectioning-induced artefacts (reviewed by Talmon, 1983; Vinson, Talmon and Walters, 1989). In particular, thin sections of samples which are normally used to prevent excessive inelastic scattering of the electron beam (reviewed by Vinson et al., 1989), made the sections weak, resulting in tearing of resin that holds the samples in place, thereby compromising the quality of some of the TEM micrographs. Nonetheless, TEM provided very useful fine details of the internal structure of the microparticles, particularly by providing information on the effects of cross-linking treatments on the microparticle vacuole sizes.

AFM was used to study the structure of the kafirin microparticles at nanoscale and to measure their mechanical properties. One challenge that was encountered with AFM images was the broadening effect, in which some sections of the micrographs showed apparently larger nanostructures than the others. This meant that the acquired surface topography image could sometimes not accurately correspond to the real surface features. The broadening effect is a well-known artefact with AFM (reviewed by Shakesheff et al., 1994). It is due to the tip-sample convolution, which results when radius of curvature of the tip is similar to or greater than the size of the feature that is imaged. Image broadening is common in rougher areas of the sample where the broader end of the tip is involved in imaging (reviewed by Shakesheff et al., 1994; Shibata-Seki, Masai, Tagawa, Sorin and Kondo, 1996). In the present study, estimated nanostructure sizes were obtained from the flat areas, which have been shown to give a more accurate approximation of particle size (Shakesheff et al., 1994). AFM at higher resolution (<100 nm) was avoided as it resulted in poor image focus. Higher resolution would have required a smaller tip radius (reviewed by Weihs, Nawaz, Jarvis and Pethica, 1991). In this study, the smallest tip available was of 8 nm radius. Despite the broadening artefact with AFM, the existence of numerous published studies using this technique demonstrates that it still a reliable method for nano scale study of biomaterials.

Another challenge found with the use of AFM was in the determination of mechanical properties of the kafirin microparticles. The drawback in this case was that the AFM technique probed a very small section of the microparticle. Hence, it was incapable of direct mechanical characterization of a whole microparticle. This is a result of the fact that the AFM cantilever tip used was 9 nm which is very small compared to kafirin microparticles, which were >1 µm. Therefore, the mechanical properties of the protein microstructures determined by the AFM technique were limited to a localized probing of mechanical parameters, which were then used to provide general information on the mechanical strength of the whole particle. In addition, the AFM technique was limited to a narrow force measurement range (nanoscale range). The use of a force-feedback microelectromechanical systems (MEMS) microgripper has been suggested as a technique for directly measuring the mechanical parameters on a whole microparticle by applying a micro-scale compression testing (reviewed by Kim, Liu, Zhang, Cheng, Wu and Sun, 2008; Kim et al., 2010). However, this equipment was not available during the present study. It may be important to note that while the use of the force-feedback MEMS microgripper would have provided a direct measurement of the general mechanical strength of the microparticles, in principle the overall

mechanical properties of the particles are directly influenced by the local mechanical parameters of the components of the microparticles (nanostructures). In fact, the profiles of the force-deformation curves obtained in the present study using AFM were generally similar to those obtained with the force-feedback MEMS microgripper when used to measure the mechanical properties of biomaterials (Kim et al., 2008). In addition, despite these limitations, biomaterial mechanical characterization technique using AFM has been used in many studies, such as in the determination of mechanical strength of insulin microparticles (Volodkin, Schmidt, Fernandes, Larionova, Sukhorukov, Duschl, Möhwald and Von Klitzing, 2012). However, as discussed, the AFM data on the microparticle mechanical properties have to be interpreted with caution in light of the fact that the method measured only a very small portion of the microparticles.

FTIR was used to determine the secondary structure of kafirin polypeptides in the microparticles. The Amide I band was used to study the secondary structure. As stated, the Amide I band is more reliable than the other Amide bands as 80% of it is due to one functional group, which is the C=O, of the protein (Pelton and McLean, 2000). A limitation of the use of FTIR in this work was that despite significant changes in the physical appearance and functional properties of the kafirin microstructures as a result of transglutaminase and glutaraldehyde treatments, the alterations in protein secondary structures due to these two treatments were rather small. This limitation of FTIR probably arises from the fact it is relatively a low-resolution spectroscopic method. Hence, it cannot establish the precise three-dimensional location of individual structural elements (reviewed by Surewicz et al., 1993).

Another limitation was that the FTIR data were presented as relative proportions of the α-helical conformations at the Amide I band. The heights of peak assigned to different types of secondary structure (i.e., α-helices and β-sheets) were measured to represent percentages of these structures in a given protein. As explained by Surewicz et al. (1993) this procedure provides only an estimate of protein secondary structure but not the absolute content of the various types of conformations. An alternative method would have been to apply X-ray crystallography (reviewed by Smyth and Martin, 2000) to get information on protein three-dimensional structure at high level of resolution. However, a challenge was the feasibility of X-ray crystallography of kafirin polypeptides, as a crystallographic study would have required high-quality single kafirin protein crystals that were not available. This is probably

because the hydrophobic nature of these proteins would lead to amorphous aggregation in aqueous solutions, rather than crystal formation. Furthermore, the relatively "static" structure in single kafirin protein crystals would not have adequately represented the protein conformation in a complex and dynamic environment that existed in a microparticle or film.

SDS-PAGE, which separates protein molecules based on their sizes (reviewed by Yada et al., 1996), was used to determine the molecular weight distribution of protein in the kafirin microparticles and kafirin microparticle films. A limitation of this method was that despite evidence of reduction of protein digestibility with heat treatment, the SDS-PAGE did not expressly show clear difference in polymerization between the control and the heat-treated kafirin microstructures, except at the extreme temperature treatment. This is probably because kafirin polymerization may also occur as a result of oxidation (reviewed by Duodu et al., 2003). An alternative approach would have been to measure the amounts of free thiol (–SH) groups using 5,5′-dithiobis-(2-nitrobenzoate) (DTNB). Heat induced disulphide cross-linking reduces the amount of free –SH groups in kafirin (Elkhalifa, Bernhardt, Bonomi, Iametti, Pagani and Zardi, 2006; Ezeogu, Duodu, Emmambux and Taylor, 2008).

It is also a concern that the SDS-PAGE data with transglutaminase treatment did not correspond with the observed changes in the physical properties of kafirin microstructures. As discussed, apart from the transglutaminase cross-linking reaction that requires lysyl side chain, the other two reactions that are catalysed by transglutaminase are deamidation and amine incorporation (Motoki and Seguro, 1998). As all these three transglutaminase-catalysed reactions result in an increase in free ammonia, measurement of ammonia may be used as a tool to monitor the overall transglutaminase reaction (Sharma, Lorenzen and Qvist, 2001). However, it is important to point out two weaknesses of this particular method. The measurement of ammonia neither differentiates among the different transglutaminase reactions nor directly measures the cross-linking effect, which was of interest in the modification of the functional properties of kafirin microstructures. A method that directly measures the cross-linking reaction is the estimation of ε-(γ-glutamyl)-lysine, the isopeptide formed during the transglutaminase reaction, as applied by Sharma et al. (2001). As this isopeptide is not broken down by proteases that hydrolyse ordinary peptide bonds (Miller and Johnson, 1999), its estimation is possible by measuring the free amino acids once the other peptides have hydrolysed. However, in the present study as kafirin is very poor in lysine, getting meaningful transglutaminase-catalysed cross-linking data with this procedure would

have been unlikely. Hence, these proposed techniques should be complemented by another technique such as size exclusion chromatography (SEC) as performed by Emmambux and Taylor (2009) who applied this technique to determine the effects of cooking on the sorghum and maize prolamin structure. The solvent should consist of 1.0 M urea and 0.02M potassium phosphate buffer (pH 3) dissolved into a liquid mixture of ethanol, water, and lactic acid at a concentration of 5:2:3 (w/w), respectively. According to Emmambux and Taylor (2009), this solvent system results in negligible amount of undissolved kafirin.

A problem was also encountered with SDS-PAGE of kafirin microparticles and collagen bound to BMP-2. Initially Coomassie Brilliant Blue staining was used but no difference was found between the bands. This was thought to be due to the very low concentration of BMP-2 with respect to the binding protein, probably making it impractical to detect possible changes in the molecular weight distribution. Then silver staining, which works on the principle that proteins bind silver ions, which can be reduced under appropriate conditions to build up a visible image made of finely divided silver metal (reviewed by Chevallet et al., 2006) was performed on the samples. It was hoped that the effect of BMP-2 binding on molecular weights would be detected due to the high sensitivity of silver staining (>100 times the sensitivity of Coomassie Brilliant Blue staining) (reviewed by Chevallet et al., 2006; Schägger, 2006). However, the very high sensitivity of silver staining resulted in occurrence of ghost (artefact) bands (reviewed by Hurkman and Tanaka, 1986), making it difficult to see differences. Hence, it was not possible to obtain meaningful data.

An ELISA type assay was used to measure the concentration of BMP-2 in supernatants after binding reactions, to determine the amount of BMP-2 bound to kafirin microstructures or collagen. The particular ELISA was relatively expensive. Hence, it was reserved for confirmatory testing for presence of BMP-2 in the supernatant following a general protein concentration measurement with Lowry protein assay. ELISA uses quantitative sandwich enzyme immunoassay technique in which a monoclonal antibody specific for the protein had been pre-coated onto a microplate (Engvall and Perlmann, 1972). A concern was the large standard deviations in the data obtained, which called for cautious interpretation of the results. This is an inherent limitation of ELISA. The main source of variability in ELISA is the variation in efficiency and uniformity of coating antigen binding or the antigen-antibody reactions (reviewed by Li, Gee, McChesney, Hammock and Seiber, 1989; Sebra, Masters, Cheung, Bowman and Anseth, 2006). Sebra et al. (2006) explained that the antigen detection

assays that rely on monolayer formation or physisorption methods to immobilize antibodies to surfaces have drawbacks due to variation in antibody coating stability and uniformity, and are often heavily dependent on substrate properties such as surface chemistry and roughness. An alternative more accurate technique for precise measurement of BMP-2 would have been mass spectrometry such as matrix-assisted laser desorption ionisation/time-of-flight mass spectrometry (MALDI/TOF-MS). This mass spectrometry technique has been applied in BMP-2 binding studies such as in the determination the binding of bioactive BMP-2 to nanocrystalline diamond by physisorption (Steinmüller-Nethl, Kloss, Najam-Ul-Haq, Rainer, Larsson, Linsmeier, Köhler, Fehrer, Lepperdinger, Liu, Memel, Bertel, Huck, Gassner and Bonn, 2006). However, it is much more expensive in comparison to ELISA. In addition, the instrumentation was not available and would have required considerable method development for kafirin as it cannot be crystallised and is not easily soluble. As the trends with the different treatments were consistent, the high standard deviations did not invalidate the ELISA findings.

Rat model assessment of safety, biodegradability and effectiveness of kafirin microparticle film-BMP-2 system in inducing bone formation was performed to establish whether the kafirin microstructures would have potential application as biomaterials for use as implantable medical devices to promote bone tissue regeneration both in animals and in people. A subcutaneous implantation site was chosen in order to rule out osteoconduction or periosteal bone formation as disturbing mechanisms in the BMP-2 induced bone formation (reviewed by Kempen et al., 2008). The choice of a rat model for this study instead of larger animals was based on several reasons. First was the ethical concern with the use of larger animals, especially for early stage investigations such as the present study. Secondly, as explained by Seeherman, Wozney and Li (2002), with small animals there is an increased number of responding cells in the bone and soft tissue elements and a more rapid rate of bone formation.

There were some limitations with the rat model study in this work. The number of animals was less than the ideal full Organisation for Economic Cooperation and Development (OECD) toxicity studies requirement of 10 animals (five animals each of both sexes) per treatment (OECD, 1981). However, the application of four treatments (implants) per animal was meant to reduce the sample size (number of animals) (reviewed by Bessa et al., 2010), while providing baseline information on tissue inflammatory response to the implants. This

use of more than one implant site with different treatments per animal may not have been ideal, but studies have been performed with a similar experimental design with different animal models such as rats (Bessa et al., 2010) and rabbits (H.-J. Wang et al., 2007). Another limitation was the difference in the physical structures of the implant materials. The collagen was in particulate form, which was very different from the structure of the kafirin microparticle film. Perhaps a better comparison would have been achieved by using binding matrices with similar physical structures.

Also, immune sensitisation of the immunocompetent rats could have had limitations as regeneration of new bone cells may have been countered by osteolysis (Prof Vinny Naidoo, personal communication), which is an immune response to bone (Roodman, 1996; Jacobs, Roebuck, Archibeck, Hallab and Glant, 2001). Immunocompromised animals such as nude mice would have been better in this case. However, since this study was also meant to investigate the safety of the implants, it was thought that the use of immunocompromised rodents would be more appropriate at a later stage of investigation.

The short period of the study (four weeks) was also a limitation. It would have been better to perform a longer study (about 12 weeks) similar to that used by Kempen et al. (2008) who investigated the *in vitro* and *in vivo* biological activities of BMP-2 released from different delivery vehicles for bone regeneration. The samples would be drawn and examined at well-distributed intervals throughout the period of implantation. This probably would have provided more information on the degradability of the implant materials and their long-term effects in the animal body.

Another concern was that the rhBMP-2 dosages used in the present study were probably too low, as discussed (section 4.3.4.4). The different levels of rhBMP-2/BMP-2 dosage, different animal models and assorted durations of assessments to induce bone morphogenesis in the literature made it difficult to make a clear-cut comparison between the kafirin microparticle film-BMP-2 system and similar systems in literature. Other researchers such as Hollinger et al. (1998) working in similar animal assays have also cited this existence of a variety of experimental conditions in similar animal studies as a challenge in their work. In addition, studies also show that high dose of BMP-2 may induce structural abnormality of bone and inflammation in rats (Zara, Siu, Zhang, Shen, Ngo, Lee, Li, Chiang, Chung, Kwak, Wu, Ting and Soo, 2011). This complicated the decision on the right dosage, as rhBMP-2 appears to be more potent than partially purified BMP for regenerating bone in rats, as discussed.

There was also concern regarding some sample preparation techniques for histological evaluations. For example, embedding tissue implant materials with paraffin wax may not have secured the implant materials optimally for histological examinations. Therefore, during sectioning with a microtome some of the implanted material appeared to have pulled away from the tissue material, causing artefacts (Prof Resia Pretorius, Department of Physiology, University of Pretoria, personal communication). However, this was a normal tissue embedding technique applied by Idexx Laboratories.

Another concern was that the sterilization process used on the implant materials could have inactivated the rhBMP-2. Gamma-irradiation was selected as a sterilization method because it is generally used to sterilize BMPs. However, the effects of the methods commonly used for BMP sterilization (γ-irradiation and ethylene oxide) on the osteoinductivity of BMPs is controversial (reviewed by Pekkarinen, 2005). In the present study, the choice of γ-irradiation as sterilization method was motivated by suggestions in literature that γ-irradiation may have only slight effects on the osteoinductivity of BMP (reviewed by Pekkarinen, 2005). Other factors that could have caused disparity in results between the present study and other studies were differences in placement site of the implants and age of the animals (Prof Vinny Naidoo, veterinarian, personal communication). Animals respond differently to growth factors depending on the site of implantation as has been shown with animal models such as rats injected with growth factors at different sites (Fujimoto, Tanizawa, Nishida, Yamamoto, Soshi, Endo and Takahashi, 1999). Similarly, studies on the effects of age on the response of rodent animal models to bone growth factors has shown a better response of younger animals than older animals as was found in a study with rabbits (Critchlow, Bland and Ashhurst, 1994).

The activity of ALP, a zinc metalloprotein enzyme that splits off a terminal phosphate group from an organic phosphate ester (reviewed by Saraç and Saygılı, 2007), was measured as a marker for early osteoblast differentiation. Bone ALP level was expected to be elevated in case of an increased osteoblastic activity, as had been shown by other workers (Farley and Baylink, 1986; Van Straalen, Sanders, Prummel and Sanders, 1991; Stucki, Schmid, Hämmerle and Lang, 2001), due to an induction by BMP-2 in the implants. ALP activity assay has been used in previous similar studies such as those on rats (Eriksson, Nygren and Ohlson, 2004; Kempen et al., 2008), rabbits (H.-J. Wang et al., 2007), humans (Rosalki, Foo, Burlina, Prellwitz, Stieber, Neumeier, Klein, Poppe and Bodenmüller, 1993; Stucki et al.,

2001) and cell lines (Kraus, Deschner, Jäger, Wenghoefer, Bayer, Jepsen, Allam, Novak, Meyer and Winter, 2012). However, a limitation of ALP activity test in measuring bone morphogenesis was that the assay is not specific for bone growth as ALP is also formed by other organs such as the liver and intestines (reviewed by Hoffmann et al., 1994), as discussed. Nonetheless, previous studies have shown that bone ALP activity could be considered a marker of bone formation *in vitro* (Farley and Baylink, 1986) and *in vivo* (Van Straalen et al., 1991; Withhold et al., 1996). Another challenge was that the collagen implant material was digested by tissue enzymes. In contrast, the kafirin microparticle film implants remained largely intact. Therefore, the collagen implant material used for ALP test appeared to have a larger proportion of animal tissue material obtained at the implant site compared to film implant material, which may have confounded the results of the assay. Perhaps an alternative ALP assay using a staining technique such as Vector Red Alkaline Phosphatase Substrate as applied by Eriksson et al. (2004) would have provided a more useful information on the ALP activity. Despite the limitation, the ALP activity data seemed to correspond to the histology study, which showed essentially no bone morphogenesis. Hence, these limitations did not really affect the precision of the results.

5.2 PROPOSED MECHANISM OF CROSS-LINKING THE KAFIRIN MICROPARTICLES WITH GLUTARALDEHYDE AND HEAT

It was found that both heat and glutaraldehyde treatments resulted in larger kafirin microparticles (Chapter 1). Images based on surface morphology examined by AFM showed that kafirin microparticles seem to comprise coalesced nanostructures of different shapes, depending on the type of treatment. The glutaraldehyde-treated kafirin microparticles were apparently made up of in spindle-shaped nanostructures, while round and irregular shaped nanostructures were obtained with heat treatment. The increase in kafirin microparticle size and difference in shapes of the nanostructures in the microparticles with heat and glutaraldehyde treatments indicated there was further assisted-assembly of kafirin polypeptides as a result of these treatments. The fact that the kafirin microparticles are apparently made up of nanostructures coalesced together evokes an analogy between the formation of kafirin microparticles and casein micelles. Casein micelles are formed by aggregation of sub-micelles (subunits made up of about 15–20 casein molecules each) and the stability of the casein micelle structure is maintained by κ-casein brush (a stabilizing coating) on the surface of the casein micelles (reviewed by Horne, 2006). Using the analogy

it could be presumed that kafirin nanostructures are stabilized by an external surface layer, probably constituted by the γ-kafirin polypeptides based on the model proposed by Taylor (2008) for kafirin microparticle formation using coacervation with acetic acid solvent. The Taylor (2008) model for kafirin microparticles formation, which is based on the structure of the spherical kafirin protein bodies (Shull, Watterson and Kirleis, 1992; Oria, Hamaker, Axtell and Huang, 2000), suggests that the α-kafirins are located at the centre of the microparticle followed by β-kafirin and then γ-kafirin layer, which stabilizes the kafirin microparticle. However, Taylor (2008) did not have data on details showing that the kafirin microparticles could be made up of nanostructures as observed in the present study. Given the similarity in scale of the sizes of the casein micelles (100–200 nm) and the kafirin nanostructures (100–300 nm), an analogy is drawn between the casein micelles and the kafirin nanostructures. Therefore, γ-kafirin polypeptide-enriched rich sub-nanostructures (subunits comprising a few molecules of kafirin sub-classes aggregating together) would be located on the surface of the kafirin nanostructures, while those sub-nanostructures deficient in γ-kafirin polypeptides would be located in the interior as shown in the proposed schematic representation (Figure 5.1A). These γ-kafirin polypeptide-rich sub-nanostructures would be analogous to the κ-casein rich casein sub-micelles as described by Horne (2006). As with casein micelle, the structure of the kafirin nanostructure would depend on the stability of the γ-kafirin-enriched polypeptide layer. Assuming that the kafirin microparticles produced by self-assembly are made of sterically stabilized kafirin nanostructures with a γ-kafirin polypeptide-enriched layer, one can relate the changes in the structure of the kafirin microparticles in response to heat or glutaraldehyde treatments by considering the behaviour of the γ-kafirin polypeptide-enriched layer in response to these treatments. This is by analogy with casein micelles where destabilizing the κ-casein brush by addition of the enzyme chymosin that breaks down the κ-casein brush, pH adjustment and addition of calcium or ethanol or combinations, leads to the collapse of the brush and thus flocculation of the micelles (reviewed by De Kruif, 1999).

With glutaraldehyde-treatment the spindle shape and unidirectional orientation of the nanostructures that seem to constitute the kafirin microparticles suggests that the mechanism of further assisted-assembly due to glutaraldehyde treatment was different from that with heat treatment. Only the main type of cross-linking between glutaraldehyde and proteins that involves the formation of Schiff bases will be discussed. The status of the γ-kafirin polypeptide-enriched rich region of the sub-nanostructures before and after collapse of the

kafirin nanostructures would influence the type of further assisted-assembly, in a similar manner to that reported with casein micelles (De Kruif, 1999). During the glutaraldehyde treatment it appears that destabilization of the γ-kafirin polypeptide-enriched layer occurs, thereby resulting in the loss of the round shape of the nanostructures as shown in the proposed schematic representation (Figure 5.1). The destabilization due to glutaraldehyde treatment probably results through formation of a γ-kafirin polypeptide-glutaraldehyde complex by covalent bonding (Figure 5.1B). This covalent bonding probably offsets the balance between the attractive forces (such as disulphide and hydrogen bonding) and repulsive (such as steric hindrance) forces between the different kafirin subclasses within the nanostructures that maintained the spherical shape. After the collapse of the spherical shapes of kafirin nanostructures, a realignment of sub-nanostructures that make up the nanostructures towards a particular direction could occur through a glutaraldehyde-assisted re-assembly driven predominantly by linear interactions as illustrated (Figure 5.1C).

The literature shows that linear aggregation of protein nanostructures requires the presence of hydrophobic rich domains and cross-linking domains as has been reported in several studies on elastin-like fibres (Bressan, Pasquali-Ronchetti, Fornieri, Mattioli, Castellani and Volpin, 1986; Bellingham, Lillie, Gosline, Wright, Starcher, Bailey, Woodhouse and Keeley, 2003; Osborne, Farmer and Woodhouse, 2008). In the present study, it is proposed that the linear attraction is likely to be driven by the kafirin polypeptide-glutaraldehyde linkage. As suggested by Migneault et al. (2004), the glutaraldehyde-protein reaction that results in a cross-linked structure consists of a linear aldol-condensed oligomer of glutaraldehyde linked to Schiff base from the protein. Treating the kafirin nanostructures with glutaraldehyde would initially result in cross-linking reaction with γ-kafirin polypeptide-enriched region on the surface of the nanostructures. Once the nanostructure has collapsed, possibly other kafirin subclasses become exposed resulting in glutaraldehyde cross-linking of the other kafirin subclasses. The formation of linear kafirin nanostructures requires the exposure of domains of the polypeptide that contain side chains that can be available for cross-linking thus promote aggregation by end-to-end alignment. In the cross-linking that results in formation of Schiff bases between carbonyl and amino-groups, glutaraldehyde preferentially reacts with basic amino acid residues that have free amino group (Migneault et al., 2004). As kafirin is poor in lysine, an alternative amino acid residue would be arginine.

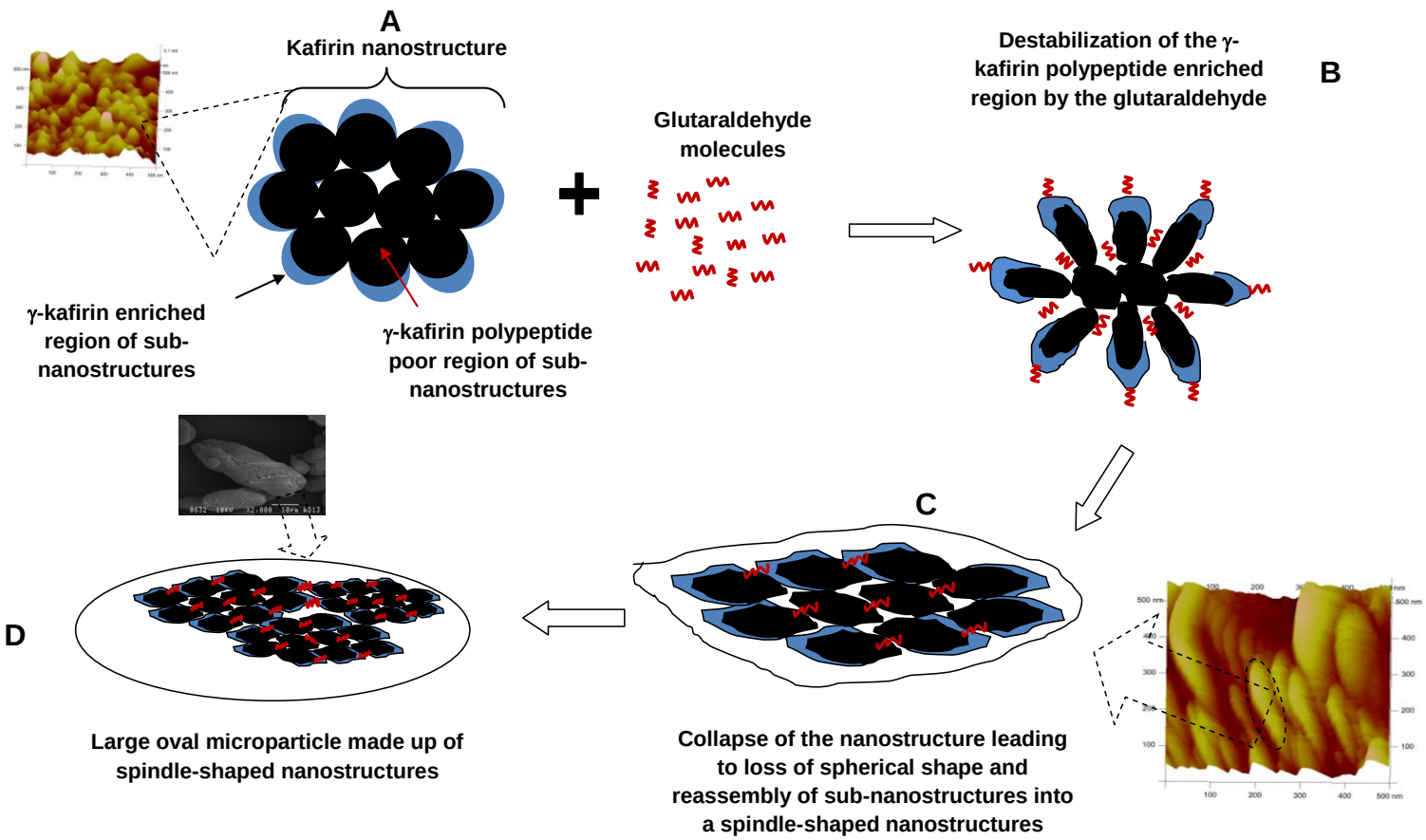

Figure 5.1 Schematic representation of proposed mechanism of glutaraldehyde cross-linking of kafirin microparticles (not drawn to scale). **A**. Kafirin nanostructure with the γ-kafirin polypeptide enriched regions of sub-nanostructures (subunits comprising a few molecules of kafirin sub-classes aggregating together) located on the surface, while regions deficient in γ-kafirin polypeptide are located in the interior. **B**. Destabilization of the γ-kafirin polypeptide-enriched layer. **C**. Loss of the round shape of the kafirin nanostructures and re-assembly of sub-nanostructures into linear spindle shapes driven by kafirin polypeptide-glutaraldehyde linkage. **D**. Cross-linking of adjacent kafirin nanostructures and merging into a large oval kafirin microparticle via kafirin polypeptide-glutaraldehyde linkage.

In addition, to achieve the hydrophobicity requirement for linear aggregation, treatment of γ-kafirin polypeptides with glutaraldehyde must reduce the number of hydrophilic groups when the aldehydes react with free amino groups. These would probably be at the basic amino acid domain Arg.His. of the γ-kafirin polypeptides, based on the amino acid sequences as given by Belton et al. (2006). Then, this in effect would increase the proportion and influence of the hydrophobic domains (with respect to the hydrophilic domains) in the γ-kafirin polypeptide, thereby favouring the linear assembly of the sub-nanostructures. The unidirectional aggregation of the kafirin nanostructures and elongation of kafirin microparticles as a result of cross-linking with glutaraldehyde also implies a sequential joining of about 500 to >2000 kafirin nanostructures. This is because measured lengths of more than 100 microparticles were distributed over a wide size range (5 to >20 µm) and the minimum length of glutaraldehyde treated nanostructure was about 100 nm. Additionally, to a less extent lateral aggregation (side-by-side association) of the kafirin nanostructures may arise from a nonspecific association, which is likely to occur between any hydrophobic sequences in the kafirin polypeptides. The increase in size of glutaraldehyde treated kafirin microparticles would result when adjacent microparticles are cross-linked through the kafirin polypeptide-glutaraldehyde covalent bonding and merging, as illustrated (Figure 5.1D).

With regard to heat cross-linking of the kafirin microparticles, the fact that the nanostructures were generally irregular in shape, apparently formed by merged spheres indicates that unlike with the glutaraldehyde treatment there was little (or less than in the case with glutaraldehyde treatment) destabilization of the γ-kafirin polypeptide-enriched layer, as illustrated in the schematic representation (Figure 5.2). This is probably because heat treatment could have reinforced the γ-kafirin coating through heat-induced disulphide cross-linking as depicted (Figure 5.2B). At nano level, the irregular shapes of the merged nanostructures through heat-treatment seems to suggest that there was a random disulphide cross-linking between γ-kafirin polypeptides on the surface of adjacent nanostructures within the same microparticle as result of the heat treatment (5.2C). The size of the microparticles increased, probably through heat-induced disulphide cross-linking of the γ-kafirin polypeptides on the surface of adjacent kafirin microparticles and merging into a larger kafirin microparticle (Figure 5.2D).

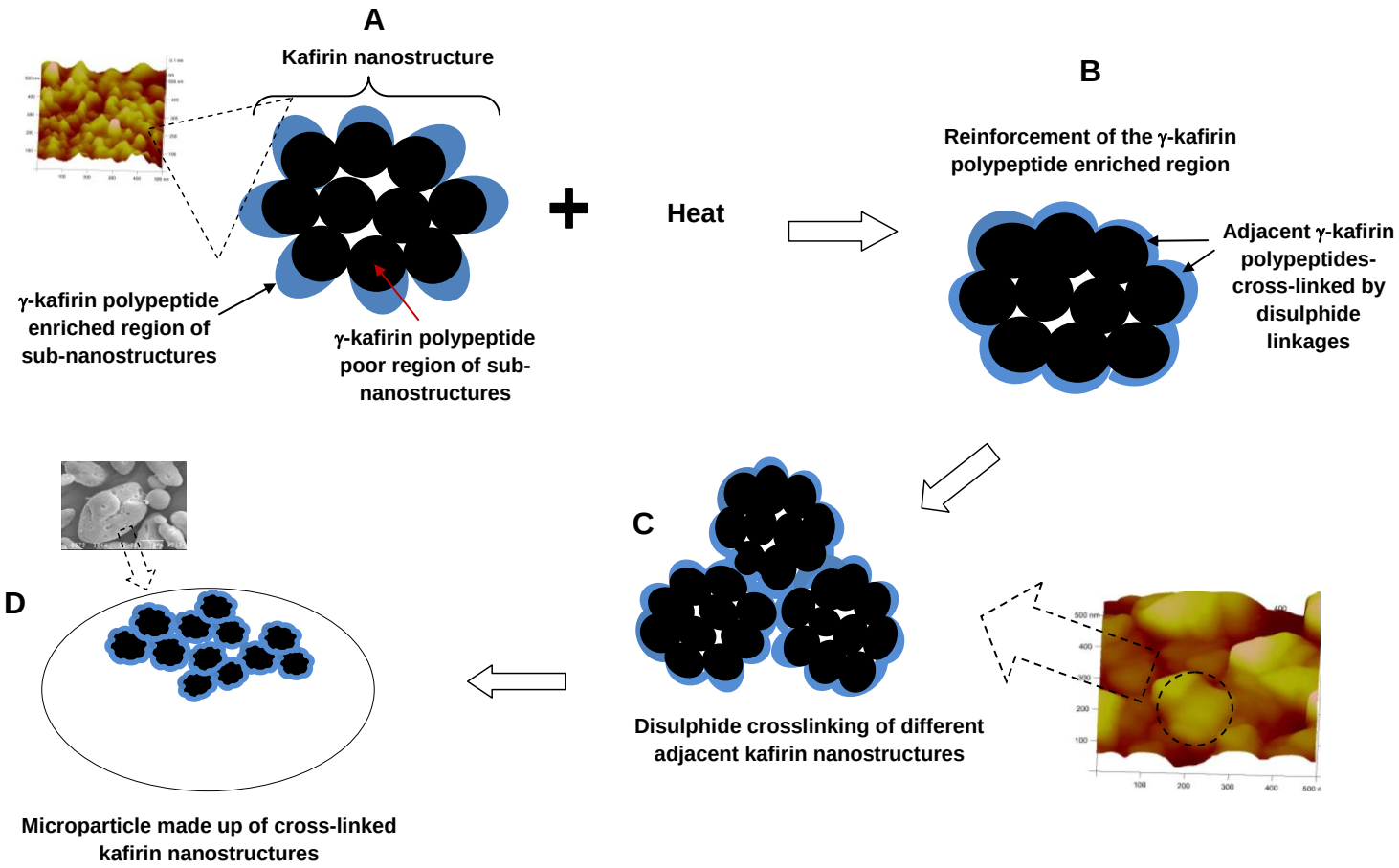

Figure 5.2 Schematic representation of proposed mechanism of heat cross-linking of kafirin microparticles (not drawn to scale). **A**. Kafirin nanostructure with the γ-kafirin polypeptide rich sub-nanostructures (subunits comprising a few molecules of kafirin sub-classes aggregating together) located on the surface, while areas deficient in γ-kafirin polypeptide are located in the interior. **B**. Reinforcement of the γ-kafirin coating through heat-induced disulphide cross-linking of adjacent sub-nanostructures. **C**. Heat-induced disulphide cross-linking of the γ-kafirin polypeptides on the surface of adjacent kafirin nanostructures. **D**. Merging of kafirin microparticles into a large microparticle.

The observed difference in shape of the smaller (spherical) and the larger (oval) heat-treated kafirin microparticles (section 4.1.4.1) was probably due to the rate of particle coalescence being inversely proportional to particle size, as proposed by Lehtinen and Zachariah (2001) who studied the effect of coalescence energy release on the temporal shape evolution of silicon and alumina nanoparticles. According to these authors, when two identical spherical nanoparticles coalescence as result of bonding between them a neck rapidly forms between the nanoparticles, which transforms into an oval shape that then slowly evolves into a sphere. As explained by these authors, the driving force for the transformation of two spherical nanoparticles into one completely fused particle is a minimization of the surface free energy reflected in a temperature increase of the resulting particle. As the characteristic coalescence time is inversely proportional to the solid-state diffusion coefficient, which is exponentially dependent on temperature, the heat release can significantly affect the overall coalescence process. This effect is significant especially for small particles since the fraction of their surface atoms is large and their overall heat capacity is small compared to larger particles. Therefore, the smaller particles are typically spherical, probably because the small size enhances coalescence rate, thereby reducing the time required to reach the final stages of shape evolution. In contrast, the larger particles have a higher heat capacity resulting in slow heating rate and slow evolution from an oval shape to a sphere. Hence, in the present study one would expect to see mainly non-spherical shapes for larger kafirin microparticles, as observed.

Cross-linking during kafirin microparticle formation resulted in relatively smaller microparticles compared to kafirin microparticles cross-linked after their formation (section 4.1.4.1). To explain the differences in size, the evidence from AFM images that showed that the kafirin microparticles are formed by coalescence of kafirin nanostructures could be applied. In the cross-linking during kafirin microparticle formation the building blocks are kafirin proteins, which are smaller in size. Therefore, this system is dominated by attractive forces between the kafirin polypeptides, which would result in smaller microparticles. In contrast, during cross-linking of pre-formed kafirin microparticles, the building units are larger as they are kafirin nanostructures. Hence, this system will be dominated by repulsive forces due to kafirin nanostructure crowding, which would result in larger microparticle size. This theory is analogous to that of Farrer and Lips (1999) who studied the mechanism of casein micelle formation from sodium caseinate. Their model demarcates two separate

regimes of close packing: below and above close packing. In this Farrer and Lips (1999) model, below close packing is expected to be sensitive to attractive interactions between sub-micelles and above close packing to be dominated by repulsive forces of micellar crowding/interpenetration.

There were differences between the sizes of the vacuoles within the kafirin microparticles cross-linked during microparticle formation and the vacuoles within microparticle cross-linked after microparticle formation. The reduction in vacuolation of microparticles cross-linked by heat during their formation was probably because of expulsion of air dissolved in the water by heat while the microparticles were being formed. In contrast, kafirin microparticles heat-treated after their formation had larger vacuoles as the air entrapped within them during their formation probably expanded with heat treatment. As discussed, air footprints have been suggested as the cause of vacuolation of the kafirin microparticles formed by coacervation (Taylor et al., 2009a). With regard to glutaraldehyde treatment, the reduction in vacuolation of the kafirin microparticles cross-linked by glutaraldehyde during their formation is probably because smaller microparticles would be dominated by attractive forces as discussed, probably resulting in reduction of vacuole sizes. On the contrary, the kafirin microparticles cross-linked after their formation were larger compared to microparticles cross-linked during their formation. Therefore, these larger glutaraldehyde cross-linked kafirin microparticles would be dominated by repulsive forces, probably resulting into larger vacuoles compared to the smaller microparticles treated with glutaraldehyde during their formation.

The glutaraldehyde-treated kafirin microparticle films had better tensile properties and water stability than control, probably mainly because of increase in covalent bonding within the film matrix as result of the kafirin polypeptide-glutaraldehyde linkages. In addition, it has been reported that the properties of the κ-casein brush, before and after collapse influences the fusion of the casein micelles thereby determining the gel properties (reviewed by De Kruif, 1999). Therefore, drawing from the analogy between the kafirin nanostructures and casein micelles and using the same reasoning, if glutaraldehyde treatment of kafirin microparticles caused a collapse of the γ-kafirin polypeptide-enriched layer as proposed, then the aggregation of the nanostructures would result in a cohesive film matrix. This would probably result in the better film tensile properties and water stability.

Another possible basis for the superiority in the quality of glutaraldehyde-treated kafirin microparticle film compared to heat-treated microparticle film may be drawn from knowledge of the possible mechanism of cast kafirin microparticle film formation with acetic acid solvent. Taylor et al. (2009c) suggested that kafirin microparticle film formation involves controlled aggregation of kafirin microparticles, followed by dissolution of the microparticles in acetic acid and drying into a cohesive film. However, the findings in the present study indicate that the aggregation is likely to be at the nanostructure level. By inference, the casting technique used to prepare the kafirin microparticle films is in principle an EISA of kafirin nanostructures. As discussed (section 4.3.4.1), EISA involves binary or tertiary solvents where preferential evaporation of one of the solvents changes the polarity of the solution, which drives the self-assembly of solutes (reviewed by Wang and Padua, 2012). As with the EISA work on zein microstructures with aqueous ethanol (70% ethanol in water) solvent (Wang et al., 2008; Wang and Padua, 2010), in the present study it is proposed that the increase in kafirin nanostructure concentration through evaporation of acetic acid solvent (25% acetic acid in water) would result in the nanostructures approaching each other. This would create sphere-to-sphere interfaces or spindle-to-spindle interfaces depending on the shape of the kafirin nanostructures. As the acetic acid solvent evaporates, the kafirin nanostructures would fuse together into a continuous film, which is in accordance with the Shin, Grason and Santangelo (2009) model for transformation of soft spherical materials. According to their model, as the concentration increases, the spheres approach each other and fuse into a bicontinuous network (sponge phase) and then into a lamellar phase. In the present study it is proposed that with the spherical heat-treated kafirin nanostructures, there would be larger interstitial spaces as illustrated (Figure 5.3A), while the packing of the spindle-shaped nanostructures would be more compact (Figure 5.3B). In addition, as the heat-treatment of kafirin nanostructures seems to enhance the stability of the γ-kafirin polypeptide-enriched layer, fusion of the kafirin nanostructures during film formation may be less cohesive. Furthermore, the bigger heat-cross-linked kafirin nanostructures may have been difficult to dissolve, thereby resulting in films with poor quality.

Generally, kafirin microparticles had higher IVPD than the films prepared from them. This may be attributed to the fact that the film formation protocol involved evaporation of the acetic acid solvent at a slightly elevated temperature (50°C) for a long time (12 h). The high temperature and long heating time may have resulted into further disulphide cross-linking of

the kafirin proteins, thereby reducing the IVPD of the films compared to the IVPD of the microparticles from which they were prepared.

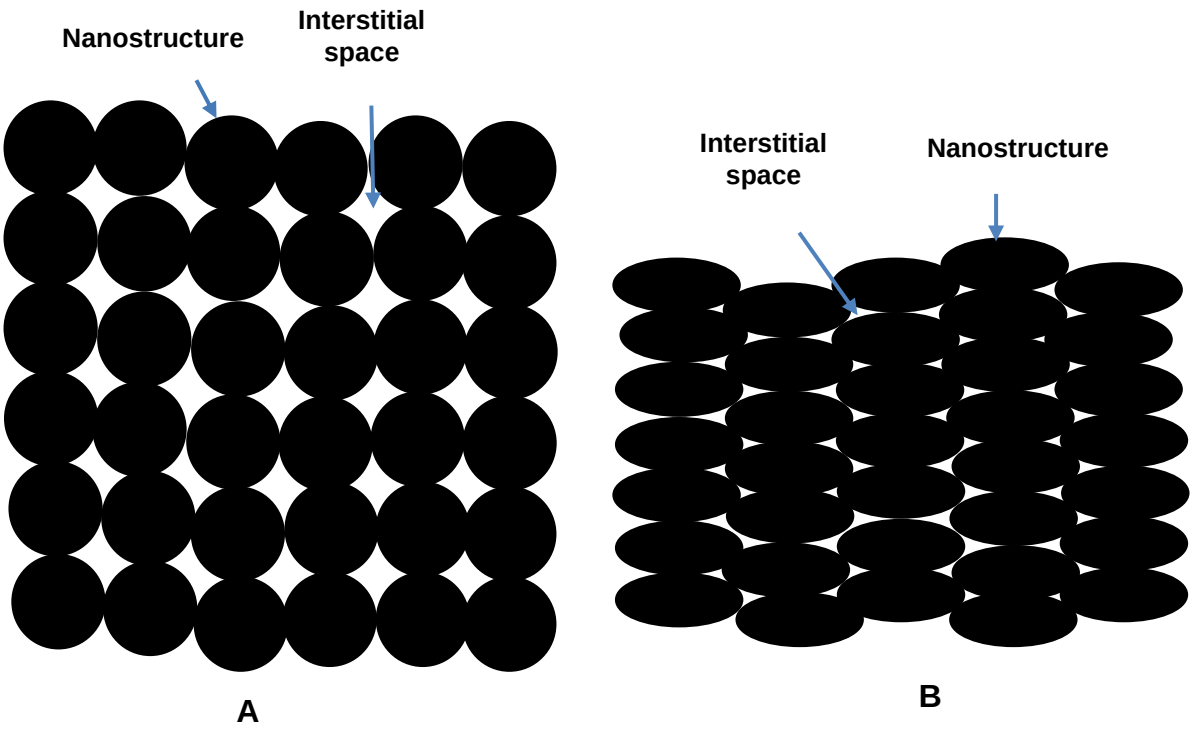

Figure 5.3 Schematic representation of hypothetical packing of kafirin nanostructures with different morphologies during film formation. **A**. Heat treated spherical nanostructures with large interstitial spaces. **B**. Glutaraldehyde-treated spindle- (oval) shaped nanostructures with smaller interstitial spaces forming a compact packing.

5.3 POTENTIAL APPLICATIONS OF KAFIRIN MICROSTRUCTURE BIOMATERIALS

The data on the safety, which indicated that the kafirin microparticle films were non-irritant when implanted in a rat model, gives kafirin microstructure biomaterials platform for many potential applications. For example, the increase in the size of modified kafirin microparticles obtained with heat and glutaraldehyde treatments makes them potentially suitable for application in scaffold-type structures for hard tissue repair that require large particles with a high degree of interconnected porosity. These kafirin microparticles could be implanted to fill a void in damaged bone tissue and subsequently seeded by the infiltration of the patient's own cells. As cells proliferate, deposition of extracellular matrix components and biodegradation of the kafirin microparticle scaffold would result in a solid, three-dimensional

tissue construct. Cell proliferation could be enhanced by loading the kafirin microparticle scaffolds with growth factors. In addition, the kafirin microparticle average size ≈20 µm obtained with heat and glutaraldehyde treatments makes them suitable as delivery devices for subcutaneous, intramuscular or intravitreal therapeutic drug administration. This is because the kafirin microparticle size is within the 10–250 µm size requirement that avoids microparticle uptake by macrophage phagocytosis and minimises inflammatory reaction (reviewed by Tran, Benoît and Venier-Julienne, 2011).

Kafirin microparticle films could be applied in skin tissue engineering for wound dressing to provide a bacterial barrier, control pain and contribute an adequate environment for epithelial regeneration due to their slow biodegradability and water stability. The kafirin microparticle films could be loaded with antimicrobial agents to avoid infection of the wound thereby enhancing the healing process. To treat an infected wound it is important to sustain sufficient drug concentration at the site of infection. Hence, the fact that kafirin microparticle film implants do not degrade rapidly could be utilised in their application as antimicrobial-loaded wound dressing.

The kafirin microparticle films could also be used in cell culture techniques. Cell culture techniques are important for the study of animal cell structure, function and differentiation and for the production of many important biological materials, such as vaccines, enzymes, hormones and antibodies. Cells could be grown on the surface of the kafirin microparticle films. The cells cultured on kafirin microparticle films could then be used as substrates for the production of viruses or cell products.

6 CONCLUSIONS AND RECOMMENDATIONS

Modification of kafirin microparticles with wet heat or glutaraldehyde treatment results in larger oval microparticles. In addition, heat treatment increases vacuole size. In contrast, transglutaminase treatment has little effect on the size of microparticles. While similar gross morphology of kafirin microparticles is obtained with heat and glutaraldehyde treatments, the shapes of presumably nanostructures that seem to coalesce to form the microparticles are very different. Heat treatment results in round-shaped nanostructures, indicative of non-linear protein aggregation in the kafirin nanostructures, probably due to disulphide cross-linking. In contrast, glutaraldehyde treatment results in spindle-shaped nanostructures, probably due to linear alignment of the kafirin nanostructures controlled by glutaraldehyde-polypeptide linkage. It is therefore apparent that with both treatments the pre-formed kafirin microparticle structures undergo some form of further assisted-assembly through different mechanisms. It seems that heat-induced disulphide cross-linking reinforces the layer, probably rich in γ-kafirin polypeptides, that stabilizes the spherical structure of the nanostructures within the kafirin microparticle. In contrast, glutaraldehyde-treatment appears to destabilize this structure-stabilizing layer through formation of γ-kafirin polypeptide-glutaraldehyde covalent bonding. This probably offsets the balance of attractive and repulsive forces between the different kafirin subclasses within the nanostructures, thereby resulting in collapse of the nanostructures and their linear realignment. Kafirin microstructures can bind BMP-2. The capacity of kafirin microparticles to bind BMP-2 is enhanced somewhat through modification by heat, transglutaminase or glutaraldehyde treatment, mainly due to increase in particle size. Thin glutaraldehyde-treated kafirin microparticle films are stable in water at ambient temperature, probably due to increase in covalent bonding within the film matrix through formation of the covalent glutaraldehyde-polypeptide linkage. Kafirin microparticle films are not toxic as kafirin is non-allergenic. The kafirin microparticle films also show a prolonged biodegradation when implanted in a mammalian tissue, probably because of the low susceptibility of kafirin to mammalian proteolytic enzymes. The large kafirin microparticles obtained with heat and glutaraldehyde treatments could have application as natural non-animal protein bioactive biomaterials for scaffold type structures used in hard tissue (e.g. bone) repair. Kafirin microparticle films could be applied in tissue engineering for soft tissue (e.g. skin) repair and in cell culture techniques for growing cells.

This study has provided valuable information on the mechanism for kafirin microparticle cross-linking with glutaraldehyde and heat. However, further work is needed in order to better understand the kafirin polypeptide self-assembly process at the molecular level so that the self-assembly process can be further manipulated to enable the formation of different structures. This will help in addressing the major challenges that remain such as production of microparticles with much larger vacuoles to allow cell migration throughout the structure, adhesion and proliferation to enable formation of functional tissues and organs. A related challenge is the production of larger films for use in large wound dressings. Research on the binding of kafirin microstructures with other types of bioactives such as nutraceuticals and antibiotic drugs is needed. A longer animal study with immunocompromised animal models to exclude the counter effects of immune sensitization in bone regeneration is recommended to provide information on long-term effect of the kafirin microstructure implants in animals.

7 REFERENCES

Allemann, E., Leroux, J.-C., Gurny, R., 1998. Polymeric nano- and microparticles for the oral delivery of peptides and peptidomimetics. Advanced Drug Delivery Reviews 34, 171–189.

American Association of Cereal Chemists (AACC International), 2000. Crude protein-combustion, Standard Method 46-30. Approved Methods of the AACC (10th ed.). The Association; St Paul, MN.

American Society for Testing and Materials (ASTM), 1997a. Annual Book of the ASTM Standards. ASTM D882-97: Standard method for tensile properties of thin plastic sheeting. The Society: West Conshohocken, PA.

American Society for Testing and Materials (ASTM), 1997b. Annual Book of the ASTM Standards. ASTM E96-97: Standard test methods for water vapor transmission of materials. The Society: West Conshohocken, PA.

Ando, H., Adashi, M., Umeda, K., Matsuura, A., Nonaka, M., Uchio, R., Tanaka, H., Motoki, M., 1989. Purification and characteristics of a novel transglutaminase derived from microorganisms. Agricultural and Biological Chemistry 53, 2613−2617.

Auriol, D.H., Paul, F.B., Monsan, P.F., 1996. Process for enzymatic synthesis of alkyl esters of peptides and peptides, and microparticles therefrom. United States Patent and Trademark Office 5554508.

Autio, K., Kruus, K., Knaapila, A., Gerber, N., Flander, L., Buchert, J., 2005. Kinetics of transglutaminase-induced cross-linking of wheat proteins in dough. Journal of Agricultural and Food Chemistry 53, 1039–1045.

Babensee, J.E., 1990. Morphological assessment of HEMA-MMA microcapsules for liver cell transplantation. PhD Thesis, University of Toronto, Toronto, Canada.

Babensee, J.E., Anderson, J.M., McIntire, L.V., Mikos, A.G., 1998. Host response to tissue engineered devices. Advanced Drug Delivery Reviews 33, 111–139.

Babiker, E.E., Kato, A., 1998. Improvement of the functional properties of sorghum protein by protein-polysaccharide and protein-protein complexes. Nahrung 42, 286–289.

Balmayor, E.R., Feichtinger, G.A., Azevedo, H.S., Van Griensven, M., Reis, R.L., 2009. Starch-poly-ε-caprolactone microparticles reduce the needed amount of BMP-2. Clinical Orthopaedics and Related Research 467, 3138–3148.

Beaulieu, L., Savoie, L., Paquin, P., Subirade, M., 2002. Elaboration and characterization of whey protein beads by an emulsification/cold gelation process: application for the protection of retinol. Biomacromolecules 3, 239–248.

Bellingham, C.M., Lillie, M.A., Gosline, J.M., Wright, G.M., Starcher, B.C., Bailey, A.J., Woodhouse, K.A., Keeley, F.W., 2003. Recombinant human elastin polypeptides self-assemble into biomaterials with elastin-like properties. Biopolymers 70, 445–455.

Belton, P.S., Delgadillo, I., Halford, N.G., Shewry, P.R., 2006. Kafirin structure and functionality. Journal of Cereal Science 44, 272–286.

Benichou, A., Aserin, A., Garti, N., 2007. W/O/W double emulsions stabilized with WPI-polysaccharide complexes. Colloids and Surfaces A: Physicochemical and Engineering Aspects 294, 20–32.

Bensaid, W., Triffitt, J.T., Blanchat, C., Oudina, K., Sedel, L., Petite, H., 2003. A biodegradable fibrin scaffold for mesenchymal stem cell transplantation. Biomaterials 24, 2497–2502.

Berkland, C., King, M., Cox, A., Kim, K.K., Pack, D.W., 2002. Precise control of PLG microsphere size provides enhanced control of drug release rate. Journal of Controlled Release 82, 137–147.

Bessa, P.C., Casal, M., Reis, R.L., 2008. Bone morphogenetic proteins in tissue engineering: the road from laboratory to clinic, Part II (BMP delivery). Journal of Tissue Engineering and Regenerative Medicine 2, 81–96.

Bessa, P.C., Balmayor, E.R., Hartinger, J., Zanoni, G., Dopler, D., Meinl, A., Banerjee, A., Casal, M., Redl, H., Reis, R.L., Van Griensven, M., 2010. Silk fibroin microparticles as carriers for delivery of human recombinant bone morphogenetic protein-2: in vitro and in vivo bioactivity. Tissue Engineering: Part C 16, 937–945.

Bharali, D.J., Siddiqui, I.A., Adhami, V.M., Chamcheu, J.C., Aldahmash, A.M., Mukhtar, H., Mousa, S.A., 2011. Nanoparticle delivery of natural products in the prevention and treatment of cancers: current status and future prospects. Cancers 3, 4024–4045.

Bigi, A., Cojazzi, G., Panzavolta, S., Roveri, N., Rubini, K., 2002. Stabilization of gelatin films by crosslinking with genipin. Biomaterials 23, 4827–4832.

Bilati, U., Allemann, E., Doelker, E., 2005. Strategic approaches for overcoming peptide and protein instability within biodegradable nano- and microparticles. European Journal of Pharmaceutics and Biopharmaceutics 59, 375–388.

Bolder, S.G., Hendrickx, H., Sagis, L.M.C., Van der Linden, E., 2006. Fibril assemblies in aqueous whey protein mixtures. Journal of Agricultural and Food Chemistry 54, 4229-4234.

Bolder, S.G., Sagis, L.M.C., Venema, P., Van der Linden, E., 2007. Effect of stirring and seeding on whey protein fibril formation. Journal of Agricultural and Food Chemistry 55, 5661–5669.

Bonnet, M., Cansell, M., Berkaoui, A., Ropers, M.H., Anton, M., Leal-Calderon, F., 2009. Release rate profiles of magnesium from multiple W/O/W emulsions. Food Hydrocolloids 23, 92–101.

Bourtoom, T., 2009. Edible protein films: properties enhancement. International Food Research Journal 16, 1−9.

Bressan, G.M., Pasquali-Ronchetti, I., Fornieri, C., Mattioli, F., Castellani, I., Volpin, D., 1986. Relevance of aggregation properties of tropoelastin to the assembly and structure of elastic fibers. Journal of Ultrastructure and Molecular Structure Research 94, 209–216.

Brown, K.V., Li, B., Guda, T., Perrien, D.S., Guelcher, S.A., Wenke, J.C., 2011. Improving bone formation in a rat femur segmental defect by controlling bone morphogenetic protein-2 release. Tissue Engineering: Part A 17, 1735–1746.

Bruno, M., Giancone, T., Torrieri, E., Masi, P., Moresi, M., 2008. Engineering properties of edible transglutaminase cross-linked caseinate-based films. Food Bioprocess Technology 1, 393–404.

Bustami, R.T., Chan, H.-K., Dehghani, F., Foster, N.R., 2000. Generation of micro-particles of proteins for aerosol delivery using high pressure modified carbon dioxide. Pharmaceutical Research 17, 1360–1366.

Byaruhanga, Y.B., Erasmus, C., Taylor, J.R.N., 2005. Effect of microwave heating of kafirin on the functional properties of kafirin films. Cereal Chemistry 82, 565–573.

Byaruhanga, Y.B., Emmambux, M.N., Belton, P.S., Wellner, N., Ng, K.G., Taylor, J.R.N., 2006. Alteration of kafirin film structure by heating with microwave energy and tannin complexation. Journal of Agricultural and Food Chemistry 54, 4198–4207.

Caillard, R., Remondetto, G.E., Subirade, M., 2009. Physicochemical properties and microstructure of soy protein hydrogels co-induced by Maillard type cross-linking and salts. Food Research International 42, 98–106.

Chambi, H., Grosso, C., 2006. Edible films produced with gelatin and casein cross-linked with transglutaminase. Food Research International 39, 458–466.

Chan, H.-K., Clark, A., Gonda, I., Mumenthaler, M., Hsu, C., 1997. Spray dried powders and powder blends of recombinant human deoxyribinuclease (rhDNase) for aerosol delivery. Pharmaceutical Research 14, 431–437.

Chan, W.-M., Ma, C.-Y., 1999. Acid modification of proteins from soymilk residue (okara). Food Research International 32, 119−127.

Charles, G., 2002. ‘Nestlé and L'Oréal in beauty food deal’. Marketing Week June 27, 2002. http://www.marketingweek.co.uk/nestlatilde169/loratilde169al-in-beauty-food-deal/2028773.article. Accessed 8 June 2012.

Charlton, A.J., Baxter, N.J., Khan, M.L., Moir, A.J.G., Haslam, E., Davies, A.P., Williamson, M.P., 2002. Polyphenol/peptide binding and precipitation. Journal of Agricultural and Food Chemistry 50, 1593–1601.

Chaudhry, Q., Scotter, M., Blackburn, J., Ross, B., Boxall, A., Castle, L., Aitken, R., Watkins, R., 2008. Applications and implications of nanotechnologies for the food sector. Food Additives and Contaminants 25, 241–258.

Chen, D., Zhao, M., Mundy, G.R., 2004. Bone morphogenetic proteins. Growth Factors 22, 233–241.

Chen, L., Subirade, M., 2007. Effect of preparation conditions on the nutrient release properties of alginate-whey protein granular microspheres. European Journal of Pharmaceutics and Biopharmaceutics 65, 354–362.

Chen, L., Subirade, M., 2009. Elaboration and characterization of soy/zein protein microspheres for controlled nutraceutical delivery. Biomacromolecules 10, 3327–3334.

Chen, L., Remondetto, G.E., Subirade, M., 2006. Food protein-based materials as nutraceutical delivery systems. Trends in Food Science Technology 17, 272–283.

Chevallet, M., Luche, S., Rabilloud, T., 2006. Silver staining of proteins in polyacrylamide gels. Nature Protocols 1, 1852–1858.

Ciacci, C., Maiuri, L., Caporaso, N., Bucci, C., Del Giudice, L., Massardo, D.R., Pontieri, P., Di Fonzo, N., Bean, S.R., Ioerger, B., Londei, M., 2007. Celiac disease: in vitro and in vivo safety and palatability of wheat-free sorghum food products. Clinical Nutrition 26, 799–805.

Clarke, A.W., Arnspang, E.C., Mithieux, S.M., Korkmaz, E., Braet, F., Weiss, A.S., 2006. Tropoelastin massively associates during coacervation to form quantized protein spheres. Biochemistry 45, 9989–9996.

Cook, R.B., Shulman, M.L., 1998. Colloidal dispersions of gluten, method of making and use therefor. United States Patent and Trademark Office 5736178.

Coombes, A.G.A., Lin, W., O'Hagen, D.T., Davis, S.S., 2003. Preparation of protein microspheres, films and coatings. United States Patent and Trademark Office 0182146.

Coombes, A.G.A., Breeze, V., Lin, W., Gray, T., Parker, K.G., Parker, T., 2001. Lactic acid-stabilised albumin for microsphere formulation and biomedical coatings. Biomaterials 22, 1–8.

Critchlow, M.A., Bland, Y.S., Ashhurst, D.E., 1994. The effects of age on the response of rabbit periosteal osteoprogenitor cells to exogenous transforming growth factor-β2. Journal of Cell Science 107, 499−516.

Csonka, F.A., Murphy, J.C., Jones, D.B., 1926. The iso-electric points of various proteins. Journal of the American Chemical Society 48, 763–768.

Cuq, B., Gontard, N., Guilbert, S., 1998. Proteins as agricultural polymers for packaging production. Cereal Chemistry 75, 1–9.

Da Silva, L.S., Taylor, J., Taylor, J.R.N., 2011. Transgenic sorghum with altered kafirin synthesis: kafirin solubility, polymerization, and protein digestion. Journal of Agricultural and Food Chemistry 59, 9265–9270.

De Freitas, F.A., Yunes, J.A., Da Silva, M.J., Arruda, P., Leite, A., 1994. Structural characterization and promoter activity analysis of the γ-kafirin gene from sorghum. Molecular and General Genetics 245, 177–186.

De Kruif, C.G., 1999. Casein micelle interactions. International Dairy Journal 9, 183–188.

DeRose, R., Ma, D.P., Kwon, I.S., Hasnain, S.E., Klassy, R.C., Hall, T., 1989. Characterisation of the kafirin gene family reveals extensive homology with zein from maize. Plant Molecular Biology 12, 245–256.

Digenis, G.A., Gold, T.B., Shah, V.P., 1994. Cross-linking of gelatin capsules and its relevance to their in vitro-in vivo performance. Journal of Pharmaceutical Sciences 83, 915–921.

Dong, J., Sun, Q., Wang, J.-Y., 2004. Basic study of corn protein, zein, as a biomaterial in tissue engineering, surface morphology and biocompatibility. Biomaterials 25, 4691–4697.

Dong, Z.-J., Xia, S.-Q., Hua, S., Hayat, K., Zhang, X.-M., Xu, S.-Y., 2008. Optimization of cross-linking parameters during production of transglutaminase-hardened spherical multinuclear microcapsules by complex coacervation. Colloids and Surfaces B: Biointerfaces 63, 41–47.

Draget, K.I., Skjåk-Bræk, G., Smidsrød, O., 1997. Alginate based new materials. International Journal of Biological Macromolecules 21, 47–55.

Dubey, R.R., Parikh, J.R., Parikh, R.R., 2003. Effect of heating temperature and time on pharmaceutical characteristics of albumin microspheres containing 5-fluorouracil. American Association of Pharmaceutical Scientists PharmSciTech 4, 1–6.

Duneas, N., 2010. Osteoinductive biomaterials. European Patent Office EP 1 539 812 B1.

Dunn, B.M., 2002. Structure and mechanism of the pepsin-like family of aspartic peptidases. Chemical Reviews 102, 4431–4458.

Duodu, K.G., Taylor, J.R.N., Belton, P.S., Hamaker, B.R., 2003. Factors affecting sorghum protein digestibility. Journal of Cereal Science 38, 117–131.

Duodu, K.G., Tang, H., Wellner, N., Belton, P.S., Taylor, J.R.N., 2001. FTIR and solid state ^{13}C NMR spectroscopy of proteins of wet cooked and popped sorghum and maize. Journal of Cereal Science 33, 261–269.

Edgcomb, S.P., Murphy, K.P., 2002. Variability in the pKa of histidine side-chains correlates with burial within proteins. Proteins 49, 1–6.

Eissa, A.S., Puhl, C., Kadla, J.F., Khan, S.A., 2006. Enzymatic cross-linking of β-lactoglobulin: conformational properties using FTIR spectroscopy. Biomacromolecules 7, 1707−1713.

El Nour, N.A., Peruffo, A.D.B., Curioni, A., 1998. Characterisation of sorghum kafirins in relations to their cross-linking behaviour. Journal of Cereal Science 28, 197–207.

Elkhalifa, A.E.O., Bernhardt, R., Bonomi, F., Iametti, S., Pagani, M.A., Zardi, M., 2006. Fermentation modifies protein/protein and protein/starch interactions in sorghum dough. European Food Research and Technology 222, 559–564.

Emmambux, N.M., 2004. Tannin binding of kafirin and its effects on kafirin films. PhD Thesis, University of Pretoria, Pretoria, South Africa

Emmambux, N.M., Taylor, J.R.N., 2003. Sorghum kafirin interaction with various phenolic compounds. Journal of the Science of Food and Agriculture 83, 402–407.

Emmambux, N.M., Taylor, J.R.N., 2009. Properties of heat-treated sorghum and maize meal and their prolamin proteins. Journal of Agricultural and Food Chemistry 57, 1045–1050.

Engvall, E., Perlmann, P., 1972. Enzyme-linked immunosorbent assay, ELISA: III. Quantitation of specific antibodies by enzyme-labeled anti-immunoglobulin in antigen-coated tubes The Journal of Immunology 109, 129–135.

Erickson, D.P., Campanella, O.H., Hamaker, B.R., 2012. Functionalizing maize zein in viscoelastic dough systems through fibrous, β-sheet-rich protein networks: An alternative, physiochemical approach to gluten-free breadmaking. Trends in Food Science and Technology 24, 74–81.

Eriksson, C., Nygren, H., Ohlson, K., 2004. Implantation of hydrophilic and hydrophobic titanium discs in rat tibia: cellular reactions on the surfaces during the first 3 weeks in bone. Biomaterials 25, 4759–4766.

Evans, D.J., Schüssler, L., Taylor, J.R.N., 1987. Isolation of reduced-soluble protein from sorghum starchy endosperm. Journal of Cereal Science 5, 61–65.

Ezeogu, L.I., Duodu, K.G., Taylor, J.R.N., 2005. Effects of endosperm texture and cooking on the in vitro starch digestibility of sorghum and maize flours. Journal of Cereal Science 42, 33–44.

Ezeogu, L.I., Duodu, K.G., Emmambux, M.N., Taylor, J.R.N., 2008. Influence of cooking conditions on the protein matrix of sorghum and maize endosperm flours. Cereal Chemistry 85, 397–402.

Ezpeleta, I., Rache, J.M., Gueguen, J., Orecchioni, A.M., 1997. Properties of glutaraldehyde cross-linked vicilin nano- and microparticles. Journal of Microencapsulation 14, 557–565.

Fadouloglou, V.E., Kokkinidis, M., Glykos, N.M., 2008. Determination of protein oligomerization state: Two approaches based on glutaraldehyde crosslinking. Analytical Biochemistry 373, 404–406.

Farley, J.R., Baylink, D.J., 1986. Skeletal alkaline phosphatase activity as bone formation index in vitro. Metabolism-Clinical and Experimental 35, 563–571.

Farrer,D., A. Lips, A., 1999. On the self-assembly of sodium caseinate. International Dairy Journal 9, 281–286.

Farris, S., Song, J., Huang, Q., 2010. Alternative reaction mechanism for the cross-linking of gelatin with glutaraldehyde. Journal of Agricultural and Food Chemistry 58, 998–1003.

Flores, I., Cabra, V., Quirasco, M.C., Farres, A., Galvez, A., 2010. Emulsifying properties of chemically deamidated corn (*Zea mays*) gluten meal. Food Science and Technology International 16, 241–250.

Fountoulakis, M., Lahm, H.-W., 1998. Hydrolysis and amino acid composition analysis of proteins. Journal of Chromatography A, 826, 109–134.

Franssen, O., Hennink, W.E., 1998. A novel preparation method for polymeric microparticles without the use of organic solvents. International Journal of Pharmaceutics 168, 1–7.

Freitas, S., Merkle, H.P., Gander, B., 2005. Microencapsulation by solvent extraction/evaporation: reviewing the state of the art of microsphere preparation process technology. Journal of Controlled Release 102, 313–332.

Friedman, M., 1996. Food browning and its prevention: an overview. Journal of Agricultural and Food Chemistry 44, 631−653.

Friess, W., Uludag, H., Foskett, S., Biron, R., Sargeant, C., 1999. Characterization of absorbable collagen sponges as rhBMP-2 carriers. International Journal of Pharmaceutics 187, 91–99.

Fu, Y.-C., Nie, H., Ho, M.-L., Wang, C.-K., Wang, C.-H., 2008. Optimized bone regeneration based on sustained release from three-dimensional fibrous PLGA/Hap composite scaffolds loaded with BMP-2. Biotechnology and Bioengineering 99, 996–1006.

Fujimoto, R. Tanizawa, T, Nishida, S., Yamamoto, N. Soshi, S., Endo, N., Takahashi, H.E., 1999. Local effects of transforming growth factor-β_1 on rat calvaria: changes depending on the dose and the injection site. Journal of Bone and Mineral Metabolism 17, 11−17.

Gan, C.-Y., Cheng, L.-H., Easa, A.M., 2008. Evaluation of microbial transglutaminase and ribose cross-linked soy protein isolate-based microcapsules containing fish oil. Innovative Food Science and Emerging Technologies 9, 563–569.

Gao, C., Taylor, J., Wellner, N., Byaruhanga, Y.B., Parker, M.L., Mills, E.N.C., Belton, P.S., 2005. Effect of preparation conditions on protein secondary structure and biofilm formation of kafirin. Journal of Agricultural and Food Chemistry 53, 306–312.

Gao, Z., Ding, P., Zhang, L., Shi, J., Yuan, S., Wei, J., Chen, D., 2007. Study of a pingyangmycin delivery system: zein/zein–SAIB in situ gels. International Journal of Pharmaceutics 328, 57–64.

Gautschi, O.P., Frey, S.P., Zellweger, R., 2007. Bone morphogenetic proteins in clinical applications. ANZ Journal of Surgery 77, 626–631.

Geiger, M., Li, R.H., Friess, W., 2003. Collagen sponges for bone regeneration with rhBMP-2. Advanced Drug Delivery Reviews 55, 1613–1629.

Gerrard, J.A., Brown, P.K., 2002. Protein cross-linking in food: mechanisms, consequences, applications. International Congress Series 1245, 211–215.

Gerrard, J.A., Brown, P.K., Fayle, S.E., 2003. Maillard crosslinking of food proteins II: the reactions of glutaraldehyde, formaldehyde and glyceraldehyde with wheat proteins in vitro and in situ. Food Chemistry 80, 35–43.

Giroux, H.J., Britten, M., 2011. Encapsulation of hydrophobic aroma in whey protein nanoparticles. Journal of Microencapsulation 28, 337–343.

Gong, J., Huo, M., Zhou, J., Zhang, Y., Peng, X., Yu, D., Zhang, H., Li, J., 2009. Synthesis, characterization, drug-loading capacity and safety of novel octyl modified serum albumin micelles. International Journal of Pharmaceutics 376, 161–168.

Gong, S., Wang, H., Sun, Q., Xue, S.-T., Wang, J.-Y., 2006. Mechanical properties and in vitro biocompatibility of porous zein scaffolds. Biomaterials 27, 3793–3799.

Gong, S.-J., Sun, S.-X., Sun, Q.-S. Wang, J.-Y., Liu, X.-M., Liu, G.-Y., 2011. Tablets based on compressed zein microspheres for sustained oral administration: design, pharmacokinetics, and clinical study. Journal of Biomaterials Applications 26, 195–208.

Gorbenko, G.P., Kinnunen, P.K.J., 2006. The role of lipid-protein interactions in amyloid-type protein fibril formation. Chemistry and Physics of Lipids 141, 72–82.

Gouranton, E., El Yazidi, C., Cardinault, N., Amiot, M.J., Borel, P., Landrier, J.F., 2008. Purified low-density lipoprotein and bovine serum albumin efficiency to internalise lycopene into adipocytes. Food and Chemical Toxicology 46, 3832–3836.

Guerrero, S., Teijón, C., Muñiz, E., Teijón, J.M., Dolores Blanco, M., 2010. Characterization and in vivo evaluation of ketotifen-loaded chitosan microspheres. Carbohydrate Polymers 79, 1006–1013.

Guo, Y., Liu, Z., An, H., Li, M., Hu, J., 2005. Nano-structure and properties of maize zein studied by atomic force microscopy. Journal of Cereal Science 41, 277–281.

Haidar, Z.S., Hamdy, R.C., Tabrizian, M., 2009. Delivery of recombinant bone morphogenetic proteins for bone regeneration and repair. Part B: Delivery systems for BMPs in orthopaedic and craniofacial tissue engineering. Biotechnology Letters 31, 1825–1835.

Hamaker, B.R., Kirleis, A.W., Mertz, E.T., Axtell, J.D., 1986. Effect of cooking on the protein profiles and in vitro digestibility of sorghum and maize. Journal of Agricultural and Food Chemistry 34, 647−649.

Hamaker, B.R., Kirleis, A.W., Butler, L.G., Axtell, J.D., Mertz, E.T., 1987. Improving the in vitro protein digestibility of sorghum with reducing agents. Proceedings of the National Academy of Sciences of the United States of America 84, 626–628.

Hamaker, B.R., Mohamed, A.A., Habben, J.E., Huang, C.P., Larkins, B.A., 1995. Efficient procedure for extracting maize and sorghum kernel proteins reveals higher prolamin contents than the conventional method. Cereal Chemistry 72, 583–588.

Haralampu, S.G., Sands, S., Gross, A., 1993. Method for producing an edible prolamine coating from aqueous latex. United States Patent and Trademark Office 5182130.

Hebrard, G., Blanquet, S., Beyssac, E., Remondetto, G., Subirade, M., Alric, M., 2006. Use of whey protein beads as a new carrier system for recombinant yeasts in human digestive tract. Journal of Biotechnology 127, 151–60.

Heritage, P.L., Loomes, L.M., Jianxiong, J., Brook, M.A., Underdown, B.J., McDermott, M.R., 1996. Novel polymer-grafted starch microparticles for mucosal delivery of vaccines. Immunology 88, 162–168.

Hernández-Muñoz, P., Kanavouras, A., Lagaron, J M., Gavara, R., 2005. Development and characterization of films based on chemically cross-linked gliadins. Journal of Agricultural and Food Chemistry 53, 8216−8223.

Herrmann, J., Bodmeier, R., 1998. Biodegradable, somatostatin acetate containing microspheres prepared by various aqueous and non-aqueous solvent evaporation methods. European Journal of Pharmaceutics and Biopharmaceutics 45, 75–82.

Higberger, J.H., 1939. The isoelectric point of collagen. Journal of the American Chemical Society 61, 2302–2303.

Hoffmann, W.E., Everds, N., Pignatello, M., Solter, P.F., 1994. Automated and semiautomated analysis of rat alkaline phosphatase isoenzymes. Toxicologic Pathology 22, 633–638.

Hollinger, J.O., Schmitt, J.M., Buck, D.C., Shannon, R., Joh, S.P., Zegzula, H.D., Wozney, J., 1998. Recombinant human bone morphogenetic protein-2 and collagen for bone regeneration. Journal of Biomedical Materials Research 43, 356–364.

Horne, D.S., 2006. Casein micelle structure: models and muddles. Current Opinion in Colloid and Interface Science 11, 148–153.

Hou, Q., De Bank, P.A., Shakesheff, K.M., 2004. Injectable scaffolds for tissue regeneration. Journal of Materials Chemistry 14, 1915–1935.

Hurkman, W.J., Tanaka, C.K., 1986. Solubilization of plant membrane proteins for analysis by two-dimensional gel electrophoresis. Plant Physiology 81, 802–806.

Hurtado-López, P., Murdan, S., 2005. Formulation and characterisation of zein microspheres as delivery vehicles. Journal of Drug Delivery Science and Technology 15, 267–272.

Hurtado-López, P., Murdan, S., 2006. An investigation into the adjuvanticity and immunogenicity of zein microspheres being researched as drug and vaccine carriers. Journal of Pharmacy and Pharmacology 58, 769–774.

Ikura, K., Goto, M., Yoshikawa, M., Sasaki, R., Chiba, H., 1984. Use of transglutaminase. Reversible blocking of amino groups in substrate proteins for a high yield of specific products. Agricultural and Biological Chemistry 48, 2347–2354.

Ishikawa, T., Terai, H., Kitajima, T., 2001. Production of a biologically active epidermal growth factor fusion protein with high collagen affinity. Journal of Biochemistry 129, 627–633.

Jackson, M., Mantsch, H.H., 1995. The use and misuse of FTIR spectroscopy in the determination of protein structure. Critical Reviews in Biochemistry and Molecular Biology 30, 95–120.

Jacobs, J.J., Roebuck, K.A., Archibeck, M., Hallab, N.J., Glant, T.T., 2001. Osteolysis: basic science. Clinical Orthopaedics and Related Research 393, 71–77.

Johnson, K.A., 1997. Preparation of peptide and protein powders for inhalation. Advanced Drug Delivery Reviews 26, 3–15.

Jones, O.G., McClements, D.J., 2010. Functional biopolymer particles: design, fabrication, and applications. Comprehensive Reviews in Food Science and Food Safety 9, 374–397.

Karageorgiou, V., Kaplan, D., 2005. Porosity of 3D biomaterial scaffolds and osteogenesis. Biomaterials 26, 5474–5491

Kawamoto, H., Mizutani, K., Nakatsubo, F., 1997. Binding nature and denaturation of protein during interaction with galloylglucose. Phytochemistry 46, 473–478.

Kaya, S., Kaya, A., 2000. Microwave drying effects on properties of whey protein isolate edible films. Journal of Food Engineering 43, 91–96.

Kempen, D.H.R., Lu, L., Hefferan, T.E., Creemers, L.B., Maran, A., Classic, K.L., Dhert, W.J.A., Yaszemski, M.J., 2008. Retention of in vitro and in vivo BMP-2 bioactivities in sustained delivery vehicles for bone tissue engineering. Biomaterials 29, 3245–3252.

Kentsis, A., Borden, K.L.B., 2004. Physical mechanisms and biological significance of supramolecular protein self-assembly. Current Protein and Peptide Science 5, 125–134.

Kiernan, J.A., 2000. Formaldehyde, formalin, paraformaldehyde and glutaraldehyde: what they are and what they do. Microscopy Today 00-1, 8–12.

Kim, C.-S., Kim, J.-I., Kim, J., Choi, S.-H., Chai, J.-K., Kim, C.-K., Cho, K.-S., 2005. Ectopic bone formation associated with recombinant human bone morphogenetic proteins-2 using absorbable collagen sponge and beta tricalcium phosphate as carriers. Biomaterials 26, 2501–2507.

Kim, K., Cheng, J., Liu, Q., Wu, X.Y., Sun, Y., 2010. Investigation of mechanical properties of soft hydrogel microcapsules in relation to protein delivery using a MEMS force sensor. Journal of Biomedical Materials Research Part A 92, 103–113.

Kim, K., Liu, X., Zhang, Y., Cheng, J., Wu, X.Y., Sun, Y., 2008. Mechanical characterization of polymeric microcapsules using a force-feedback MEMS microgripper. In: Engineering in Medicine and Biology Society, 2008. EMBS 2008. 30th Annual International Conference of the IEEE, 20–25 August 2008, Vancouver, Canada, pp.1845–1848.

Kim, S., Kang, Y., Krueger, C.H., Sen, M., Holcomb, J.B., Chen, D., Wenke, J.C., Yang, Y., 2012. Sequential delivery of BMP-2 and IFG-1 using a chitosan gel with gelatin microspheres enhances early osteoblastic differentiation. Acta Biomaterialia 8, 1768–1777.

King, G.N., Cochran, D.L., 2002. Factors that modulate the effects of bone morphogenetic protein-induced periodontal regeneration: a critical review. Journal of Periodontology 73, 925–936.

Kocamustafaogullari, G., Ishii, M., 1995. Foundation of the interracial area transport equation and its closure relations. International Journal of Heat and Mass Transfer 38, 481–493.

Krake, B., Damasche, B., 2000. Measurement of nanohardness and nanoelasticity of thin gold films with scanning force microscope. Applied Physics Letters 77, 361–363.

Kraus, D., Deschner, J., Jäger, A., Wenghoefer, M., Bayer, S., Jepsen, S., Allam, J.P., Novak, N., Meyer, R., Winter, J., 2012. Human β-defensins differently affect proliferation, differentiation, and mineralization of osteoblast-like MG63 cells. Journal of Cellular Physiology 227, 994–1003

Krebs, M.R.H., Devlin, G.L., Donald, A.M., 2007. Protein particulates: another generic form of protein aggregation? Biophysical Journal 92, 1336–1342.

Krochta, J.M., 2002. Proteins as raw materials for films and coatings: definitions, current status, and opportunities. In: Gennadios, A. (Ed.), Protein-Based Films and Coatings. CRC Press: Boca Raton, FL, pp. 1−41.

Kumar, V., Kang, J., Hohl, R.J., 2001. Improved dissolution and cytotoxicity of camptothecin incorporated into oxidized-cellulose microspheres prepared by spray drying. Pharmaceutical Development and Technology 6, 459–467.

La, W.-G., Kang, S.-W., Yang, H.S., Bhang, S.H., Lee, S.H., Park, J.-H, Kim, B.-S., 2010. The efficacy of bone morphogenetic protein-2 depends on its mode of delivery. Artificial Organs 34, 1150–1153

Lai, H.-M., Padua, G.W., 1997. Properties and microstructure of plasticized zein films. Cereal Chemistry 74, 771–775.

Lai, H.-M., Padua, G.W., Wei, L.S., 1997. Properties and microstructure of zein sheets plasticized with palmitic and stearic acids. Cereal Chemistry 74, 83–90.

Lambert, J.M., Weinbreck, F., Kleerebezem, M., 2008. In vitro analysis of protection of the enzyme bile salt hydrolase against enteric conditions by whey protein-gum Arabic microencapsulation. Journal of Agricultural and Food Chemistry 56, 8360–8364.

Lantto, R., 2007. Protein cross-linking with oxidative enzymes and transglutaminase. Effects in meat protein systems. PhD Thesis, University of Helsinki, Helsinki, Finland.

Larré, C., Chiarello, M., Blanloeil, Y., Chenu, M., Gueguen, J., 1993. Gliadin modifications catalyzed by guinea pig liver transglutaminase. Journal of Food Biochemistry 17, 267–282.

Latha, M.S., Rathinam, K., Mohanan, P.V., Jayakrishnan, A., 1995. Bioavailability of theophylline from glutaraldehyde cross-linked casein microspheres in rabbits following oral administration. Journal of Controlled Release 34, 1–7.

Laurine, E., Gregoire, C., Fandrich, M., Engemann, S., Marchal, S., Thion, L., Mohr, M., Monsarrat, B., Michel, B., Dobson, C.M., Wanker, E., Erard, M., Verdier, J.-M., 2003. Lithostathine quadruple-helical filaments form proteinase K-resistant deposits in Creutzfeldt-Jakob disease. Journal of Biological Chemistry 278, 51770–51778.

Lawton, J.W., 2002. Zein: a history of processing and use. Cereal Chemistry 79, 1–18.

Lawton, J.W., 2004. Plasticizers for zein: their effect on tensile properties and water absorption of zein films. Cereal Chemistry 81, 1–5.

Lee, C., Wei, X., Kiser, J.W., Hone, J., 2008. Measurement of the elastic properties and intrinsic strength of monolayer grapheme. Science 321, 385–388.

Lee, H.-J., Soles, C.L., Vogt, B.D., Liu, D.-W., Wu, W.-I., Lin, E.K., Kim, H.-C., Lee, V.Y., Volksen, W., Miller, R.D., 2008. Effect of porogen molecular architecture and loading on structure of porous thin films. Chemistry of Materials 20, 7390–7398.

Lee, S.J., Rosenberg, M., 1999. Preparation and properties of glutaraldehyde cross-linked whey protein-based microcapsules containing theophylline. Journal of Controlled Release 61, 123–136.

Lee, S.J., Rosenberg, M., 2000. Whey protein-based microcapsules prepared by double emulsification and heat gelation. Lebensmittel-Wissenschaft und-Technologie 33, 80–88.

Lee, W., Park, J., Yang, E.H., Suh, H., Kim, S.H., Chung, D.S., Choi, K., Yang, C.W., Park, J., 2002. Investigation of the factors influencing the release rates of cyclosporin A-loaded micro- and nanoparticles prepared by high-pressure homogenizer. Journal of Controlled Release 84, 115–123.

Lehtinen, K.E.J., Zachariah, M.R., 2001. Effect of coalescence energy release on the temporal shape evolution of nanoparticles. Physical Review B 63, 205402-1–205402-7.

Li, Q.X., Gee, S.J., McChesney, M.M., Hammock, B.D., Seiber, J.N., 1989. Comparison of an enzyme-linked immunosorbent assay and a gas chromatographic procedure for the determination of molinate residues. Analytical Chemistry 61, 819–823.

Liggins, R.T., Toleikis, P.M., Guan, D., 2008. Microparticles with high loadings of a bioactive agent. United States Patent and Trademark Office 0124400.

Liu, X., Sun, Q., Wang, H., Zhang, L., Wang, J.Y., 2005. Microspheres of corn protein, zein, for an ivermectin drug delivery system. Biomaterials 26, 109–115.

Livney, Y.D., 2010. Milk proteins as vehicles for bioactives. Current Opinion in Colloid and Interface Science 15, 73–83.

López-Rubio, A., Lagaron, J.M., 2012. Whey protein capsules obtained through electrospraying for the encapsulation of bioactives. Innovative Food Science and Emerging Technologies 13, 200–206

Lowik, D., Van Hest, J.C.M., 2004. Peptide based amphiphiles. Chemical Society Reviews 33, 234−245.

Lowry, O.H., Rosebrough, N.J., Farr, A.L., Randall, R.J., 1951. Protein measurement with the Folin phenol reagent. Journal of Biological Chemistry 193, 265–275.

Lundin, L., Golding, M., Wooster, T.J., 2008. Understanding food structure and function in developing food for appetite control. Nutrition and Dietetics 65 (Suppl. 3), S79–S85.

Maa, Y.-F., Nguyen, P.-A., Sweeney, T., Shire, S.J., Hsu, C.C., 1999. Protein inhalation powders: spray-drying vs spray freeze drying. Pharmaceutical Research 16, 249–254.

MacAdam, A.B., Shaft, Z.B., James, S.L., Marriott, C., Martin, G.P., 1997. Preparation of hydrophobic and hydrophilic albumin microspheres and determination of surface carboxylic acid and amino residues. International Journal of Pharmaceutics 151, 47–55.

Madhan, B., Muralidharan, C., Jayakumar, R., 2002. Study on the stabilisation of collagen with vegetable tannins in the presence of acrylic polymer. Biomaterials 23, 2841–2847.

Maghsoudi, A., Shojaosadati, S.A., Farahani, V., 2008. 5-Fluorouracil-loaded BSA nanoparticles: formulation optimization and in vitro release study. AAPS PharmSciTech 9, 1092–1096.

Marketing Week , 2003. 'Laboratoires Innéov set to roll out first product line'. Marketing Week March 20, 2003. http://www.marketingweek.co.uk/laboratoires-innov-set-to-roll-out-first-product-line/2033890.article. Accessed 8 June 2012.

Marquié, C., Tessier, A.-M., Aymard, C., Guilbert, S., 1997. HPLC determination of the reactive lysine content of cottonseed protein films to monitor the extent of cross-linking by formaldehyde, glutaraldehyde, and glyoxal. Journal of Agricultural and Food Chemistry 45, 922–926.

Marteau, P., Minekus, M., Havenaar, R., Huis In't Veld, J.H.J., 1997. Dairy foods: survival of lactic acid bacteria in a dynamic model of the stomach and small intestine: validation and the effects of bile. Journal of Dairy Science 80, 1031–1037.

Mathiowitz, E., Bernstein, H., Morrel, E., Schwaller, K., 1993. United States Patent and Trademark Office 5271961.

Mathiowitz, E., Chickering III, D., Jong, Y.S., Jacob, J.S., 2000. Process for preparing microparticles through phase inversion phenomena. United States Patent and Trademark Office 6143211.

Matsudomi, N., Kato, A., Kobayashi, K., 1982. Conformation and surface properties of deamidated gluten. Agricultural and Biological Chemistry 46, 1583−1586.

McMaster, T.J., Miles, M.J., Kasarda, D.D., Shewry, P.R., Tatham, A.S., 2000. Atomic force microscopy of A-gliadin fibrils and in situ degradation. Journal of Cereal Science 31, 281–286.

Meade, S.J., Miller, A.G., Gerrard, J.A., 2003. The role of dicarbonyl compounds in non-enzymatic crosslinking: a structure–activity study. Bioorganic and Medicinal Chemistry 11, 853–862.

Micard, V., Belamri, R., Morel, M.-H., Guilbert, S., 2000. Properties of chemically and physically treated wheat gluten films. Journal of Agricultural and Food Chemistry 48, 2948–2953.

Migneault, I., Dartiguenave, C., Bertrand, M.J., Waldron, K.C., 2004. Glutaraldehyde: behavior in aqueous solution, reaction with proteins, and application to enzyme crosslinking. BioTechniques 37, 790−802.

Militello, V., Vetri, V., Leone, M., 2003. Conformational changes involved in thermal aggregation processes of bovine serum albumin. Biophysical Chemistry 105, 133–141.

Miller, M.L., Johnson, G.V.W., 1999. Rapid, single-step procedure for the identification of transglutaminase-mediated isopeptide crosslinks in amino acid digests. Journal of Chromatography B 732, 65–72.

Mizutani, Y., Matsumura, Y., Imamura, K., Nakanishi, K., Mori, T., 2003. Effects of water activity and lipid addition on secondary structure of zein in powder systems. Journal of Agricultural and Food Chemistry 51, 229–235.

Mohanty, B., Bohidar, H.B., 2005. Microscopic structure of gelatin coacervates. International Journal of Biological Macromolecules 36, 39–46.

Mokrane, H., Lagrain, B., Gebruers, K., Courtin, C.M., Brijs, K., Proost, P., Delcour, J.A., 2009. Characterization of kafirins in Algerian sorghum cultivars. Cereal Chemistry 86, 487–491.

Motoki, M., Seguro, K., 1998. Transglutaminase and its use for food processing. Trends in Food Science and Technology 9, 204–210.

Motoki, M., Seguro, K., Nio, N., Takinami, K., 1986. Glutamine-specific deamidation of α_{s1}-casein by transglutaminase. Agricultural and Biological Chemistry 50, 3025−3030.

Mussatto, S.I., Dragone, G., Roberto, I.C., 2006. Brewers' spent grain: generation, characteristics and potential applications. Journal of Cereal Science 43, 1–14.

Muthuselvi, L., Dhathathreyan, A., 2006. Simple coacervates of zein to encapsulate gitoxin. Colloids and Surfaces B: Biointerfaces 51, 39–43.

Nag, S., Banerjee, R., 2012. Fundamentals of medical implant materials. In: Narayan, R. (Ed.), ASM Handbook: Materials for Medical Devices. ASM International: Russell Township, OH, Vol. 23, pp. 6–17.

Narita, Y., Oda, S., Moriyama, A., Kageyama, T., 2002. Primary structure, unique enzymatic properties, and molecular evolution of pepsinogen B and pepsin B. Archives of Biochemistry and Biophysics 404, 177–185.

Nickel, J., Dreyer, M.K., Kirsch, T., Sebald, W., 2001. The crystal structure of the BMP-2:BMPR-IA complex and the generation of BMP-2 antagonists. Journal of Bone and Joint Surgery 83-A (Suppl. 1, Part 1), S7–S14.

Ohtsuka, T, Sawa, A., Kawabata, R., Nio, N., Motoki, M., 2000. Substrate specificities of microbial transglutaminase for primary amines. Journal of Agricultural and Food Chemistry 48, 6230–6233.

Önal, U., Langdon, C., 2005. Performance of zein-bound particles for delivery of riboflavin to early fish larvae. Aquaculture Nutrition 11, 351–358

Organisation for Economic Cooperation and Development (OECD), 1981. OECD Guideline for Testing of Chemicals 410. Repeated Dose Dermal Toxicity: 21/28-day Study. OECD: Paris, France.

Oria, M.P., Hamaker, B.R., Axtell, J.D., Huang, C.-P., 2000. A highly digestible sorghum mutant cultivar exhibits a unique folded structure of endosperm protein bodies. . Proceedings of the National Academy of Sciences of the United States of America 97, 5065–5070.

Orliac, O., Rouilly, A., Silvestre, F., Rigal, L., 2002. Effects of additives on the mechanical properties, hydrophobicity and water uptake of thermomoulded films produced from sunflower protein isolate. Polymer 43, 5417–5425.

Osborne, J.L., Farmer, R., Woodhouse, K.A., 2008. Self-assembled elastin-like polypeptide particles. Acta Biomaterialia 4, 49–57.

Panchapakesan, C., Sozer, N., Dogan, H., Huang, Q., Kokini, J.L., 2012. Effect of different fractions of xeon on the mechanical and phase properties of zein films at nano-scale. Journal of Cereal Science 55, 174–182.

Park, H.J., Chinnan, M.S., 1995. Gas and water vapor barrier properties of edible films from protein and cellulosic materials. Journal of Food Engineering 25, 497–507.

Parris, N., Coffin, D.R., 1997. Composition factors affecting the water vapor permeability and tensile properties of hydrophilic zein films. Journal of Agricultural and Food Chemistry 45, 1596−1599.

Parris, N., Cooke, P.H., Hicks, K.B., 2005. Encapsulation of essential oils in zein nanospherical particles. Journal of Agricultural and Food Chemistry 53, 4788–4792.

Patel, A., Hu, Y., Tiwari, J.K., Velikov, K.P., 2010. Synthesis and characterisation of zein–curcumin colloidal particles. Soft Matter 6, 6192–6199.

Patel, Z.S., Yamamoto, M., Ueda, H., Tabata, Y., Mikos, A.G., 2008. Biodegradable gelatin microparticles as delivery systems for the controlled release of bone morphogenetic protein-2. Acta Biomaterialia 4, 1126–1138.

Patil, G.V., 2003. Biopolymer albumin for diagnosis and in drug delivery. Drug Development Research 58, 219–247.

Patten, G.S., Augustin, M.A., Sanguansri, L., Head, R.J., Abeywardena, M.Y., 2009. Site specific delivery of microencapsulated fish oil to the gastrointestinal tract of the rat. Digestive Diseases and Sciences 54, 511–521.

Paulis, J.W., Wall, J.S., 1979. Distribution and electrophoretic properties of alcohol-soluble proteins in normal and high-lysine sorghums. Cereal Chemistry 56, 20–23.

Pekkarinen, T., 2005. Effect of sterilization and delivery systems on the osteoinductivity of reindeer bone morphogenetic protein extract. PhD Thesis, University of Oulu, Oulu, Finland.

Pelton, J.T., McLean, L.R., 2000. Spectroscopic methods for analysis of protein secondary structure. Analytical Biochemistry 277, 167–176.

Pérez-Pérez, C., Regalado-González, C., Rodríguez-Rodríguez, C.A., Barbosa-Rodríguez, J.R., Villaseñor-Ortega, F., 2006. Incorporation of antimicrobial agents in food packaging films and coatings. In: Guevara-González, R.G. and Torres-Pacheco, I. (Eds.), Advances in Agricultural and Food Biotechnology. Research Signpost; Trivandrum, India, pp. 193−216.

Phani, K.K., Niyogi, S.K., 1987. Young's modulus of porous brittle solids. Journal of Materials Science 22, 257–263.

Picot, A., Lacroix, C., 2004. Encapsulation of bifidobacteria in whey protein-based microcapsules and survival in simulated gastrointestinal conditions and in yoghurt. International Dairy Journal 14, 505–515.

Poole, A.J., Church, J.S., Huson, M.G., 2008. Environmentally sustainable fibers from regenerated protein. Biomacromolecules 10, 1−8.

Prata, A.S., Zanin, M.H.A., Ré, M.I., Grosso, C.R.F., 2008. Release properties of chemical and enzymatic crosslinked gelatin-gum Arabic microparticles containing a fluorescent probe plus vetiver essential oil. Colloids and Surfaces B: Biointerfaces 67, 171–178.

Quirk, R.A., France, R.M., Shakesheff, K.M., Howdle, S.M., 2004. Supercritical fluid technologies and tissue engineering scaffolds. Current Opinion in Solid State and Materials Science 8, 313–321.

Quispe-Condori, S., Saldaña, M.D.A., Temelli, F., 2011. Microencapsulation of flax oil with zein using spray and freeze drying. LWT-Food Science and Technology 44, 1880–1887.

Rayment, I., 1997. Reductive alkylation of lysine residues to alter crystallization properties of properties. Methods in Enzymology 276, 171–179.

Reddy, N., Yang, Y., 2011. Potential of plant proteins for medical applications. Trends in Biotechnology 29, 490–498.

Reddy, N., Tan, Y., Li, Y., Yang, Y., 2008. Effect of glutaraldehyde crosslinking conditions on the strength and water stability of wheat gluten fibers. Macromolecular Materials and Engineering 293, 614–620.

Reis, C.P., Neufeld, R.J., Ribeiro, A.J., Veiga, F., 2006. Nanoencapsulation II. Biomedical applications and current status of peptide and protein nanoparticulate delivery systems. Nanomedicine: Nanotechnology, Biology, and Medicine 2, 53–65.

Remondetto, G.E., Subirade, M., 2003. Molecular mechanisms of Fe^{2+}-induced β-lactoglobulin cold gelation. Biopolymers 69, 461–469.

Ripamonti, U., Duneas, N., Van Den Heever, B., Bosch, C., Crooks, J., 1997. Recombinant transforming growth factor-β1 induces endochondral bone in the baboon and synergizes with recombinant osteogenic protein-1 (bone morphogenetic protein-7) to initiate rapid bone formation. Journal of Bone and Mineral Research 12, 1584–1595.

Rippey, J.J., 1994. General Pathology. Illustrated Lecture Notes. (Second edition), Wits University Press; Johannesburg, South Africa, pp. 151–152.

Roodman, G.D, 1996. Advances in bone biology: the osteoclast. Endocrine Reviews 17, 308–332.

Roos, N., Lorenzen, P.C., Sick, H., Schrezenmeir, J., Schlimme, E., 2003. Cross-linking by transglutaminase changes neither the in vitro proteolysis nor the in vivo digestibility of caseinate. Kieler Milchwirtschaftliche Forschungsberichte, 55, 261–276.

Rosalki, S.B., Foo, A.Y., Burlina, A., Prellwitz, W., Stieber, P., Neumeier, D., Klein, G., Poppe, W.A., Bodenmüller, H., 1993. Multicenter evaluation of iso-ALP test kit for measurement of bone alkaline phosphatase activity in serum and plasma. Clinical Chemistry 39, 648–652.

Ruhé, P.Q., Boerman, O.C., Russel, F.G.M., Spauwen, P.H.M., Mikos, A.G., Jansen, J.A., 2005. Controlled release of rhBMP-2 loaded poly(DL-lactic-co-glycolic acid)/calcium phosphate cement composites in vivo. Journal of Controlled Release 106, 162–171.

Safanama, D.S., Marashi, P., Hesari, A.Z., Firoozi, S., Aboutalebi, S.H., Jalilzadeh, S., 2012. Elastic modulus measurement of nanocomposite materials by atomic force microscopy. International Journal of Modern Physics: Conference Series 5, 502–509.

Saraç, F., Saygılı, F., 2007. Causes of high bone alkaline phosphatase. Biotechnology and Biotechnological Equipment 21, 194–197.

Schägger, H., 2006. Tricine–SDS-PAGE. Nature Protocols 1, 16–22.

Scheufler, C., Sebald, W., Hülsmeyer, M., 1999. Crystal structure of human bone morphogenetic protein-2 at 2.7 Å resolution. Journal of Molecular Biology 287, 103–115.

Schrier, J.A., DeLuca, P.P., 1999. Recombinant human bone morphogenetic protein-2 binding and incorporation in PLGA microsphere delivery systems. Pharmaceutical Development and Technology 4, 611–621.

Schrooyen, P.M.M., Van der Meer, R., De Kruif, C.G., 2001. Micrencapsulation: its application in nutrition. Proceedings of the Nutrition Society 60, 475–479.

Sebra, R.P., Masters, K.S., Cheung, C.Y., Bowman, C.N., Anseth, K.S., 2006. Detection of antigens in biologically complex fluids with photografted whole antibodies. Analytical Chemistry 78, 3144–3151.

Secundo, F., Guerrieri, N., 2005. ATR-FT/IR study on the interactions between gliadins and dextrin and their effects on protein secondary structure. Journal of Agricultural and Food Chemistry 53, 1757−1764.

Seeherman, H., Wozney, J., Li, R., 2002. Bone morphogenetic protein delivery systems. Spine 27, S16–S23.

Seguro, K., Kumazawa, Y., Kuraishi, C., Sakamoto, H., Motoki, M., 1996. The ε-(γ-glutamyl)lysine moiety in crosslinked casein is an available source of lysine for rats. Journal of Nutrition 126, 2557–2562.

Selling, G.W., Woods, K.K., Sessa, D., Biswas, A., 2008. Electrospun zein fibers using glutaraldehyde as the crosslinking reagent: effect of time and temperature. Macromolecular Chemistry and Physics 209, 1003–1011.

Semo, E., Kesselman, E., Danino, D., Livney, Y.D., 2007. Casein micelle as a natural nanocapsular vehicle for nutraceuticals. Food Hydrocolloids 21, 936–942.

Sessa, D.J., Mohamed, A., Byars, J.A., 2008. Chemistry and physical properties of melt-processed and solution-cross-linked corn zein. Journal of Agricultural and Food Chemistry 56, 7067–7075.

Sessa, D.J., Mohamed, A., Byars, J.A., Hamaker, S.A., Selling, G.W., 2007. Properties of films from corn zein reacted with glutaraldehyde. Journal of Applied Polymer Science 105, 2877–2883.

Shah, P, Keppler, L., Rutkowski, J., 2011. A review of bone morphogenic protein : an elixir for bone grafting. Journal of Oral Implantology (in press). DOI: http://0-dx.doi.org.innopac.up.ac.za/10.1563/AAID-JOI-D-10-00196.

Shakesheff, K.M., Davies, M.C., Jackson, D.E., Roberts, C.J., Tendler, S.J.B., Brown, V.A., Watson, R.C., Barrett, D.A., Shaw, P.N., 1994. Imaging the surface of silica microparticles with the atomic force microscope: a novel sample preparation method. Surface Science Letters 304, L393–L399.

Sharma, R., Lorenzen, P.C., Qvist, K.B., 2001. Influence of transglutaminase treatment of skim milk on the formation of ε-(γ-glutamyl)lysine and the susceptibility of individual proteins towards crosslinking. International Dairy Journal 11, 785–793.

Shibata-Seki, T., Masai, J., Tagawa, T., Sorin, T., Kondo, S., 1996. In-situ atomic force microscopy study of lipid vesicles adsorbed on a substrate. Thin Solid Films 273, 297–303.

Shin, H., Grason, G.M., Santangelo, C.D., 2009. Mesophases of soft-sphere aggregates. Soft Matter 5, 3629–3638.

Shoyele, S.A., Cawthorne, S., 2006. Particle engineering techniques for inhaled biopharmaceuticals. Advanced Drug Delivery Reviews 58, 1009–1029.

Shull, J.M., Watterson, J.J., Kirleis, A.W., 1991. Proposed nomenclature for the alcohol-soluble proteins (kafirins) of *Sorghum bicolor* (L. Moench) based on molecular weight, solubility and structure. Journal of Agricultural and Food Chemistry 39, 83–87.

Shull, J.M., Watterson, J.J., Kirleis, A.W., 1992. Purification and immunocytochemical localization of kafirins in *Sorghum bicolor* (L. Moench) endosperm). Protoplasma 171, 64–74.

Shutava, T. G., Balkundi, S. S., Lvov, Y.M., 2009. (-)-Epigallocatechin gallate/gelatin layer-by-layer assembled films and microcapsules. Journal of Colloid and Interface Science 330, 276–283.

Silva, G.A., Ducheyne, P., Reis, R.L., 2007. Materials in particulate form for tissue engineering. 1. Basic concepts. Journal of Tissue Engineering and Regenerative Medicine 1, 4–24.

Singleton, V.L., Rossi, J., 1965. Colorimetry of total phenolics with phosphomolybdic-phosphotungstic acid reagents. American Journal of Enology and Viticulture 16, 144–158.

Sinha, V.R., Trehan, A., 2003. Biodegradable microspheres for protein delivery. Journal of Controlled Release 90, 261–280.

Smart, J.D., Nicholls, T.J., Green, K.L., Rogers, D.J., Cook, J.D., 1999. Lectins in drug delivery: a study of the acute local irritancy of the lectins from *Solanum tuberosum* and *Helix pomatia*. European Journal of Pharmaceutical Sciences 9, 93–98.

Smidsrød, O., Skjåk-Bræk, G., 1990. Alginate as immobilization matrix for cells. Trends in Biotechnology 8, 71–78.

Smyth, M.S., Martin, J.H.J., 2000. X-ray crystallography. Journal of Clinical Pathology: Molecular Pathology 53, 8–14.

Soliman, E.A., Eldin, M.S.M., Furuta, M., 2009. Biodegradable zein-based films: influence of γ-irradiation on structural and functional properties. Journal of Agricultural and Food Chemistry 57, 2529–2535.

Stark, L.E., Gross, A.T., 1991. Hydrophobic protein microparticles and preparation thereof. United States Patent and Trademark Office 5021248.

Stark, L.E., Gross, A.T., 1994. Hydrophobic protein microparticles. United States Patent and Trademark Office 5330778.

Steinmüller-Nethl, D., Kloss, F.R., Najam-Ul-Haq, M., Rainer, M., Larsson, K., Linsmeier, C., Köhler, G., Fehrer, C., Lepperdinger, G., Liu, X., Memel, N., Bertel, E., Huck, C.W., Gassner, R., Bonn, G., 2006. Strong binding of bioactive BMP-2 to nanocrystalline diamond by physisorption. Biomaterials 27, 4547–4556.

Stokes, R.H., Robinson, R.A., 1949. Standard solutions for humidity control at 25^{o}C. Industrial and Engineering Chemistry 41, 2013.

Stucki, U., Schmid, J., Hämmerle, C.F., Lang, N.P., 2001. Temporal and local appearance of alkaline phosphatase activity in early stages of guided bone regeneration. A descriptive histochemical study in humans. Clinical Oral Implants Research 12, 121–127.

Subirade, M., Kelly, I., Guéguen, J., Pézolet, M., 1998. Molecular basis of film formation from a soybean protein: comparison between the conformation of glycinin in aqueous solution and in films. International Journal of Biological Macromolecules 23, 241–249.

Sugiarto, M., Ye, A., Singh, H., 2009.Characterisation of binding of iron to sodium caseinate and whey protein isolate. Food Chemistry 114, 1007–1013.

Sun, Y., Hayakawa, S., Izumori, K., 2004. Modification of ovalbumin with a rare ketohexose through the Maillard reaction: effect on protein structure and gel properties. Journal of Agricultural and Food Chemistry 52, 1293–1299.

Surewicz, W.K., Mantsch, H.H., Chapman, D., 1993. Determination of protein secondary structure by Fourier transform infrared spectroscopy: a critical assessment. Biochemistry 32, 389–394.

Suzuki, T., Sato, E., Matsuda, Y., Tada, H., Unno, K., Kato, T., 1989. Preparation of zein microspheres conjugated with antitumor drugs available for selective cancer chemotherapy and development of a simple colorimetric determination of drugs in microspheres. Chemical and Pharmaceutical Bulletin 37, 1051–1054.

Talmon, Y., 1983. Staining and drying-induced artifacts in electron microscopy of surfactant dispersions. Journal of Colloid and Interface Science 93, 366–382.

Tamber, H., Johansen, P., Merkle, H.P., Gander, B., 2005. Formulation aspects of biodegradable polymeric microspheres for antigen delivery. Advanced Drug Delivery Reviews 57, 357–376.

Tan, M.L., Choong, P.F.M., Dass, C.R., 2010. Recent developments in liposomes, microparticles and nanoparticles for protein and peptide drug delivery. Peptides 31, 184–193.

Tang, C.-H., Li, L., Yang, X.-Q., 2006. Influence of transglutaminase-induced cross-linking on in vitro digestibility of soy protein isolate. Journal of Food Biochemistry 30, 718–731.

Tang, C.-H., Jiang, Y., Wen, Q.-B., Yang, X.-Q., 2005. Effect of transglutaminase treatment on the properties of cast films of soy protein isolates. Journal of Biotechnology 120, 296–307.

Taylor, J., 2008. Preparation, characterisation and functionality of kafirin microparticles. PhD Thesis, University of Pretoria, Pretoria, South Africa.

Taylor, J., Taylor, J.R.N., 2002. Alleviation of the adverse effects of cooking on sorghum protein digestibility through fermentation in traditional African porridges. International Journal of Food Science and Technology 37, 129–137.

Taylor, J., Taylor, J.R.N., Belton, P.S., Minnaar, A., 2009a. Formation of kafirin microparticles by phase separation from an organic acid and their characterisation. Journal of Cereal Science 50, 99–105.

Taylor, J., Taylor, J.R.N., Belton, P.S., Minnaar, A., 2009b. Kafirin microparticle encapsulation of catechin and sorghum condensed tannins. Journal of Agricultural and Food chemistry 57, 7523–7528.

Taylor, J., Taylor, J.R.N., Belton, P.S., Minnaar, A., 2009c. Preparation of free-standing films from kafirin protein microparticles: mechanism of formation and functional properties. Journal of Agricultural and Food Chemistry 57, 6729–6735.

Taylor, J., Taylor, J.R.N., Dutton, M.F., De Kock, S., 2005a. Glacial acetic acid-a novel food-compatible solvent for kafirins extraction. Cereal Chemistry 82, 485–487.

Taylor, J., Taylor, J.R.N., Dutton, M.F., De Kock, S., 2005b. Identification of kafirin film casting solvents. Food Chemistry 32, 149−154.

Taylor, J.R.N., Novellie, L., Liebenberg, Nv.d.W., 1985. Protein body degradation in the starchy endosperm of germinating sorghum. Journal of Experimental Botany 36, 1287–1295.

Tice, T. R., Gilley, R.M., 1985. Preparation of injectable controlled-release microcapsules by a solvent evaporation process. Journal of Controlled Release 2, 343–352.

Tran, V.-T., Benoît, J.-P., Venier-Julienne, M.-C., 2011. Why and how to prepare biodegradable, monodispersed, polymeric microparticles in the field of pharmacy? International Journal of Pharmaceutics 407, 1–11.

Tsugita, A., Scheffler, J.-J., 1982. A Rapid method for acid hydrolysis of protein with a mixture of trifluoroacetic acid and hydrochloric acid. European Journal of Biochemistry 124, 585–588.

Tu, J., Wang, H., Li, H., Dai, K., Wang, J., Zhang, X., 2009. The in vivo bone formation by mesenchymal stem cells in zein scaffolds. Biomaterials 30, 4369–4376.

Utesch, T., Daminelli, G., Mroginski, M.A., 2011. Molecular dynamics simulations of the adsorption of bone morphogenetic protein-2 on surfaces with medical relevance. Langmuir 27, 13144–13153.

Van der Linden, E., Venema, P., 2007. Self-assembly and aggregation of proteins. Current Opinion in Colloid and Interface Science 12, 158–165.

Van Straalen, J.P., Sanders, E., Prummel, M.F., Sanders, G.T.B., 1991. Bone-alkaline phosphatase as indicator of bone formation. Clinica Chimica Acta 201, 27–34.

Vandelli, M.A., Rivasi, F., Guerra, P., Forni, F., Arletti, R., 2001. Gelatin microspheres crosslinked with D,L-glyceraldehyde as a potential drug delivery system: preparation, characterisation, in vitro and in vivo studies. International Journal of Pharmaceutics 215, 175–184.

Vandelli, M.A., Romagnoli, M., Monti, A., Gozzi, M., Guerra, P., Rivasi, F., Forni, F., 2004. Microwave-treated gelatin microspheres as drug delivery system. Journal of Controlled Release 96, 67–84.

Vinson, P.K., Talmon, Y., Walters, A., 1989. Vesicle-micelle transition of phosphatidylcholine and octyl glucoside elucidated by cryo-transmission electron microscopy. Biophysics Journal 56, 669–681.

Visser, R., Arrabal, P.M., Becerra, J., Rinas, U., Cifuentes, M., 2009. The effect of an rhBMP-2 absorbable collagen sponge-targeted system on bone formation in vivo. Biomaterials 30, 2032–2037.

Volodkin , D.V., Schmidt, S., Fernandes, P., Larionova, N.I., Sukhorukov, G.B., Duschl, C., Möhwald, H., Von Klitzing, R., 2012. One-step formulation of protein microparticles with tailored properties: hard templating at soft conditions. Advanced Functional Materials 22, 1914–1922.

Wagner, J.R., Gueguen, J., 1995. Effects of dissociation, deamidation, and reducing treatment on structural and surface active properties of soy glycinin. Journal of Food Biochemistry 43, 1993−2000.

Wang, E.A., Rosen, V., D'Alessandro, J.S., Bauduy, M., Cordes, P., Harada, T., Israel, D.I., Hewick, R.M., Kerns, K.M., Lapan, P., Luxenberg, D.P., McQuaid, D., Moutsatsos, I.K., Nove, J., Wozney, J.M., 1990. Recombinant human bone morphogenetic protein induces bone formation. Proceedings of the National Academy of Sciences of the United States of America 87, 2220–2224.

Wang, H.-J., Lin, Z.-X., Liu, X.-M., Sheng, S.-Y., Wang, J.-Y., 2005. Heparin-loaded zein microsphere film and hemocompatibility. Journal of Controlled Release 105, 120–131.

Wang, H.-J., Gong, S.-J., Lin, Z.-X., Fu, J.-X., Xue, S.-T., Huang, J.-C., Wang, J.-Y., 2007. In vivo biocompatibility and mechanical properties of porous zein scaffolds. Biomaterials 28, 3952–3964.

Wang, Q., Yin, L., Padua, G.W., 2008. Effect of hydrophilic and lipophilic compounds on zein microstructures. Food Biophysics 3, 174–181.

Wang, Q., Crofts, A.R., Padua, G.W., 2003. Protein-lipid interactions in zein films investigated by surface plasmon resonance. Journal of Agricultural and Food Chemistry 51, 7439–7444.

Wang, X., Wenk, E., Matsumoto, A., Meinel, L., Li, C., Kaplan, D.L., 2007. Silk microspheres for encapsulation and controlled release. Journal of Controlled Release 117, 360–370.

Wang, X., Wenk, E., Hu, X., Castro, G.R., Meinel, L., Wang, X., Li, C., Merkle, H., Kaplan, D., 2007. Silk coatings on PLGA and alginate microspheres for protein delivery. Biomaterials 28, 4161–4169.

Wang, Y., Padua, G.W., 2010. Formation of zein microphases in ethanol-water. Langmuir 26, 12897–12901.

Wang, Y., Padua, G.W., 2012. Nanoscale characterization of zein self-assembly. Langmuir 28, 2429−2435.

Wang, Y., Tilley, M., Bean, S., Sun, X.S., Wang, D., 2009. Comparison of methods for extracting kafirin proteins from sorghum distillers dried grains with solubles. Journal of Agricultural and Food Chemistry 57, 8366–8372.

Weihs, T.P., Nawaz, Z., Jarvis, S.P., Pethica, J.B., 1991. Limits of imaging resolution for atomic force microscopy of molecules. Applied Physics Letters 59, 3536–3538.

Weiler, A., Helling, H.-J., Kirch, U., Zirbes, T.K., Rehn, K.E., 1996. Foreign-body reaction and the course of osteolysis after polyglycolide implants for fracture fixation. Journal of Bone and Joint Surgery [Br] 78-B, 369–376.

Weiss, J., Takhistov, P., McClements, D.J., 2006. Functional materials in food nanotechnology. Journal of Food Science 71, 107–116.

Weiss, P., Layrolle, P., Clergeau, L.P., Enckel, B., Pilet, P., Amouriq, Y., Daculsi, G., Giumelli, B., 2007. The safety and efficacy of an injectable bone substitute in dental sockets demonstrated in a human clinical trial. Biomaterials 28, 3295–3305.

Whitesides, G.M., Mathias, J.P., Seto, C., 1991. Molecular, self-assembly and nanotechnology: a chemical strategy for synthesis of nanostructures. Science 254, 1312–1319.

Whittlesey, K.J., Shea, L.D., 2004. Delivery systems for small molecule drugs, proteins, and DNA: the neuroscience/biomedical interface. Experimental Neurology 190, 1–16.

Wieser, H., Koehler, P., 2008. The biochemical basis of celiac disease. Cereal Chemistry 85, 1–13.

Wine, Y., Cohen-Hadar, N., Freeman, A., Frolow, F., 2007. Elucidation of the mechanism and end products of glutaraldehyde crosslinking reaction by x-ray structure analysis. Biotechnology and Bioengineering 98, 711–718.

Withhold, W., Schulte, U., Reinauer, H., 1996. Method for determination of bone alkaline phosphatase activity: analytical performance and clinical usefulness in patients with metabolic and malignant bone diseases. Clinical Chemistry 42, 210–217.

Xiao, D., Davidson, P.M., Zhong, Q., 2011. Spray-dried zein capsules with coencapsulated nisin and thymol as antimicrobial delivery system for enhanced antilisterial properties. Journal of Agricultural and Food Chemistry 59, 7393–7404.

Xing, F., Cheng, G., Yang, B., Ma, L., 2004. Microencapsulation of capsaicin by the complex coacervation of gelatin, acacia and tannins. Journal of Applied Polymer Science, 91, 2669–2675.

Xu, H., Jiang, Q., Reddy, N., Yang, Y., 2011. Hollow nanoparticles from zein for potential medical applications. Journal of Materials Chemistry 21, 18227–18235.

Xu, W., Reddy, N., Yang, Y., 2007. An acidic method of zein extraction from DDGS. Journal of Agricultural and Food Chemistry 55, 6279–6284.

Yada, R.Y., Jackman, R.L., Smith, J.L., Marangoni, A.G., 1996. Analysis: quantification and physical characterization. In: Nakai, S. and Modler, H.W. (Eds.). Food Proteins: Properties and Characterization. Willey-VCH; New York, pp. 333–403.

Yang, H., Wang, Y., Lai, S., An, H., Li, Y., and Chen, F., 2007. Application of atomic force microscopy as a nanotechnology tool in food science. Journal of Food Science 72, 65–75.

Yasko, A.W., Lane, J.M., Fellinger, E.J., Rosen, V., Wozney, J.M., Wang, E.A., 1992. The healing of segmental bone defects, induced by recombinant human bone morphogenetic protein (rhBMP-2). A radiographic, histological, and biomechanical study in rats. Journal of Bone and Joint Surgery 74-A, 659–670.

Yeates, T.O., Padilla, J.E., 2002 Designing supramolecular protein assemblies. Current Opinion in Structural Biology 12, 464–470.

Yeo, J.-H., Lee, K.-G., Lee, Y.-W., Kim, S.Y., 2003. Simple preparation and characteristics of silk fibroin microsphere. European Polymer Journal 39, 1195–1199.

Yokoyama, K., Nio, N., Kikuchi, Y., 2004. Properties and applications of microbial transglutaminase. Applied Microbiology and Biotechnology 64, 447–454.

Young, S. L., Sarda, X., Rosenberg, M., 1993. Microencapsulating properties of whey proteins. 1. Microencapsulation of anhydrous milk fat. Journal of Dairy Science 76, 2868–2877.

Yu, Z., Rogers, T.L., Hu, J., Johnston, K.P., Williams III, R.O., 2002. Preparation and characterization of microparticles containing peptide produced by a novel process: spray freezing into liquid. European Journal of Pharmaceutics and Biopharmaceutics 54, 221–228.

Zara, J.N., Siu, R.K., Zhang, X., Shen, J., Ngo, R., Lee, M., Li, W., Chiang, M., Chung, J., Kwak, J., Wu, B.M., Ting, K., Soo, C., 2011. High doses of bone morphogenetic protein 2 induce structurally abnormal bone and inflammation in vivo. Tissue Engineering: Part A 17, 1389–1399.

Zhang, B., Luo, Y., Wang, Q., 2011. Effect of acid and base treatments on structural, rheological, and antioxidant properties of α-zein. Food Chemistry 124, 210–220.

Zhang, H., Mittal, G., 2010. Biodegradable protein-based films from plant resources: a review. Environmental Progress and Sustainable Energy 29, 203–220.

Zhang, S., 2002. Emerging biological materials through molecular self-assembly. Biotechnology Advances 20, 321–339.

Zhang, W., Zhong, Q., 2009. Microemulsions as nanoreactors to produce whey protein nanoparticles with enhanced heat stability by sequential enzymic cross-linking and thermal pretreatments. Journal of Agricultural and Food Chemistry 57, 9181–9189.

Zhang, W., Zhong, Q., 2010. Microemulsions as nanoreactors to produce whey protein nanoparticles with enhanced heat stability by thermal pretreatment. Food Chemistry 119, 1318–1325.

Zhong, Q., Jin, M., Davidson, P.M., Zivanovic, S., 2009. Sustained release of lysozyme from zein microcapsules produced by a supercritical anti-solvent process. Food Chemistry 115, 697–700.

Zimet, P., Livney, Y.D., 2009. Beta-lactoglobulin and its nanocomplexes with pectin as vehicles for omega-3 polyunsaturated fatty acids. Food Hydrocolloids 23, 1120–1126.

8 PUBLICATIONS MADE BASED ON THIS RESEARCH

Anyango, J.O., Taylor, J., Taylor, J.R.N., 2011. Improvement in water stability and other related functional properties of thin cast kafirin protein films. Journal of Agricultural and Food Chemistry 59, 12674–12682.

Anyango, J.O., Duneas, N., Taylor, J.R.N., Taylor, J., 2012. Physico-chemical modification of kafirin microparticles and their ability to bind bone morphogenetic protein-2 (BMP-2), for application as a biomaterial. Journal of Agricultural and Food Chemistry 60, 8419–8426.

9 ANNEX

Annex 1: Approval document

Annex 2: Idexx Laboratories Report

ANNEX 1: APPROVAL DOCUMENTS

UNIVERSITEIT VAN PRETORIA
UNIVERSITY OF PRETORIA
YUNIBESITHI YA PRETORIA

ANIMAL USE AND CARE COMMITTEE
Private Bag X04
0110 Onderstepoort

Tel +27 12 529 8434 / Fax +27 12 529 8300
e-mail: aucc@up.ac.za

Ref: H016-11

19 April 2011

Prof JRN Taylor
Department of Food Science
University of Pretoria
(john.taylor@up.ac.za)

Dear Prof Taylor

H016-11 : Subcutaneous bioassay of novel osteoconductive protein microstructure for alternative autograft bone transplant scaffold *(J Anyango)*

The application for ethical approval, dated on 31 March 2011 was approved, by the Animal Use and Care Committee at its meeting held on 18 April 2011.

Kind regards

E Mostert

Elmarie Mostert

AUCC Coordinator

Copy Prof V Naidoo

J Anyango

UNIVERSITEIT VAN PRETORIA
UNIVERSITY OF PRETORIA
YUNIBESITHI YA PRETORIA

ANIMAL USE AND CARE COMMITTEE
Private Bag X04
0110 Onderstepoort

Tel +27 12 529 8434 / Fax +27 12 529 8300
e-mail: aucc@up.ac.za

Ref: H016-11 (Amendment 1)

1 February 2012

Prof JRN Taylor
Department of Food Science
University of Pretoria
(john.taylor@up.ac.za)

Dear Prof Taylor

H016-11 (Amendment 1) : Subcutaneous bioassay of novel osteoconductive protein microstructure for alternative autograft bone transplant scaffold *(J Anyango)*

The amendment to the application for ethical approval, dated 19 December 2011 was approved by the Animal Use and Committee at its meeting held on 30 January 2012.

Kind regards

E Mostert

Elmarie Mostert

AUCC Coordinator

Copy Prof V Naidoo

J Anyango

ANNEX 2: IDEXX LABORATORIES REPORT

UNIVERSITY OF PRETORIA
BIOMEDICAL RESEARCH CENTRE
PRIVATE BAG X04
ONDERSTEPOORT
0110

2012/04/04

For attention: Prof Vinny Naidoo and Ilse Janse van Rensburg

STUDY H16/11: SUBCUTANEOUS BIOASSAY OF NOVAL OSTEOCONDUCTIVE PROTEIN MICROSTRUCTURE FOR ALTERNATIVE AUTOGRAFT BONE TRANSPLANT SCAFFOLD: IDEXX REF 2000/12 AND 2892/12

INTRODUCTION:

We have received two groups of Sprague-Dawley rats, namely group 1 with our reference 2000/12 on the 21st of February 2012, and a second group with our reference 2892/12 on the 13th of March 2012. All of these rats had four implantation sites on the dorsal body wall, which we allocated the numbering system A1 and A2 on the left hand side anterior and posterior respectively, and on the right hand side B1 and B2 anterior and posterior respectively. The implantation sites were evaluated and measured and the findings are recorded in Table 1A and 1B of both these groups.

We were requested to evaluate the implant sites as well as the standard histology on organs with a special request to look at the bone morphogenesis of the implant sites and to record the findings as well as the digital photos of specific morphological findings. In the second group 2892/12 two of the implantation sites were collected by the researcher for additional testing and were not available for histopathology. Histopathology results of the implantation sites were tabulated and the findings recorded (Tables 2A and 2B for 21/2/12 and 13/3/12 respectively).

METHODOLOGY:

Necropsies were performed and the implantation sites were all collected separately in 10% buffered formalin as indicated above, while organs were collected for the standard histopathology profile in a separate formalin container.

After sufficient fixation (2 days) selected blocks of tissue as well as a cross section of the implantation site were cut and processed in an automated histological tissue processor according to our standard operating procedure for our Idexx laboratory (PTA-his-SOP-27). After overnight tissue processing, wax blocks were produced and histological sections of 6µm were cut on a microtome (PTA-his-SOP-30). The slides were then stained with Haematoxylin and Eosin staining in an automated histological stainer (PTA-his-SOP-25).

The macroscopical findings of the implantation sites for these two groups of rats are recorded in Table 1A and 1B.

Histological observations of the implantation sites for these two groups of rats are given in Table 2A and 2B.

MACROSCOPICAL FINDINGS OF IMPLANTATION SITES

***UPBRC Ref*: H16/11 *Our Ref*: 2000/12**

***Date received*: 21/02/2012**

Macroscopical evaluation of implantation sites				
Rat no	***UPBRC ref***	***Histo ref***	***Morphological Appearance***	***Size (mm)***
14	14/1	2000-14 A1/12	Cystic granuloma	20
	14/3	2000-14 A2/12	Small cystic lesion	15
	14/2	2000-14 B1/12	Cystic granuloma	20
	14/4	2000-14 B2/12	Round nodule	10
15	15/1	2000-15 A1/12	Hard flat implant	10
	15/3	2000-15 A2/12	Hard flat implant	10
	15/2	2000-15 B1/12	Hard flat implant	15
	15/4	2000-15 B2/12	Hard flat implant	20
16 F	16/1	2000-16F A1/12	Round flat nodule	18
	16/3	2000-16F A2/12	Cystic granuloma	22
	16/2	2000-16F B1/12	Cystic granuloma implant	10
	16/4	2000-16F B2/12	Cystic granuloma	25
16 M	16/1	2000-16M A1/12	Granulomatous nodule	15
	16/3	2000-16M A2/12	Flat hard implant	18
	16/2	2000-16M B1/12	Flat nodule	12
	16/4	2000-16M B2/12	Round granulomatous nodule	15
17	17/1	2000-17 A1/12	Cystic granuloma	20
	17/3	2000-17 A2/12	Flat hard implant	15
	17/2	2000-17 B1/12	Cystic nodule	15
	17/4	2000-17 B2/12	Hard flat implant	15
18	18/1	2000-18 A1/12	Hard flat implant	10
	18/3	2000-18 A2/12	Hard flat implant	15
	18/2	2000-18 B1/12	Hard flat implant	10
	18/4	2000-18 B2/12	Hard flat implant	10
19	19/1	2000-19 A1/12	Hard flat implant	10
	19/3	2000-19 A2/12	Hard flat implant	15
	19/2	2000-19 B1/12	Hard flat implant	10
	19/4	2000-19 B2/12	Minimal lesion	5
20	20/1	2000-20 A1/12	Granulomatous cystic implant	10
	20/3	2000-20 A2/12	Flat lesion	10
	20/2	2000-20 B1/12	Cystic pyogranuloma	20
	20/4	2000-20 B2/12	Pyogranuloma	20

Table 1B

MACROSCOPICAL FINDINGS OF IMPLANTATION SITES

***UPBRC Ref*: H16/11 *Our Ref*: 2892/12**

***Date received*: 19/03/2012**

Macroscopical evaluation of implantation sites				
Rat no	***UPBRC ref***	***Histo ref***	***Morphological Appearance***	***Size (mm)***
1	1/1	2892-1 A1/12	Granuloma cystic	20
	1/3	2892-1 A2/12	Cystic	15
	1/2	2892-1 B1/12	Flat implant	20
	1/4	2892-1 B2/12	Granulomatous lesion	15
3	3/1	2892-3 A1/12	Flat implant	20
	3/3	2892-3 A2/12	Flat implant	20
	3/2	2892-3 B1/12	Minimal visible	10
	3/4	2892-3 B2/12	Minimal visible	10
4	4/1	2892-4 A1/12	Flat implant	15
	4/3	2892-4 A2/12	Flat implant	15
	4/2	2892-4 B1/12	Minimal visible	10
	4/4	2892-4 B2/12	Minimal visible	7
5	5/1	2892-5 A1/12	Flat implant	20
	5/3	2892-5 A2/12	Minimal lesion	5
	5/2	2892-5 B1/12	Minimal visible	3
	5/4	2892-5 B2/12	Minimal visible	10
6	6/1	2892-6 A1/12	Flat implant	15
	6/3	2892-6 A2/12	Flat implant	15
	6/2	2892-6 B1/12	Minimal visible	3
	6/4	2892-6 B2/12	Focal granuloma	10
7	7/1	2892-7 A1/12	No lesion	-
	7/3	2892-7 A2/12	No lesion	-
	7/2	2892-7 B1/12	No lesion	-
	7/4	2892-7 B2/12	Granuloma	20
8	8/1	2892-8 A1/12	Minimal visible	2
	8/3	2892-8 A2/12	Minimal visible	3
	8/2	2892-8 B1/12	Minimal visible	2
	8/4	2892-8 B2/12	Minimal visible	2
9	9/1	2892-9 A1/12	Minimal visible	2
	9/3	2892-9 A2/12	No lesion	-
	9/2	2892-9 B1/12	Flat implant	15
	9/4	2892-9 B2/12	No lesion	-

Rat no	*UPBRC ref*	*H*	*ical Appearance*	*Size (mm)*
10	10/1	2892-10 A1/12	Flat implant	12
	10/3	2892-10 A2/12	Flat implant	10
	10/2	2892-10 B1/12	Minimal lesion	5
	10/4	2892-10 B2/12	Flat implant	15
11	11/1	2892-11 A1/12	No lesion	-
	11/3	2892-11 A2/12	Minimal lesion	3
	11/2	2892-11 B1/12	No lesion	-
	11/4	2892-11 B2/12	Cystic lesion	15
12	12/1	2892-12 A1/12	No lesion	-
	12/3	2892-12 A2/12	Focal pyogranuloma	15
	12/2	2892-12 B1/12	No lesion	-
	12/4	2892-12 B2/12	Flat and 2nd pyogranuloma	10 - 15
13	13/1	2892-13 A1/12	Minimal lesion	2
	13/3	2892-13 A2/12	No lesion	-
	13/2	2892-13 B1/12	Flat implant	2
	13/4	2892-13 B2/12	Flat implant	5

RESULTS:

A. MORPHOLOGICAL FINDINGS OF THE STANDARD ORGANS SELECTED FOR HISTOLOGICAL EVALUATION

GROUP RECEIVED 21 FEBRUARY 2012: OUR REF 2000/12

RAT 14: OUR REFERENCE 2000-14/12

MACROSCOPICAL ANATOMICAL PATHOLOGY FINDINGS

1. No lesions are observed during macroscopical evaluation.
2. The animal is in good condition with normal body fat depots present.

HISTOPATHOLOGY

Adrenal:	Normal
Brain:	Sections from the brain which include both the cerebellum and the cerebrum do not show any neuropathology.
Gonad:	The ovary and female internal genitalia are normal.
Heart:	No lesions are observed in the myocardium.
Intestine, large:	No pathology is present.
Intestine, small:	Normal morphological features
Kidney:	No lesions are recorded.
Liver:	Normal morphological features. Mild congestion is visible.
Lung:	Mild congestion is observed. The peribronchial lymphoid tissue appears normal.
Pancreas:	No pathology is present.
Spleen:	The lymphoid tissue in the splenic white pulp appears normal while mild extramedullary haemopoiesis is observed in the red pulp. The red pulp is moderately congested.
Stomach:	No specific morphological changes are detected.
Thymus:	The thymic lymphoid tissue appears morphologically normal.
Urinary bladder:	Normal

COMMENT:

The examination is negative for specific pathology in the organs of this rat.

RATC 15: OUR REFERENCE 2000/15-12

MACROSCOPICAL ANATOMICAL PATHOLOGY FINDINGS

1. No lesions are observed in this animal.
2. The animal is in good condition with normal fat reserves visible.

HISTOPATHOLOGY

Adrenal:	No lesions are present in the adrenal sections.
Brain:	The histological evaluation does not show any lesions in the brain section. Mild leptomeningeal congestion is visible.
Heart:	No pathology is observed in the section from the heart muscle.

Gonad:	The ovary
Intestine, large:	No pathology is observed in the section from the large intestine. The gut-associated lymphoid tissue appears active.
Intestine, small:	No specific lesions are found in the small intestine.
Kidney:	No specific pathological changes are observed in the kidney section.
Liver:	No morphological pathology is visible.
Lung:	No abnormalities are present.
Pancreas:	Sections of the pancreas are morphologically normal.
Spleen:	Moderate haemosiderosis and extramedullary haemopoiesis are found. .
Stomach:	Normal morphological features are present in the stomach section.
Thymus:	The thymic lymphoid tissue appears normal while no lesions could be confirmed in the interstitial stroma.
Urinary bladder:	No lesions are found.

COMMENT:

No specific morphological pathology is observed in the organs examined from this rat.

RAT 16 FEMALE: OUR REFERENCE 2000-16F/12

MACROSCOPICAL ANATOMICAL PATHOLOGY FINDINGS

1. No macroscopical lesions are found.
2. The stomach contains normal food contents.
3. Good body condition and normal fat depots are found.

HISTOPATHOLOGY

Adrenal:	The medulla is mildly congested.
Brain:	Normal
Gonad:	No pathology is observed in the section from the female internal genitalia.
Heart:	Normal morphology. No lesions are recorded.
Intestine, large:	No abnormalities are observed. Active gut-associated lymphoid tissue is normal.
Intestine, small:	No pathology is visible.
Kidney:	Mild medullary congestion could be demonstrated in the kidney section.
Liver:	No anatomical pathological changes present
Lung:	The section from the lung could not demonstrate any pathological changes in the pulmonary tissues.
Pancreas:	Normal architecture of the exocrine pancreas is present.
Spleen:	Normal splenic red pulp and white pulp are visible. Mild haemosiderosis is found.
Stomach:	No pathology is observed.
Thymus:	Mild congestion of the thymic medulla is present.
Urinary bladder:	Normal

COMMENT:

No specific lesions are detected in the organs examined from this rat.

MACROSCOPICAL ANATOMICAL PATHOLOGY FINDINGS

1. No specific pathology is observed in the organs examined.
2. The rat is in good body condition with normal fat depots visible.
3. Normal male genitalia observed.

HISTOPATHOLOGY

Adrenal:	Normal cortex and medulla are present.
Brain:	No lesions could be recorded in the several sections from the brain.
Gonad:	The testis sections appear normal and no lesions are observed in these sections. Normal spermatogenesis is confirmed.
Heart:	The myocardium appears morphologically normal and no lesions are present in the section from the heart.
Intestine, large:	The large intestine is normal without lesions visible in the mucosa and wall of the intestinal tract.
Intestine, small:	No pathology is observed.
Kidney:	The kidney shows only mild congestion.
Liver:	No lesions are observed.
Lung:	Mild focal atelectasis
Pancreas:	Normal
Spleen:	Active lymphoid tissue is present in the splenic white pulp while mild extramedullary haemopoiesis and haemosiderosis of the red pulp are found.
Stomach:	No lesions are recorded.
Thymus:	The thymic lymphoid tissue appears normal.
Urinary bladder:	No pathology is found in the urinary bladder.

COMMENT:

No specific lesions are observed. No lesions suggestive of intoxication are found.

RAT 17: OUR REFERENCE 2000-17/12

MACROSCOPICAL ANATOMICAL PATHOLOGY FINDINGS

1. Mild congestion of the intestinal tract
2. The rat is in good body condition.

HISTOPATHOLOGY

Adrenal:	Normal cortex and medulla.
Brain:	Normal
Gonad:	Normal functional ovary and uterine horns
Heart:	No pathology is visible.
Intestine, large:	No lesions are observed.
Intestine, small:	Normal morphological features are found with mild congestion of the mucosa is present.
Kidney:	No pathological changes are detected.
Liver:	Normal histology
Lung:	No lesions are observed in the lung sections. The peribronchial lymphoid tissue appears active and normal.
Pancreas:	Normal pancreatic acini and ductal system are visible.
Spleen:	Normal splenic white pulp and red pulp with mild extramedullary haemopoiesis are detected.
Stomach:	No lesions are observed in the gastric mucosa and stomach wall.

Thymus:	The lympl nd medulla appears morphologically normal.
Urinary bladder:	No specimen

COMMENT:

No specific morphological anatomical pathology is present. Negative for any pathology in the organs examined.

RAT 18: OUR REFERENCE 2000-18/12

MACROSCOPICAL ANATOMICAL PATHOLOGY FINDINGS

1. No macroscopical pathological lesions are observed in the organs of this rat.
2. The female rat is in good body condition with fat reserves visible.

HISTOPATHOLOGY

Adrenal:	Normal morphological features are found.
Brain:	Normal
Gonad:	Normal inactive female genital organs.
Heart:	Negative for pathological lesions
Intestine, large:	No pathology is present.
Intestine, small:	Normal morphological features are visible.
Kidney:	No pathology is detected. Moderate congestion of the renal cortex is present.
Liver:	No lesions are found in the liver sections.
Lung:	Focal atelectasis is present.
Pancreas:	No lesions are observed.
Spleen:	Normal active splenic white pulp and normal red pulp are found.
Stomach:	No pathological changes are detected in the stomach wall including the mucosa
Thymus:	Mild congestion is detected.
Urinary bladder:	Normal morphology

COMMENT:

Specific pathological lesions are not observed in the organs examined from this rat

RAT 19: OUR REFERENCE 2000-19/12

MACROSCOPICAL ANATOMICAL PATHOLOGY FINDINGS:

1. The rat is in good body condition.

HISTOPATHOLOGY

Adrenal:	Normal
Brain:	Several sections were produced from the brain and show no morphological pathology.
Gonad:	Active productive ovary and normal internal tubular genitalia.
Heart:	No lesions are observed in the myocardium
Intestine, large:	Normal morphological features are present in the large intestine.
Intestine, small:	No morphological pathology is found.
Kidney:	Normal morphology
Liver:	No lesions are observed.
Lung:	No specific pathology is detected. Mild atelectasis is found.

Pancreas: No lesions
Spleen: Active white pulp is visible in the splenic section.
Stomach: The stomach appears morphologically normal
Thymus: The thymic lymphoid tissue is normal and no lesions could be observed in the interstitial stroma.
Urinary bladder: No lesions are recorded.

COMMENT:

The organs examined appeared normal.

RAT 20: OUR REFERENCE 2000-20/12

MACROSCOPICAL ANATOMICAL PATHOLOGY FINDINGS

1. The rat is in good body condition with fat depots visible.

HISTOPATHOLOGY

Adrenal: Congested
Brain: Normal
Gonad: The section from the ovary and uterus reveals no lesions.
Heart: No morphological pathological lesions are present.
Intestine, large: Normal morphology
Intestine, small: No lesions are observed.
Kidney: No pathology is visible.
Liver: The hepatic parenchyma appears morphologically normal.
Lung: Normal morphology is found.
Pancreas: Normal pancreas
Spleen: Moderate extramedullary haemopoiesis is observed in the splenic red pulp. The splenic white pulp appears active and normal.
Stomach: No lesions are detected.
Thymus: The thymic lymphoid tissue and interstitial stroma are normal.
Urinary bladder No pathology is observed in the urinary bladder.

COMMENT:

Histological evaluation could not demonstrate any specific morphological pathology.

GROUP RECEIVED 13 MARCH 2012 FOR STANDARD HISTOPATHOLOGY OF ORGANS: OUR REF 2892-12

RAT 1: OUR REF 2892-1/12

HISTOPATHOLOGY

Adrenal gland:	Normal
Brain:	No lesions could be recorded in the neuroparenchyma and leptomeninges of the cerebral and cerebellar sections.
Gonad:	Numerous follicles and corpora lutea are present in the functional ovary. The uterus is normal.
Heart:	No lesions are observed in the myocardium.
Intestine, large:	Normal large intestinal morphology is visible in the different sections.
Intestine, small:	Normal morphological features
Kidney:	No lesions are found in the kidney section.
Liver:	No morphological microscopical pathology could be confirmed in the liver section.
Lung:	Mild atelectasis and emphysema are visible. Mild congestion is observed.
Pancreas:	Normal
Spleen:	The lymphoid tissue in the splenic white pulp appears normal while mild extramedullary haemopoiesis is observed in the red pulp. The red pulp is congested.
Stomach:	No specific morphological changes are detected.
Thymus:	Normal lymphoid tissue is present in the section.
Urinary bladder:	Normal mucosa and bladder wall

COMMENT

No specific anatomical pathological lesions are observed in the sections examined of this rat.

RAT 3: OUR REF 2892-3/12

HISTOPATHOLOGY

Adrenal gland:	Normal adrenal cortex and medulla
Brain:	No pathology could be confirmed in the sections from the cerebrum and cerebellum.
Gonad:	Normal functional ovary and uterus
Heart:	No pathology is observed in the section from the heart muscle.
Intestine, large:	Normal large intestinal mucosa is observed.
Intestine, small:	No specific lesions are observed in the small intestine.
Kidney:	Sections from both kidneys were evaluated without any tubular, interstitial and glomerular pathology present.
Liver:	No pathological changes could be observed in the hepatic parenchyma as well as the stromal tissue, portal tracts and biliary system of the liver.
Lung:	No abnormalities are observed. Mild atelectasis and active peribronchial lymphoid tissue are visible.
Pancreas:	The pancreatic acini, interstitial stromal tissue and islands of Langerhans appear morphologically normal.
Spleen:	Moderate congestion of the red pulp is found.
Stomach:	Normal morphological features are present in the stomach section.
Thymus:	Normal
Urinary bladder:	Normal

COMMENT

No specific morphological pathology could be demonstrated in this female rat.

RAT 4: OUR REF 2892-4/12

HISTOPATHOLOGY

Adrenal gland:	Normal
Brain:	Normal
Gonad:	The ovary and uterus of this female rat appears functional and normal.
Heart:	Normal morphology. No lesions are recorded.
Intestine, large:	No lesions could be confirmed in the large intestinal tract.
Intestine, small:	No pathology is visible.
Kidney:	Mild renal cortico-medullary congestion.
Liver:	No lesions are recorded in the sections from the liver.
Lung:	Focal mild atelectasis is found.
Pancreas:	Normal
Spleen:	Moderate congestion. Normal splenic red pulp and white pulp are visible
Stomach:	No pathology is observed.
Thymus:	No lesions are observed in the thymic lymphoid tissue and stroma.
Urinary bladder:	Normal

COMMENT

No diagnostic specific morphological pathology is observed during histopathology of the organs mentioned.

RAT 5: OUR REF 2892-5/12

HISTOPATHOLOGY

Adrenal gland:	Normal adrenal gland
Brain:	No neuropathology is observed in the neuroparenchyma with leptomeninges present.
Gonad:	Normal functional female internal genitalia
Heart:	No lesions are observed in the myocardium.
Intestine, large:	No pathology is observed in the large intestinal mucosa, gut-associated lymphoid tissue and intestinal wall
Intestine, small:	No pathology is present.
Kidney:	Sections were produced from the kidney and show only mild congestion.
Liver:	There is mild congestion and focal sinusoidal dilatation observed, but no lesions could be recorded in the hepatic parenchyma.
Lung:	Normal morphology of the lung.
Pancreas:	No pathology could be observed in the pancreatic sections.
Spleen:	Normal lymphoid tissue of the splenic white pulp is found with moderate congestion of the red pulp.
Stomach:	No lesions are recorded.
Thymus:	The thymic lymphoid tissue is morphologically normal.
Urinary bladder:	Normal morphology

COMMENT

No specific morphological pathology could be confirmed in this rat.

RAT 6: OUR REF 2892-6/12

HISTOPATHOLOGY

Adrenal gland:	Normal adrenal glands are observed.
Brain:	Pathology could not be confirmed in several sections of the brain of this rat.
Gonad:	The ovary, Fallopian ducts and uterus are all normal.
Heart:	No lesions could be confirmed, but there is mild congestion visible in the myocardium.
Intestine, large:	No lesions are observed.
Intestine, small:	Normal morphological features are present.
Kidney:	No pathological changes are detected.
Liver:	No microscopical pathological lesions could be recorded in the liver.
Lung:	No lesions are observed in the lung sections.
Pancreas:	Normal morphology, mild autolytic changes are found.
Spleen:	Normal splenic white pulp, red pulp and severe congestion are detected.
Stomach:	No lesions are observed in the gastric mucosa and stomach wall.
Thymus:	The thymic section reveals normal lymphoid tissue and stroma.
Urinary bladder:	Normal histology of the urinary bladder.

COMMENT

The macroscopical pathology and histopathology could not confirm any specific anatomical pathological changes.

RAT 7: OUR REF 2892-7/12

HISTOPATHOLOGY

Adrenal gland:	The adrenal glands appear morphologically normal.
Brain:	Several sections were produced from different areas in the brain and could not demonstrate any anatomical pathological lesions.
Gonad:	Normal and active functional ovary and tubular genitalia are present.
Heart:	Negative for pathological lesions
Intestine, large:	Normal gut associated lymphoid tissue is detected in the intestinal mucosa. No pathology is present.
Intestine, small:	Normal morphological features are visible.
Kidney:	No pathology is detected.
Liver:	No lesions are observed in the liver parenchyma as well as in the portal tracts.
Lung:	No lesions are found in the sections from the lungs. The peribronchial lymphoid tissue appears morphologically normal.
Pancreas:	Normal anatomical features are observed in the pancreatic section. No lesions are found.
Spleen:	Normal splenic white pulp and red pulp are present.
Stomach:	No pathological changes are detected in the stomach.
Thymus:	Normal
Urinary bladder:	Normal

COMMENT

The microscopical evaluation as well as the macroscopical necropsy did not show any specific pathological changes.

RAT 8: OUR REF 2892-8/12

HISTOPATHOLOGY

Adrenal gland:	Normal
Brain:	The microscopical evaluation could not detect any pathological changes in the neuroparenchyma and leptomeninges.
Gonad:	Normal internal female genitalia
Heart:	No lesions are observed in the myocardium
Intestine, large:	Normal morphological features are present in the large intestine.
Intestine, small:	No morphological pathology is present.
Kidney:	No pathological lesions are visible in the kidney sections.
Liver:	The liver appears morphologically normal and no microscopical pathological lesions are found.
Lung:	The lung alveoli and bronchial tree as well as the interstitial tissue appear morphologically normal.
Pancreas:	Normal morphology is visible.
Spleen:	Active white pulp is visible in the splenic section.
Stomach:	The stomach appears morphologically normal.
Thymus:	The thymic lymphoid tissue appears normal and the cortex and medulla of the thymic lobules are well-populated with lymphocytic cells.
Urinary bladder:	Normal histological morphology

COMMENT

The anatomical pathological evaluations do not reveal pathological changes that can be associated with this experiment.

RAT 9: OUR REF 2892-9/12

HISTOPATHOLOGY

Adrenal gland:	Normal
Brain:	Normal morphological features are seen in sections from the cerebrum and cerebellum.
Gonad:	The section from the ovary shows a normal functional organ. The uterus appears normal also.
Heart:	No morphological pathological lesions are present.
Intestine, large:	Normal morphology
Intestine, small:	No lesions are observed.
Kidney:	Mild renal congestion is present.
Liver:	Mild congestion is observed, but the rest of the hepatic parenchyma appears morphologically normal.
Lung:	Normal morphology is present.
Pancreas:	There are no pathological lesions observed in the pancreatic section.
Spleen:	Moderate congestion is observed in the splenic red pulp
Stomach:	No lesions are found.
Thymus:	The thymus is morphologically normal.
Urinary bladder:	Normal

COMMENT

Macroscopical and histological evaluation could not demonstrate any specific morphological pathology.

RAT 10: OUR REF 2892-10/12

HISTOPATHOLOGY

Adrenal gland:	The sections from both adrenal glands do not show any pathological changes.
Brain:	Normal
Gonad:	Normal ovary, Fallopian ducts and uterus are confirmed.
Heart:	No lesions are recorded in the myocardium.
Intestine, large:	The sections from the large intestine show normal intestinal mucosa and no parasites or any lesions could be demonstrated in the large intestine.
Intestine, small:	No pathology is detected.
Kidney:	Normal morphology
Liver:	The liver appears morphologically normal.
Lung:	Normal lung alveoli and airways are visible.
Pancreas:	Normal
Spleen:	Normal splenic white and red pulp. Moderate congestion is visible. Mild haemosiderosis is also present.
Stomach:	No pathology is observed.
Thymus:	Normal morphological features
Urinary bladder:	No pathology is found.

COMMENT

No specific lesions are detected in the organs from this rat.

RAT 11: OUR REF 2892-11/12

HISTOPATHOLOGY

Adrenal gland:	Normal
Brain:	Histological evaluation of different sections from the brain could not demonstrate any pathological lesions.
Gonad:	Normal ovarian and uterine architecture is present.
Heart:	Normal anatomical features. Mild congestion is found.
Intestine, large:	No lesions are recorded in the intestinal wall and mucosa.
Intestine, small:	No pathology is detected in the small intestine.
Kidney:	No lesions are observed in the kidney section.
Liver:	The liver appears morphologically normal and no lesions could be recorded in the liver sections.
Lung:	Sections from the lung show no pathological changes. The bronchial associated lymphoid tissue is normal.
Pancreas:	Normal morphology
Spleen:	Normal splenic white pulp is visible. Mild congestion and haemosiderosis are observed in the splenic red pulp.
Stomach:	No lesions are found in the gastric wall.
Thymus:	The lymphoid tissue of the thymus appears normal.
Urinary bladder:	Normal morphology observed.

COMMENT

No specific lesions are observed in the organs of this rat.

RAT 12: OUR REF 2892-12/12

HISTOPATHOLOGY

Adrenal gland:	Sections from the adrenal glands do not show any pathology.
Brain:	No lesions are recorded in several sections from the brain.
Gonad:	Normal functional female genitalia is present.
Heart:	Normal morphological features
Intestine, large:	The sections from the large intestine do not reveal any pathology.
Intestine, small:	No lesions are observed in the small intestinal sections.
Kidney:	The kidney is normal.
Liver:	The hepatic parencnhyma and stromal tissues as well as portal tracts appear morphologically normal.
Lung:	The lung shows appears normal. No inflammation is present in the lung.
Pancreas:	Normal
Spleen:	Mild extramedullary haemopoiesis and congestion are found in the splenic red pulp.
Stomach:	No lesions are observed.
Thymus:	Normal lymphoid tissue is present in the thymic follicles.
Urinary bladder:	No pathology is found.

COMMENT

Evaluation of this rat does not show specific pathological changes.

RAT 13: OUR REF 2892-13/12

HISTOPATHOLOGY

Adrenal gland:	The adrenal glands are morphologically normal.
Brain:	No lesions are found.
Gonad:	Normal functional internal genitalia
Heart:	The myocardium is normal.
Intestine, large:	No pathology is detected.
Intestine, small:	Normal microscopical findings
Kidney:	No lesions could be observed in the kidney sections. Mild congestion is visible.
Liver:	No histological pathological changes could be confirmed in the section from the liver.
Lung:	Normal morphology of the lung is found.
Pancreas:	No lesions are found in the pancreas sections.
Spleen:	Moderate extramedullary haemopoiesis is visible in the splenic red pulp
Stomach:	Normal anatomy
Thymus:	The thymic lymphoid tissue and stroma appear morphologically normal.
Urinary bladder:	Normal

COMMENT

The anatomical pathology could not demonstrate specific lesions associated with the experimental procedure.

RESULTS

B: EVALUATION OF IMPLANTATION SITES

IMPLANTATION SITES OF GROUP RECEIVED 21ST OF FEBRUARY 2012: OUR REF 2000/12

See Table 2A attached.

Implanted material

The microscopical examination of the implantation sites in the rats received on 21 February 2012 is recorded in Table 2A. There were two types of implanted material consisting of osteoid matrix type implant where an eosinophilic homogenous stroma with lacunae of the osteocytic cells could be detected, and these eosinophilic implants resemble osteoid matrix of bone.

The second type of implant appears to be long filamentous threads of homogenous eosinophilic material without any cells or structures internally present. The threads show a constant width. This is recorded as filamentous implant in the tables.

Foreign body reaction

The foreign body reaction is part of the inflammatory process consisting mainly of epitheloid macrophages as well as multinucleated giant cells responsible for phagocytosis and resorption of foreign material such as the implanted osteoid and filamentous material or any other foreign material which includes hair etc. Small microgranulomas are observed around the implanted proteinaceous material, typical for a foreign body inflammatory reaction.

In this study the foreign body inflammatory reaction appears to be more prominent where the osteoid matrix implant was used when compared to those sites where a filamentous implant is visible.

Granulomatous reaction

The granulomatous inflammatory reaction is intermingled and present in and around both the osteoid matrix as well as the filamentous implants. It consisted of macrophages as well as mononuclear cells and few polymorphonuclear leukocytes around the implanted material. There appears to be minimal inflammatory oedema present and the granulomatous inflammation is localized only around the different implants.

The granulomatous inflammation is most prominent and more severe in the implantation sites where the osteoid matrix implant was identified in the majority of the implantation sites. The granulomatous inflammatory process could be identified in all of the different implantation sites as recorded in Table 2A.

Osteolysis

Osteolysis refers to the fragmentation and resorption of the eosinophilic proteinaceous implanted material, both osteoid matrix as well as the filamentous implant conducted by mainly osteoclastic cells and some of these osteoclasts are also multinucleated, similar to the multinucleated macrophages of the foreign body reaction. Osteoclasts accumulate, especially on the surface of the implanted material and is responsible for resorption of the eosinophilic proteinaceous implanted material.

The osteolytic process varies from mild to severe in the osteoid matrix implants, while it is minimal (negative) where the filamentous implant was used in this study.

Osteogenesis:

Osteogenesis refers to the process of new bone deposition which in this case would be intramembranous bone formation where existing osteoid matrix and implants are re-populated with osteocytic cells in the osteoid lacunae and proteinaceous stroma, while osteoblasts accumulate on the external surface of the proteinaceous stromal tissue and produce osteoid on the external surface of the membranous / proteinaceous eosinophilic material of the implant.

Osteogenesis appears to be absent in the majority of these implants sites and could be graded only as mild in a few of the osteoid matrix implant sites.

Ulcerated skin

The areas of ulceration are small and microscopically confirmed at the implantation site on the surface of the skin showing superficial exudative crusts and some areas of full-thickness epithelial necrosis, while mild inflammation is present in the dermis underneath the ulcerated skin. External irritation (scratching) may have a part in the pathogenesis.

Superficial ulceration is recorded in Table 2A and is found in both the osteoid matrix implant sites as well as the filamentous implant sites.

IMPLANTATION SITES OF GROUP RECEIVED 13 MARCH 2012: OUR REF 2892/12

See Table 2B attached. The grading of the histological findings in the implantation sites on the group of rats received on the 13th of March 2012 is similar to that reported above.

Implanted material

Again the two types of implanted material which is reported as osteoid matrix implant and filamentous implant were found in the implantation sites.

The filamentous implant was in some of the sites easily disrupted during tissue sectioning and is not so tightly adhered to the subcutaneous stroma as what is found with the osteoid matrix implant.

Foreign body reaction

A foreign body reaction could be confirmed in all of the implantation sites.

The foreign body reaction varied from mild to severe and there is little difference between the foreign body inflammatory process recorded for the osteoid matrix implants compared to the filamentous implants.

Granulomatous reaction

The granulomatous inflammatory process consisting of macrophages and epitheloid cells and also some lymphocytic inflammatory infiltrates which point towards a chronic inflammatory reaction. The body recognized the foreign material, while in some of the implantation sites, especially where the filamentous material was used, pyogranulomatous inflammation could be detected with the presence of numerous heterophils also visible in the central part of the granuloma.

Osteolysis

The osteolytic process of resorption and breakdown of the osteoid matrix and filamentous implant could be confirmed in most of the implantation sites as indicated in Table 2B. Disruption and resorption of the filamentous implant could be confirmed also in the majority of implantation sites.

Osteogenesis

The osteogenic or regenerative process with new bone development and re-population of osteoid lacunae with osteocytes was graded as mild and could be detected only in one of the osteoid matrix implant sites.

Ulcerated skin

Superficial ulceration in the epidermis was found in only three of the implantation sites, all of the osteoid matrix implant areas, while dermal scarring due to the implantation was present underneath these ulcers as well as in some of the non-ulcerated sites. This latter dermatofibrosis and scarring is part of the normal healing process where the osteoid matrix or filamentous implant was implanted into the subcutis.

DISCUSSION:

The morphological findings are recorded under the results, while grading of the pathological changes at the implantation sites are given in the tables attached.

These findings must be correlated with the history and while it appears in the earlier group of rats with our reference 2000/12 that the filamentous implantation sites show less of a foreign body reaction as well granulomatous inflammation and osteolysis, there is no prominent difference between this inflammatory process and osteolysis in the group of rats received later with our reference 2892/12. In this latter group the osteolytic process and resorption of the different implants are already advanced and complete healing should develop in a short time.

Osteogenesis could be demonstrated in some of the implantation sites of in the osteoid matrix group characterized by re-population of the lacuni with osteocytic cells and superficial osteoid production on the surface of the spicules of osteoid matrix that was implanted in the subcutaneous tissues. None of the filamentous implantation sites reveal any signs of osteogenesis.

Yours faithfully

DR W S BOTHA

UNIVERSITY OF PRETORIA
BIOMEDICAL RESEARCH CENTRE
PRIVATE BAG X04
ONDERSTEPOORT
0110

2012/04/04

For attention: Ilse Janse van Rensburg

STUDY H16/11: SUBCUTANEOUS BIOASSAY OF NAVAL OSTEOCONDUCTIVE PROTEIN MICROSTRUCTURE FOR ALTERNATIVE AUTOGRAFT BONE TRANSPLANT SCAFFOLD: IDEXX REF 2000/12 AND 2892/12

PROFORMA INVOICE / FAKTUUR	
1. Histopathology/Histopatologie x 70 @ R203 each	R 14210.00
2. Post mortem x 8 @ R203 each	R 1624.00
3. Handling fee	R 152.00
4. Photography: ½ hour	R 559.00
TOTAL / TOTAAL	R 16393.00

TABLE 2A: HISTOPATHOLOGICAL FINDINGS ON IMPLANTATION SITES: STUDY H16/11 OUR REF: 2000/12

TREATMENT	CC	CL	CH	KL	KP	KC	KG	KP	KG	CH	CH	CH	CC	KP	KC	CC
IMPLANT SITE	14/1	14/3	14/2	14/4	15/1	15/3	15/2	15/4	16/1M	16/3M	16/2M	16/4M	16/1F	16/3F	16/2F	16/4F
IDEXX REF	14 A1	14A 2	14B 1	14B 2	15A 1	15A 2	15 B1	15B2	16A1	16A2	16B1	16B 2	16A1	16A2	16B1	16B2
Implanted material	0	0	0	*ƒ*	*ƒ*	*ƒ*	*ƒ*	*ƒ*	*ƒ*	0	0	0	0	*ƒ*	*ƒ*	0
Foreign body reaction	2+	1+	2+	-	-	-	-	1+	-	2+	2+	3+	2+	2+	-	3+
Granulomatous reaction	3+	2+	3+	1+	1+	1+	1+	1+	1+	3+	3+	3+	3+	3+	1+	3+
Osteolysis	3+	1+	3+	-	-	-	-	-	-	1+	2+	2+	2+	-	-	2+
Osteogenesis	-	-	-	-	-	-	-	-	-	-		-		-	-	-
Ulcerated skin	-	-	1+	2+	1+	2+	1+	-	-	-	1+	1+	2+	1+	1+	1+

Legend:

0	Osteoid matrix implant (collagen)	CC	Collagen control	KG	Kafirin microparticle film treated with glutaraldehyde
ƒ	Filamentous implant (kafirin microparticle film)	CL	Collagen low BMP-2 loading	KP	Kafirin microparticle film treated with polyphenol
-	Negative / No Lesion	CH	Collagen high BMP-2 loading		
1+	Mild	KC	Kafirin microparticle film control		
2+	Moderate	KL	Kafirin microparticle film low BMP-2 loading		
3+	Severe	KH	Kafirin microparticle film high BMP-2 loading		

TABLE 2B: HISTOPATHOLOGICAL FINDINGS ON IMPLANTATION SITES: STUDY H16/11 OUR REF: 2892/12

TREATMENT	CC	CC	CC	CC	CL	CL	CL	CL	CH	CH	CH	CH	KC	K C	KC	K C	KL	KL	KL	KL	K H	K H	KH	K H
IMPLANT SITE	4/2	6/2	5/3	12/ 1	13/1	5/4	8/1	4/4	11/3	13/2	7/3	1/4	1/3	6/ 4	10/ 1	9/ 3	12/ 3	7/ 1	3/ 1	11/ 4	3/ 4	8/ 4	9/2	10 /3
IDEXX REF	4B 1	6B1	5A2	12A 1	13A 1	5B2	8A1	4B2	11A 2	13B 1	7A2	1B 2	1A 2	6B 2	10 A1	9A 2	12 A2	7A 1	3A 1	11 B2	3B 2	8B 2	9B 1	10 A2
Implanted material	0	0	0	0	0	0	0	0	0	0	0	0	*ƒ*	*ƒ*	*ƒ*	*ƒ*	*ƒ*	0	*ƒ*	*ƒ*	*ƒ*	*ƒ*	*ƒ*	*ƒ*
Foreign body reaction	3+	3+	3+	1+	2+	2+	2+	2+	2+	2+	3+	3+	2+	1+	2+	1+	2+	1+	2+	2+	2+	2+	2+	1+
Granulomatous reaction	3+	3+	3+	2+	3+	1+	2+	3+	2+	2+	1+	3+	2+	3+	2+	1+	3+	1+	3+	2+	2+	1+	3+	2+
Osteolysis	2+	2+	3+	2+	1+	2+	1+	2+	2+	2+	2+	3+	3+	2+	2+	-	1+	-	2+	2+	2+	-	1+	1+
Osteogenesis	-	-	-	-	-	-	-		-	-	-	1+	-	-	-	-	-	-	-	-	-	-	-	-
Ulcerated skin	-	1+	-	-	-	1+	-	-	1+	-	-	-	-	-	-	-	-	-	-	-	-	-	-	-

Legend:

0	Osteoid matrix implant (collagen)	CC	Collagen control
ƒ	Filamentous implant (kafirin microparticle film)	CL	Collagen low BMP-2 loading
-	Negative / No Lesion	CH	Collagen high BMP-2 loading
1+	Mild	KC	Kafirin microparticle film control
2+	Moderate	KL	Kafirin microparticle film low BMP-2 loading
3+	Severe	KH	Kafirin microparticle film high BMP-2 loading

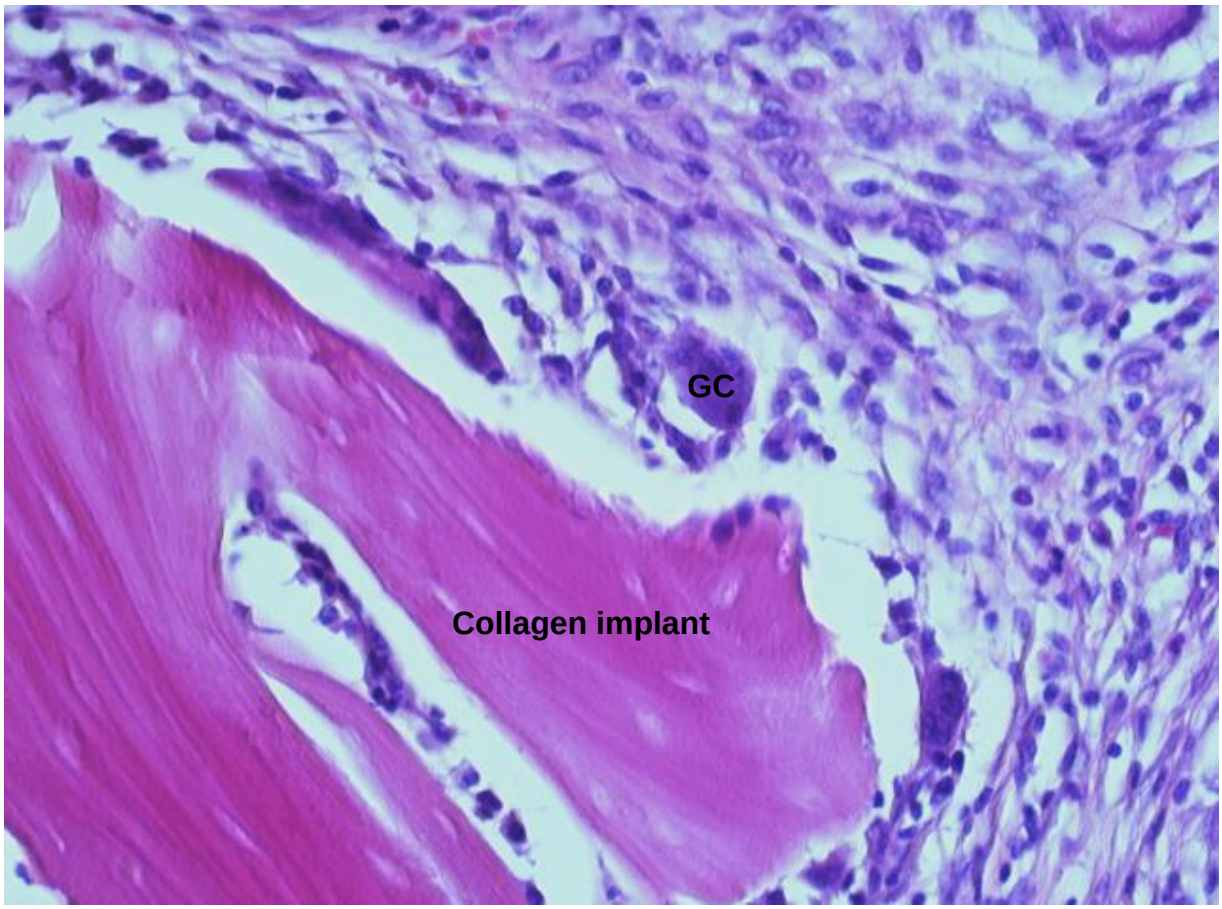

Figure A1. Image of haematoxylin–eosin stained sections of collagen implant in the subcutaneous site showing foreign body giant cells Day 7 post implantation. **GC**-Giant cell. Magnification x 200

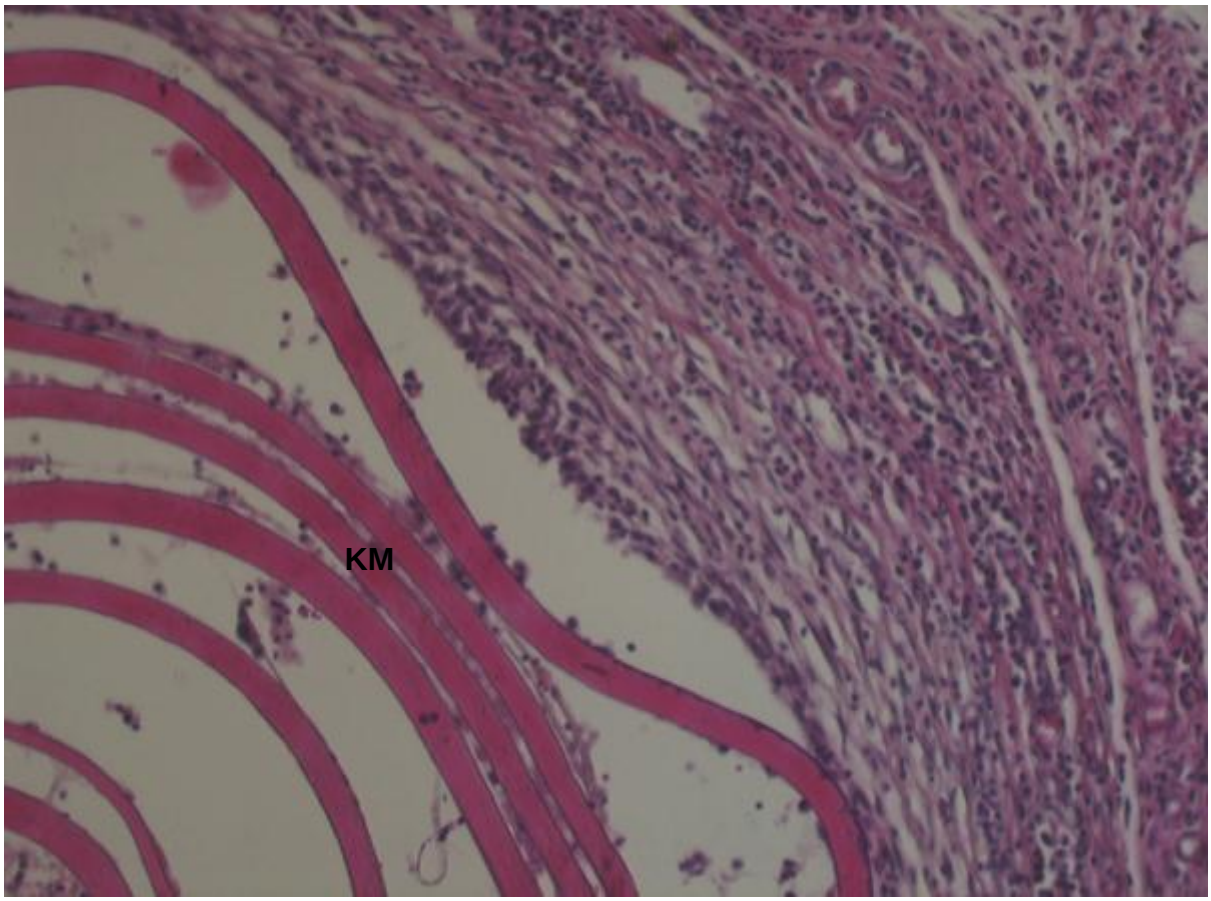

Figure A2. Image of haematoxylin–eosin stained sections of kafirin microparticle film implants in the subcutaneous site showing intact kafirin microparticle film implant and inflammation by Day 28 post implantation. **KM** - Kafirin microparticle film implant. Magnification x 100.

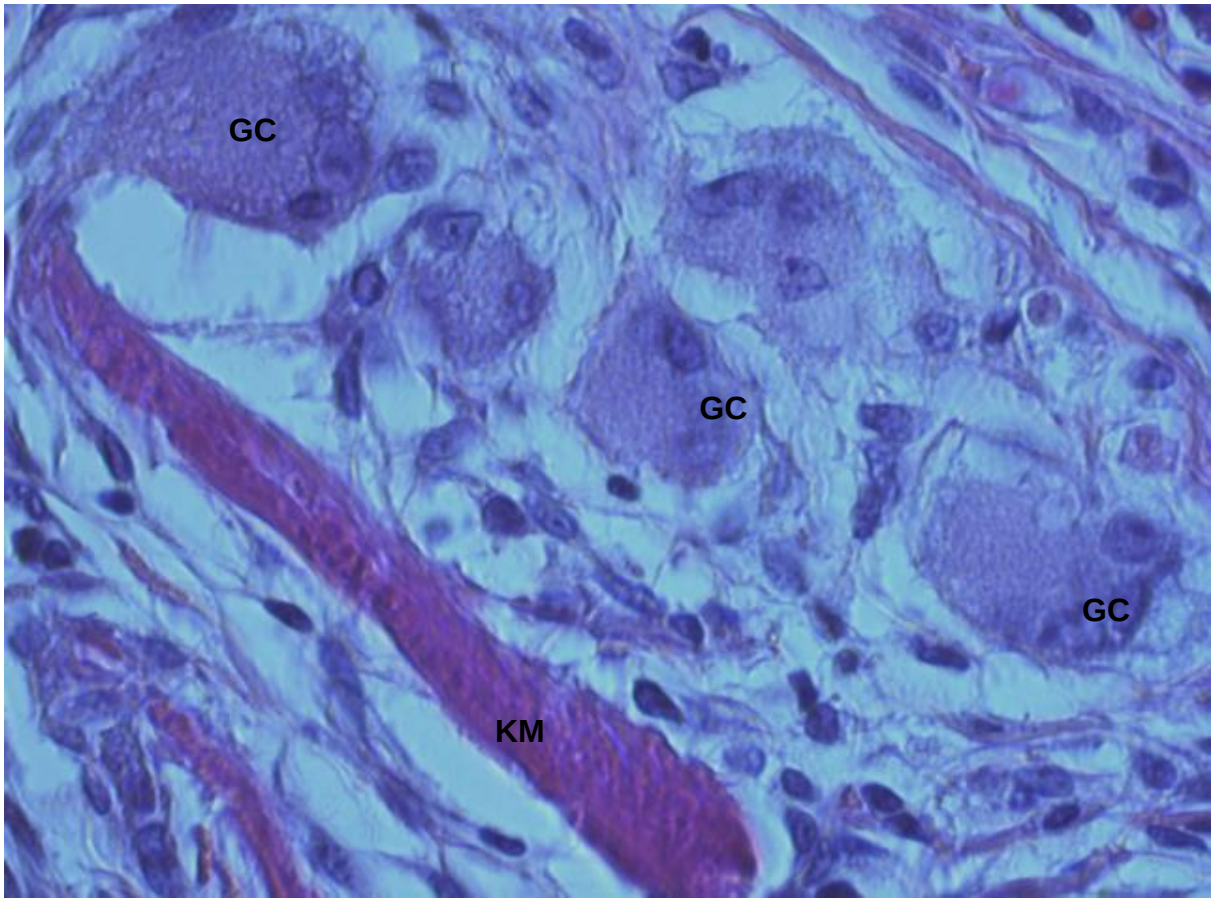

Figure A1. Image of haematoxylin–eosin stained sections of kafirin microparticle film implant in the subcutaneous site showing foreign body giant cells Day 28 post implantation. **KM**- kafirin microparticle film implant. **GC**-Giant cell. Magnification x 400.

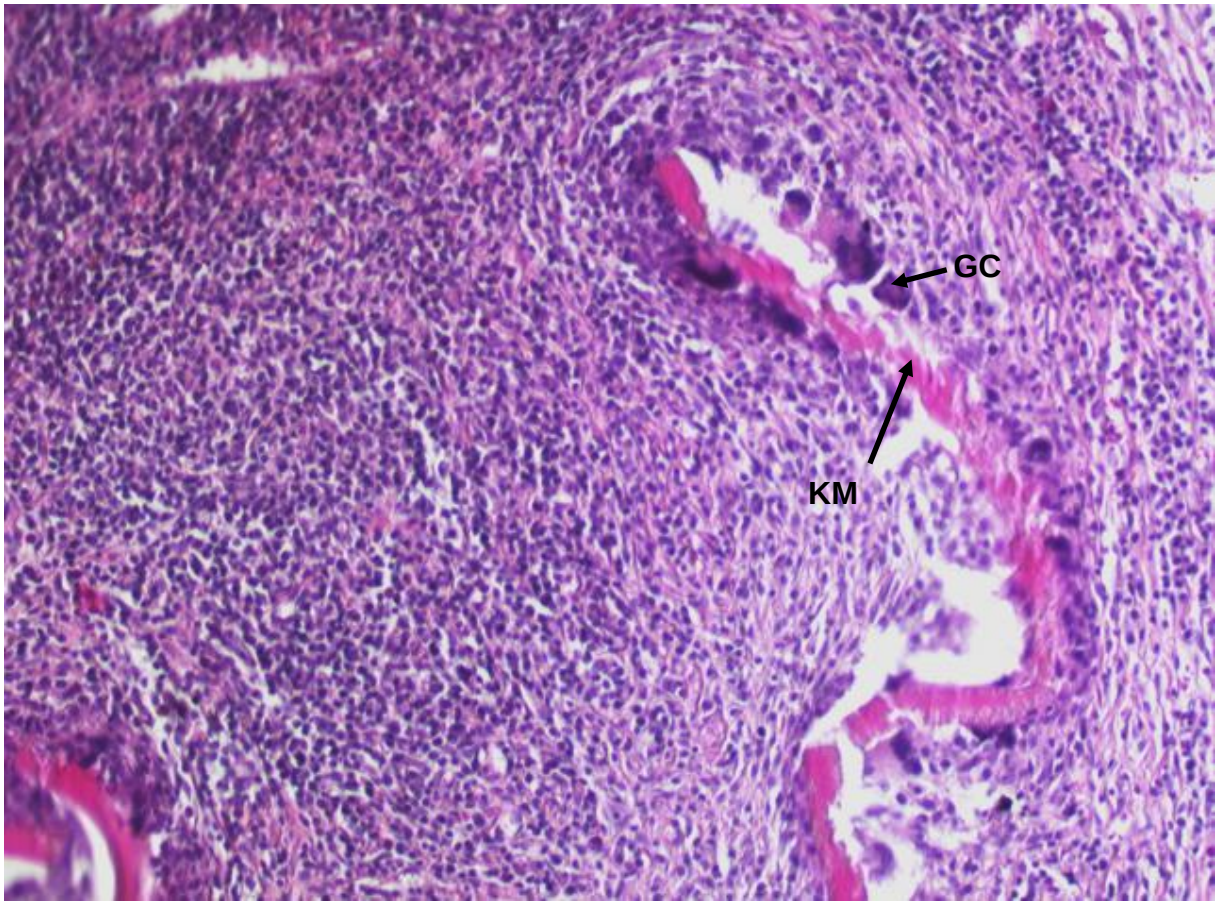

Figure A2. Image of haematoxylin–eosin stained sections of kafirin microparticle film implant in the subcutaneous site showing lysis (degradation) of kafirin microparticle film and inflammation by Day 28 post implantation. **KM** – Kafirin microparticle film implant **GC**-Giant cell. Magnification x 100.

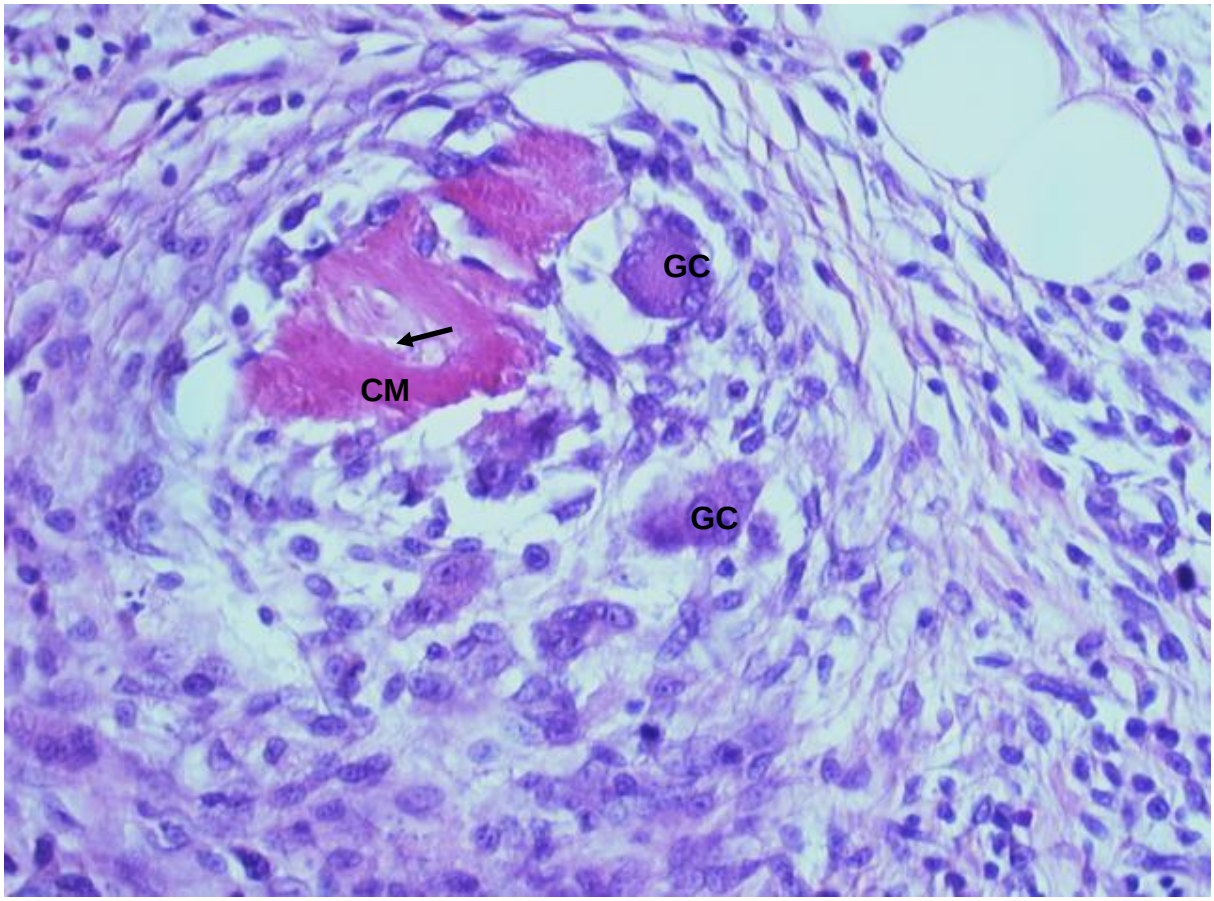

Figure A3. Image of haematoxylin–eosin stained sections of collagen implant in the subcutaneous site showing Osteolysis of collagen implant Day 7 post implantation. **CM**-Collagen implant. **GC**-Giant cell. Arrow is pointing at site of osteolysis. Magnification x 200.

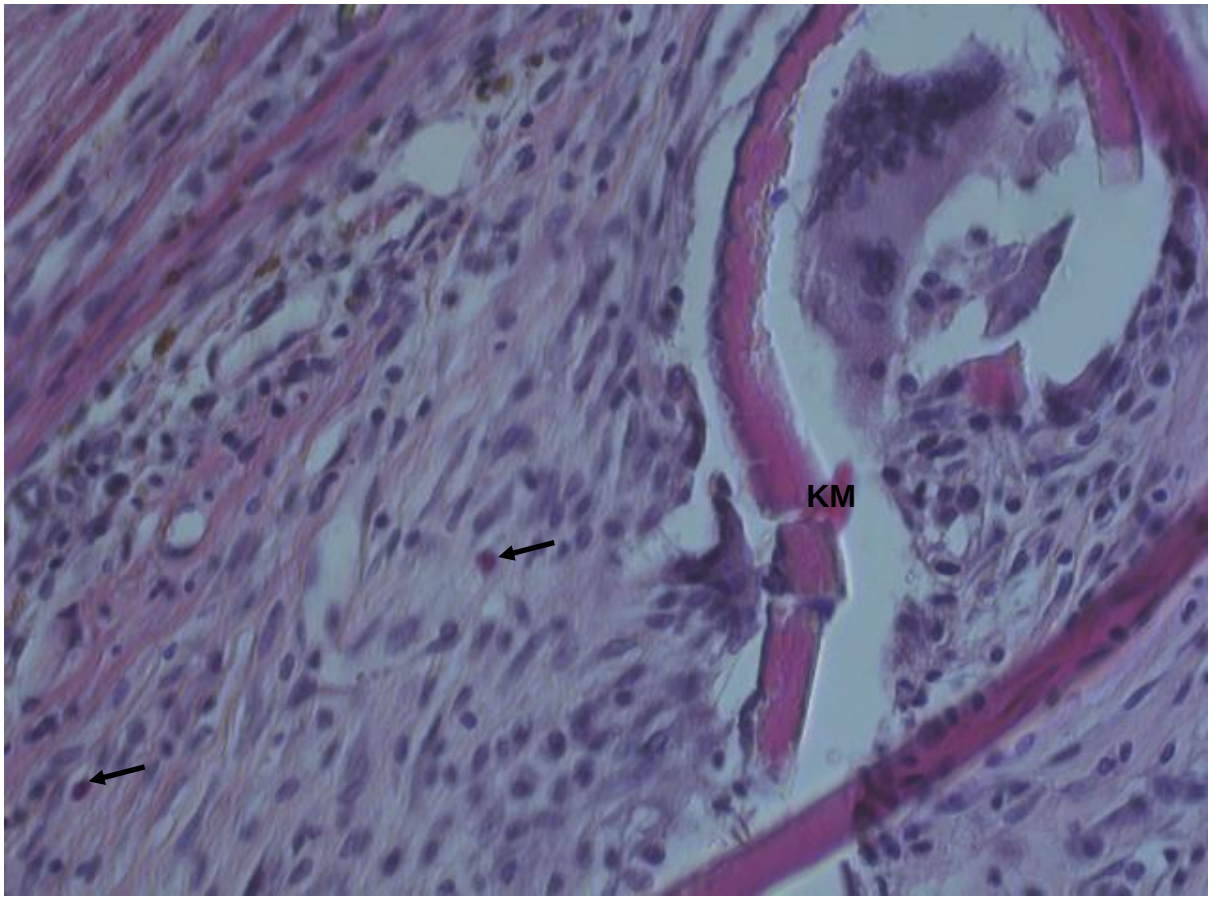

Figure A4. Image of haematoxylin–eosin stained sections of kafirin microparticle film implant in the subcutaneous site showing granulomatous inflammatory reaction with kafirin microparticle film implant 28 days post implantation. **KM** – kafirin microparticle film implant. Arrows pointing at heterophils, which indicate granulomatous inflammatory reaction. Magnification x 200.

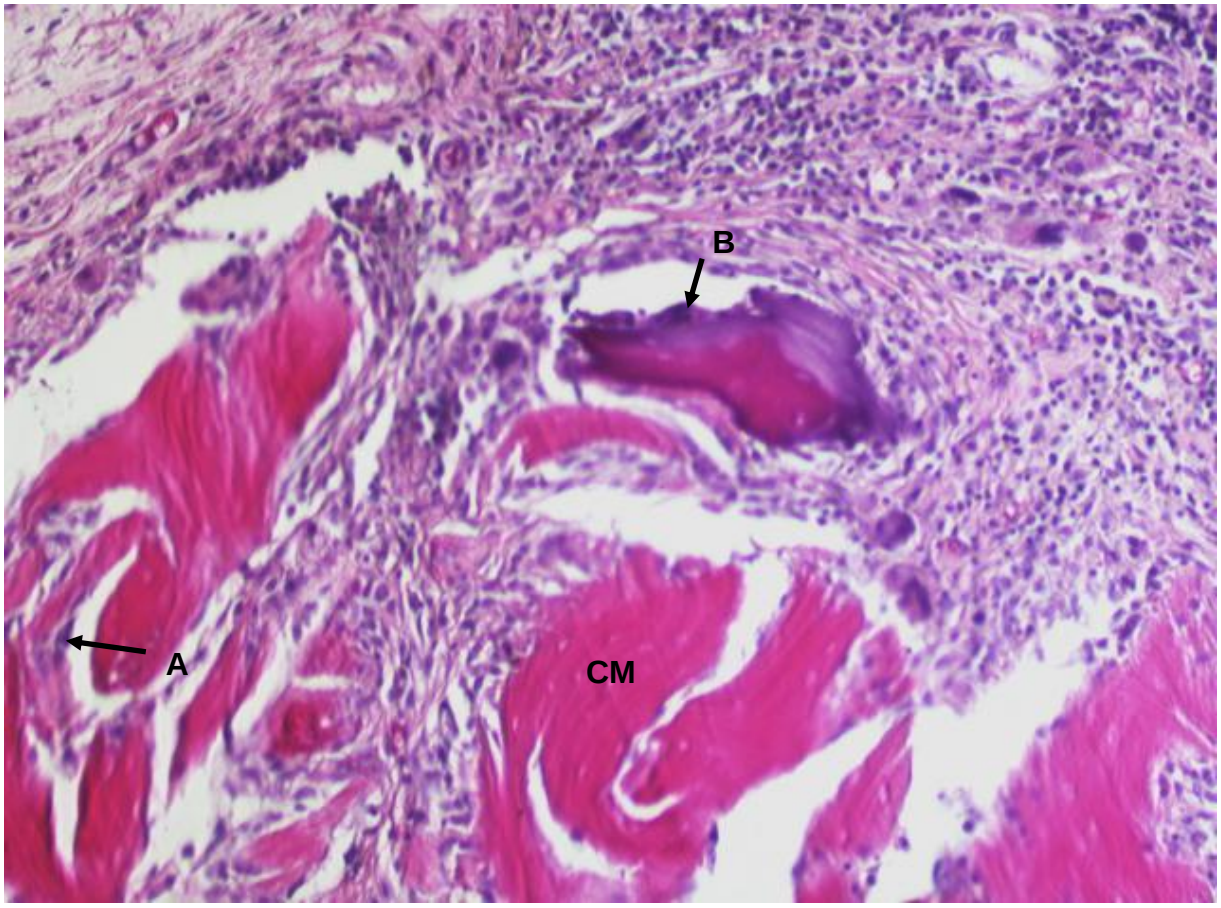

Figure A5. Image of haematoxylin–eosin stained sections of collagen implant showing mild osteogenesis after the implantation for 28 days. CM -Collagen implant. **A.** Shows the repopulation of the osteoid lacunae with osteocytes. **B.** Bluish staining at the edge of the collagen implant indicate presence of osteoblasts. Magnification x 100.